TABLE OF CONTENTS

Page

LIST OF TABLES

Page

LIST OF FIGURES

Page

LIST OF ABREVIATIONS

A-GPS	Assisted GPS
ANSS	Augmentation Navigation Satellite Systems
ASIC	Application Specific Integrated Circuit
A-TOA	Adapted Time Of Arrival
BER	Bit-Error-Rate
BJ	Bump and Jump
BOC	Binary Offset Carrier
C/A	Coarse Acquisition
CBOC	Composite BOC
CCRW	Code Composite Ranging Waveform
CD	Collective Detection
CDMA	Code Division Multiple Access
CGR	Cognitive GNSS Radio
CGR-DB	CGR Data Base
CNR	Carrier-to-Noise Ratio
CP	Cooperative Positioning
CPS	Cognitive Positioning System
CR	Cognitive Radio
CRLB	Cramer-Rao Lower Band
CS	Control Station
CW	Continuous Waveform
DBZP	Double Block Zero Padding
DFT	Discrete Fourier transform
DGPS	Differential Global Positioning System
DLL	Delay-Locked Loop
DoD	Department of Defense
DPLL	Differential Phase-Locked Loop
DSP	Digital Signal Processor
EDSM	Enhanced Dynamic Spectrum Management

EGNOS	European Geostationary Navigation Overlay Service
EITHSCD	Efficient and Innovative Technique of High Sensitivity Collective Detection
EKF	Extended Kalman Filter
ÉTS	École de Technologie Supérieure
FDMA	Frequency Division Multiple Access
FFT	Fast Fourier Transform
FPGA	Field Programmable Gate Array
FM	Frequency Modulation
FT	Fourier Transform
GAGAN	GPS Aided GEO Augmented Navigation
GPS	Global Positioning System
GNSS	Global Navigation Satellite System
GSM	Global System for Mobile communication
GSS	Générateur de Signal Synthétique
GTRF	Galileo Terrestrial Reference Frame
HEDSM	Hybrid Enhanced Dynamic Spectrum Management
HS-CD	High Sensitivity Collective Detection
HS-CGR	High Sensitivity Cognitive GNSS Receiver
HS-GNSS	High Sensitivity GNSS
HS-GPS	High Sensitivity GPS
IDFT	Inverse Discrete Fourier Transform
IF	Intermediate Frequency
IGS	International GNSS Service
IGSO	Inclined GeoSynchronous Orbit
INS	Inertial Navigation System
IoT	Internet of Things
IR	Infra-Red
ISAE	Institut Supérieur de l'Aéronautique et de l'Espace
ISP	Intelligent Signal Processing
JNR	Jammer-to-Noise Ratio

LASSENA	Laboratoire Spécialisé en Systèmes Embarqués, Navigation et Avionique
LBS	Location-Based Services
LHCP	Left Hand Circularly Polarized
LORAN	LOng-RAge Navigation
LOS	Line of Sight
MBOC	Multiplexed BOC
MCS	Master Control Station
MEDLL	Multipath-Estimating Delay Locked Loop
MSAS	MTSAT Satellite Augmentation System
MTLL	Mean Time to lose Lock
MTTA	Mean Time To Acquire
MUSIC	Multiple Signal Classification
PA	Partition and Add
PC	Personal Computer
PDA	Personal Data Assistant
PFA	Probability of False Alarm
PLL	Phase-Locked Loop
PND	Personal Navigation Devise
PRN	Pseudorandom Noise
RF	Radio Frequency
RFID	Radio Frequency Identification
RISC	Reduced Instruction Set Computer
RNSS	Regional Navigation Satellite Systems
SBAS	Satellite-Based Augmentation System
SCAN	Signal, Communication, Antenna and Navigation
SCP	Spectral Compression Positioning
SDN	Software Defined Navigation
SDR	Software Defined Radio
SNR	Signal-To-Noise Ratio
SoOP	Signal of Opportunity

TMBOC	Time Multiplexed BOC
TOA	Time of Arrival
TSI	Traitement de Signal Intelligent
TTFF	Time To First Fix
ULS	UpLoad Station
UWB	Ultra Wide Band
VHF	Very High Frequency
VOR	VHF Omnidirectional Radio range
WAAS	Wide Area Augmentation System
WGS	World Geodetic System
WLAN	Wireless Local Area Network
WSN	Wireless Sensor Network

LIST OF SYMBOLS

α	Doppler offset change rate
β	Maximum tolerance code phase estimation error in CD algorithm
δf_d	Doppler offset search grid resolution
$\delta\tau$	Code phase search grid resolution
Δb	User clock bias
Δf_d	Doppler offset
$\Delta\tau$	Code phase estimation error
$\Delta\rho$	Differential pseudorange
ρ	Pseudorange
θ	Angle of circular search in CD algorithm
τ	Code phase offset
ζ	Signal travel time
c	Speed of light
C/N_0	Carrier-to-Noise Ratio
D_{ind}	Individual detection metric
D_{CD}	Collective Detection metric
f_s	Sampling frequency
N_c	Number of samples per code period
P_d	Probability of detection
P_{fa}	Probability of false alarm
R	Radius of circular search in CD algorithm
$R(\tau)$	PRN signal autocorrelation function
t_{RX}	Reception time of satellite signal
t_{TX}	Transmission time of satellite signal
T_c	Chip period
T_s	Sampling period
T_{coh}	Coherent integration period
X	Vector of position and clock-bias

CHAPTER 1

INTRODUCTION

In recent years, the interest in positioning and navigation has been increasing, as being evidenced by the systems and services developed in this sense. The use of global navigation satellite system (GNSS) receivers has increased considerably with the integration of GNSS chips in cellular phones and mobile devices which are used for potential applications in several areas like location-based service (LBS). Since the deployment of the first constellation of satellites by the US military 35 years ago, the number of devices equipped with GPS (Global Positioning System) is steadily increasing and is currently almost 4 billion. GPS devices have been used in various applications: aviation, maritime, rail, car guidance, topography, agriculture, critique infrastructure, medicine, human security, etc.

This first chapter introduces a contextualization of the GNSS positioning field and its importance in several areas. Then, the motivations that led us to carry out this PhD project will be developed as well as the objectives of this work. The structure of the thesis and the publications made during the period of this research work are described at the end of this chapter.

1.1 Background and GNSS systems overview

Currently, the technology of the global navigation satellite system (GNSS) continues to evolve in a very competitive climate. Four major systems exist and can be exploited: GPS (USA), Galileo (European Union), GLONASS (Russia) and BeiDou (China). Navigation and positioning technique becomes one of the most popular research and development topics with the arising of new satellite navigation (Galileo and BeiDou) systems and the modernization of GPS and GLONASS systems, with new satellites, new frequencies and modern signals. The number of satellites able to transmit the navigation signals will increase in order to have a wider coverage and above all a greater availability allowing to have more precise positioning.

Apart from the four biggest GNSS systems, some GNSS augmentation systems, SBAS (Satellite-Based Augmentation System), exist to complement the GPS system such as WAAS (Wide Area Augmentation System) in USA, MSAS (MTSAT Satellite Augmentation System) in Japan, EGNOS (European Geostationary Navigation Overlay Service) in Europe and GAGAN (GPS Aided Geo Augmented Navigation) in India. Other regional navigation systems also exist such as QZSS (Quasi-Zenith Satellite System) in Japan, IRNSS (Indian Regional Navigation Satellite System) in India, etc.

The increase in the number of satellite signals and the diversity of GNSS satellites is a great advantage because it can improve the overall performance of the signal processing in a multi-constellation multi-frequency hybrid architecture. Thus, traditional satellite navigation receivers should be improved in order to able to receive all GNSS signals (current and future). The receivers should be designed to acquire as many satellite signals as possible from different constellations. The improvement of the GNSS signals will improve the issue of availability, however, the signals degradation remain challenging including the high attenuations and shadowing in harsh environments like in urban environments.

The combined use of different GNSS signals motivates the use of traditional receivers that are not favorable in some areas of the globe. Similarly, positioning in non-ideal environments (inside buildings, in forest, in large canyons, under tunnels, etc.) has become possible thanks to the use of these different systems in a single architecture. Given that each system uses its own transmission frequency band, the combined use of GNSS systems makes the reception of navigation signals more flexible, especially with the use of the new L5 and E5 broadband signals in addition to the standard signals L1 and E1.

This diversity and redundancy of GNSS measurements will further open the door to new developments and applications that are impossible to attend with actual receivers, designed for outdoor environments. Increasing the number of signals and the diversity of GNSS satellites has significant benefits for many areas of application, because it can improve the sensitivity and the overall performance of the signal processing in a hybrid architecture combining all

GNSS signals. However processing multi-band signals is costly and presents different technical challenges.

Several sectors are affected and covered by GNSS applications such as:
Science: topography, geographic information system (GIS), archeology, atmospheric science, geophysics, geodesy, oceanography, etc.;
Transport: land, air, maritime, rail, fleet management, congestion reduction, etc.;
Industry: telecommunications, public safety, agriculture, medicine, tourism, etc.;
Military: precise target location, missile guidance, etc.

1.2 Thesis motivations

In urban environments, the use of GNSS receivers has increased considerably with the integration of GNSS chips in cellular phones and mobile devices which are used for potential applications in several areas like location-based service. This requires obtaining of high positioning accuracy and resolution of the various problems encountered in GNSS denied environments. Navigation and positioning techniques become one of the most popular research and development fields with the coming of new satellite navigation Galileo and BeiDou systems and the modernization of GPS and GLONASS systems, with new satellites, new frequencies and modern signals. The increase in the number of satellite signals and the diversity of GNSS satellites is a great advantage because it can improve the overall performance of the signal processing in a multi-constellation multi-frequency hybrid architecture.

Due to the growing interest in positioning and navigation in challenging environments like urban and indoors, the development of new techniques for weak GNSS signal acquisition and tracking is required. Received satellites signals can be attenuated in urban areas with tall buildings, indoors, in forested areas, in many suburban neighborhoods, and can be affected by several sources of errors such as multipath and Non-line-of-sight (NLOS) reflexions, masking, interferences and jamming. The receiver then provides a position often affected by an error of

several tens of meters; otherwise it will be really impossible to compute its position. In such environments, acquisition of weak satellite signals requires advanced signal processing techniques to improve the sensitivity of the GNSS receivers.

Different obstacles traversed by the signals emitted from the satellite can also cause their degradation at reception, especially inside buildings. Three phenomena are possible: reflection, diffusion and diffraction. The reflection characterizes the fact that part of the wave is reflected by an obstacle and returns to its point of origin. The diffusion characterizes the fact that the wave or part of the wave passes through the obstacle but each takes some direction. Diffraction characterizes the angle between the boundary of the obstacle traversed and the direction of the wave. Thus, the reception of the signals reflected, diffused and diffracted or all of them combined on the receiving antenna forms the multipath phenomenon.

Figure 1.1 and Figure 1.2 show the challenges in urban and indoor positioning with the various obstacles encountered by the satellite signals and especially the different materials which cause the signal attenuation.

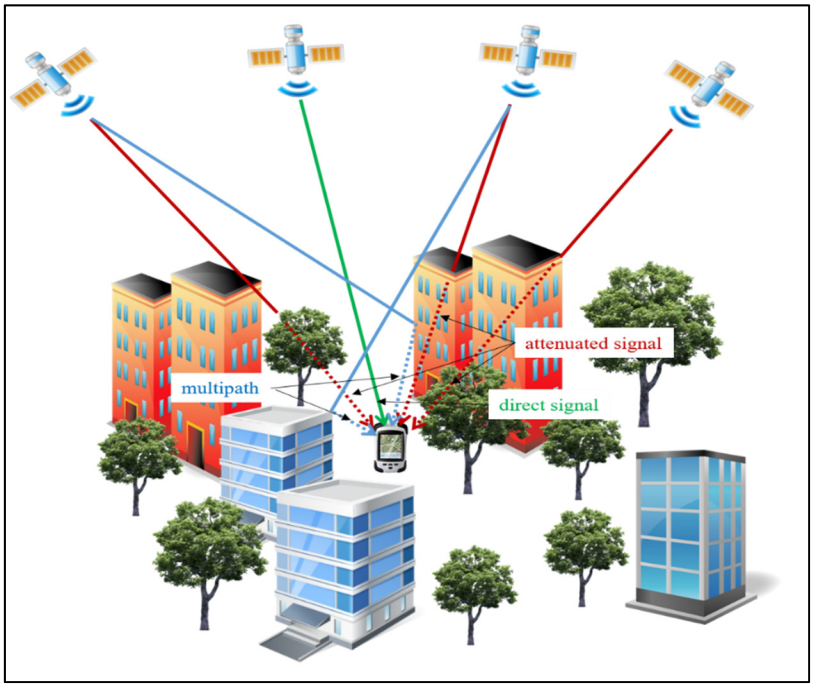

Figure 1.1 Challenges in a typical urban environment (tall buildings, trees, etc.)

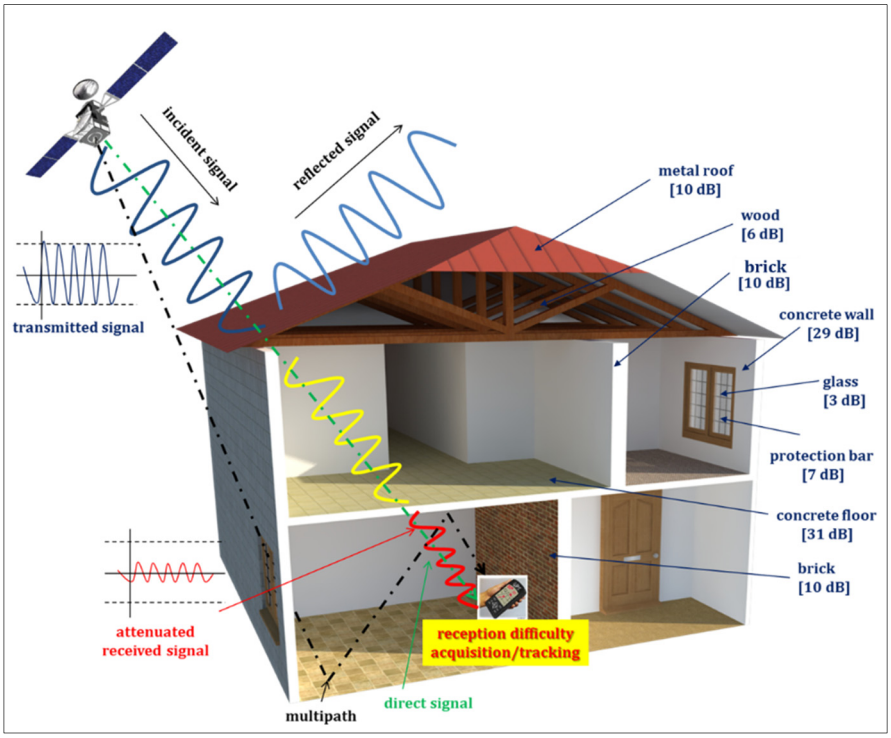

Figure 1.2 Challenges in indoor GNSS positioning

The values of the signal attenuation caused by some obstacles are shown in Table 1.1 (Taken from (van Diggelen, 2009).

Table 1.1 Signal attenuation caused by different materials

Obstacles	**Range of attenuations [dB] at 1.5 GHz**		
	minimum	**median**	**maximum**
Drywall	1	1	1
Plywood	1	2	3
Glass	1	3	4
Lumber	2	6	9
Rebar grid	2	-	11
Brick	5	10	31
Concrete	12	29	43
Reinforced concrete	29	-	33
Metal tinted glass	-	10	-

GPS receivers still have weaknesses in terms of availability (presence and consistency of signals), integrity (compliance with operating standards), accuracy (accuracy, fineness and validity of positioning) and electromagnetic vulnerability (RF interference). Degradation of precision can have many sources: satellite errors (selective availability, orbit error, clock error), atmosphere (ionosphere and troposphere), local and multipath obstruction, receiver noise, etc.

Due to the modernization of GNSS signals and the growing interest in navigation and positioning in harsh environments, the development of techniques and methods for weak satellite signal processing is needed. Significant techniques and technologies making mobile phones capable of determining their position have been developed recently for Assisted-GPS by the wireless service providers

At the system level, many modernization steps and improvements have been introduced for ephemeris precision, satellites errors reduction, etc. At the user level, a better way to overcome this problem of positioning in hostile environments is the use of high sensitivity (HS) and robust receivers. Several techniques have been proposed to deal with this problem of receiving weak signals. For indoor environments, many technologies have been proposed for localization purposes because the GNSS signals cannot be received with a sufficiently high signal-to-noise ratio (Seco-Granados et al., 2012). Moreover, most existing techniques require a dedicated physical infrastructure.

To improve the robustness and especially the sensitivity of future GNSS receivers inside buildings, or generally in non-ideal environments, some intra-receiver and extra-receiver approaches have been proposed such as the use of the advanced processing techniques of high sensitivity acquisition and tracking, multipath mitigation and anti-jamming, the use of all existing navigation system signals (current and future), the use of navigation assistance techniques (Differential GPS (DGPS), Relative Kinematic Positioning (RKP), Precise Point Positioning (PPP), Inertial Navigation System (INS), Signals of Opportunity (SoOP), etc.).

GNSS signals are already weak (-130 dBm) when they attend the earth surface. So, the receiver should be more sensitive to be able to acquire the attenuated satellites signals. Moreover, High Sensitivity (HS) receiver is required for GNSS positioning in hostile environment. Compared to a standard GNSS receiver, a high sensitivity receiver is able to perform correlation for longer times, and therefore, can acquire very weak satellite signals. Under the same conditions, HS receivers have faster Time To First Fix (TTFF) and re-acquisition times than standard receivers. In order to acquire GNSS signal with very low power, HS receivers use coherent and non-coherent integration, and some of them take advantage of massive parallel processing in order to dwell the receiver for longer periods of correlation (Schmid, 2009) (O'Driscoll, 2007a). Other correlation techniques have been proposed including the self Doppler aiding and differential integration (Esteves, 2013) (Sahmoudi et al., 2010).

Although high sensitivity receivers are capable to acquire weak satellite signals, there are more problematic in urban and indoor environments compared to other challenged environments such as high attenuation, multipath, etc. So, only high sensitivity receivers are not enough for positioning and navigation in deep urban canyons. Many techniques have been developed for urban and indoor positioning and can be categorized into two groups: the first group includes the techniques using other signals than GNSS signals like Ultra Wide Band (UWB), Wireless Local Area Network (WLAN) positioning, Wireless Sensor Networks (WSN), Radio Frequency Identification (RFID), ultrasound, camera, Bluetooth, FM radio signals, infrared (IR), etc. These techniques have the common drawback that they cannot provide a continuous positioning solution between two buildings (from a building to another one) because the range of coverage for these technologies is limited and it requires an additional equipment to be installed (Seco-Granados et al., 2012) (van Diggelen (2009). The second group consists of different techniques that use some sort of assistance in addition to GNSS signals like Assisted GNSS (A-GNSS) and integrated INS/GNSS using inertial sensors (accelerometers, magnetometers and gyroscopes). In this thesis, we are interested in the second group in which the positioning techniques are based on GNSS signals using aiding information. The assistance data allows the GNSS receiver to reduce the search space by providing information such as satellite ephemeris, reference time and a priori position. Two major approaches to A-GNSS

exist: MS-assisted and MS-based GNSS. MS (Mobile Station) designates the GNSS receiver. The position is computed at a server (reference station) in MS-assisted GNSS whereas it is computed by the receiver itself in MS-based GNSS. In MS-assisted GNSS, the receiver only performs the signal acquisition and sends the measurements to the reference station (van Diggelen, 2009).

The greater motivation of this research study is due to the growth of mobile devices in urban areas which can be useful to help other receivers in bad condition of reception as a cooperative GNSS solution. It is a kind of connected receivers or collaborative positioning (crowd positioning) but it is based only on satellite signals. Figure 1.3 shows the main motivation of the developed research work. This idea shows that we are not limited to a static base station as used in A-GPS and standard Real Time Kinematic (RTK) positioning, but allows a mobile receiver in challenging reception conditions to get help from another mobile stations or other cooperative users in a good reception conditions. Under these conditions, we must be able to process highly degraded or very short signals that do not allow the receiver to go through the tracking process. Thus, this leads us to the need to rethink the architecture of GNSS receiver for modern applications.

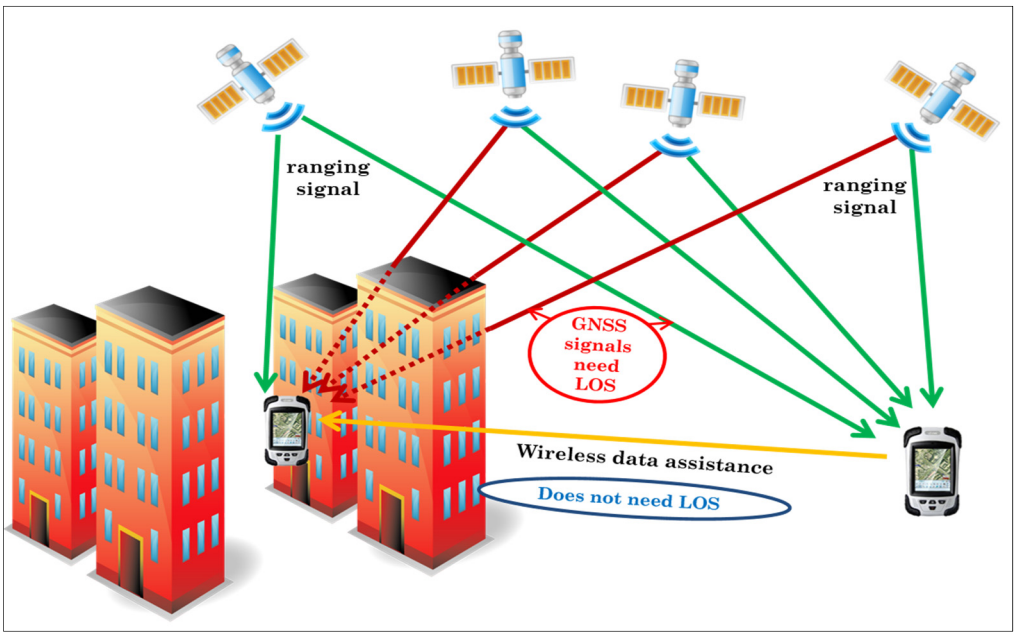

Figure 1.3 Motivation of the developed research work

Despite the various benefits of the "Collective Detection (CD)" approach, this technique also has some drawbacks: the number of candidate points to be scanned is very significant which makes its practical implementation very difficult; the horizontal position error is quite large (acceptability according to the applications) due to the technique of direct positioning (DP); the dependence on several assistance information to help the collaborative acquisition; and the existence of maximum satellites to better benefit from this technique.

1.3 Thesis objectives

The focus of this thesis is on signal processing in GNSS receivers, particularly with weak satellite signals, i.e., lower than their nominal values. High sensitivity acquisition techniques are used to process weak satellites signals. This research project consists of developing new methods and architectures of high sensitivity GNSS receiver while developing new integrated algorithms in a hybrid GNSS receiver capable of operating in deep urban areas using all GNSS signals. The methodology involves the use of the new concept of "Collective Detection (CD)", also called “collaborative acquisition”. The collaborative approach that treats multi-satellite signals all together opens an interesting solution. Many techniques exist in the literature to solve the problems of positioning in urban environments, but we propose the new Collective Detection approach because of its performance as both a Direct Positioning (DP) method, providing a coarse position/clock-bias solution directly from acquisition, and High-Sensitivity (HS) acquisition method, by application of vector detection of all satellites in view. Indeed, the correct combination of the correlation values of several satellites can reduce the required Carrier-to-Noise Ratio (C/N_0) level of the satellite signals which cannot be acquired individually by standard signal processing (acquisition and tracking) but make it possible to use them constructively to a positioning solution. The combination of different GNSS signals can considerably increase the acquisition sensitivity of the receiver.

Despite the various benefits of the CD approach, this technique also has some drawbacks. So, the different proposals in this thesis should address the resolution of important performance metrics for CD techniques applied to process satellite signals in constrained environments:

increase sensitivity (collaboration of some signals with low C/N_0 level), reduce complexity (reducing the number of candidate points, optimizing the computational load, acceleration of computation), maintain good positioning accuracy margin (minimizing the positioning error), and minimize reliance on assistance and help to reduce costs associated with the installation of additional positioning equipment in GNSS denied environments.

The proposals make it possible to improve the sensitivity of a GNSS receiver via the CD approach by using: collaborative acquisition techniques of several satellite signals; better technique for Doppler frequency estimation to obtain finer estimates and more accurate; and longer coherent integration and non-coherent accumulation. In addition, the proposals are able to reduce the complexity of the CD by: optimizing the search process for candidate points in position/clock-bias domain; applying a circular uncertainty area in which the local horizontal search is a polar Rho-theta referential instead of a North-East referential; reducing the search space by varying the resolutions in the uncertainty area of the position and the clock-bias; applying a hybrid scheme of collective and sequential acquisition; and accelerating FFT calculations using bi-dimensional parallel search in code and frequency. Finally, one of the main objectives is to apply the CD technique to Cooperative GNSS Positioning for modern navigation in harsh environments as a practical application of this interesting approach. Related to this idea, the ultimate goal is to propose an architecture of a smart receiver "High Sensitivity Cognitive GNSS Receiver (HS-CGR)" to optimally receive and process weak GNSS signals according to various parameters (C/N_0 level, elevation angle, geometric configuration of the satellites) and the environment where the user is located. Algorithms for optimally exploiting receiver resources by selecting the best satellites or the reference station will be developed based on a smart processing according to the received parameters. The implementation of an intelligent selection of one or more reference stations and the selection of the best satellites in the exploitation of the CD approach must be carried out in order to achieve the objective of increasing the overall sensitivity performance of the receiver and reducing the complexity while maintaining good positioning accuracy.

Thus, in order to achieve the thesis goal, the following objectives are called for:

- Study different acquisition techniques for very degraded GNSS signals in deep urban environments,
- Use the new Collective Detection approach because of its performance as a High Sensitivity (HS) acquisition method, by application of vector detection of all satellites in view.,
- Propose new algorithms and methods to improve receiver sensitivity using all existing GNSS signals,
- Propose new algorithms and methods to reduce receiver complexity in position/clock-bias domain.
- Manage the trade-off between important metrics: increasing sensitivity while reducing complexity and maintaining good accuracy,
- Minimize reliance on assistance information that requires additional hardware architectures,
- Propose new alternatives and new applications of the developed CD approaches such as Cooperative GNSS positioning,
- Develop new algorithms of an intelligent selection of one or more reference stations and the selection of the best satellites in the exploitation of the CD approach,
- Perform a simulation development of the new algorithms proposed using Matlab/Simulink to evaluate their performance,
- Perform tests with real GNSS signals and measurements to evaluate the practical feasibility of the case studies.

To achieve these objectives, the work of this thesis focuses mainly on signal processing at the acquisition and navigation level as presented Figure 1.4 showing the various signal processing steps within a GNSS receiver. To analyze the performance of the developed acquisition algorithms, the sensitivity and the complexity (mean acquisition time) must be taken into account. On the one hand, the sensitivity is defined as the minimum signal power required for a specified reliability of correct acquisition. On the other hand, the mean acquisition time is the average time to detect the signal, meaning to reach successful acquisition.

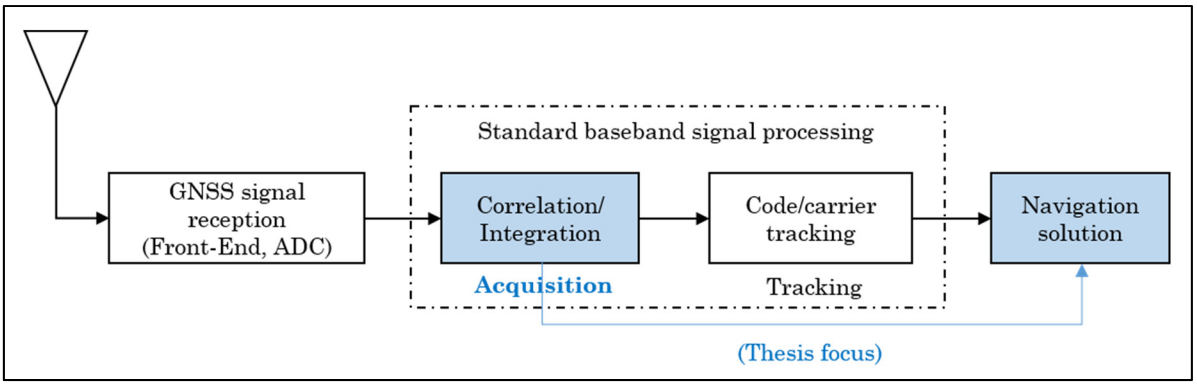

Figure 1.4 General view of the GNSS signal processing

To deepen the exploitation of the CD approach, the idea of collaboration between several receivers will also be developed in the thesis. The basic idea is presented in Figure 1.5.

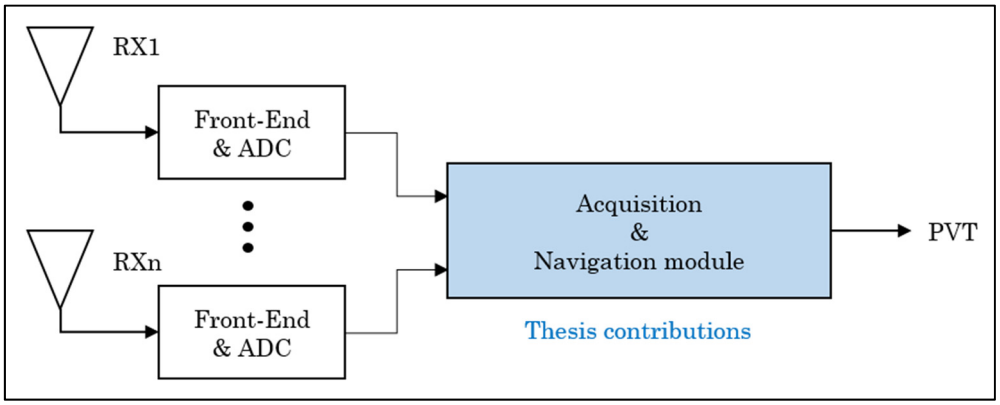

Figure 1.5 Collaborative GNSS positioning using Collective Detection

1.4 Thesis outline

The aim of this thesis is to present different high sensitivity techniques and to develop a new architecture for the future generation of hybrid GNSS receivers of high sensitivity and robustness, capable of using all possible GNSS signals within the new CD approach and which can be used for positioning in deep urban environment.

To properly deal with this problem and to achieve the objectives, this thesis dissertation is organized in six chapters. The main body of the thesis is divided into two major parts. The first part, which consists of chapters CHAPTER 2, CHAPTER 3 and CHAPTER 4, presents detailed studies of techniques for GNSS signals acquisition and the methods for acquiring weak satellite signals as high sensitivity techniques. The second part, which consists of chapters CHAPTER 5 and CHAPTER 6, presents the main contributions to this thesis concerning the new algorithms and architectures proposed to treat weak signals in urban environments. Thus, this dissertation is organized as follows:

CHAPTER 1 specifies the scientific context of the thesis work and its motivations. The objectives and the main contributions in this work are then presented.

CHAPTER 2 presents the signals of the different GNSS constellations and how they are transmitted. It also provides the basic architecture and working principles of GNSS receivers to describe all the steps of processing until obtaining the position of the receiver.

CHAPTER 3 describes the principle of satellite signals acquisition. State-of-the-art of acquisition techniques is developed. Problem formulation of acquisition process and the various methods of acquisition are then presented.

CHAPTER 4 is devoted to techniques for acquiring weak GNSS signals in non-ideal environments. It begins with the investigation of the different sources of signal degradation in urban environments and the architecture of high-sensitivity receivers including coherent and non-coherent integration methods. Then, Assisted GNSS technique and some combined acquisition approaches are presented to which the major contributions in this thesis are focused. The presence of secondary codes in modern GNSS signals as well as optimization techniques for processing them are also provided.

CHAPTER 5 presents in detail the Cooperative or Collective Detection (CD) approach and several contributions to this approach. CD technique can be considered as one of the promising

approaches to meet the requirements of signal processing in GNSS challenging environments. Much of the original contributions in this thesis are developed in this chapter such as the proposal for the use of a mobile reference station in the CD approach, the use of an International GNSS Service (IGS) station applied in CD, the use of a better Doppler frequency estimation technique to improve the performance of the CD approach in terms of sensitivity, the proposal of a hybrid architecture of CD with conventional acquisition technique to improve the performance in terms of complexity.

CHAPTER 6 develops a new concept of Collaborative GNSS positioning using Collective Detection approach. New architecture of high sensitivity cognitive GNSS receiver (HS-CGR) is proposed. Smart approach of CD technique is applied to navigation and GNSS positioning according to certain criteria such as the C/N_0 level, the elevation angle, and the geometric configuration of the visible satellites. The major contributions are made on: the possibility of using the CD approach with two reference stations to help a receiver in difficulty in challenging environments as a cooperative positioning; the exploitation technique of the best satellites by the receiver (reference station); and also the operation of the receiver according to the environment in which it operates to achieve the final objective of this thesis.

The last part of this dissertation discusses the results and accomplishments of this thesis work, draws conclusions and propose some topics for future works.

Figure 1.6 summarizes the structure of this thesis with the different chapters as well as the various corresponding contributions. Indeed, contribution C8 corresponds to CHAPTER 4, C1 – C5 correspond to CHAPTER 5 and C6 – C7 correspond to CHAPTER 6.

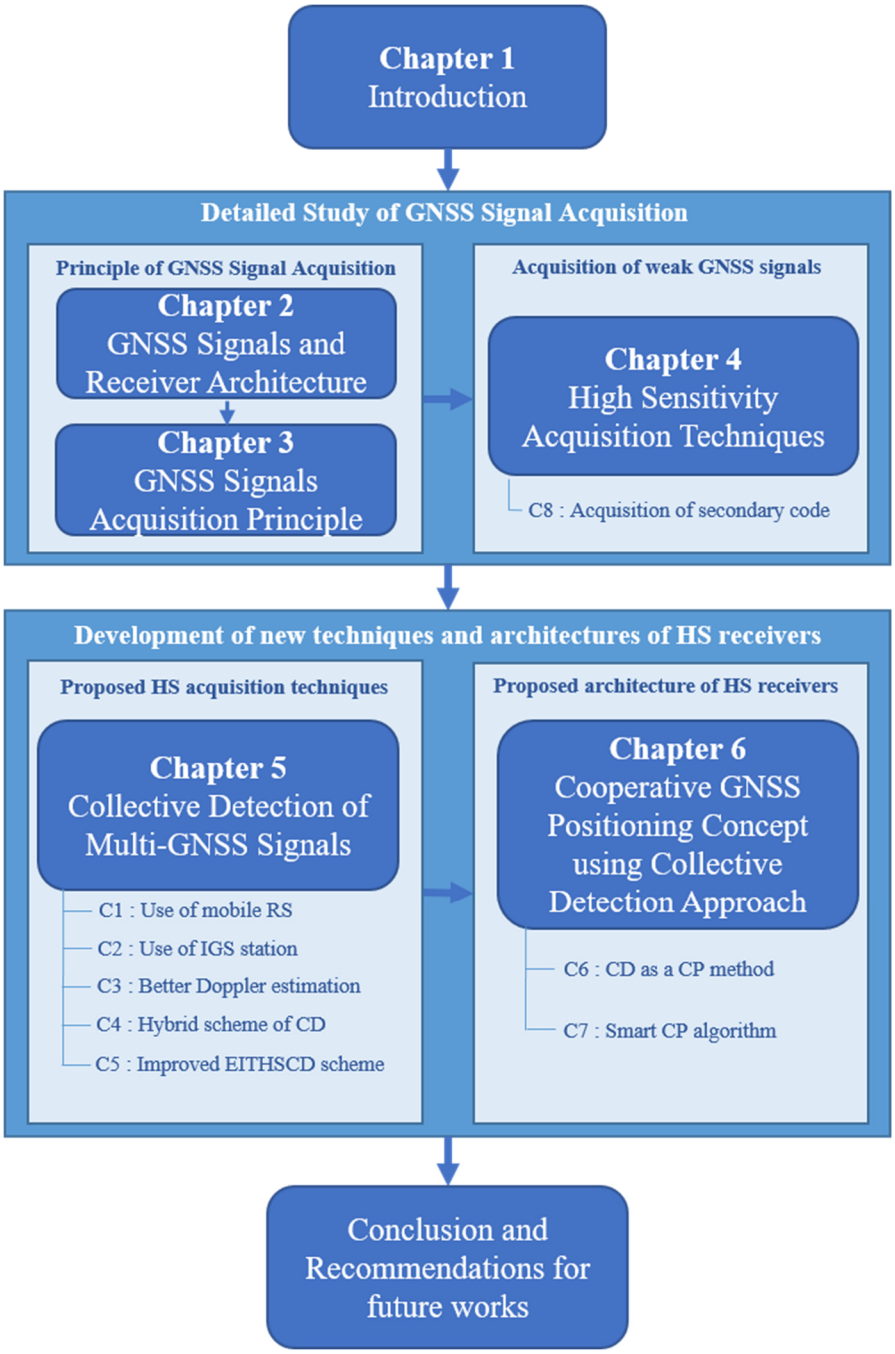

Figure 1.6 Structure of the thesis and overview of contributions

1.5 Publications and thesis contributions

Several articles have been published during those few years of research and development project.

Publications in International Conferences

P1 Andrianarison, M., M. Sahmoudi and R. Jr. Landry. 2015. « Cooperative Detection of Multiple GNSS Satellite Signals in GNSS-Challenged Environments ». In Proceedings of *ION GNSS+ 2015*. (Tampa, Florida, USA), p. 370-380.

P2 Andrianarison, M., M. Sahmoudi and R. Jr. Landry. 2016. « Innovative Techniques for Collective Detection of Multiple GNSS Signals in Challenging Environments ». In Proceedings of *IPIN 2016*. (Alcala de Henares, Madrid, Spain).

P3 Omar, A. B., M. Sahmoudi, P. Esteves, L. Ries, M. Andrianarison and R. Jr. Landry. 2014. « A New Method of Collective Acquisition of Multiple GNSS Satellite Signals in Challenging Environments ». In Proceedings of the 7th ESA Workshop on Satellite Navigation Technologies NAVITEC'2014, ESA/ESTEC, (Noordwijk, The Netherlands).

P4 Leclère, J., M. Andrianarison and R. Jr. Landry. 2017. « Efficient GNSS secondary code correlations for high sensitivity acquisition ». In *European Navigation Conference (ENC) 2017*. (Lausanne, Switzerland, May 9 - 12, 2017).

Publications in International Journals/Magazines

P5 Andrianarison, M., M. Sahmoudi and R. Jr. Landry. 2017. « Efficient and Innovative Techniques for Collective Acquisition of Weak GNSS Signals ». *Journal of Computer and Communications,* vol. 5, n^{o} 06, p. 84-113, https://doi.org/10.4236/jcc.2017.56006.

P6 Andrianarison, M., M. Sahmoudi and R. Jr Landry. 2018. « New Strategy for Collaborative Acquisition of Connected GNSS Receivers in Deep Urban Environments », *Journal of Positioning*, vol. 9, n^{o} 03, p. 23-46., https://doi.org/10.4236/pos.2018.93003.

P7 Andrianarison, M. and R. Jr Landry. 2018. « New Approach of High Sensitivity Techniques using Collective Detection Method with Multiple GNSS Receivers », *Journal of Sensors*, vol. 18, n^{o} 11, p. 3690, https://doi.org/10.3390/s18113690.

The original contributions and some proposals of this thesis are summarized as follow:

- **C1:** In the first contribution, we propose the use of a mobile reference station in the CD approach. In fact, all previous studies about CD are based on the use of a fixed reference station that provides sets of data assistance to the mobile station receiver so that it can estimate roughly its position. In this work, we are not limited to a static reference station and it is possible for a mobile receiver in challenging reception condition to get help from another mobile station or a cooperative user in a good reception situation. The compensation of the mobility effect is proposed. This contribution corresponds to the publication P1 (CHAPTER 5).

- **C2:** In this contribution, we propose the use of a reference station from the IGS network in the CD approach. This work presents an algorithm taking advantage of the availability of data from a well-known reference station. The idea consists in calculating the user mobile position based on reference points that exist somewhere as a network reference point with a known position (IGS service). IGS represents a better alternative in the case that there is no other reference receiver to assist the user receiver. Knowing that there is a network of over 350 continuously operating dual-frequency GPS stations in the world, we do not have the constraint of using our own reference station in areas where there is IGS stations. Given that reference station position and ephemeris can be obtained with IGS service, the MS can estimate its approximate position using the CD approach, even in harsh environments. This contribution corresponds to the publication P1 (CHAPTER 5).

- **C3:** In this contribution, we propose the computation of the CD metrics in function of both the code phase and the Doppler frequency for all satellites in view by applying an efficient technique to estimate the Doppler frequency. In this work, we apply the Spectral Peak Location (SPL) delta-correction technique within the CD algorithm, to improve the accuracy of the Doppler estimation through FFT, and therefore enhancing the correlation energy. Then, the Bi-dimensional Parallel Search acquisition method (BPS) correlation method is proposed, because it is able to effectively reduce the number of computations. This contribution corresponds to the publication P2 (CHAPTER 5)

- **C4:** In this proposal, we present a new method for reducing the complexity of CD without compromising the sensitivity of this method while hybridizing the standard correlation approach with the CD in a multi-stage method with different code delay and position resolution. A new architecture of a hybrid scheme correlation is proposed. It is important to note that I participated in this proposal but it does not correspond to an original personal contribution. This proposal corresponds to the publication P3 (CHAPTER 5).

- **C5:** In this contribution, we present the operation of the CD approach incorporating new methods and architectures to address both the complexity and sensitivity problems. The first method consists of hybridizing the CD approach with some correlation techniques and coupling it with a better technique for Doppler frequency estimate. A new CD scheme with less computational load is proposed in order to accelerate the detection and location process. High sensitivity acquisition techniques using long coherent integration and non-coherent integration are also used in order to improve the performance of the proposed EITHSCD (Efficient and Innovative Techniques for High Sensitivity Collective Detection) algorithm. This contribution corresponds to the publication P5 (CHAPTER 5)

- **C6:** In this contribution, we show how to use the CD approach to deal with the concept of collaborative or cooperative positioning. In collaborative positioning concept, a network of GNSS receivers which are interconnected may collectively receive any available satellite signals, and each receiver can receive measurements from other receivers via a communication link. In this work, we develop new techniques allowing a receiver in deep urban environment to compute its location using the CD approach while overcoming its complexity problem. The idea consists in applying the CD method in the case of two receivers to assist a receiver in a difficult situation. This contribution is a generalization of previous works to the case of more than two cooperative users and corresponds to the publication P6 (CHAPTER 6).

- **C7:** In this contribution, we propose an algorithm that consists in choosing a receiver from several connected receivers to be a reference station to assist the other receivers in

difficulty, as a smart cooperative navigation concept. In this work, new metrics of CD with optimal weighting of visible satellites are exploited. Analyze of optimization method in order to use better satellites in CD process according to some defined parameters (C/N_0 level, elevation angle, and geometric configuration of the visible satellites) is carried out. A new architecture of a new high sensitivity cognitive GNSS receiver is proposed. This work treats the exploitation of the best satellites and the working environment by the receiver in order to achieve a certain level of intelligence and making it capable of operating even in harsh environments like deep urban canyons and indoor. This contribution corresponds to the publication P7 (CHAPTER 6).

- **C8:** In this proposal, we consider the case of the new GNSS signals and propose an optimal method to reduce the complexity of the secondary code correlation by decomposing the local secondary code in two codes and using recursion while performing an exhaustive search. Good results have been obtained for the GPS L5, Galileo E1 and E5 signals. It is important to note that I participated in this proposal but it does not correspond to an original personal contribution. This proposal corresponds to the publication P4 (introduced in CHAPTER 4 and developed in ANNEX V).

CHAPTER 2

GNSS SIGNALS AND RECEIVER ARCHITECTURES

After describing the research problem and the objectives of this thesis in the previous chapter, we will now introduce the various GNSS signals (current and future) and present techniques and methods for processing these signals, in particular the acquisition process. This chapter starts by providing an overview of GNSS systems with a description of the currently available and future planned systems worldwide. Transmission of GNSS signals and the working principle of a GNSS receiver are then presented. Next, the role of acquisition within a GNSS receiver is presented as well as the challenges that are currently faced by acquisition modules, and various existing acquisition methods are described at the end.

2.1 General principle of GNSS

2.1.1 Satellite-based navigation

The positioning system is based on the principle of trilateration. Trilateration is a technique that uses geometry to determine the position of a point in a given space using reference points as shown in Figure 2.1. Trilateration is based only on distances to determine the position of a point contrary to the principle of triangulation which uses both angles and distances from reference points.

If the position of each of the points A, B and C at x and y, i.e. x_A, y_A, x_B, y_B, x_C and y_C, and their respective distance r_A, r_B and r_C with respect to a point P are known, then it is possible to determine the exact position of this point P in the same space. Considering the unknowns x_P and y_P, the three nonlinear equations to solve can be expressed using the Pythagorean theorem as:

$$
\begin{aligned}
r_A &= \sqrt{(x_A - x_P)^2 + (y_A - y_P)^2} \\
r_B &= \sqrt{(x_B - x_P)^2 + (y_B - y_P)^2} \\
r_C &= \sqrt{(x_C - x_P)^2 + (y_C - y_P)^2}
\end{aligned} \tag{2.1}
$$

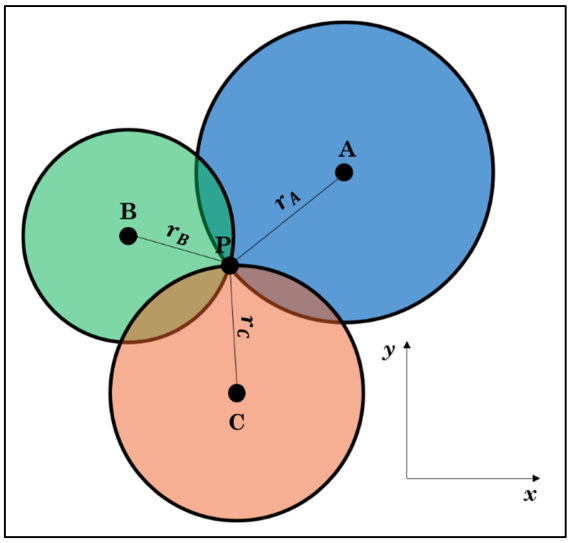

Figure 2.1 Trilateration principle in two-dimension

Trilateration can also be used for three-dimensional positioning. The principle of 3D trilateration is most commonly used for satellite positioning. Therefore, the use of a minimum of three reference points becomes necessary in order to determine the position of a point in space. In addition, at least four reference points must be used in order to remove the ambiguity on the positioning solution due to the time bias caused by the non-synchronization of transmitters clocks and receivers. In reality, the positions of the satellites represented by the points A, B and C are expressed in 3D, which means that the z-axis is added. Consider a fourth reference point D, the four non-linear equations derived from the Pythagorean theorem are:

$$
\begin{aligned}
r_A &= \sqrt{(x_A - x_P)^2 + (y_A - y_P)^2 + (z_A - z_P)^2} \\
r_B &= \sqrt{(x_B - x_P)^2 + (y_B - y_P)^2 + (z_B - z_P)^2} \\
r_C &= \sqrt{(x_C - x_P)^2 + (y_C - y_P)^2 + (z_C - z_P)^2} \\
r_D &= \sqrt{(x_D - x_P)^2 + (y_D - y_P)^2 + (z_D - z_P)^2}
\end{aligned} \tag{2.2}
$$

If (x_k, y_k, z_k) and (x_r, y_r, z_r) represent the satellite and user 3D coordinates respectively, the navigation equation is expressed as (Borre et al., 2007; Kaplan et Hegarty, 2006; Parkinson et Spilker, 1996; Pratap et Enge, 2006; Tsui, 2005):

$$\rho_k = r_k + c \cdot \Delta b = \sqrt{(x_k - x_r)^2 + (y_k - y_r)^2 + (z_k - z_r)^2} + c \cdot \Delta b_r \qquad (2.3)$$

where ρ_k is the pseudorange of the satellite k seen by the user r, r_k represents the geometric range between the user and the satellite, c is the speed of the light in the vacuum and Δb_r is the user clock bias with respect to the GNSS constellation time.

The satellite positioning therefore involves four main unknowns: the position of the user on the three axes and the receiver clock bias. This requires a minimum of four satellites to solve a four-equation system and four unknowns.

The pseudorange can be also calculated by the travel time of the signal from the satellite to the receiver which is the difference of reception and transmission times ($\zeta_k = t_{RX} - t_{TX}$) multiplied by the speed of light:

$$\rho_k = c \cdot \zeta_k \qquad (2.4)$$

Unlike other navigation systems, the satellite-based navigation makes it possible to obtain a three-dimensional position (the altitude of a user can also be determined) from several satellites simultaneously. Each satellite constellation has characteristics specific to the navigation signals that the satellites transmit (navigation data structures, modulation type, data length, etc.).

The measured pseudorange is affected by different sources of errors which are modeled by the following equation (Meng et al., 2004; Tsui, 2005):

$$\rho_k = \rho_{r,k} + \Delta P_k - c \cdot (\Delta b_k - \Delta b_u) + c \cdot (\Delta T_k + \Delta I_k + \upsilon_k + \Delta \upsilon_k) \qquad (2.5)$$

where:

- $\rho_{r,k}$: true value of pseudorange from user to satellite k
- ΔP_k: satellite position error effect on range
- Δb_k: satellite clock error
- Δb_u: user clock bias error
- ΔT_k: tropospheric delay error
- ΔI_k: ionospheric delay error
- υ_k: receiver measurement noise error
- $\Delta \upsilon_k$: relativistic time correction

Errors induced by the tropospheric delay and the ionospheric delay can be corrected using well known models but that caused by the receiver clock bias is impossible with the information received by the receiver. This is why the term corresponding to the receiver clock bias always remains an unknown in the navigation equation.

2.1.2 GNSS systems worldwide

In GNSS system, three segments are necessarily correlated to finally obtain the desired coordinates. First there is the indispensable space segment in orbit, then the traditional components of the user segment on the ground, and finally the control segment which ensures the coherence of the whole.

The space segment consists of a constellation of several satellites in orbit, distributed between several planes, but the number of satellites in service at a specific date may vary depending on the operations decided by the control segment. The constellation is organized by 24 to 30 main satellites according to the system to ensure the global availability of GNSS systems, which implies having at least four satellites visible from the ground all over the world. There is always more satellites in orbit to maintain a complete coverage of these locations even in case of failure.

The control segment is composed of a network of several stations on Earth. It consists of a master control station (MCS) and control stations (CS) that monitor the satellite signals and upload new correction data to satellites. The CS takes care of the maintenance of the satellites as well as their good functioning.

The user segment concerns all the equipment and devices that receive the satellite signals transmitted from the spatial segment. These devices process GNSS signals in order to calculate their position or for specific applications. Since the deployment of the first constellation of satellites by the US military in 1978, the total number of GPS receiver is estimated at 3.6 billion in 2014; smartphones with integrated GPS are the most numerous with 3.08 billion followed by 260 million navigation devices for road applications.

Note that this thesis consists of the GNSS signal processing which is part of the user segment.

Satellite navigation systems continue to evolve, many systems are operational and others are under development. The four great GNSS systems (GPS, GLONASS, Galileo and BeiDou) provide a fully operational global coverage of almost the entire globe. Their specifications are summarized in Table 2.1.

Taking into account these four GNSS systems and also all Augmentation and Regional Navigation Satellite Systems (ANSS and RNSS) as GAGAN, MSAS, EGNOS, WAAS, QZSS and IRNSS, the evolution of the number of satellite constellations is presented in Figure 2.2 [Adapted from (Electric Co., 2014)].

Knowing that GPS (https://www.gps.gov/systems/gps/space/), GLONASS (https://www.glonass-iac.ru/en/guide/) and Galileo (https://www.gsa.europa.eu/) are already operational, it can be noted that BeiDou (http://en.chinabeidou.gov.cn/) is in development and still growing until 2021.

Table 2.1 Summary of GNSS constellations

System	GPS	GLONASS	Galileo	BeiDou
Number of satellites (in-orbit)	31 (24)	28 (24)	24 (18)	27 MEO (20) 3 IGSO 5 GEO
Spare satellites	8 active	3 active	3 planned	3; 0; 0 planned
Status	Fully operational	Fully operational	Partially operational	22 satellites operational
Orbit	6 MEO	3 MEO	3 MEO	3 MEO 3 IGSO 1 GEO
Orbital altitude [km]	20180	19130	23222	23150 35816 35816
Orbital inclination [°]	55	64.8	56	55 55 0
Revolution period	11h 58mn	11h 16mn	14h 07mn	12h 38mn
Reference geodesic system	WGS-84	PZ-90.02	GTRF	CGCS2000
Reference time system	UTC + 16s	UTC + 3h	UTC + 16s	UTC ± 100ns

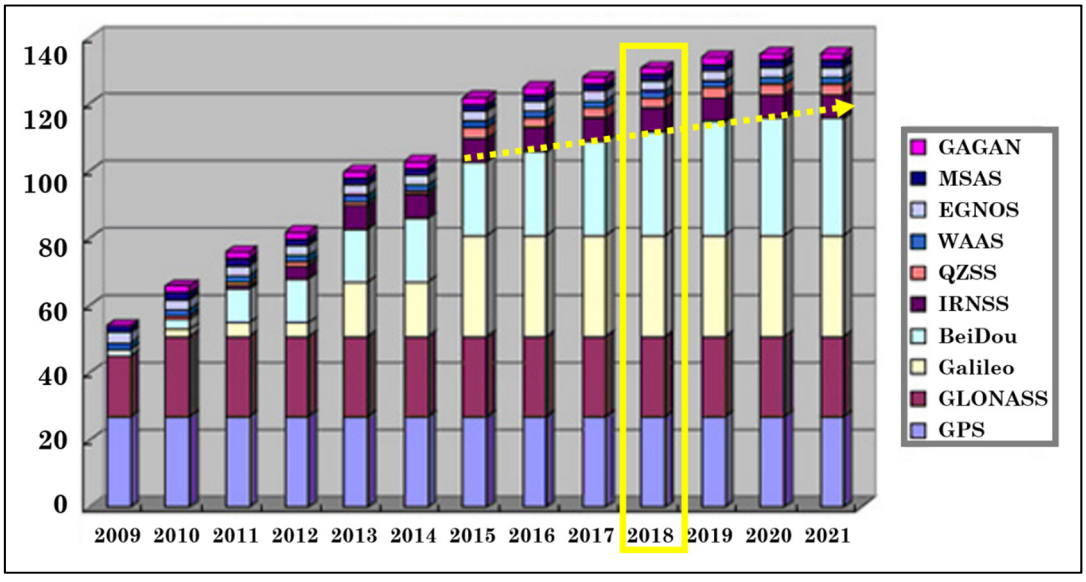

Figure 2.2 Evolution of number of satellites in multi-GNSS systems

The most widely used system is the American GPS, specifically the L1 C/A signal. All existing GNSS signals are summarized in the Figure 2.3 with their respective frequencies [Adapted from (NovAtel, 2017)].

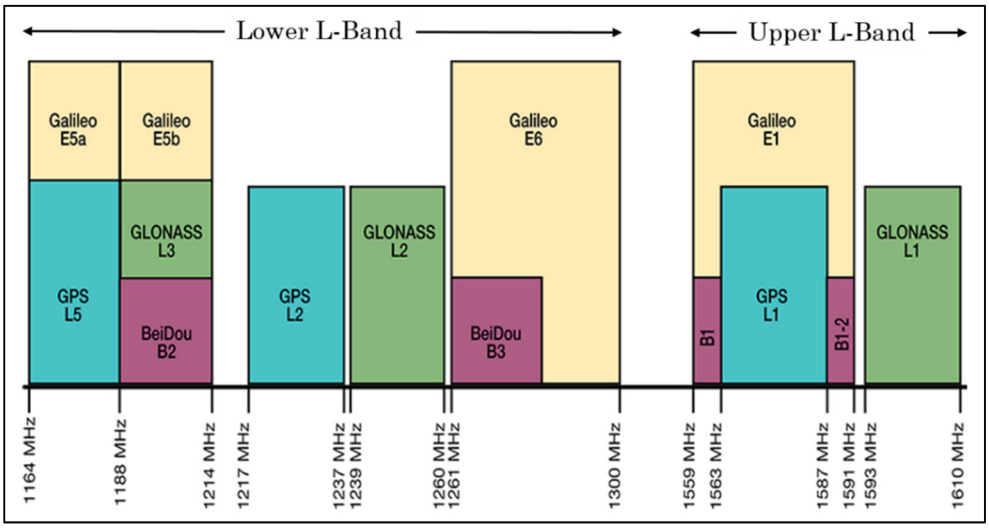

Figure 2.3 GNSS navigational frequency bands

The work carried out in this thesis focuses only on GPS L1 C/A and L5 signals, and Galileo E1 and E5 signals which are transmitted in the L-band, especially in L1/E1 band (GPS L1 C/A and Galileo E1 OS signals) and in L5/E5 band (GPS L5 and Galileo E5a and E5b signals). These signals are shown in the framed in dotted lines in Figure 2.4 which represents the different frequency bands used by the different systems. [Adapted from (Datta, 2016)].

By using different GNSS signals, GNSS receivers are able to improve the main weaknesses of navigation systems such as availability (increasing the number of visible satellites to determine the receiver position), integrity (more reliable navigation messages), accuracy (several frequencies allowing better correction of certain errors) and electromagnetic vulnerability (use of different modulation techniques).

GNSS signals are heterogeneous because of some differences in principles on signal components, spectra, modulation type, navigation messages, time references, etc. Each system has its advantages and limitations depending on the application and the environment.

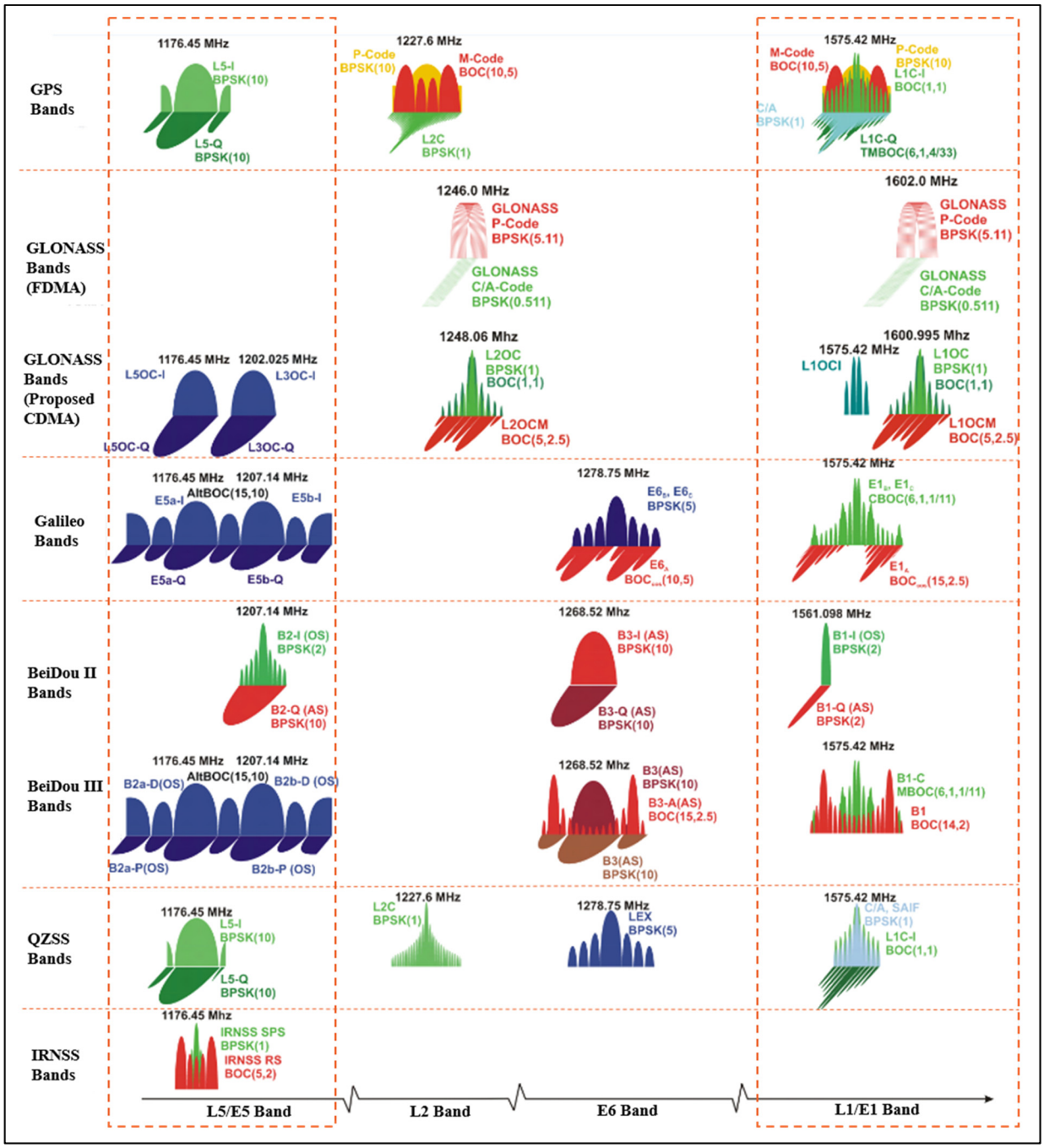

Figure 2.4 Different GNSS frequency bands used by different systems

Moreover, it is really interesting to make a combined use of the three functional systems (GPS/Galileo/Glonass) making the GNSS receivers more robust and more accurate than the current receivers. Thus, the combined use of GNSS signals requires interoperability between the different systems.

2.1.3 GNSS signals structure

Some methods exist to multiplex multiple signals within the same communication channel. The most known multiple access technique is probably the Frequency Division Multiple Access (FDMA), which consists in subdividing a channel into several different frequency bands. There is also the Time Division Multiple Access (TDMA), where the strategy consists in temporally segmenting access to a communication channel. While in both cases the communication channel must be split, another method, called Code Division Multiple Access (CDMA), allows several transmitters to communicate simultaneously over the same frequency bands (Gerakoulis, 2001).

Before being transmitted, CDMA signals are generally modulated by a sinusoidal carrier. The two most commonly used modulations are the Binary Phase Shift Keying (BPSK) and the Frequency Shift Keying (FSK). BPSK modulation is generally preferred because it is easier to implement. A simple multiplication of the CDMA signal by the carrier is then required, hence the name of CDMA with spread spectrum by direct sequence (DS-CDMA - Direct Sequence CDMA). The FSK modulation produces a spectrum spread signal by frequency hopping (FH-CDMA - Frequency Hopping CDMA). DS-CDMA modulation technique is used for GPS and Galileo systems which are used in this thesis (Galileo-OS-SIS-ICD, 2016; ICD-GPS-200, 2000). CDMA signals also offer some robustness against interferences and jammers. For more details about CDMA principles, please refer to (Bruno, 2007).

Signals transmitted from satellites to Earth have three essential components: a carrier, a spreading code and navigation data or navigation message. More details on GNSS signals structure are presented in (Avila-Rodriguez et al., 2008; Subirana, Zornoza et Hernandez-Pajares, 2014).

Table 2.2 Summary of frequency characteristics of GNSS signals

GNSS	Access technique	Band	Center frequency [MHz]	Bandwidth [MHz]
GPS	CDMA	L1	1575.420	20.460
		L2	1227.600	20.460
		L5	1176.450	24.000
Galileo	CDMA	E1	1575.420	24.552
		E5-A	1176.450	25.575
		E5-B	1207.140	25.575
		E6	1278.750	40.920
Glonass	FDMA	L1	1603.688	11.813
		L2	1247.313	9.188
	CDMA	L1	1575.420	8.190
		L3	1211.261	10.035
		L5	1176.450	16.380
BeiDou	CDMA	B1	1561.098	4.092
		B1-BOC	1575.420	16.368
		B2	1207.140	24.000
		B2-BOC	1207.140	30.690
		B3	1268.52	24.000
		B3-BOC	1268.52	35.805
		L5	1176.45	24.000

The carrier is a continuous radio frequency sinusoidal signal whose frequency is the central L-band (band between 1 and 2 GHz). It is denoted f_L. For example, f_L = 1575.42 MHz for GPS L1 C/A signal. Table 2.2 summarizes the current and future signals of each system GNSS with their carrier frequency.

The spreading code, denoted c_n, consists of a finite known long binary sequence of +1 and -1 transmitted at high frequency rate and specific to each satellite. The spreading codes are rather based on pseudo-random sequences called Pseudo-Random Noise (PRN) or PRN codes due to their noise-like characteristics (very low cross-correlation with other signals, a high autocorrelation only in 0 and lower elsewhere). Spreading codes are repeated at regular intervals and each signal uses a unique spreading code that is orthogonal to others. PRN codes are said to be pseudo-orthogonal since some cross-correlation noise remains between the channels (Gerakoulis, 2001). So sufficiently long spreading codes are used to minimize this effect. A very large number of different codes can be produced by polynomial generators, but generally only those with the lowest levels of cross-correlation are retained. PRN codes allow the receiver to determine the transmitting satellite and the signal travel time between the satellite and the receiver which makes it possible to have precise ranging and to let the satellites to broadcast signals at the same frequency. The value of a PRN code is expressed in "chip" instead of "bit" to assert that they do not carry information.

The navigation message, transmitted at low rate, is a binary-coded message of +1 or -1 which includes some useful information in particular the ephemerides (orbital information) allowing the calculation of the position of the satellites, as well as information on their internal clock (bias, drift and acceleration parameters), almanac (reduced accuracy data set of the constellation satellites), satellite health status, coordinated universal time conversion, ionospheric information, etc. The navigation message, denoted d, also includes the necessary corrections to the frequency measured in orbit. The duration of one data bit T_d is a multiple of one PRN code period duration T_c which itself contains N_c chips. (ICD-GPS-200, 2000).

GPS L1 C/A signals

The L1 C/A GPS signals are based on DS-CDMA modulation, a combination of CDMA techniques for multiple access and BPSK for carrier modulation. A clock with a frequency of 10.23 MHz is used on board the GPS satellites in order to synchronize the data and the spreading code. The rhythm of the data is 50 bps (low rate) and that of the spreading code is

1.023 Mcps (high rate). The data bits are thus combined with the spreading code (using a modulo-2 sum) before being multiplied by a carrier whose nominal frequency is 1575.42 MHz. The BPSK signal formed is finally amplified to a minimum power of 33 W and limited to a bandwidth of 20.46 MHz before being transmitted to the ground (Kaplan et Hegarty, 2006). Given the long distance of the satellites from the users, GPS signals have only about -160 dBW of power when received on the ground. Combined with ambient thermal noise, this corresponds to an SNR of the order of -30 dB (ICD-GPS-200, 2000).

The spreading codes used for GPS L1 C/A are Gold codes of 1023 chips length and repeated every millisecond (37 different Gold codes) (Gold, 1967). Since the data bits have a period of 20 ms, there are thus 20 repetitions of the C/A code, or epochs, between each of the data bits. In terms of data, they are segmented into frames, subframes, and words: each frame contains five subframes, which in turn contain ten 30-bit words (i.e. 300 bits per subframe). Each word is then composed of 24 bits of data and 6 bits of parity. A complete navigation message has 25 frames, representing 37 500 bits of data transferred in 12.5 minutes.

The illustration of the code PRN $c(t)$ and navigation data $d(t)$ synchronization for GPS L1 C/A signal is shown in Figure 2.5.

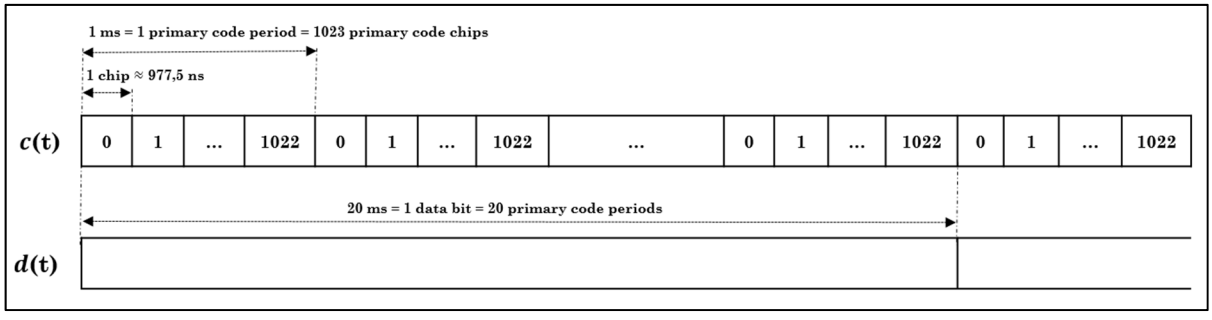

Figure 2.5 Synchronization of the data and PRN code for GPS L1 C/A signal

Thus, in the case of GPS L1 C/A the transmitted signal is represented in Figure 2.6.

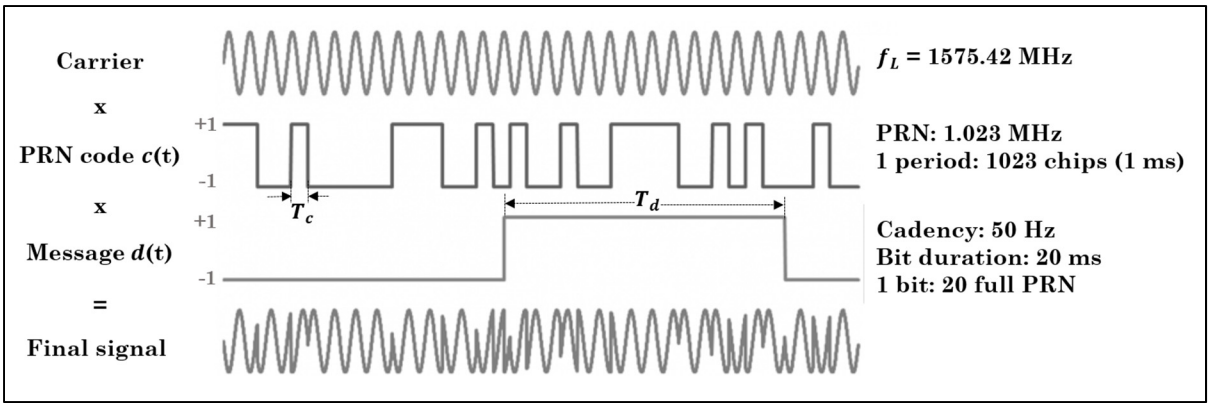

Figure 2.6 Structure of GPS L1 C/A signal (figure is not scale)

This transmitted signal by satellite k can be expressed as:

$$s_{e,k}(t) = \sqrt{2P_e}\, c_k(t)\, d_k(t) \cos(2\pi f_{L1} t + \varphi_{e,k}) \tag{2.6}$$

where the term "e" indicates emitted or transmitted signal, t is the time, P_e is the signal power, $c_k(t)$ is the PRN code, $d_k(t)$ is the navigation data, f_{L1} is the L1 carrier frequency, and $\varphi_{e,k}$ is the phase of the received carrier.

Modern signals

Some of the modernized GNSS signals use other types of modulations than the BPSK used by the GPS L1 C/A. The most used is the Binary Offset Carrier (BOC) modulation which is the result of the multiplication of the PRN code with a square sub-carrier which is mathematically obtained by taking the sign of a sine waveform of frequency. Based on BOC modulations, different modulations are implemented in modernized satellite signals: Composite BOC (CBOC) for the Galileo E1 OS signal, Time Multiplexed BOC (TMBOC) for the GPS L1C signal, and Alternative BOC (AltBOC) for the Galileo E5 signals (Betz, 2015).

Modern signals have introduced some new components such as a secondary code, a sub-carrier and a pilot channel (Turunen, 2007). The secondary code is a binary code repeating

continuously transmitted at lower chipping rate (1 kchip/s at most). Each chip of the secondary code multiplies one period of the primary code as shown in Figure 2.7. The product of the primary and secondary codes is then usually called the tiered code (Betz, 2015). The secondary code helps the synchronization with the data bits. The sub-carrier leads to the new BOC modulation and modifies the signals spectrum. Finally, the pilot channel component includes only the spreading code and the carrier. The data is excluded from the pilot channel that provides some advantages for the detection of the satellite signal. The data channel and pilot channel are usually denoted I channel (In-phase) and Q channel (Quadrature-phase) respectively.

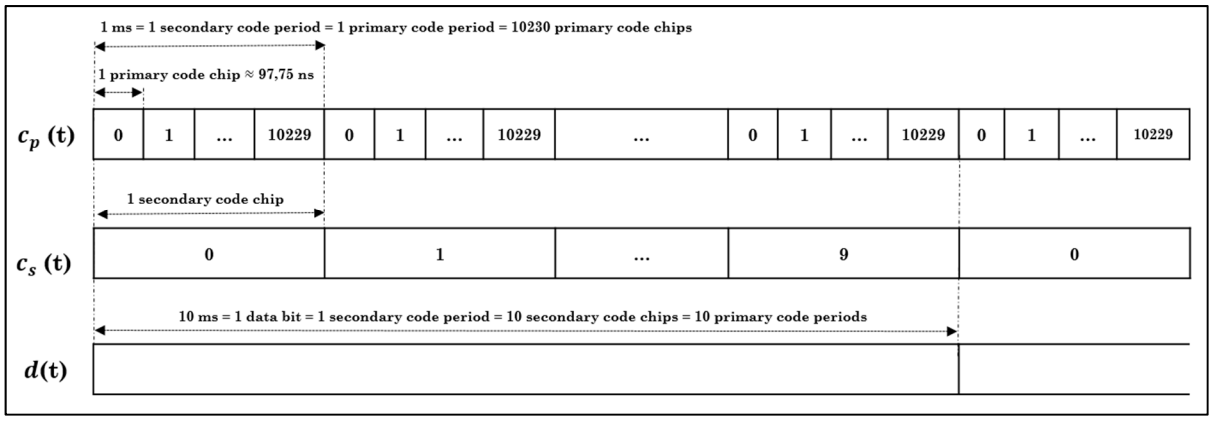

Figure 2.7 Synchronization of the data and PRN code for GPS L5 signal

For GPS L5, Galileo E5a and E5b signals, the data and pilot channels are in quadrature and the modulation is a Quadrature Phase Shift Keying (QPSK) while each channel is BPSK modulated.

Galileo offers users a total of ten signals including three free of charge. In fact, five services are planned to be offered: a freely accessible Open Service (OS) suitable for mass-market applications, a Commercial Service (CS) allowing development of applications for professional or commercial use, a Safety-of-Life service (SoL) for contribution to integrity monitoring, a public encrypted service (PRS) restricted to government-authorized users intended for security and strategic infrastructure, and a Search And Rescue service (SAR) to

forward the distress signals to a rescue coordination center by detecting the transmitted emergency signals. The OS service is distributed over the signals E1, E5a and E5b. The signal E1 employs CBOC modulation and is transmitted on the same frequency as the GPS signal L1 C/A at 1575.42 MHz. E5a and E5b signals are derived from a single signal E5, exploiting AltBOC modulation, thereby enabling E5a and E5b to be processed as two QPSK signals. The Galileo E1 OS signals use memory codes, i.e. they have to be stored in receiver memory and cannot be obtained from a code generator algorithm. For Galileo E1 OS, 100 codes of length 4092 have been defined (Galileo OS-SIS-ICD, 2016).

The characteristics of the signals exploited in this thesis (GPS L1 C/A, GPS L5, Galileo E1 OS and Galileo E5) are summarized in Table 2.3.

Table 2.3 Features of some GNSS signals used in this thesis

Signal		**Carrier frequency [MHz]**	**Modulation**	**Spreading code**			
				Type	**T_c [ms]**	**N_c [chip]**	**Data rate [bit/s]**
GPS	L1	1575.42	BPSK	Gold code	1	1023	50
	L5	1176.45	QPSK	Combination and short-cycling of M-sequence	1	10203	100
Galileo	E1 OS	1575.42	CBOC	Memory code	4	4092	250
	E5a	1176.45	QPSK	M-sequence	1	10230	50
	E5b	1207.14	QPSK	M-sequence	1	10230	250

Table 2.4 shows the properties of primary and secondary codes for each signal.

So, if the data and pilot channels are in quadrature, the emitted composite GNSS signal by satellite k is defined as:

$$s_{e,k}(t) = \sqrt{2P_e}\, c_{p,i,k}(t)\, c_{s,i,k}(t)\, sc_{i,k}(t)\, d_k(t) \cos\left(2\pi f_L t + \varphi_{e,k}\right) + \sqrt{2P_e}\, c_{p,q,k}(t)\, c_{s,q,k}(t)\, sc_{q,k}(t)\, \sin\left(2\pi f_L t + \varphi_{e,k}\right) \quad (2.7)$$

where :

- P_e is the power of the emitted signal on each channel (assuming the same power on both channels),
- "p" and "s" indicate respectively "primary" and "secondary" terms,
- "i" and "q" indicate respectively "in-phase" and "quadrature" components,
- $c_{p,i,k}(t)$ and $c_{p,q,k}(t)$ are the primary codes of the data and pilot channels,
- $c_{s,i,k}(t)$ and $c_{s,q,k}(t)$ are the secondary codes of the data and pilot channels,
- $sc_{i,k}(t)$ and $sc_{q,k}(t)$ are the sub-carriers of the data and pilot channels modulating the spreading codes.

Table 2.4 Primary and secondary codes properties of some GPS and Galileo signals

Signal			**Primary code**			**Secondary code**		
			chipping rate [Mchip/s]	**length**		**chipping rate [chip/s]**	**length**	
				[chip]	**[ms]**		**[chip]**	**[ms]**
GPS	L1 C/A		1.023	1023	1	-	-	-
	L5	I	10.23	10230	1	1000	10	10
		Q					20	20
Galileo	E1 OS		1.023	4092	4	250	25	100
	E5a	I	10.23	10230	1	1000	20	20
		Q					100	100
	E5b	I	10.23	10230	1	1000	4	4
		Q					100	100

2.2 Transmission of GNSS signals

Measurements from GNSS signals are contaminated by different sources of error. In general, these errors can come either from the satellites or from the receiver, or can be caused by the propagation of the signals. Moreover, the geometry of the satellites is also an important factor that can affect the accuracy of the navigation solution calculated by a GNSS receiver. From the satellites to the earth, through the atmospheric layers (troposphere and ionosphere), the signals are affected by several elements of errors. Here are some important effects to consider when transmitting satellite signals.

2.2.1 Free space loss

Despite the transmission of the satellite signals with enough power level, the signals arrive at the receivers with low power because of the long distance of propagation traversed. This is caused by the free space loss. For example, GPS satellites signals are emitted at a power level of 13.4 dBW. With an effective gain of 13.4 dB the radiated power rises to 26.8 dBW. But because of the great distance and the free space loss the signal received at the receiver antenna is ~ -160 dBW for L1 band. This loss can be 10 dB to 182.4 dB for a satellite at the zenith (20000 km away) and 184.7 dB for a satellite on the horizon (26000 km away) (Macgougan, 2003).

The free space loss is defined as:

$$L_f = \frac{P_r}{P_e} \tag{2.8}$$

where P_r is the received power and P_e is the emitted power.

The received power is expressed as:

$$P_r = \frac{P_e A_r}{(4\pi d^2)} \tag{2.9}$$

where d represents the radial distance between the satellite and the receiver antenna and A_r is the antenna aperture defined as:

$$A_r = \frac{\lambda^2}{(4\pi)} \tag{2.10}$$

where λ is the wavelength of the carrier (approximately 19 cm for L1) as:

$$\lambda = \frac{c}{f} \tag{2.11}$$

where c is the speed of the light in m/s and f is the carrier frequency in Hz.

Thus, in the logarithmic scale, the free space loss is expressed as:

$$L_f(dB) = 10\log_{10}\left(\frac{P_r}{P_e}\right) = 10\log_{10}\left(\frac{\lambda^2}{(4\pi d)^2}\right) = 20\log_{10}\left(\frac{c}{4\pi f d}\right) \tag{2.12}$$

For GPS L1 C/A signal (f = 1575.42 MHz and d = 24092 km), the signal budget is summarized in Table 2.5.

Based on Equation 2.12, the minimum power received for the GPS L5, Galileo E1, Galileo E5a and Galileo E5b signals are presented in the Table 2.6.

Note that the values of the received power for GPS L5 correspond to the signals of block III GPS satellites. The power is -127.9 dBm for block IIF satellites.

Table 2.5 Power of received GPS L1 C/A signal

Parameters	Values
Satellite antenna power	13.4 dBW
Satellite antenna gain	13.4 dBW
Free space loss	-184.4 dB
Atmospheric attenuation	-2.0 dB
Depolarization loss	-3.4 dB
User antenna gain	3.0 dB
User receiver power	-160.0 dB

Table 2.6 Minimum received power at the receiver antenna

Signal			Received power [dBm]
GPS	L5	I	-127
		Q	-127
Galileo	E1 OS	D	-130
		P	-130
	E5a	I	-128
		Q	-128
	E5b	I	-128
		Q	-128

In harsh environments, particularly in indoor, the satellites signals are highly attenuated and the power can drop to -160 dBm because of the presence of obstacles (van Diggelen, 2009). Knowing that the antenna of the receiver also plays an important role in this, the received signal can drop to -170 dBm if the receiver has a poor performance antenna. Thus, to compensate for all these losses, signal processing at the receiver is really essential. The requirement in signal processing is proportional to the level of power of the received signal. This is why the work of this thesis.

2.2.2 Doppler effect

Positioning satellites, such as GPS satellites for example, generally travel at high speed along an average orbit (MEO). This has the consequence of introducing a significant Doppler effect on the signals received. In fact, the Doppler effect characterizes the frequency shift of an electromagnetic wave between transmission and reception which occurs when a relative velocity exists between the transmitter and the receiver. Indeed, the Doppler shift of a GNSS signal is defined as the difference between the carrier frequency received by the receiver and that transmitted by a satellite. Since the Doppler shift is directly proportional to the relative speed between a satellite and a receiver (the relativistic effects are neglected here), it is therefore possible to measure this shift in order to determine the speed of the movement of a user:

$$\Delta f = -\frac{\dot{\rho}}{\lambda} = -\frac{f\dot{\rho}}{c} \tag{2.13}$$

where:

- Δf is the Doppler shift
- $\dot{\rho}$ is the relative velocity between a satellite and the receiver
- λ is the carrier wavelength
- f is the carrier frequency (without Doppler effect)
- c is the speed of light

The relative speed between the receiver and a satellite can also be expressed in terms of variation of the pseudorange measurement. Indeed, the pseudorange change of a satellite is defined as the projection of the relative velocity between the receiver and the satellite in line of sight to the satellite. Based on this definition, the variation of the pseudorange measurement can be obtained such that:

$$\dot{\rho} = \vec{e}_k(\vec{v}_k - \vec{v}_r) = -\vec{e}_k(\vec{v}_r - \vec{v}_k) = -\Delta f \cdot \lambda \tag{2.14}$$

where

- $\vec{v}_k$ is speed vector of the satellite k
- $\vec{v}_r$ is the GNSS receiver speed vector
- $\vec{e}_k$ is the unit vector oriented along the line of sight to the satellite k, and defined as

$$\vec{e}_k = \frac{[(x_k - x_r) \quad (y_k - y_r) \quad (z_k - z_r)]^T}{\sqrt{(x_k - x_r)^2 + (y_k - y_r)^2 + (z_k - z_r)^2}} \tag{2.15}$$

The Doppler frequency which affects the received signal is composed of three components: the satellite's Doppler due to the movement of the satellite, the user's Doppler due to the user motion, and the oscillator's Doppler-like effect due to the oscillator deviation. Table 2.7 shows the Doppler shift experienced by a typical GNSS receiver due to the major contributing sources of frequency shift (Monnerat et al., 2004).

Table 2.7 Main frequency offset sources for GNSS receivers

Signal	**Value [Hz]**
Satellite motion	± 4880
Uncompensated user	± 190
Oscillator deviation	± 440
Total	± 5510

GPS satellites are moving at a speed about 3874 m/s and the maximum relative speed between a GPS satellite and a stationary receiver on the ground, i.e. maximum Doppler velocity, is approximately 929 m/s (Tsui, 2005). For Galileo, the maximum relative speed between a satellite and a static receiver on Earth is 789.4 m/s. The Doppler effect may be significant for received signal even for a stationary receiver on the ground. There are carrier Doppler and code Doppler in Doppler frequency shift caused by the satellite motion. For the GPS L1 C/A, the Doppler frequency shift on C/A code is quite small because it is emitted at low rate (1.023

MHz) which is lower 1540 times than the carrier frequency (1575.42 MHz/1.023 MHz). The Doppler effect then differs for each GNSS system depending on the altitude of the satellites since this impacts the relative speed between the satellite and the receiver. The values of maximum Doppler shift for GPS and Galileo signals are shown in Table 2.8.

Table 2.8 Maximum Doppler shift for a stationary receiver

Signal		**Carrier Doppler [kHz]**	**Code Doppler [Hz]**
GPS	L1	4.88	3.17
	L5	3.64	31.7
Galileo	E1	4.15	2.69
	E5a	3.10	26.9
	E5b	3.18	26.9

For a static receiver, the maximum Doppler frequency shift is around ±5 kHz. This value is considered in the design of a GPS receiver equivalent to a low speed vehicle. If a high-speed vehicle is considered, it is better to assume a Doppler frequency value of ±10 kHz. These values determine the search area according to frequencies in the acquisition process (Tsui, 2005). According to (van Diggelen, 2009), if the receiver is moving, this affects the observed GPS Doppler by up to 1.46 Hz for each 1 km/h of speed. The Doppler effect then depends on the speed of the receiver. For GPS L1 C/A, the Doppler effect caused by the mobility of the receiver can be resumed in Table 2.9.

Table 2.9 Carrier Doppler due to the user motion

Dynamics	**Example of application**	**Velocity [km/h]**	**Doppler shift [Hz]**
Low dynamics	Pedestrian, robot	5	7.3
Medium dynamics	Car in urban city, drone	50	73
High dynamics	Car in a highway	120	175.2

2.2.3 Rate of change of the Doppler frequency

According to (Tsui, 2005), the Doppler effect due to the relative velocity between a satellite and the receiver is changing over the time. To find the Doppler frequency rate of change, we can estimate either the average rate of change or the maximum rate of change of the Doppler frequency. For example for a stationary receiver at L1 frequency band, the average rate of change is about 0.54 Hz/s and the maximum rate of change of the carrier Doppler shift is about 0.936 Hz/s. These values depend on the latitude of the receiver.

In reality, the Doppler change rate is not constant over time period and can be much higher if the user is moving. According to (Tsui, 2005), a receiver that moves with an acceleration of 9.8 m/s^2 toward a satellite can cause a Doppler rate of change about 51.5 Hz/s. For example, an aircraft flying with a high acceleration of 68.7 m/s^2, the rate of change of the Doppler frequency is close to 360 Hz/s. Despite the fact that the acceleration of the receiver is the dominant factor in the rate of change caused by the motions of the satellite and the receiver, the rate of change value of the carrier Doppler shift is different according to the orbit. In fact, for L1 C/A signal (Dion, Calmettes et Boutillon, 2007), it can reach up at 62 Hz/s for a receiver on low orbit, 14 Hz/s on medium orbit and 5.5 Hz/s on geostationary orbit (Capuano, Botteron et Farine, 2013).

Note that the change rate of the code Doppler shift is not so significant to the carrier Doppler shift. For example, if the rate of change for the L1 C/A signal is 0.94 Hz/s for the carrier Doppler, it corresponds to 0.61 mHz/s for the code Doppler (Leclère, 2014).

2.2.4 Error sources in GNSS

Apart from the attenuation and Doppler effect, there are other sources that deteriorate the positioning solution of the GNSS system also exist.

2.2.4.1 Satellite and Receiver Clock errors

Despite the use of high-precision atomic clocks (cesium and rubidium clocks), the clock on board the satellites is not perfect and its instability can affect the pseudorange measurements calculated by the GNSS receivers. The error on the time measurement can reach up to 17 ns which corresponds to approximately 5.1 m of pseudorange (El-Rabbany, 2002). However, the performance of these clocks is carefully observed by the ground stations of the control segment and the information on the clock bias is calculated and transmitted to the users within the navigation message. The error caused by the instability of the satellite clock can therefore be directly corrected without any additional calculation, but this is not the case for the GNSS receiver clock error which must instead be estimated inside the navigation filter.

The clock used within the commercial GNSS receivers generally consists of a low cost quartz clock whose error is much larger than the one on the satellite clock. Moreover, this error is generally unstable and cannot generally be considered as constant or predicted. Thus, the clock bias and clock drift parameters must be constantly estimated within the navigation filter of the GNSS receiver in order to achieve a certain level of accuracy. These parameters can be estimated inside the Kalman filter of the GNSS receiver.

2.2.4.2 Tropospheric delays

The troposphere is the lowest part of the atmosphere. It rises up to 7 km at the poles whereas it can reach up to 20 km of altitude at the equator. The troposphere constitutes a problematic gaseous layer for the propagation of satellite signals. In fact, it is mainly composed of dry gases and water vapor, which causes the phenomenon of refraction of the GPS signals, thus creating a propagation delay which directly affects the pseudorange measurement. According to (Bruno, 2007), this delay is generally in the order of 2.5 m (1σ[1]) at the zenith and 25 m (1σ) at

[1] 1σ means the error at standard deviation and represents the confidence level attributed to this error. Assuming normal and centered distributions, 1σ represents a probability of 68.3% in one-dimensional distributions.

5° elevation for a receiver located at sea level. There are some models in the literature that considerably reduce the effect of this atmospheric layer on the propagation of satellites signals, such as (Dodson et al., 2001) that developed the tropospheric model of EGNOS. For further details on the definition of the RMS[2] (Root Mean Square) errors (1σ, 2σ, 3σ), see ANNEX IV.

2.2.4.3 Ionospheric delays

The ionosphere is a part of the atmosphere that extends from about 70 km to 1000 km above the surface of the Earth. The ionospheric delays are mainly caused by the fact that the solar and cosmic radiation present in this atmospheric layer cause ionization of gaseous atoms and molecules, thus generating free electrons that can interfere with the satellite signal. The propagation of GNSS signals through the ionosphere is one of the main sources of error on the pseudorange measurement. According to (Bruno, 2007), this error can reach up to 15 m (1σ) at the zenith and up to 50 m (1σ) for satellites with a low degree of elevation. And the use of a 10° elevation mask would reduce the effect of this error to about 10 m (1σ). The intensity of this phenomenon depends on several factors (time, season, geographic location, solar and geomagnetic activities, etc.) which makes this error very difficult to predict. Some methods exist to reduce this effect as proposed by (Bruno, 2007) for the use of a correction model whose parameters are broadcast in the navigation message.

2.2.4.4 Effect of geometry of satellites on positioning accuracy

As we saw in paragraph 2.1.1, the position of a GNSS receiver is calculated using the principle of trilateration. In reality, random errors are present on the distance measurements and consequently the position obtained is no longer an exact point as shown in Figure 2.1 but rather a statistical region, a region of probability represented by the hatched region in Figure 2.8.

---

[2] RMS represents the square root of the average of the squared error. RMS measurement is an average but assuming that the error follows a normal distribution and corresponds to the percentile 68.3% in one-dimensional distributions.

Each satellite is surrounded by an uncertainty area which represents the total equivalent error that may affect the pseudorange measurements called User Equivalent Range Error (UERE).

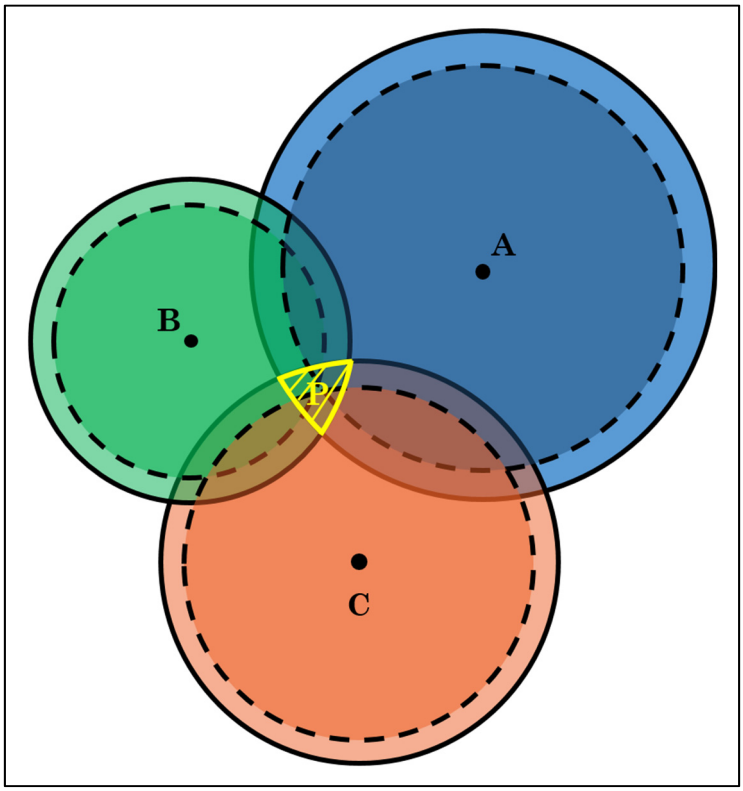

Figure 2.8 Effect of the geometry of the satellites and uncertainties on trilateration

The precision of a navigation solution is directly influenced by the spatial arrangement of the satellites in visibility. For a conventional navigation solution with four satellites, the satellites offering the best spatial distribution will be selected from the satellites in view. In fact, the geometrical position of the satellites used in the calculation of the receiver position directly influences the surface area of the statistical region representing the uncertainty on the calculated position P. Thus, for a good geometry of the satellites, i.e. a uniform spatial distribution, a relatively small region of uncertainty will be obtained at the navigation solution. However, this region of uncertainty will tend to increase as the geometry of the satellites deteriorates.

The geometry of satellites is characterized by a series of indices, called Dilution of Precision (DOP) (Kaplan et Hegarty, 2006). The geometric precision of dilution (GDOP), which is the most general index, makes it possible to estimate, from a global point of view, the positioning and clock bias errors of a navigation solution. In fact, GDOP assesses the effect of the geometry of the satellites on the positioning error. The DOP can also be divided into various other indices, such as PDOP (Position 3D DOP) to estimate 3D positioning errors or TDOP (Time DOP) to estimate clock bias separately. Thus, the dilution of precision can be expressed as a number of separate measurements: GDOP, PDOP, TDOP, VDOP (Vertical DOP), HDOP (Horizontal DOP), EDOP (East DOP) and NDOP (North DOP). For further details on the calculation of these parameters, see ANNEX III.

2.3 Reception of GNSS signals and receiver architectures

After passing through the propagation channel, the signal arrives at the receiver unit. GNSS receivers usually consist of three modules: the RF (Radio Frequency) front-end to capture and condition the satellite signals, the IF (Intermediate Frequency) circuit to demodulate the signals, and the baseband processor to process the signals in order to extract the user position. With more details, the architecture of a GNSS receiver generally consists of the following elements (Parkinson et Spilker, 1996):

- The receiving antenna,
- The RF signal processing module,
- An analog-to-digital converter (ADC) associated with an automatic gain control (AGC) module,
- Digital reception channels,
- The reception channel processing block which controls the management of the channels according to the received information (acquisition and tracking modules),
- A module for determining the navigation solution decoding the navigation message from the previous data,
- The power supply,
- The user interface.

The RF front-end receives the GNSS signals through the antenna, and after amplification and filtering, converts the RF signal to IF signal. Then, the ADC module converts the analog IF to digital IF signal. After that, the digital mixer strips down the carrier from the received GNSS signal, and the down converted signal is correlated with the locally generated version of it. Then, the correlation results are searched to find the correlation peak and decide the acquisition of a satellite. If a satellite is detected during the acquisition process, the satellite signal is tracked in the tracking module. Finally, the navigation solution module takes the information from the tracking module, and decodes the navigation message in order to calculate the user position. The generic architecture of a GNSS receiver can be shown in Figure 2.9.

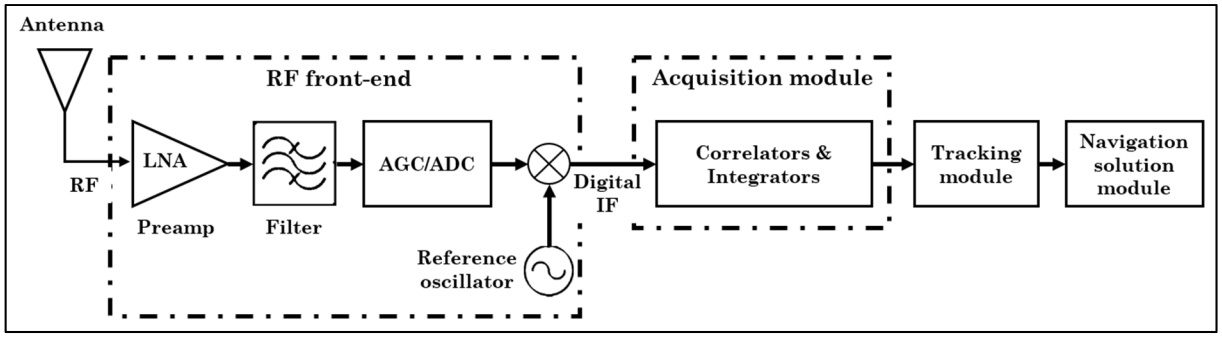

Figure 2.9 Generic GNSS receiver architecture

2.3.1 Antenna

The antenna is the first important element of a GNSS receiver. It is used to convert the electromagnetic wave from the satellites into an electrical signal. For various applications, GNSS receiver antennas are developed for maximum integration (Pigeon, 2011). Thus, their size, weight and cost are reduced to the maximum. The choice of thin antennas minimizing these parameters is relevant. Several features can be found on the antenna itself:

- The selectivity: the antenna must limit the power of incoming interference (spectral filtering). Indeed, the antenna must be able to reject the signals from different frequency bands from those concerned (L1, L2, L5 etc.), so the interest of narrowband or multiband antennas for multi-frequency antennas;

- The ratio between the gain of the antenna and the elevation: the gain of the antenna is ideal if it is constant for all satellites above a given elevation angle. In fact, it is necessary that the gain is high for angles above a certain elevation mask, in order to further amplify the signals transmitted by the satellites;
- The optimization deal with multipath: the gain should be low for negative or low elevations in order to reject multipath and interferences. It is important that the antenna rejects a maximum of multipaths. In fact, multipath are often derived from reflection at ground level which is therefore below a certain elevation mask.
- The physical characteristics: constraints related to the operating environment exist due to the objective of integrating the antenna into a functional device. This defines characteristics such as size, shape and material used.
- The polarization: it is of great importance for all satellite navigation signals as well as the receiver antennas are right-hand circularly polarized (RHCP) so that the signals reflected an odd number of times (i.e. circularly polarized to the left) are strongly attenuated by the antenna. The signals reflected an even number of times represent a major weakness of the receivers.

Like any electrical device, there is thermal noise at the output of the antenna. This noise varies according to the direction in which it points, its radiation pattern and its environment. The noise captured by the antenna is the noise of the sky and the noise due to the terrestrial radiation. The signal received at the antenna consists of the signals from K different satellites combined with noise as:

$$s_r(t) = \sum_{k=1}^{K} s_{r,k}(t) + \eta(t) \tag{2.16}$$

where $s_{r,k}(t)$ is the received signal from satellite k and $\eta(t)$ is the noise component.

Considering the data and pilot channels in the signal received from satellite k, the expression of the received signal from satellite k with the Doppler effect is:

$$s_{r,k}(t) = \sqrt{2P_{e,k}}\, c_{i,k}(t-\tau_k)\, d_k(t-\tau_k) \cos\left(2\pi\left(f_L + f_{d,k}\right)t + \varphi_{r,k}\right) + \sqrt{2P_{e,k}}\, c_{q,k}(t-\tau_k)\, \sin\left(2\pi\left(f_L + f_{d,k}\right)t + \varphi_{r,k}\right) \quad (2.17)$$

where $P_{e,k}$ is the received power on each channel, τ_k is the delay due to the distance traveled by the signal from the satellite k to the receiver, $f_{d,k}$ is the carrier Doppler frequency, and $\varphi_{r,k}$ is the phase of the received carrier such as $\varphi_{r,k} = \varphi_{e,k} - 2\pi f_L \tau_k$. It is noted that the signals are received with different delays and different power due to attenuation.

This signal will now pass through the RF front-end where some processing will be performed.

2.3.2 RF front-end

The RF front-end is an indispensable element in GNSS receivers to facilitate the processing of satellite signals. Its purpose is to provide digital signal samples as clean as possible to the signal processing block. For this, its functions are:

- Selection of the useful signal,
- Out-of-band interference filtering,
- Reduction of interference,
- Amplification of the signal,
- Down-conversion of the signal to an intermediate frequency (IF),
- Sampling and signal identification.

The various elements of the RF front-end allowing to perform its role are presented in Figure 2.10 where $s_r(t)$ is the received signal from a satellite k, $s_b(t)$ is the baseband signal from a satellite k, $s_b(nT_s)$ is the discrete baseband signal for a satellite k, f_L is the carrier frequency, f_{IF} is the intermediate frequency, f_{LO} is the local oscillator frequency, f_{ref} is the reference frequency of the receiver, and f_s is the sampling frequency.

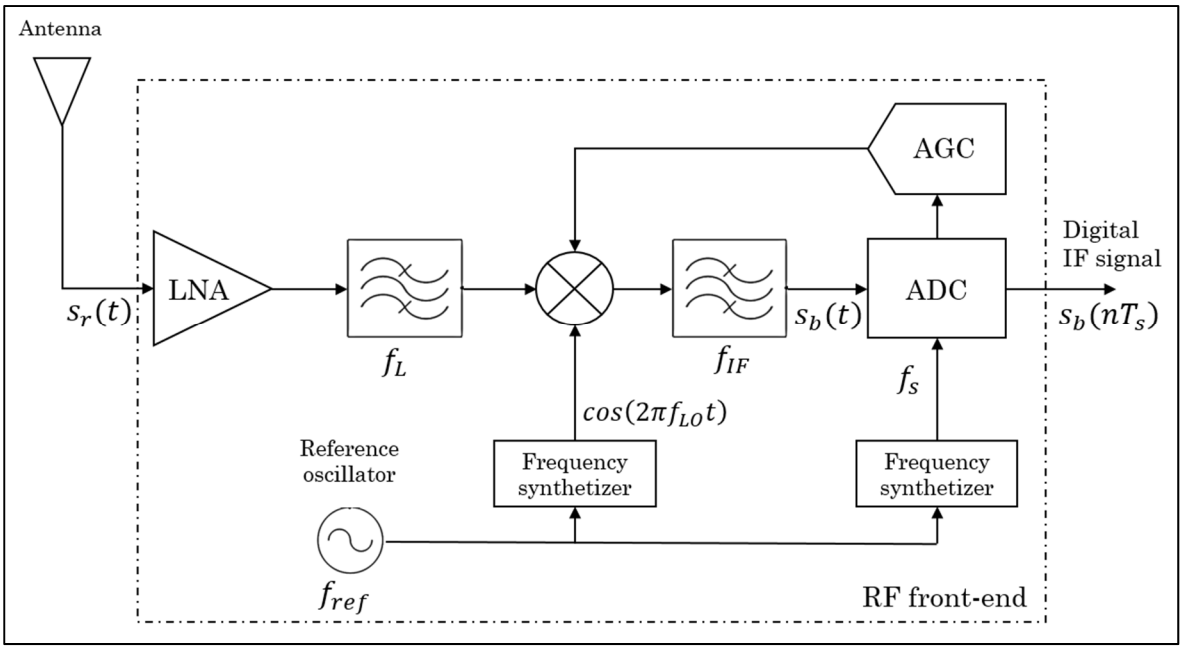

Figure 2.10 RF front-end of a GNSS receiver

Since the signal is embedded under noise, it is important to amplify it before handling through a series of electronic components using a Low Noise Amplifier (LNA) at the input of the receiver, which is mainly characterized by its gain and its noise figure. Moreover, the LNA has limits in terms of gain. So, it may therefore be necessary to use several amplifiers (higher gain but less noise resistant) interspersed with filters to eliminate the noise that can be generated.

Once the signal is amplified, it is important to regulate the amplitude of the signal using an automatic gain control (AGC) with the intention that it remains within the linear range of electronic components. To achieve this, a feedback loop that is an adaptive system is required. The AGC serves to preserve the signal within the input range of the individual filters. However, this device is limited by its linear operating range (amplitude of the output signals) and by the dynamics of its responses (time of rise and fall of the alternating signals).

To evaluate the parameters of the incoming signal, the receiver generates reference signals, which are compared to the incoming signal. A local reference oscillator (LO) is used to generate a local carrier. The LO is very important since the performance of the GNSS receiver

depends highly on it which is characterized by the stability and the sensitivity on vibration. The incoming signal is mixed with the local generated sine wave and filtered to remove all the unwanted signal and provide a good rejection of out-of-band interference.

Typically, the low conversion to the IF range is performed in two steps, although it is possible to achieve this in a single step. The frequency conversion therefore makes it possible to reduce the bandwidth of interest to an intermediate frequency that is easier to process by the electronics. To achieve this, bandpass filters are first used to select the frequency ranges of interest and thus minimize the bandwidth of the signal. Thereafter, a frequency offset of the original signal f_L is performed by a synthesized frequency f_{LO}. It results in two copies centered at frequencies $f_{IF} = f_L - f_{LO}$. In addition to providing the frequency needed to shift the RF content to IF, the frequency synthesizer must also derive the sampling frequency f_s. The receiver reference is characterized by a clock jitter. Since this variation cannot be correctly predicted, it must be estimated at each epoch. Indeed, there is a single clock source in the receiver, from which all the required frequencies are extrapolated. To reduce the cost, weight and size of the receivers, their clock is not as precise and stable as those found on satellites, whose clocks are cesium and rubidium. The clock of the receiver is actually a crystal of quartz which contracts periodically when subjected to a voltage, which is much less accurate than the atomic radiations of the clocks of the satellites.

In a GNSS receiver, multi-purpose filters are used. In particular, it is used to reduce the signal strength (i.e. immunity to noise) before amplifying it, in order to limit the bandwidth of a signal to be sampled (anti-aliasing filter), in order to select/reject a frequency range using a selection/rejection filter. Using these types of filters, it is possible to soften or integrate a signal or even help to generate frequencies from a reference. Thus, the first filter of a receiver serves as immunity to noise while the second filter is of anti-aliasing type. The other filters are used for the manipulation and synthesis of frequencies. In the case of an anti-aliasing filter, it is important that the characteristic of the bandwidth be uniformly flat (i.e. few oscillations), that the rejected range be strongly attenuated and that the transition between these two ranges abruptly. Moreover, the higher the order of a filter, the steeper the slope and the more complex

the implementation. To compensate for this limitation, the sampling frequency must be greater than the bandwidth of the desired signal. Regarding the selection of filters, it is generally difficult to create a narrow filter whose slopes are abrupt, especially at high frequencies (apart from resonant filters which allow only one frequency to pass). Thus, it would be possible to let through a large bandwidth, from which would be intersected other ranges so obtaining the desired range with the desired characteristics using different cascaded filters (Psiaki, Akos et Thor, 2005).

Before sampling, the frequency shifted signal must be filtered by an anti-aliasing filter so that it is a given bandwidth. According to (Tsui, 2005), the rate of the spectral spreading code is 1023000 ± 6 Hz, the total Doppler effect has a maximum effect of ± 6 Hz on the code, the sampling frequency should not be a multiple of this frequency range. Moreover, for a standard sampling, the sampling theorem of Nyquist-Shannon specifies that the sampling frequency must be at least twice the bandwidth of the signal to be sampled so that the digitized signal is completely representative. Given the limitations of the filters in passing one frequency but in cutting the next ones, a certain margin of oversampling is necessary to compensate, i.e. to sample at a frequency of 2.5 times the bandwidth. The bandwidth of a filter is normally proportional to its center frequency. Otherwise, there may be spectral aliasing or reframing, which results in a frequency and phase inversion. With regard to direct sampling of the RF band, there are two possibilities: sampling at a very high rate or sub-sampling, which amounts to causing voluntary spectral folding. The disadvantage of sub-sampling is the high attenuation of the digitized signals: the smaller the sub-sampling factor, the lower the resulting cardinal sinus component (Lamontagne, 2009).

The expression of the baseband signal for a satellite k is:

$$s_{b,k}(t) = \sqrt{2P_{b,k}}\, c_{i,k}(t-\tau_k)\, d_k(t-\tau_k) \cos\left(2\pi f_{b,k} t + \varphi_{b,k}\right) + \sqrt{2P_{b,k}}\, c_{q,k}(t-\tau_k)\, \sin\left(2\pi f_{b,k} t + \varphi_{b,k}\right) \quad (2.18)$$

where $P_{b,k}$ is the power on each channel, $f_{b,k}$ is the baseband frequency ($f_{b,k} = f_{IF} + f_{d,k}$), and $\varphi_{b,k}$ is the phase of the carrier. In reality, a term Δf_{IF} has to be considered in the resulted intermediate frequency f_{IF}, i.e. $f_{IF} = f_{IF} - \Delta f_{IF}$ because of the imperfection of the reference oscillator. For detailed information, please refer to (van Diggelen, 2009).

In the ADC module, the received continuous signal is transformed to a discrete digital signal, with a sampling period T_s, as $T_s = \frac{1}{f_s}$. Then, the ADC quantizes the signal in order to map the infinite set of sampled signal values to a small set. The number of samples per spreading code is denoted N_s. One of the weaknesses of the samplers is its jitter, this is the opening time of the ADC. If the time of sampling deviates from its period, the values thus obtained will have an amplitude error. In fact, the jitter of the opening time affects the high-frequency signals more. In addition, high-speed converters generally have fewer effective bits. According to (Tsui, 2005), another complexity is to design a narrow filter at such a high frequency, normally characterized by a relatively high loss.

The discrete baseband signal for a satellite k is expressed as:

$$\begin{aligned} s_{b,k}(nT_s) = \sqrt{2P_{b,k}}\, c_{i,k}(nT_s - \tau_k)\, d_k(nT_s - \tau_k) \cos\left(2\pi f_{b,k} nT_s + \varphi_{b,k}\right) \\ + \sqrt{2P_{b,k}}\, c_{q,k}(nT_s - \tau_k)\, \sin\left(2\pi f_{b,k} nT_s + \varphi_{b,k}\right) \end{aligned} \tag{2.19}$$

In addition, it is possible to sample in a complex way, thus obtaining two series of data: real and imaginary. In fact, it is rather a quadrature sampling, where the second series of data is out of phase 90^o relative to the first. Since there are two data channels, the sampling frequency must only be greater than the bandwidth of the signal to be scanned and not double. (Tsui, 2005) states that there is no real gain in using quadrature conversion in the intermediate range compared to a standard conversion for GNSS receivers. For example, it resolves the image frequency problem but it requires two paths instead of one. However, direct sampling allows multiple narrow bands to be folded into the same tape base. It also allows us to have a lower IF and a lower sampling frequency than for a real sampling. According to (Tsui, 2005), a

sampling frequency of 1.25 times the bandwidth can be adopted to accommodate the limitations of anti-aliasing filters.

In this case, the discrete baseband signal $s_b(nT_s)$ can be modeled as a complex signal, where $s_i(nT_s)$ and $s_q(nT_s)$ are the real part and the imaginary part respectively. Thus, the expression of the discrete baseband signal for a satellite k is:

$$\begin{aligned} s_{b,k}(nT_s) &= s_i(nT_s) + j\, s_q(nT_s) \\ &= \sqrt{2P_{b,k}}\, \Big(c_{i,k}(nT_s - \tau_k)\, d_k(nT_s - \tau_k) \\ &\quad - j\, c_{q,k}(nT_s - \tau_k) \Big) e^{j(2\pi f_{b,k} nT_s + \varphi_{b,k})} \end{aligned} \tag{2.20}$$

where $j = \sqrt{-1}$.

After the ADC, once the GNSS receiver has performed these measurements at a given time interval called discrete measurements, the signal will have to be encoded with a finite number of bits, thus obtaining an approximation of the actual signal. The error generated by this process is called quantization error and can usually be neglected for a receiver digital. Also, total system jitter, quantization noise and thermal noise of the ADC form the three main sources of noise. The last two sources have a direct effect on the SNR. Although a single quantization bit is generally sufficient to recover the shifted navigation message in the spectrum, it may be worthwhile to use more bits to develop a more robust algorithm for acquiring and tracking low amplitude signals.

2.3.3 Acquisition

Acquisition process is the next step of the GNSS receiver after the RF front-end. First, acquisition of a satellite signal begins with a process of searching for visible satellites of the receiver. Acquisition is the most difficult step to perform by the receiver. The search time of visible satellites depends on the type of start (hot, warm or cold). If a satellite k is visible,

acquisition process must determine the two properties of the signal: the frequency and the code phase. In fact, the purpose of acquisition process is to obtain a rough estimation of the baseband frequency $f_{b,k}$ noted $\hat{f}_{b,k}$, and the delay of the spreading code transmitted τ_k noted $\hat{\tau}_k$ (more precisely, τ_k modulo one code period). The Doppler frequency shift may be up to 10 kHz if the maximum satellite speed is combined with a very fast user displacement and never exceeds 5 kHz for a fixed receiver. The phase of the code designates the point in the data block where the PRN code begins. If a 1 ms data block is examined, then the data includes an entire PRN code (Borre et al., 2007).

More precisely, acquisition is a process of searching, in the time-frequency space, the values of τ_k and $f_{b,k}$ which maximize the correlation product between the received signal and a replica of this signal. The correlation value is high if $\hat{f}_{b,k}$ is close to $f_{b,k}$ and if $\hat{\tau}_k$ is close to τ_k, then we can talk about a successful acquisition if it exceeds a predefined threshold. Moreover, the correlation value is low if $\hat{f}_{b,k}$ is far from $\hat{f}_{b,k}$ or if $\hat{\tau}_k$ is far from τ_k. This will be detailed in Chapter 3. In order to find the peak which exceeds a predefined threshold, this process is repeated for different values of $\hat{f}_{b,k}$ and $\hat{\tau}_k$. If all possibilities have been tested but no peak exceeds the threshold, the signal is therefore not detected and we can say that this satellite is not visible or we have missed it (Ziedan, 2006).

The acquisition process can be summarized in Figure 2.11 which shows the four steps of the processing: multiplication with a complex exponential of frequency (search of frequency $\hat{f}_b$), multiplication with the spreading code of a satellite (search of the delay $\hat{\tau}$), accumulation of the signal samples to increase the SNR, and calculation of the signal power (magnitude) (Leclère, Botteron et Farine, 2010b).

In figure 2.11, the expression $r_k(\hat{f}_b, \hat{\tau})$ is called the cross ambiguity function (CAF) which is the expression of the accumulation over all signal samples.

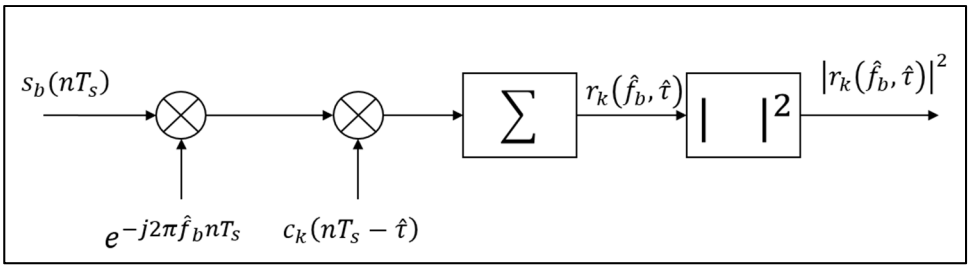

Figure 2.11 Basic principle of acquisition process

Note that the main work of this thesis is focused on acquisition techniques. The basic principle of this process will be detailed in Chapter 3 as well as the different techniques; the acquisition of GNSS signals in challenging environments will be addressed in Chapter 4; and methods of collective or collaborative acquisition (vector acquisition) will be developed in Chapter 5 where there are all the major contributions of this work.

2.3.4 Tracking

The tracking of GNSS signals is done after the satellites in view localization which is the acquisition process. The tracking mode requires as much precision as the acquisition mode. The main aim of the tracking is to refine the coarse values of the code phase $\hat{\tau}$ and the frequency $\hat{f}_b$ due to the frequency and code variations by the Doppler effect which is itself generated by the relative motion between the satellites and the receiver; and then keep track of it as the properties of the signals change over time. The tracking operation is similar to the one in acquisition: the incoming signal is multiplied with a local carrier and a local code, and the result is then accumulated.

The tracking process contains two parts: code tracking and carrier frequency/phase tracking. Code tracking is often implemented as a Delay-Locked Loop (DLL) where three local codes (replicas) are generated and correlated with the incoming signal. The three replicates designate the replica of the early (*E*), prompt (*P*), and late (*L*) versions of the PRN code, which are slightly shifted versions of each other, and are often separated by a half-length (less than one chip). The other part of the process consists in the tracking of the carrier wave which can be

done in two ways: either the tracking of the signal phase using a Phase Locked-loop (PLL) or the tracking of the frequency using a Frequency Locked-loop (FLL), but usually PLL is used for better performance. The tracking process must be continuously performed to monitor the frequency evolution over time. The receiver must take into account the possible variations on the frequency and the code in order to remain synchronized with the signals of the satellites. If the receiver loses track of a satellite, a new acquisition must be carried out for that particular satellite (Borre et al., 2007).

PLL and DLL are used most of the time during the tracking period of the navigation signals. The tracking loops generate the replicas of the received signals and try to set to zero the phase errors between these signals in order to maintain the phase lock. Tracking loops are more efficient in environments where the C/N_0 level of the signal is high and users are less dynamic. The carrier tracker discriminator defines the type of tracking loop, whether it is a PLL, a Costa PLL or a FLL. The PLL and the Costa loop are more precise but they are more sensitive to the signal dynamics than the FLL. When the signal is tracked correctly, it is then possible to measure the pseudorange characterized by the margins of error σ_{PLL} and σ_{DLL}. To minimize the phase error, narrow correlator must be used (Kaplan et Hegarty, 2006).

Several methods have been proposed for tracking navigation signals at all levels. The difference between tracking weak signals and high power signals is that the tracking of weak signals requires a larger data length using long coherent integration (Tsui, 2005).

The tracking mode consists of feedback loops to update the measurements at each iteration, and which makes it possible to update the carrier local oscillators and the code delay offset. This principle of tracking process is illustrated in Figure 2.12 showing code and carrier tracking loops.

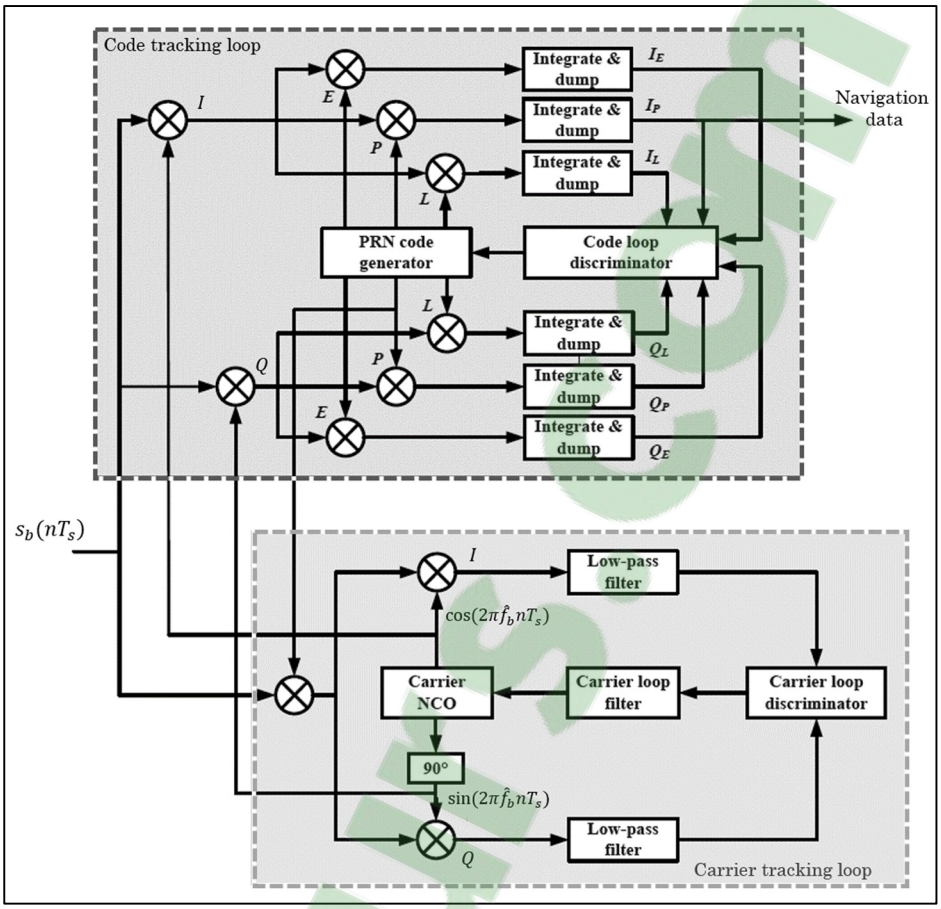

Figure 2.12 Basic principle of tracking process

2.3.5 Navigation

The calculation of the navigation solution is the last stage of the GNSS receiver. In particular, it makes it possible to determine the position, the velocity and the time (PVT) of the receiver. To achieve this, the observation measurements obtained in the preceding steps are used to determine the distance between the receiver and the various satellites. The position of the satellites is determined from the navigation messages. The navigation data bits can be extracted once a satellite signal is tracked which requires a significant amount of time.

Another element to be considered is the synchronization between the clock of the receiver and that of the satellites since this synchronization is paramount for the precision of the receiver.

Indeed, an error of only 1 ns implies an error of 0.3 m on the pseudorange measurement. This problem is solved when calculating the navigation solution by adding an unknown to the calculation. An unknown must be added for each constellation. As we saw in section 2.1.1, the representation of the position of an object on Earth requires three axes. There are therefore three unknowns of position to be identified. To these three unknowns is added that of the synchronization known as the clock bias. The position of the receiver is thus represented by four variables if a single constellation is considered (Pratap et Enge, 2006).

To determine the PVT of the receiver, the system of 4-unknown equations must be solved using a Kalman filter in the receiver. The Kalman filter is a recursive estimator to estimate the current state from the previous state and the current measurements. It thus combines the four position/time variables and the four velocity/clock drift variables of the receiver. However, these notions of stochastic mathematics go beyond the objective of this thesis and will not be studied in depth. For more information on this subject, the reader is invited to read (Kaplan et Hegarty, 2006).

2.3.6 Global architecture of GNSS receiver

Traditional GNSS receivers are composed of analog part (RF front-end) and digital part. The analog part consists of the antenna, a low noise amplifier with automatic gain control, a frequency conversion module, a local oscillator, a frequency synthesizer, filters and power supply. The digital part consists of reception channels where there are all digital signal processing such as acquisition and tracking. In addition, the navigation solution (decoding of the navigation message, pseudorange measurement, error correction, etc.) is implemented in a software part. Currently, we move to all-digital architecture as shown in Figure 2.13. Indeed, the current receivers are designed with integrated digital components and receivers acquire GNSS signals over several channels at a time, thereby accelerating the Time To First Fix (TTFF). The TTFF is the time when the receiver gets its first corrected position whether assisted or unassisted which is the most important criterion for evaluating the performance of high sensitivity receivers.

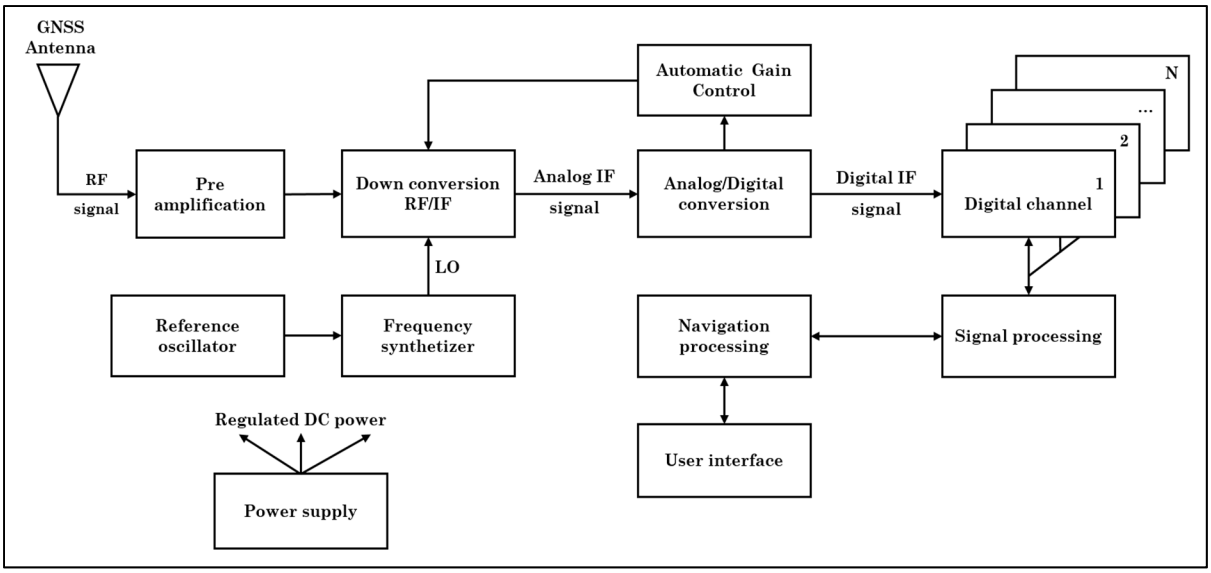

Figure 2.13 Block diagram of a modern digital GNSS receiver
Adapted from (Kaplan et Hegarty, 2006)

The main segments of the GNSS receiver are generally implemented within one or more integrated circuits, also called ASIC (Application Specific Integrated Circuit). The design of an ASIC is time-consuming, expensive and not very flexible, making it difficult for manufacturers to respond quickly to changes in the arrival of new GNSS signals. However, a much more flexible new approach, called Software Defined Radio (SDR), solves the problem. In fact, GNSS receivers are becoming increasingly miniaturized and require low power consumption with a sensitivity to weak signals. All this motivated the evolution of GNSS receivers towards the software concept. We also talk about Software Defined Navigation (SDN) in navigation field. This software architecture was designed to meet a number of criteria that were always required, such as flexibility, sensitivity and performance. Benefiting from its flexibility, the use of the receiver in a software way also facilitates the development and validation of new algorithms. The SDR, a concept dating back to the early 1990s, relies on the exclusively digital processing of signals using reprogrammable components (Bruno, 2007). In other words, it will be attempted in an SDR navigation receiver to digitize the GNSS signals as close as possible to the antenna (using an analog to digital converter) in order to minimize the number of hardware components required. Since a maximum of processing is performed by software, it is possible to quickly modify the architecture of an SDR receiver, even after its

sale to a customer. In most current software receivers, only the antenna and the low noise amplifier are not software.

The most commonly considered components for the development of SDR receivers are Digital Signal Processor (DSP) and general purpose digital processors such as those encountered in personal computers. These components typically accomplish the tasks associated with the baseband, which consist of a series of sequential mathematical operations. However, it becomes difficult to efficiently process the IF signals, despite the power of the current processors, since a large number of operations must be carried out in parallel. FPGA (Field-Programmable Gate Array) is another component used occasionally for the development of SDR receivers. Indeed, the FPGA is a reprogrammable logic circuit; it operates in a parallel way, unlike the digital processors that operate sequentially. The development of parallel architectures within an FPGA allows thus treating IF signals at very high speeds and delivering unmatched performance. Given the high density of current FPGA, it is also possible to implement a large number of GNSS reception channels without sacrificing the receiver performance. This is very beneficial given the large number of satellites and current and future GNSS signals.

2.4 Summary

In this chapter, we presented the basic principle of positioning by satellites, GNSS signals and the principle of GNSS receivers. The various sources that may affect the reception of GNSS signals as well as those that may degrade navigation solutions have also been introduced. These elements are necessary for understanding the following chapters.

We have talked about modern GNSS signals that have introduced some new components such as a secondary code, a sub-carrier and a pilot channel. These signals that have adopted a variety of features not used for the GPS L1 C/A signal are the future of positioning and navigation systems.

We have also seen that the received signal is affected by a code delay and a Doppler frequency which both should be estimated in the first step of baseband processing, i.e. acquisition process. Indeed, the frequency of the signal from a specific satellite may be different from its nominal value. The receiver converts the RF signal to intermediate frequency IF. And the signals are affected by the relative motion of the satellite causing the Doppler effect.

Finally, we have discussed that acquisition is the most difficult step to be accomplished by the receiver. The search time of visible satellites depends on the type of start (hot, warm or cold). Note that the main work of this thesis is focused on acquisition techniques. The basic principle of this process will be detailed in the next chapter.

CHAPTER 3

GNSS SIGNALS ACQUISITION PRINCIPLE

The acquisition is the most difficult step to be accomplished by the receiver. The task of an acquisition channel is to determine the presence of a signal emitted by a particular satellite from all the signals received simultaneously, and to initialize the estimation of its time delay and Doppler frequency shift. The search time of visible satellites depends on the type of start (hot, warm or cold). The acquisition module provides only a rough estimate of the Doppler frequency and the code delay. These estimates are used to calculate the pseudorange between the satellite and the receiver. At the implementation level, during the acquisition stage we do not require as much accuracy as the tracking mode. In this chapter, the principle of GNSS signals acquisition is described. State-of-the-art of acquisition techniques is reviewed. Problem formulation of acquisition process and the various methods of acquisition are then presented.

3.1 State of the art of common acquisition methods

According to (Tsui, 2005), less than 11 satellites are visible at a time according to both the date and the receiver position. The search delay is more or less long, depending on the type of start. Indeed, in the case of a cold start, the receiver has no idea where it is and its time reference may be outdated, as well as the last ephemerides (describing the position of the satellites in orbit). The search for satellite signals is thus a process that can be quite long given that the duration of a complete GPS navigation message may take 12.5 minutes. Current acquisition techniques are based on the use of several channels in parallel to accelerate the TTFF.

Parallel methods can use two approaches: Discrete Fourier Transform (DFT) or a faster Delay and Multiply method characterized by a low SNR (Tsui, 2005). It is therefore understood that the DFT approach is more sensitive and therefore more efficient in the presence of signals of low amplitudes. In the case of very weak signals, a long acquisition period is required. However, the transitions in the navigation message and the Doppler effect on the code can degrade the acquisition performance thus limiting the integration time. But with the new GNSS

signals, it is possible to have a longer integration time since the pilot component of the signal is no longer modulated by the navigation message (Tsui, 2005).

During the acquisition of a satellite k, the incoming signal is multiplied by the generated local PRN code corresponding to this satellite k. The cross-correlation between the PRN codes of other satellites makes it possible to suppress signals from other satellites. To avoid deleting the desired signal component, the locally generated PRN code must be aligned in time so that the code phase is correct (Borre et al., 2007). During the acquisition of any given satellite, signals from other satellites are treated as noise (Kaplan et Hegarty, 2006).

Once the signal has been acquired, a PLL can take over. In the case of a GPS PLL, two successive integration times of 10 ms ensure that at least one of the two integrations is not affected by a transition since the period of the navigation message is 20 ms. However, this type of search imposes frequency hops of only 100 Hz, thus multiplying by five the required computation effort (Tsui, 2005). Coherent processing of long navigation data is a better approach for acquiring weak SNR signals.

Some weak signal acquisition techniques have been introduced by (Ziedan, 2006) such as: circular correlation and delay and multiply approach. Circular correlation is an alternative approach based on the Fast Fourier Transform (FFT) method. It calculates the coherent integration for all code delays and each Doppler shift in the same process. The delay and multiply approach eliminates all Doppler errors.

The basic elements of the GNSS signal acquisition schemes consist of two main blocks: the correlation block and the detection scheme. Based on these fundamental modules, most GNSS signal acquisition schemes found in literature include additional features, such as data preprocessing (Pany, 2010; Ziedan, 2006), feedback loops (Rovelli et al., 2010), multi-trial detection (Borre et al., 2007; Foucras et al., 2012; Parkinson et Spilker, 1996), fusion with other data sources (Kubrak et al., 2008; Pany et al., 2009), inclusion of additional blocks to refine the coarse estimates before the handover to tracking (Sagiraju, Akopian et Valio, 2006).

Several methods of correlation exist such as: Serial Search (SS), Parallel Frequency Search (PFS), Parallel Code Search (PCS) (Borre et al., 2007; Tsui, 2005), Bi-Dimensional Parallel Search (BPS) based on spectral shifting with Doppler pre-processing (Akopian, 2005; Pany, 2010; Sagiraju, Raju et Akopian, 2008), and the Double Block Zero Padding (DBZP) (Foucras et al., 2012; Lin et Tsui, 2000; Ziedan, 2006; Ziedan et Garrison, 2004). Other methods of correlation exist in the literature but all are based on the above-mentioned methods, such as the improved fast modified DBZP in (Zhang et Ghogho, 2010) or reconfigurable acquisition scheme for time-frequency in (Borio et Presti, 2008). Although there are many methods, they can be divided into two categories: the time-domain acquisition method (serial search) and the frequency-domain acquisition methods which encompasses all other methods. FFT-based techniques are performed in frequency-domain in order to reduce the computational complexity.

To evaluate the performance of high sensitivity receivers, some criteria should be considered. One important criterion is the TTFF, the time when the receiver gets its first corrected position whether assisted or unassisted. Also the sensitivity is a key feature of a receiver, which measures the lower level of C/N_0 of a signal that an acquisition method could acquire. It is also necessary to consider the SNR of the received signal to evaluate the sensitivity of the receiver, it is the calculation of the receiver gain and the post-correlation SNR measured during the acquisition and tracking period. Similarly, the evaluation of the robustness against radio interference from different non-intentional and intentional sources (wireless networks, mobile phone, criminal transmitters, etc.) is very important, it is the calculation of JNR (Jammer to Noise Ratio).

3.2 Problem formulation

In the real case, the received signal is the combination of several signals coming from different satellites plus a noise term. Then, the composite GNSS signal entering the correlation block must take account of the noise component. So, the expression of the signal at the RF front-end output is:

$$s_{b,k}(nT_s) = \sqrt{2P_{i,b,k}}\, c_{i,k}(nT_s - \tau_k)\, d_k(nT_s - \tau_k) \cos\left(2\pi f_{b,k} nT_s + \varphi_{b,k}\right) + \sqrt{2P_{q,b,k}}\, c_{q,k}(nT_s - \tau_k)\, \sin\left(2\pi f_{b,k} nT_s + \varphi_{b,k}\right) + \eta(nT_s) \tag{3.1}$$

where $P_{i,b,k}$ and $P_{q,b,k}$ are the respective carrier powers for the in-phase and quadrature phase carrier components, τ_k is the delay due to the distance traveled by the signal from the satellite k to the receiver, $f_{b,k}$ is the carrier Doppler frequency, $\varphi_{b,k}$ is the phase of the received carrier, and $\eta(nT_s)$ is the incoming noise which is assumed to be an Additive White Gaussian Noise (AWGN) with centered Gaussian distribution. The noise is assumed to be characterized with a constant two-sided power spectral density (PSD) equal to $\frac{N_0}{2}$ dBW/Hz, where N_0 is defined as:

$$N_0 = k_B T_{eff} \tag{3.2}$$

where k_B is the Boltzmann constant and T_{eff} is the effective temperature of the entire RF front-end which depends on the noise figure of the front-end, on the ambient temperature and on the effective temperature of the antenna.

In general formulation of GNSS signal, $d(t)$ is the 50-bps (bits per second) data modulation, $c(t)$ and $p(t)$ are the respective C/A and P pseudorandom code waveforms, ω is the L1 carrier frequency in radians per second, and θ is a common phase shift in radians. The quadrature carrier power $P_{q,b,k}$ is approximately 3 dB less than $P_{i,b,k}$. In contrast to the L1 signal, the L2 signal is modulated with only the 50-bps (bits per second) data and the P-code, although there is the option of not transmitting the 50-bps (bits per second) data stream.

Knowing that the noise is also filtered with the signal, if we assume an ideal filter of two-sided bandwidth 2B, the noise power is expressed by:

$$\sigma_\eta^2 = \frac{N_0}{2} 2B = N_0 B \tag{3.3}$$

The noise power is proportional to the filter front-end bandwidth (van Diggelen, 2009). The noise power then depends on the desired signal, for example the GPS L5 signal bandwidth is ten times that of GPS L1 C/A signal.

To consider $\eta(nT_s)$ as an AWGN, we should consider $B = \frac{f_s}{2}$ for a real sampling, or $B = f_s$ for a complex sampling. It is almost impossible to make an ideal filter, thus a precise analysis can be carried out only when the transfer function of the front-end filter is known (Leclère, 2014). Since the noise power depends on the front-end bandwidth (or on the sampling frequency), the SNR at the front-end output may be different for signals of the same power but a different bandwidth. To determine the noise power, the carrier power-to-noise density ratio is usually used (Joseph, 2010), defined as:

$$C/N_0 = \frac{P_r}{N_0} \tag{3.4}$$

which is usually expressed in log scale as:

$$C/N_0 = 10\log_{10}\left(\frac{P_r}{N_0}\right) = 10\log_{10} P_r - 10\log_{10} N_0 \tag{3.5}$$

Using this formula, a signal power of -160 dBW (corresponding to a received signal in an open sky view) received by a front-end with an effective temperature of 300 K is equal to C/N_0 = 43.8 dBHz.

The signal received from satellite k before the correlation step can be expressed as:

$$s_{b,k}(nT_s) = \sqrt{2P_{b,k}}\, c_{i,k}(nT_s - \tau_k)\, d_k(nT_s - \tau_k) e^{j\{2\pi(f_{IF} + f_{d,k})nT_s + \varphi_{b,k}\}} + \eta(nT_s) \tag{3.6}$$

In order to obtain a position solution, a GNSS receiver must be able to process the signal received from a number of satellites which is performed during a sufficient duration time. For that, a synchronization between the transmitter and the receiver is required. This synchronization is usually carried out in two steps: a coarse synchronization stage, acquisition, and a fine tuning process, tracking. To achieve the first step, the acquisition process can be considered as a combined estimation/detection problem (Borio, 2008; He et Petovello, 2014; Hurd, Statman et Vilnrotter, 1987; O'Driscoll, 2007b).

3.2.1 Estimation problem

According to the signal expression in equation (3.6), the unknown signal parameters corresponding to a given satellite are (O'Driscoll, 2007b):

1) The satellite identification number, k;
2) The instantaneous signal power, $P_{b,k}$;
3) The code phase, τ_k;
4) The current data bit value, d_k;
5) The Doppler frequency offset, $f_{d,k}$;
6) The initial phase offset, $\varphi_{b,k}$.

From the unknown parameters listed above, the main parameters to be estimated during the acquisition stage are the code phases τ and the Doppler offsets $f_d = f_b - f_{IF}$ of the incoming signals, jointly with each satellite identification number. As stated before in this report, the acquisition problem can be formulated as a parameter estimation problem.

Let the vector $\boldsymbol{\theta} = [\tau, f_d]$ represent the set of main parameters to be estimated in acquisition stage, and $\widehat{\boldsymbol{\theta}}$ its estimates. A number of observations (N observations) of the received signal are carried out by the estimator. The observation vector is denoted as $\boldsymbol{s_r} = \{s_{r_0}, s_{r_1}, \dots, s_{r_{N-1}}\}$. Suppose that $f_{\boldsymbol{s_r}|\widehat{\boldsymbol{\theta}}}(\boldsymbol{s_r}|\widehat{\boldsymbol{\theta}})$ is the Probability Density Function (PDF) of the received signal conditioned on its estimated parameters. This PDF denotes the *a priori* probability of observing

the vector $\boldsymbol{s_r}$ and it represents the measure of the likelihood that the true parameter vector is $\widehat{\boldsymbol{\theta}}$. Since we know $\boldsymbol{s_r}$, but we do not know $\widehat{\boldsymbol{\theta}}$, let consider $f_{\boldsymbol{s_r}|\widehat{\boldsymbol{\theta}}}(\boldsymbol{s_r}|\widehat{\boldsymbol{\theta}})$ to be a function of $\widehat{\boldsymbol{\theta}}$ parameterised by $\boldsymbol{s_r}$. Thus, $f_{\widehat{\boldsymbol{\theta}}|\boldsymbol{s_r}}(\widehat{\boldsymbol{\theta}}|\boldsymbol{s_r})$ is referred to as the likelihood function (O'Driscoll, 2007b).

Since $f_{\widehat{\boldsymbol{\theta}}|\boldsymbol{s_r}}(\widehat{\boldsymbol{\theta}}|\boldsymbol{s_r})$ is known as the likelihood function, several estimators allowing to estimate the set of parameters, code phase and Doppler frequency, during the acquisition stage can be used, such as: the minimum mean square error (MMSE) estimator (Papoulis, 1965; Scharf, 1991), the maximum *a posteriori* (MAP) estimator (Henkel et Kiam, 2013), the maximum likelihood (ML) estimator (O'Driscoll, 2007b; Proakis, 2008).

The MMSE estimator is an optimal estimator. If $\varepsilon = \widehat{\boldsymbol{\theta}} - \boldsymbol{\theta}$ represent the error between the estimated and the true signal parameters, then the MMSE estimator has to minimize the mean square error, given by $E[\varepsilon^T \varepsilon]$, where $E[\boldsymbol{x}]$ represents the excepted value of the random variable $\boldsymbol{x}$ and $\boldsymbol{x^T}$ is the transpose of the vector $\boldsymbol{x}$. The MMSE estimator is based on a knowledge of the a posteriori distribution of the true parameter vector corresponding to the observation vector $f_{\widehat{\boldsymbol{\theta}}|\boldsymbol{s_r}}(\widehat{\boldsymbol{\theta}}|\boldsymbol{s_r})$. Therefore, the MMSE estimator provides, on average, the best estimate in the mean-square sense. Then, the MMSE estimate is expressed as:

$$\widehat{\boldsymbol{\theta}}_{MMSE} = E\left[\widehat{\boldsymbol{\theta}}|\boldsymbol{s_r}\right] \tag{3.7}$$

The MAP estimator is a related estimator. In a similar way to the MMSE, the MAP estimate is the estimate $\widehat{\boldsymbol{\theta}}_{MAP}$ maximizing the posterior probability that the estimate is correct, given that the vector $\boldsymbol{s_r}$ was received. Then, the MAP estimate is the solution of the equation:

$$\widehat{\boldsymbol{\theta}}_{MAP} = \arg\max_{\widehat{\boldsymbol{\theta}}} f_{\widehat{\boldsymbol{\theta}}|\boldsymbol{s_r}}(\widehat{\boldsymbol{\theta}}|\boldsymbol{s_r}) \tag{3.8}$$

The MMSE and the MAP estimates of $\boldsymbol{\theta}$, the true parameter vector, coincide if the expected value and the peak of the *a posteriori* distribution coincide (O'Driscoll, 2007b). This is true for

certain cases only, based on different optimization criteria and for certain types of *a posteriori* distributions. In practice, the MMSE and the MAP cannot be used for GPS signal acquisition because of the reliance on the availability of $f_{\widehat{\boldsymbol{\theta}}|\boldsymbol{s_r}}(\widehat{\boldsymbol{\theta}}|\boldsymbol{s_r})$ and the fact that we do not have expressions for $f_{\widehat{\boldsymbol{\theta}}}(\widehat{\boldsymbol{\theta}})$ and $f_{\boldsymbol{s_r}}(\boldsymbol{s_r})$ in the Bayes' theorem which are used in MMSE and MAP. For further information, see (Proakis, 2008).

Thus, an alternate estimate, the maximum likelihood estimate is commonly used. The likelihood function of the parameter $\widehat{\boldsymbol{\theta}}$ is simply the *a priori* probability of the received data signal $\boldsymbol{s_r}$ given $\widehat{\boldsymbol{\theta}}$. Then, the ML estimate is given by the solution of the equation:

$$\widehat{\boldsymbol{\theta}}_{ML} = \arg\max_{\widehat{\boldsymbol{\theta}}} f_{\boldsymbol{s_r}|\widehat{\boldsymbol{\theta}}}(\boldsymbol{s_r}|\widehat{\boldsymbol{\theta}}) \tag{3.9}$$

According to (O'Driscoll, 2007b), a decision statistic $D_k(\widehat{\boldsymbol{\theta}})$ for satellite k can be defined from the likelihood function containing the same information as $\widehat{\boldsymbol{\theta}}_{ML}$ and that is the maximum for the same set of parameters $\widehat{\boldsymbol{\theta}}_{ML}$. The ML estimate of the true desired parameter vector $\boldsymbol{\theta}$ is given by $\widehat{\boldsymbol{\theta}} = [\hat{\tau}, \hat{f}_d]$, such that the next expression (3.10) is maximized:

$$\left| \int_0^{NT_S} s_r(t) c_{i,k}(t - \hat{\tau}_k)\, e^{j\{2\pi(f_{IF} + \hat{f}_{d,k})nT_S\}} \right|^2 \tag{3.10}$$

The discrete-time equivalent is given by the metric:

$$D_k(\widehat{\boldsymbol{\theta}}) = \left| \boldsymbol{s_r} \cdot \boldsymbol{s}_k(\widehat{\boldsymbol{\theta}}) \right|^2 \tag{3.11}$$

where $\boldsymbol{s}_k(\widehat{\boldsymbol{\theta}}) = \left\{ c_k(nT_s - \hat{\tau}_k)\, e^{-j2\pi(f_{IF} + \hat{f}_{d,k})nT_S} \right\}_{n=0,1,\ldots,N-1}$. The expression of $D_k(\widehat{\boldsymbol{\theta}})$ corresponds to the four steps of the acquisition process as shown in Figure 2.11 (multiplication of the incoming signal with the spreading code of the satellite k with a delay $\hat{\tau}_k$, multiplication

of the incoming signal with a complex exponential of frequency $\hat{f}_{b,k}$, accumulation of the signal samples in order to increase the SNR and computation of the magnitude of the signal).

Moreover, treatment of the acquisition as a simple estimation problem is not adequate with the goal of the acquisition step, because we are not certain that the ML estimate really corresponds to the best approximation of real signal parameters, as it is also possible that the signal tested is absent. In this case, the estimate simply corresponds to the noise peak. Thus, it is necessary to move on to another estimation step which will be able to evaluate and test the presence or absence of the signal. Hence, we treat the acquisition problem as a detection problem.

3.2.2 Detection problem

Estimation of signal power values allows to decide if the received GNSS signals are sufficient in number and strength. Furthermore, this argument can be seen as a signal-detection problem: deciding between different hypotheses whether one or more GNSS signals are received within the recorded signal or if only noise is received (Pany, 2010). Once the decision statistic is obtained for different combinations of the code phase and Doppler offsets under test, these statistics are then used to decide the presence of signal (Esteves, 2014b). In the case of detection problem, the decision statistic, defined in Equation 3.11, is known as the *detection metric*. In GNSS signal theory detection, two conditions of signal presence and absence are defined. A binary hypothesis-testing problem is then set up (Pany, 2010):

1) Hypothesis H_0, called *null hypothesis*, corresponding to the situation in which the desired signal is absent (only noise is received); and
2) Hypothesis H_1, called *alternate hypothesis*, corresponding to the situation in which the navigation signal is actually present.

Two decisions can be taken from these two hypotheses:

- The decision that H_0 is true, called as Decision D_0; and
- The decision that H_1 is true, called as Decision D_1.

According to D_0 and D_1, four possibilities may result, two under H_0 and two under H_1:

- Correct rejection: Decision D_0 given that H_0 is true;
- False alarm: Decision D_1 given that H_0 is true;
- Missed detection: Decision D_0 given that H_1 is true; and
- Correct detection: Decision D_1 given that H_1 is true;

Probabilities are related to these different possibilities of decision/detection, such as:

- Probability of correct rejection: P_{cr};
- Probability of false alarm: P_{fa};
- Probability of missed detection: P_{md}; and
- Probability of correct detection, often called probability of detection: P_d;

Several criteria must be considered in order to have an optimal choice between the two possible decisions. According to (Pany, 2010), Bayesian and Neyman-Pearson detectors can be used to solve this problem. The first detector minimizes the Bayesian risk. The second detector is based on the Neyman-Pearson criterion in which the detection is made to maximize the probability of detection under the constraint that the probability of false alarm does not exceed a predefined threshold γ and maximize the probability of correct decision among others (Yang et al., 2007). Both tests are based on the likelihood ratio $\Lambda(\boldsymbol{s_r})$ of the vector $\boldsymbol{s_r}$ and compare this ratio to the threshold γ. If the likelihood ratio value exceeds the detection threshold γ, then the decision D_1 is made, otherwise, the decision D_0 is chosen. Both Bayesian and Neyman-Person detectors are optimal since they achieve the objectives of minimum risk or maximum probability of detection. Thus, optimization under all the criteria to be taken into account, the likelihood ratio test is defined as:

$$\Lambda(\boldsymbol{s_r}) = \frac{f_{\boldsymbol{s_r}|H_1}(\boldsymbol{s_r}|H_1)}{f_{\boldsymbol{s_r}|H_0}(\boldsymbol{s_r}|H_0)} \underset{D_0}{\overset{D_1}{\gtrless}} \gamma \tag{3.12}$$

Since signal acquisition in a GNSS receiver is considered as an estimation and detection problem, a generalized likelihood ratio test (GLRT) which is a common approach to addressing

a composite hypothesis-test problem can be used. A GLRT is based on the likelihood ratio, defined in Equation 3.12, and replaces the unknown parameters $\widehat{\boldsymbol{\theta}} = [\hat{\tau}, \hat{f}_d]$ with their ML estimates $\widehat{\boldsymbol{\theta}}_{ML}$ (Borio, 2008). Thus, the GLRT can be expressed as:

$$\Lambda_G(\boldsymbol{s_r}) = \max_{\widehat{\boldsymbol{\theta}}} \frac{f_{\boldsymbol{s_r}|H_1,\widehat{\boldsymbol{\theta}}}(\boldsymbol{s_r}|H_1, \widehat{\boldsymbol{\theta}})}{f_{\boldsymbol{s_r}|H_0}(\boldsymbol{s_r}|H_0)} = \max_{\widehat{\boldsymbol{\theta}}} \Lambda(\boldsymbol{s_r}|\widehat{\boldsymbol{\theta}}) = \Lambda(\boldsymbol{s_r}|\widehat{\boldsymbol{\theta}}_{ML}) \tag{3.13}$$

Similar to the estimation problem, the likelihood function can be directly related to the detection metric, knowing that the distribution of the received signal vector under H_0 is independent of the parameter signal vector $\boldsymbol{s_r}$. Thus, the detection metric is expressed as:

$$D_k(\widehat{\boldsymbol{\theta}}_{ML}) \underset{D_0}{\overset{D_1}{\gtrless}} \gamma \tag{3.14}$$

As we have seen previously, the threshold setting process in satellite signal acquisition is performed using the Neyman-Person criterion which optimizes the detection probability under the constraint of a limited false alarm, i.e. the probability of detection is attempted to be maximized for a fixed false alarm probability. The probability density function of the detection metric under both hypotheses must then be known.

Based on the detection threshold γ, the probability of detection P_d and the probability false alarm P_{fa} are respectively given by:

$$P_d = \int_{\gamma}^{\infty} f_{D_k(\widehat{\boldsymbol{\theta}}|H_1)}(x|H_1) \cdot dx \tag{3.15}$$

and

$$P_{fa} = \int_{\gamma}^{\infty} f_{D_k(\hat{\boldsymbol{\theta}}|H_0)}(x|H_0) \cdot dx \tag{3.16}$$

The different probabilities that represent the main measures of performance of the acquisition as a detection problem are summarized in Figure 3.1.

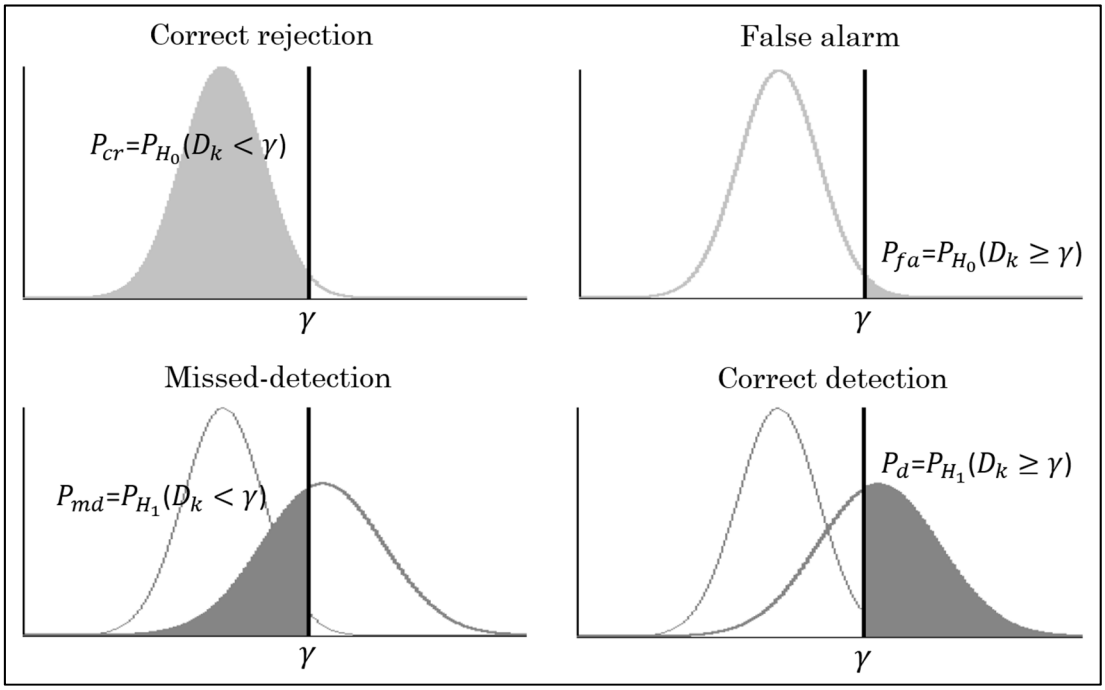

Figure 3.1 GNSS signal acquisition characterization as a detection problem

3.2.3 Structure of GNSS acquisition schemes

To track and decode the information in the GNSS signal, an acquisition method must be used to detect the presence of the signal. It is necessary to know how much data is needed to complete the acquisition; the longer the data, the longer the processing time. There are two factors that limit the choice of data length: the length of navigation data that is 20 ms, and the Doppler frequency change. The length of the navigation data is 20 ms, so the maximum length is 10 ms; this is based on the fact that if the first 10 ms of the data contain a phase transition due to the bit of the navigation data, there will be no phase transition in the next 10 ms of data. It is then sufficient to carry out the acquisition on a 1 ms of information; if there is a transition

in the duration of 1 ms of navigation information, there will be no data transition for the next 19 ms. Thus, at least a few milliseconds of data must be used for the acquisition to be successful. A rule of thumb is to use one or two thousandths of a second of data for strong signals, and use around five to ten milliseconds of data for weaker signals. But, the problem is how to know if a signal from a given satellite is strong or weak before acquisition. Then, it is recommended to acquire at least two sets of consecutive data (Tsui, 2005).

Thus, in order to achieve its ends, the acquisition process can be presented as the composition of two processing blocks: correlation and detection (Borio, 2008; O'Driscoll, 2007b). This structure of the GNSS signal acquisition process is shown in Figure 3.2 [Adapted from (Esteves, 2014b)].

The correlation block consists of scanning the search space for unknown parameters (code phase and Doppler frequency), generating for each set of different candidate parameters a metric that corresponds to the correlation output and that is a function of the code phase and Doppler frequency estimate values. The metric corresponds to the product of the GNSS incoming signal and the correlation of its code with a locally generated circularly shifted replica. Different methods can be used to perform this search process, we will see them in the next section. On the other hand, the detection block consists of generating a detection metric from the output of the correlation block in order to decide the presence of the satellite signal under test. Different signal integration techniques exist for the detection of GNSS signals depending on signal strength, signal structure or expected parameters.

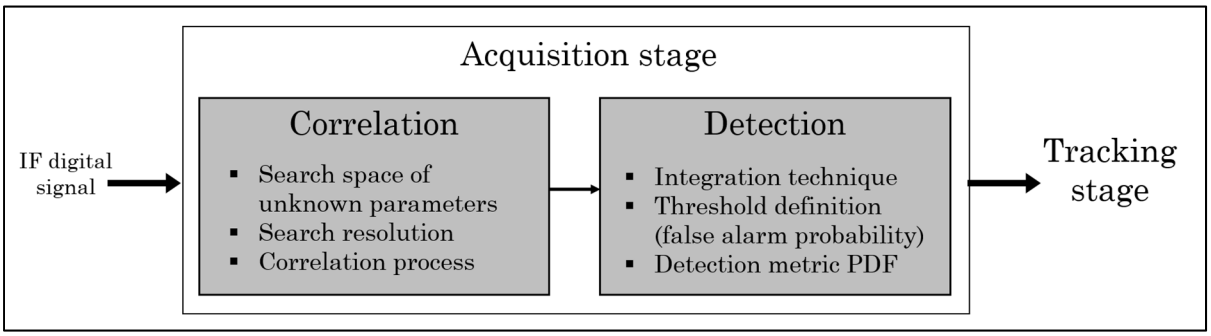

Figure 3.2 Structure of GNSS signal acquisition scheme

3.3 Correlation operation

As we have seen previously, the task of an acquisition channel is to determine the presence of a signal emitted by one satellite in particular from all the signals received simultaneously and provides a rough estimation of the code phase and the Doppler frequency of the incoming signal. To do this, a two-dimensional (2D) search space is defined to scan all possible combinations of code and Doppler which is composed of an infinite number of options. The usual approach is to establish a search grid to cover this 2D space where all the points are evaluated. The search process for all sets of code delay and Doppler frequency is shown in Figure 3.3 that represents the acquisition search grid, in which ΔT and $\delta\tau$ represent the code delay uncertainty range and the code delay search grid resolution respectively; and, ΔF_d and δf_d represent the Doppler shift uncertainty range and the Doppler shift search grid resolution respectively.

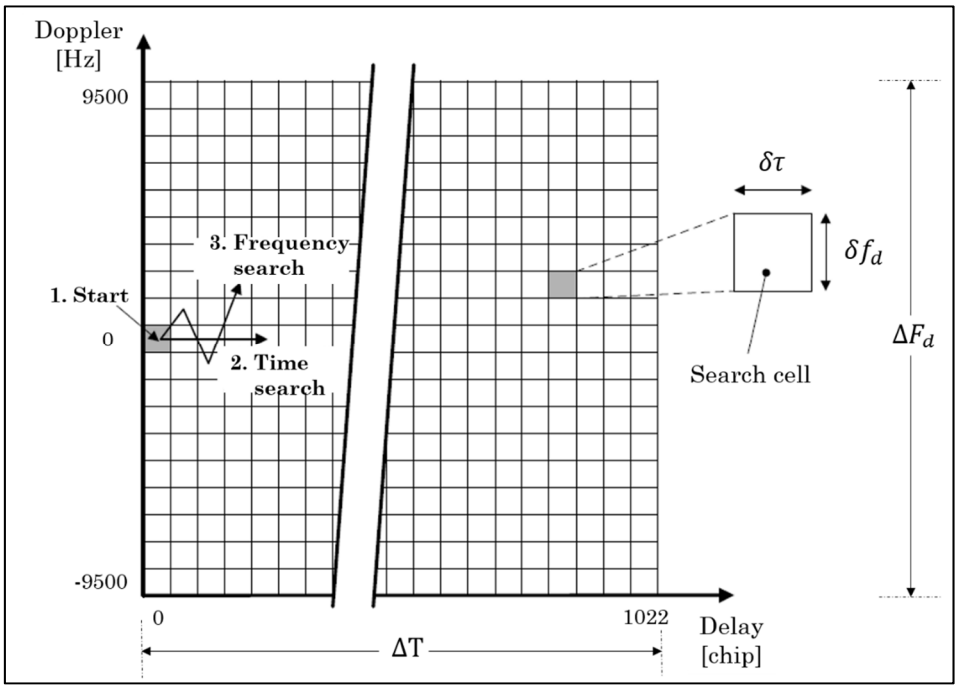

Figure 3.3 Acquisition search principle

Each search cell represents a combination of code delay and Doppler frequency and consists of a candidate code delay $\hat{\tau}_i = i \cdot \delta\tau$ and Doppler shift $\hat{f}_{d_j} = j \cdot \delta f_d - \Delta F_d/2$. We call "correct

cell" the cell corresponding to the best approximation of the true values of the parameters τ and f_d. Using the correlation operation, the aim of the acquisition process is to determine the code delay and the Doppler frequency of the received signal. The error in the estimation of the code delay is denoted by $\Delta\tau = \tau - \hat{\tau}$ and the Doppler frequency estimation error is denoted by $\Delta f_d = f_d - \hat{f}_d$. Then, the maximum estimation error that may be incurred at the right search cell (representing the good set of code delay and Doppler) is half of the search grid resolution (Kaplan et Hegarty, 2006). Indeed, the worst-case estimation errors on the correlation output at the good search cell has to be considered in the search resolutions for each parameter.

To achieve the objectives of the acquisition, the receiver first correlates the received GNSS signal with a replica of the carrier and the spreading code generated by the receiver itself. The incoming signal is then multiplied by a sinusoid and a local spreading code. As we saw in Figure 2.11, the signal is then integrated in order to generate the in-phase correlator output I. To get the quadrature-phase correlator output Q, the same process is carried out with a shifted sinusoid of $\pi/2$ (Tsui, 2005).

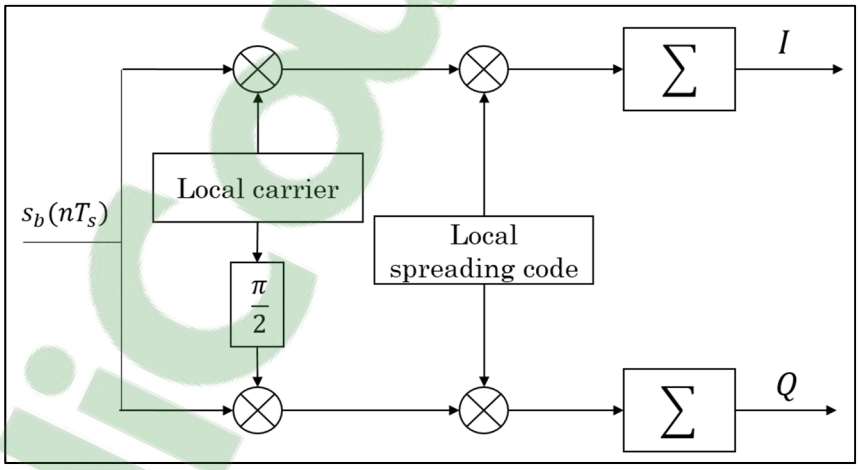

Figure 3.4 Correlation operation architecture

Assuming that $\hat{\tau}$ and $\hat{f}_d$ represent the estimated values of the code delay and the Doppler, we compute the accumulation terms in-phase I and quadrature-phase Q such that:

$$I = \sum_{n=0}^{N_s-1} s_b(nT_s) \cdot c_k[(1+\alpha_k)nT_s - \hat{\tau}_k] \cos\left(2\pi(f_{IF} + \hat{f}_{d,k})nT_s\right) \tag{3.17}$$

$$Q = -\sum_{n=0}^{N_s-1} s_b(nT_s) \cdot c_k[(1+\alpha_k)nT_s - \hat{\tau}_k] \sin\left(2\pi(f_{IF} + \hat{f}_{d,k})nT_s\right) \tag{3.18}$$

where α_k represents the Doppler effect on the code which is neglected which is often neglected to simplify the signal model.

Code step

The correlation operation is dependent upon the GNSS signals properties, particularly the spreading code properties. When the spreading code is correlated to itself, two cases are possible: the result of the correlation is equal to 1 for a perfect alignment and close to zero for a misalignment. Similarly, the correlation result is zero when two different spreading codes are correlated. The correlation between two discrete signals is defined as:

$$R_{c_x}(\tau) = \frac{1}{N_s} \sum_{n=0}^{N_s-1} c_x(nT_s) c_x(nT_s - \tau) \tag{3.19}$$

In continuous form, this correlation operation is expressed as:

$$R_{c_x}(\tau) = \frac{1}{T_{c_x}} \int_0^{T_{c_x}} c_x(t) c_x(t-\tau) dt \tag{3.20}$$

where the index "x" on c_x indicates whether it is a primary or secondary code, likewise to differentiate whether it is a code on pilot component or on data component.

For example, the auto-correlation function between the local and the incoming spreading code of the GPS L1 C/A (PRN 2) is shown in Figure 3.5.

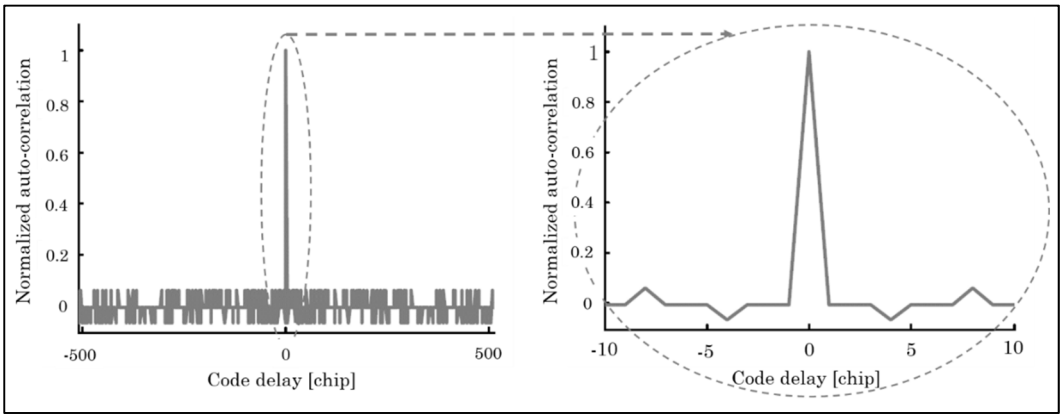

Figure 3.5 Auto-correlation function of the GPS L1 C/A (PRN 2)

As we have seen previously, the correlation operation depends on the spreading code properties. In fact, the spreading codes used in GNSS have been carefully selected according to their auto-correlation and cross-correlation properties. The spreading codes are selected in order to have cross-correlation values as low as possible, and auto-correlation values as low as possible except only if it is aligned with itself which corresponds to the maximum value when the chip code of the received signal is perfectly aligned with that one of the local copy. The auto-correlation and cross-correlation functions for GPS L1 code, GPS L5 code and Galileo E1 code are presented respectively in (Figure 3.6), (Figure 3.7) and (Figure 3.8).

The correlation of secondary codes will be discussed in Section 4.7 where we will discuss the proposal in a way to reduce complexity for the acquisition of new signals with longer secondary codes. We will see that the longer is the code, the better are the correlation properties (Leclère, Andrianarison et Landry, 2017).

According to (Foucras, 2015), the secondary peaks maximum values, in dB, of the auto-correlation and the cross-correlation for the GPS L1 C/A and Galileo E1 OS signals are summarized in Table 3.1. For that, all the PRN codes (or all couple of PRN codes) are

computed and the Doppler frequency range is [-10 kHz, 10 kHz]. CBOC modulation is considered for the Galileo E1 OS signal.

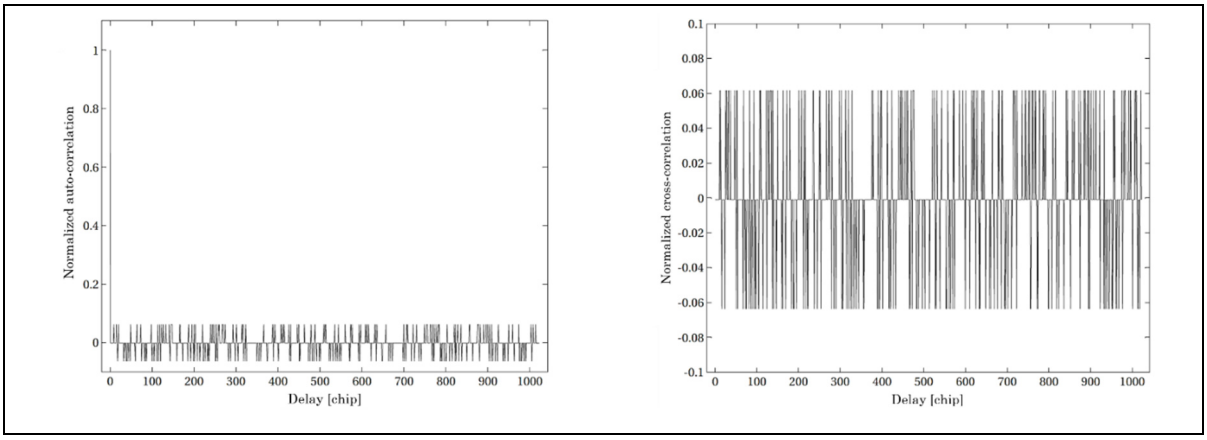

Figure 3.6 Auto-correlation (left) and cross-correlation (right)
of a GPS L1 C/A code (1023 chips)

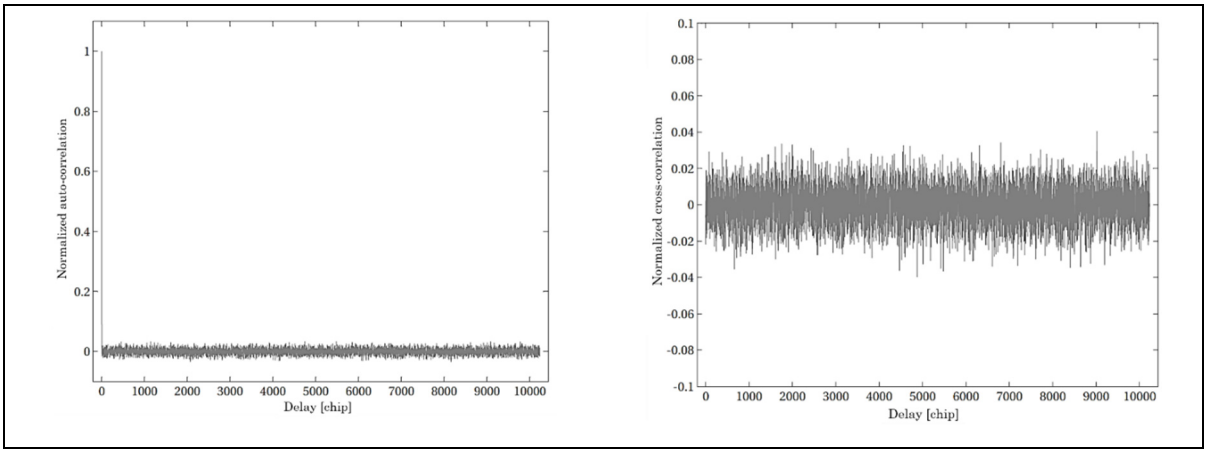

Figure 3.7 Auto-correlation (left) and cross-correlation (right)
of a GPS L5 code (10230 chips)

Table 3.1 Maximum secondary peaks values of the correlation function

Signals	**Auto-correlation [dB]**		**Cross-correlation [dB]**	
	$f_d = 0$ **Hz**	$f_d \in$ **[0,10] kHz**	$f_d = 0$ **Hz**	$f_d \in$ **[0,10] kHz**
GPS L1 C/A	-23.94	-19.18	-23.94	-19.08
Galileo E1 OS	-25.39	-23.44	-26.66	-25.16

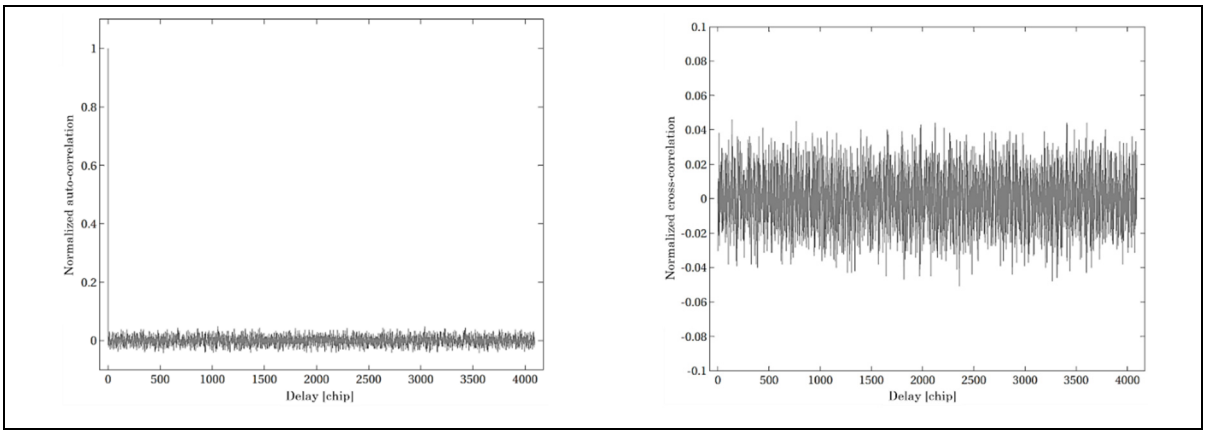

Figure 3.8 Auto-correlation (left) and cross-correlation (right)
of a Galileo E1 code (4092 chips)

Note that the values of cross-correlation for Galileo E1 OS in Table 3.1 correspond to the values for the same satellites. For different satellites, the maximum values for the secondary peaks are -24.49 dB and -22.82 dB for $f_d = 0$ Hz and $f_d \in [0,10]$ kHz respectively.

The number of code delay to be tested is equal to the number of samples per code period, N_s, which is a multiple of the number of chips per code, N_c. The parameter $\hat{\tau}$ takes a finite number of values, which is $i \cdot \delta\tau$ where i is an integer between 0 and $N_s - 1$. During search process, the best case is that the code delay of the incoming signal falls exactly on a code delay tested ($\hat{\tau} = \tau_k$), i.e. $\tau_k = i \cdot \delta\tau$; and the worst case is that the code delay of the incoming signal falls exactly on the middle of two delays tested, i.e. $\tau_k = (i + \frac{1}{2})\delta\tau$. To better estimate the code, some proposals of the step have been used in the literature. For example, for a BPSK modulation, $\delta\tau$ is chosen for a half of a chip; and for a BOC(1,1) modulation, $\delta\tau$ is chosen for one sixth of a chip (van Diggelen, 2009). Figure 3.9 shows the best case that may happen during the search corresponding to the BPSK and the BOC(1,1) modulation, i.e. $\tau_k = i \cdot \delta\tau$. And the worst cases for both modulation are shown in Figure 3.10, in which the code delay mismatch between τ_k and the closest code bin is $\delta\tau/2$. In Figure 3.9 et Figure 3.10, $\delta\tau$ is half a chip for BPSK modulation and one sixth of a chip for BOC(1,1) modulation.

Note that the maximum loss, due to code delay mismatch, depends on the step used in code search. For example, the loss corresponding to the code step for a BPSK modulation is summarized in Table 3.2 (van Diggelen, 2009).

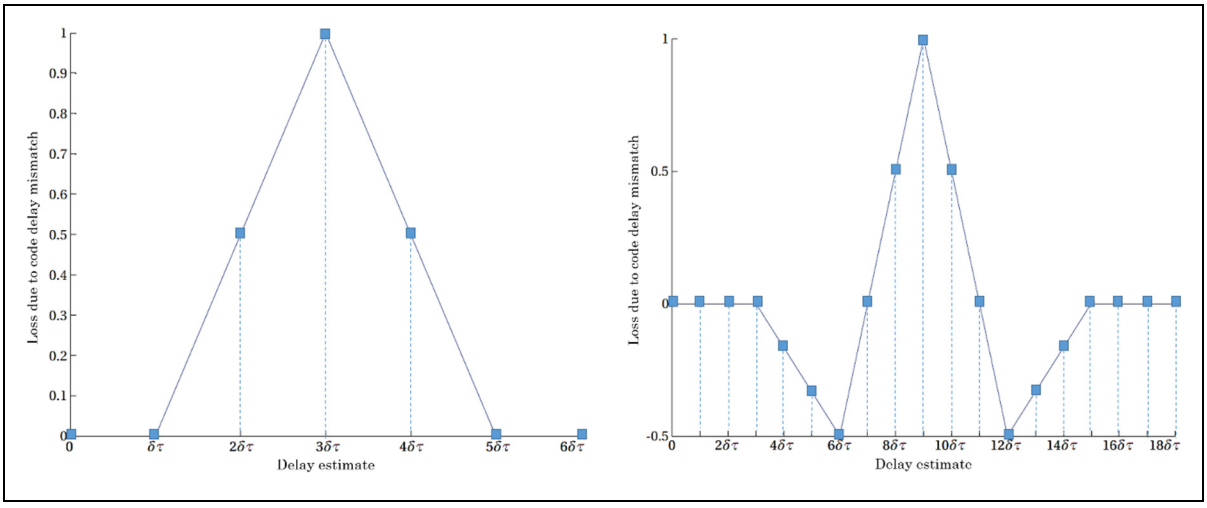

Figure 3.9 Loss due to the code step in the best case
for a BPSK modulation (left) and for a BOC(1,1) modulation (right)

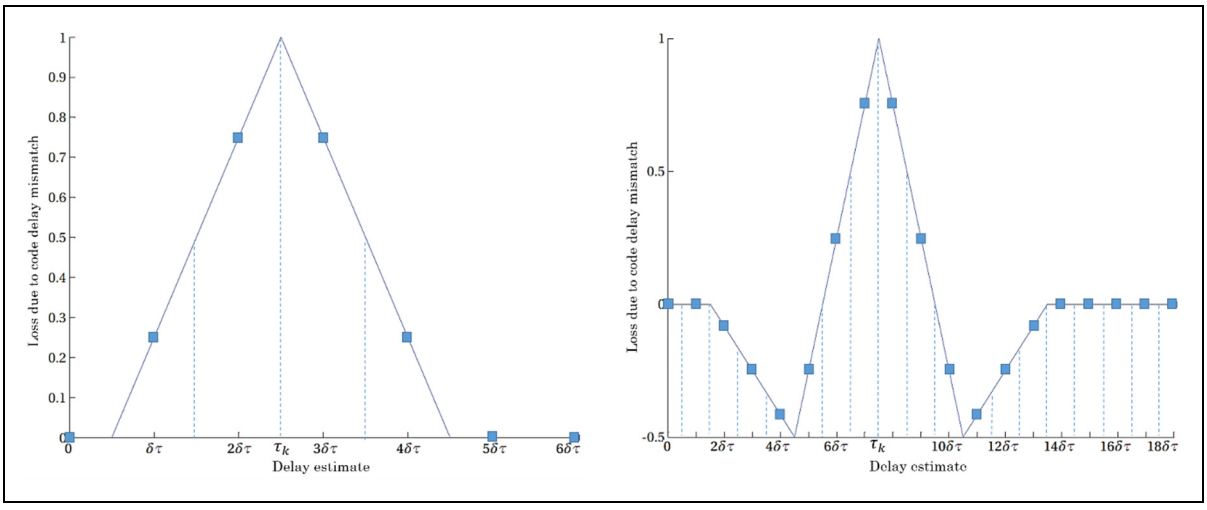

Figure 3.10 Loss due to the code step in the worst case
for a BPSK modulation (left) and for a BOC(1,1) modulation (right)

Table 3.2 Loss due to the code delay mismatch w.r.t the code step (BPSK modulation)

Code step	1 chip	$\frac{1}{2}$ chip	$\frac{1}{3}$ chip	$\frac{1}{4}$ chip
Maximum code delay error	$\frac{1}{2}$ chip	$\frac{1}{4}$ chip	$\frac{1}{6}$ chip	$\frac{1}{8}$ chip
Maximum loss [dB]	-6.0206	-2.4988	-1.5836	-1.1598
Average loss [dB]	-2.4988	-1.1598	-0.7558	-0.5606

Frequency step

Similarly as $\hat{\tau}$, the parameter $\hat{f}_d$ takes a finite number of values during the search process. The same approach as the code delay search is followed. The number of the parameter $\hat{f}_d$ depends on the range of the frequency search space and the search grid resolution over the frequency, which is defined according to the maximum estimation error of the Doppler shift. The number of frequency bins to be scanned is N_{f_d} that is obtained as the ratio between the uncertainty in the Doppler frequency dimension and the chosen grid resolution. The values taken by $\hat{f}_d$ are $j \cdot \delta f_d - \Delta F_d/2$, where j is an integer.

Based on the estimation of the parameters τ and f_d, the correlation output, which is the module of $S_k(\hat{\tau}, \hat{f}_d)$, is expressed as:

$$
\begin{aligned}
\left|S_k(\hat{\tau}, \hat{f}_d)\right| &= \left|\sum_{n=0}^{N_s-1} s_b(nT_s) \cdot c_k(nT_s - \hat{\tau}_k)\, \mathrm{e}^{\{-\mathrm{j}2\pi(f_{IF}+\hat{f}_{d,k})nT_s\}}\right| \\
&= \sqrt{2P_{b,k}}\left|\sum_{n=0}^{N_s-1} c_k(nT_s - \tau_k)c_k[nT_s \right. \\
&\quad \left. - \hat{\tau}_k]\, \mathrm{e}^{\{\mathrm{j}2\pi(f_{IF}+f_{d,k})nT_s+\varphi_{b,k}\}}\mathrm{e}^{\{-\mathrm{j}2\pi(f_{IF}+\hat{f}_{d,k})nT_s\}} + \eta(nT_s)\right| \\
&= \sqrt{2P_{b,k}}\left|\sum_{n=0}^{N_s-1} c_k(nT_s - \tau_k)c_k(nT_s - \hat{\tau}_k)\, \mathrm{e}^{\{\mathrm{j}2\pi\Delta f_d nT_s\}} + \eta(nT_s)\right| \qquad (3.21)
\end{aligned}
$$

Thus, this correlation can be approximated by:

$$\left|S_k\left(\hat{\tau}, \hat{f}_d\right)\right| \approx \sqrt{2P_{b,k}}\, N|R(\Delta\tau)||\mathrm{sinc}(\Delta f_d N T_s)| + \eta_n \tag{3.22}$$

where $R(\Delta\tau)$ represents the auto-correlation function of $c_k[nT_s]$ evaluated at the relative code delay $\Delta\tau$, and $\mathrm{sinc}(\Delta f_d N T_s) = \frac{\sin(\pi \Delta f_d N T_s)}{\pi \Delta f_d N T_s}$, represents the transfer function of the matched filter as a low-pass filter. Thus, any frequency estimation error can be considered as an attenuation through the sinc function into the correlation output. The loss due to the frequency mismatch is function of the product $\Delta f_d N T_s$.

During search process, the best case is that the received frequency of the incoming signal falls exactly on a frequency tested ($\hat{f}_d = f_{d_k}$), i.e. $f_{d_k} = j \cdot \delta f_d - \Delta F_d/2$; and the worst case is that the frequency of the incoming signal falls exactly on the middle of two frequencies tested, i.e. $f_{d_k} = (j + \frac{1}{2})\delta f_d - \Delta F_d/2$. To better estimate the frequency, some proposals of the step have been used in the literature, and the maximum loss is different according to the step used. For example, two typical choices of the Doppler search resolution are: $\delta f_d = \frac{1}{2T_c}$ and $\delta f_d = \frac{2}{3T_c}$ (Kaplan et Hegarty, 2006; van Diggelen, 2009). Using $\delta f_d = \frac{1}{T_c}$, the best case and the worst case of the loss due to the frequency step are shown in Figure 3.11.

The maximum loss of the correlation output due to the Doppler frequency estimation error is:

$$L_{\Delta f_d,\max} = 10\log_{10}\left|\mathrm{sinc}\left(\frac{\delta f_d}{2} N T_s\right)\right| \tag{3.23}$$

Knowing that the maximum loss is different according to the step used, the loss due to the Doppler frequency mismatch for a coherent integration time T_c is summarized in Table 3.3 (Kaplan et Hegarty, 2006; van Diggelen, 2009).

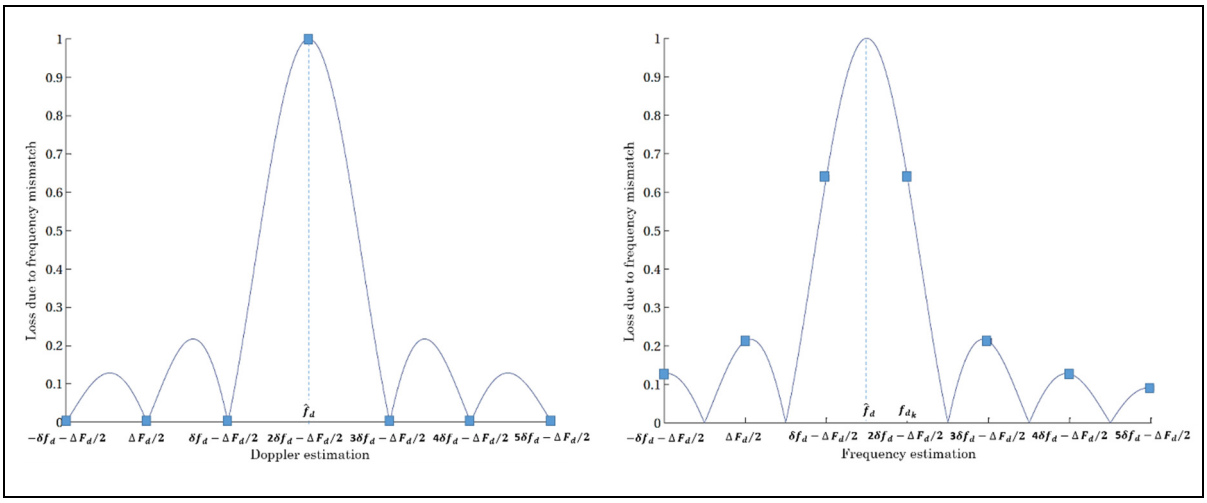

Figure 3.11 Loss due to the frequency step
in the best case (left) and in the worst case (right)

Table 3.3 Loss due to the Doppler frequency mismatch

Frequency step	$\frac{1}{T_c}$	$\frac{2}{3T_c}$	$\frac{1}{2T_c}$
Maximum frequency error	$\frac{1}{2T_c}$	$\frac{1}{3T_c}$	$\frac{1}{4T_c}$
Loss [dB]	-3.9224	-1.6500	-0.9121

Finally, the total number of search cells to be scanned within acquisition is $N_s \times N_{f_d}$. According to the GNSS applications, this number can reach the order of 10^6 points. Thus, the search space is very large which involves high complexity and requires faster processing. Treatment of this compromise is part of the work of this thesis.

As we saw previously, the existing correlation methods can be classified into two categories: the time-domain acquisition method (serial search) and the frequency-domain acquisition methods which encompasses all other methods. The next section will develop the different methods of acquisition SS, PFS, PCS, and other methods) with their performance comparison.

3.4 Acquisition methods

3.4.1 Serial search

At the start of a GNSS receiver, the device is confronted with the following problem. The receiver does not know the phase of the PRN code inside the sampled signal as well as the frequency of the carrier since it receives a Doppler effect due to the movement of the satellites and the receiver. The exact role of the acquisition module is therefore to provide an approximation of the phase of the PRN code and the frequency of the carrier. As its name suggests, the serial or sequential acquisition is performed by attempting to correlate the incoming signal with all possible combinations of frequencies and code phases. It is the simplest GNSS correlation method where the CAF is computed for one couple $\left(\hat{f}_d, \hat{\tau}\right)$ at a time, and the computation is repeated for different $\hat{f}_d$ and different $\hat{\tau}$. It corresponds to the CAF expression:

$$S_k\left(\hat{\tau}, \hat{f}_d\right) = \sum_{n=0}^{N_s-1} s_b(nT_s) c_k(nT_s - \hat{\tau}_k)\, \mathrm{e}^{\{-\mathrm{j}2\pi(f_{IF}+\hat{f}_{d,k})nT_s\}} \tag{3.24}$$

The block diagram proposed by (Borre et al., 2007) corresponding to the serial search is shown in Figure 3.12:

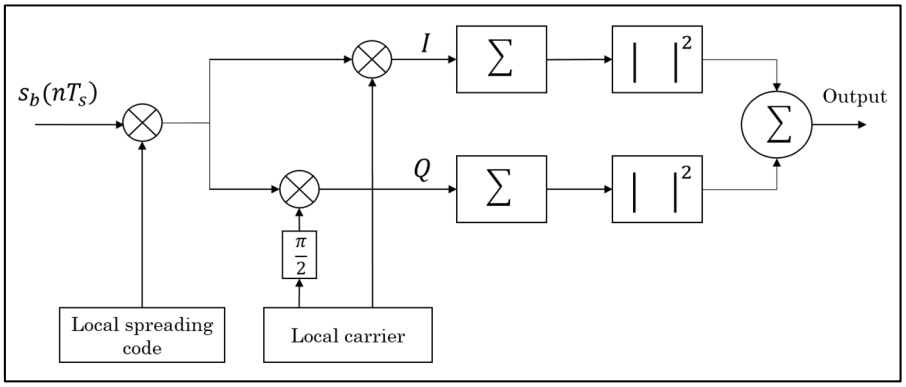

Figure 3.12 Block diagram of a serial search acquisition

The first step is to multiply a replica of the spreading code having a certain phase with the signal in order to correlate it. This result is then multiplied by a replica of the carrier frequency having a certain Doppler. These operations are performed for a certain integration period (typically 1 ms for GPS L1 C/A code) for sampling a complete period of the PRN code. Finally, the results are compared with a threshold to determine whether there has been a correlation or not. If so, the information is transmitted to the tracking module, and if not, it passes to the next phase increment or frequency.

Assuming one chip spacing between the code delay values (N_c = 1023), and Doppler frequency search space of (IF ± 10 kHz) and Doppler bin spacing of 500 Hz, 41943 combinations have to be searched. This large number of operations is a weak point for the SS algorithm. Thus, in order to reduce the acquisition search complexity, FFT technique can be used to eliminate one of these parameters and perform the search in parallel and in one dimension.

3.4.2 Parallel code search

The first mention of parallelism during the GNSS signal acquisition were introduced in (Van Nee et Coenen, 1991). They proposed to parallelize the research on the code phases in order to reduce the number of iterations of the algorithm. Indeed, using the circular correlation property of the signal, the algorithm does not need to generate the 1023 versions of the same PRN code. The circular correlation is the result of the product, in the frequency domain, between the incoming signal and the conjugate complex of a version of the PRN code. After reconverting the correlation in the time domain, we can determine whether the signal strength is greater than the acquisition threshold. The block diagram presented in (Tsui, 2005) corresponding to the parallel code search (PCS) is shown in Figure 3.13.

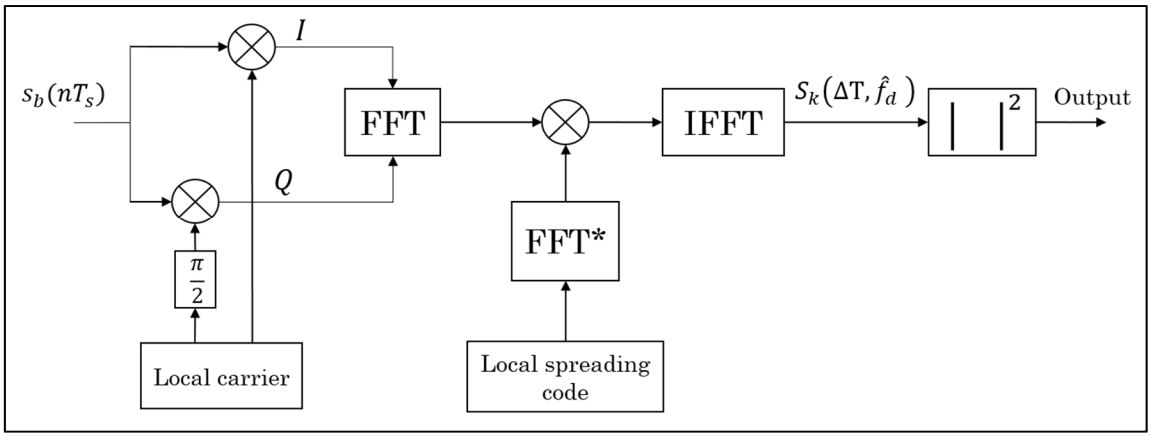

Figure 3.13 Block diagram of the parallel code search acquisition

The objective of this method is to propose a new acquisition architecture to solve the defects of the serial acquisition method, such as the execution time (large number of operations). This is always a correlation between the incoming signal and a replica of the code generated by the receiver. In order to gain in execution time (reduce the number of operations), the PCS method uses the circular correlation between the input signal and the PRN code generated Figure 3.13 instead of a correlation of the 1023 shifted replicas (serial acquisition).

The multiplication of the input signal with the replica of the code generated by the receiver gives rise to the phase I and quadrature phase Q components of the signal. The signal resulting at the input of the FFT is then $s(n) = I(n) + jQ(n)$. On the other hand, the generated PRN code is obtained in the frequency domain after passing through the FFT. The conjugate of the resulting complex signal is then calculated. The two signals resulting from the FFT of $s(n)$ and the FFT of the PRN code are then multiplied and are then brought back to the time domain by an inverse FFT (IFFT). The correlation between the input signal and the PRN code is then given by the module of the signal at the output of the IFFT. If a correlation peak appears, the coordinates of this peak define the delay of the code and the Doppler frequency shift. However, the code delay is expressed in number of samples and not in code chips, as in the SS method.

The theory behind the PCS method is described in the following (Pany, 2010). The *N*-point DFT of a finite length sequence, $[k]$, with length *N*, is:

$$X[k] = \sum_{n=0}^{N-1} x[n]\, \mathrm{e}^{-\mathrm{j}2\pi kn/N} \tag{3.25}$$

The PCS method uses the convolution theorem which states that the convolution of two sequences in the time-domain can be obtained through multiplication of these sequences in the frequency-domain. So, the circular cross-correlation between two finite sequences, $x[n]$ and $c[n]$, both of the length N, is obtained as:

$$h[n] = \frac{1}{N} \sum_{m=0}^{N-1} x[m]c[m+n] \tag{3.26}$$

Then, the *N*-point DFT of $h[n]$ is expressed as:

$$\begin{aligned} H[k] &= \sum_{n=0}^{N-1} \sum_{m=0}^{N-1} x[m]c[m+n]\mathrm{e}^{-\frac{\mathrm{j}2\pi kn}{N}} \\ &= \sum_{n=0}^{N-1} \sum_{m=0}^{N-1} x[-m]c[m-n]\mathrm{e}^{-\frac{\mathrm{j}2\pi kn}{N}} \\ &= \sum_{m=0}^{N-1} x[m]\mathrm{e}^{\frac{\mathrm{j}2\pi km}{N}} \sum_{n=0}^{N-1} c[m+n]\mathrm{e}^{-\frac{\mathrm{j}2\pi k(m+n)}{N}} \\ &= X^*[k]C[k] \end{aligned} \tag{3.27}$$

where $X^*[k]$ is the complex conjugate of $X[k]$.

The PCS concept can be used to efficiently calculate the correlation of the incoming signal with the local replica of the PRN code. The advantage of this method is the reduction in the number of operations and the accuracy with respect to the SS and PFS methods. On the one hand, the PRN code is generated once for all the frequency domain scanning operations. On the other hand, the precision is now on the number of samples (N_s = 60000 samples for a f_s = 60 MHz) instead of 1023 chips. The method is used in most of the FFT-based acquisition

methods and software receivers because of its superior performance, low computational complexity, and fast execution time.

For example, using the PCS acquisition method, Figure 3.14 shows the acquisition results after 1 ms of coherent integration, corresponding to PRN 19 of GPS L1 C/A signal, in which the correlation peak is clearly visible, it means that acquisition is successful. The frequency search is performed on [-5 kHz, +5 kHz].

Despite the advantages of the PCS method, there are nevertheless two major drawbacks: the dependence with the sampling frequency and the sensitivity to the transition of bits.

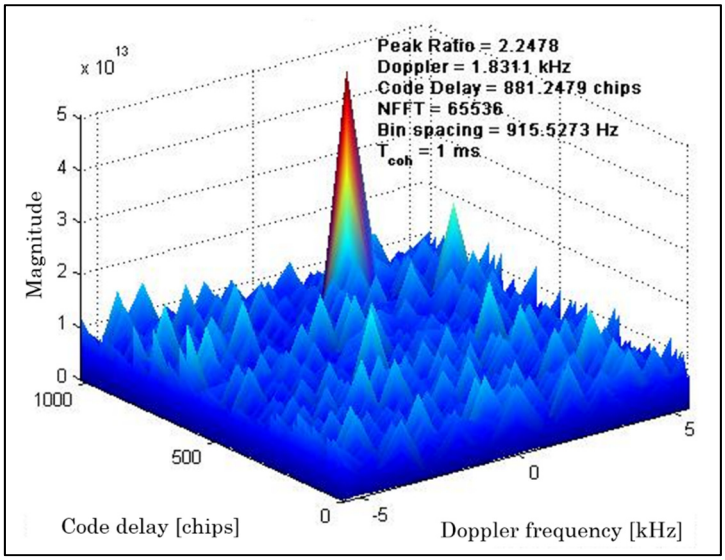

Figure 3.14 Acquisition results for PRN 19
(GPS L1 C/A signal) with T_{coh} = 1 ms

On the one hand, the FFT length being the number of samples in a code period, it directly depends on the sampling frequency. However, the choice of the length is sometimes limited, so a problem can arise when the length of the FFT does not correspond to the length of a code period, and it is not possible to extend the sequences using more samples or zero padding (Ziedan, 2006). Thus, a peak maximum reduction could have occurred which results in a reduction of the SNR. According to (Leclère, Botteron et Farine, 2010a), the number of points

to be scanned should be at least twice the number of samples in a code period to ensure that there will be any loss. On the other hand, unlike the SS method, one period of the incoming code is sufficient to search for all code phases (sequential search uses two periods). Therefore, the existence of a bit transition can result in losses. The bit transition may be from data or a secondary code. This problem can be solved by doubling the size of the FFT and filling the local code replica with zero (Foucras, 2015).

3.4.3 Parallel frequency search

We have seen that the serial search method is very expensive in execution time. Therefore, it is necessary to eliminate one of the two parameters to be searched, or if necessary to do so in parallel. The parallel frequency search (PFS) method proposed in this paragraph consists in parallelizing the search for a single parameter which is the frequency. Thus, the scanning of the frequency space is no longer performed, thus eliminating the corresponding search operations. This method is similar to that of the serial search method, where the incoming signal is multiplied by a PRN code corresponding to a well-defined satellite, with a code delay ranging from 0 to 1022. The resulting signal is then obtained in the frequency domain by the Fourier Transform. If the number of samples in the input sequence is a power of 2, the FFT can be used. For further details on FFT, the reader may refer to Annex VII.

(Van Nee et Coenen, 1991) proposes to use a FFT on the result of the multiplication of the input signal and a local version of the given PRN code in order to know the power of its frequency spectrum. This method uses the CDMA demodulation properties. In the event that the incoming signal would be aligned with the local replica of the PRN code, the result of their multiplication would be a pure sinusoidal wave. One of the modes of the FFT will be very high in the case of an alignment and it will make it possible to detect an approximation of the carrier frequency. If the coefficients all have a similar amplitude, the code is not aligned and the algorithm is repeated by shifting the code of a chip. The block diagram of the parallel frequency search method is shown in Figure 3.15.

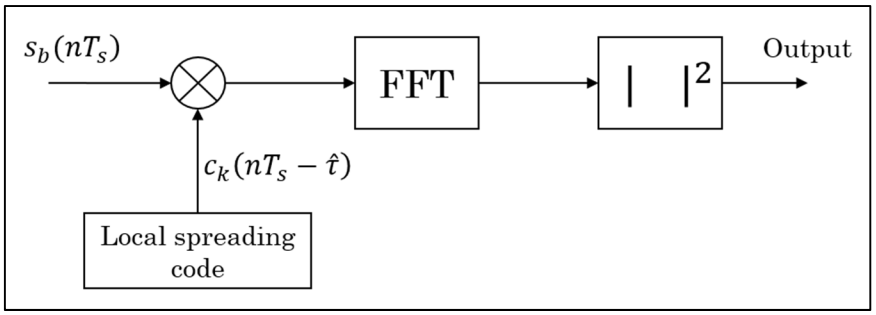

Figure 3.15 Block diagram of the parallel frequency search acquisition

The signal at the output of the FFT is then complex. If the PRN code generated by the receiver is perfectly aligned with the incoming signal, we can see in this case a correlation peak located at a frequency f_b which is equal to the sum of the desired Doppler shift and the intermediate frequency. The precision of this method at the frequency level depends on the number of samples existing in the processed data. For example, for a sampling frequency f_s = 60 MHz and for 1 ms code duration, we have $N_s = \frac{f_s}{1000} = 60000$ samples. The scanning in this method is done only on 1023 chips of code, which implies a significant gain in computation time compared to the SS method. However, it loses in terms of accuracy.

The idea of reducing the acquisition time by parallelizing the search in the frequency search space can be observed by the operation carried out after the code removal for different $\hat{f}_d$:

$$S_k(\hat{\tau}, \hat{f}_d) = \sum_{n=0}^{N_c-1} s_b(nT_s)c_k(nT_s - \hat{\tau}_k)\, \mathrm{e}^{\{-\mathrm{j}2\pi(f_{IF}+\hat{f}_{d,k})nT_s\}} \tag{3.28}$$

A parallel with the DFT of a sequence $x[n]$ of N_c points can be performed using Equation 3.25, in which $x[n] = s_b(nT_s)c_k(nT_s - \hat{\tau}_k)$ and $\frac{kn}{N_c} = \left(f_{IF} + \hat{f}_{d,k}\right)nT_s$, i.e. $\hat{f}_{b,k} = \frac{k}{N_cT_s} = \frac{k}{T_c}$.

With the PFS method, the CAF for all the frequencies simultaneously for a specific $\hat{\tau}$ is obtained. However, this approach has major disadvantages. First, a large FFT may be required

depending on the sampling frequency and the coherent integration time; which is a limitation for some implementations. In addition, the frequency search space is imposed by the FFT and could be too large. The sampling frequency f_s is about several MHz while the useful frequency search space is only an order of a several kHz, which is inefficient because most of the points computed are not used. The other inconvenient is that the use of a step of $\frac{1}{T_c}$ can induce a loss of about 3.92 dB according to the
Table 3.3. However, if we reduce the frequency step by zero-padding the sequence before doing the FFT operation, it involves an increase in size, and is not practical as we saw previously.

3.4.4 Other methods

Other methods based on parallel search over code or frequency exist. For example, double-block zero padding (DBZP) is a method that mixes the PCS and the PFS (Foucras et al., 2012; Ziedan, 2006; Ziedan et Garrison, 2004). The DBZP method performs a search simultaneously several carrier frequencies as the PFS does, but the small accumulation carried out before the FFT operation is computed for several code phases using small FFTs. As its name suggests, we have to pad with zeros the portions of local code since the correlation is not circular. Despite its effectiveness, the DBZP suffers from the occurrence of data bit transitions. Indeed, the acquisition of the modernized GNSS signals can be seriously affected by the presence of bit sign transitions at each spreading code period. Hence the need to use an acquisition method that is insensitive to the bit sign transition. To overcome this problem, (Foucras, 2015) proposed the Double-Block Zero-Padding Transition Insensitive (DBZPTI) which is an improved and innovative acquisition method of the DBZP.

(Akopian, 2005) also proposed an alternative method that mixes the PCS and the PFS, which uses FFT to simultaneously search over the code and the frequency dimension. However, this proposal requires an increase in the memory in order to store intermediate results.

A variant of the PCS algorithm has been proposed in (Akopian, 2005) to overcome its greatest disadvantage in terms of execution complexity, i.e. the fact that the required FFTs are taken over the whole data blocks. This acquisition method, called bi-dimensional parallel search (BPS), is developed in which the entire data block is broken down into sub-blocks equivalent in length to the number of samples per code period, N_s. In (Pany, 2010), this acquisition method is called the "spectral shifting with Doppler preprocessing". The BPS method improves the search algorithm in both dimensions, code and Doppler frequency, which starts by breaking down the whole data block into the equivalent to one code period blocks, averaging the incoming signal over the total number of code periods contained in the signal, N_c. The block diagram of the BPS method is illustrated in Figure 3.16.

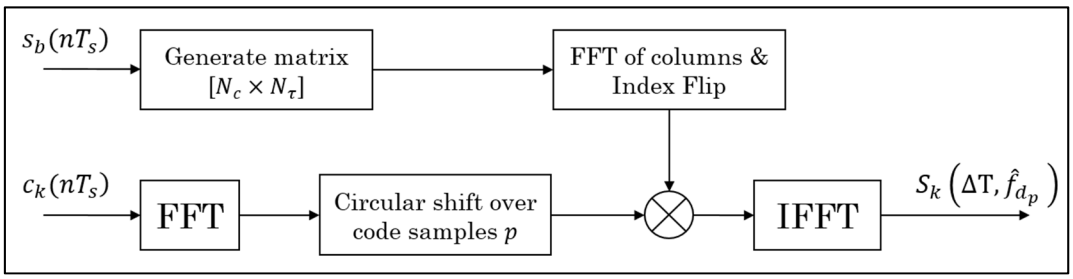

Figure 3.16 Block diagram of the bi-dimensional parallel search method

In Figure 3.16, the FLIP$\{x[n]\}$ operation inverts the positions of the entries of the $x[n]$ sequence, i.e. the last entry goes to the first place, and so on. For real-valued sequences, we have FLIP$\{\text{FFT}\{c[\cdot]\}\} = \text{FFT}^*\{c[\cdot]\}$.

3.4.5 Comparison between the three classical methods

The design of a GNSS receiver is based on one of the three methods presented above (SS, PCS or PFS). In order to make an informed choice, several factors must be taken into account. Of these, the two main factors to be considered are the execution time and the resources needed to implement the acquisition method. Table 3.4 highlights the comparison of the complexity for the different acquisition methods (Molino et al., 2008), in which: N_{f_d} represents the number of Doppler bins in the search space, N_s represents the number of samples in one integration period, N_c

represents the code delay resolution (typically 2 for half a chip resolution) and L_c represents the PRN code length (1023 for GPS L1-C/A).

Table 3.4 Complexity comparison for different acquisition algorithms

Method	**Multiplications**	**Summations**	**Repetitions**	**Complexity of implementation**
SS	$4N_{f_d}N_cN_sL_c$	$4N_{f_d}N_cN_sL_c$	$N_{f_d}N_cL_c$	Low
PCS	$N_{f_d}(4N_s\log_2 4N_s)$ $+ 4N_s\log_2 4N_s$	$N_{f_d}(6N_s\log_2 6N_s)$ $+ 3N_s\log_2 6N_s$	N_{f_d}	High
PFS	$4N_cN_sL_c$	$4N_cN_sL_c$	N_cL_c	Medium

From this comparison, it can be easily determined that acquisition using the PCS is the fastest method. Considering the fact that this method must calculate successively a FFT and an IFFT in the same iteration, it performs approximately 10 times less expensive operations than the PFS. Using the same approach, it can be said that PCS is about 10000 times faster than SS method acquisition. However, the PCS method is the most costly in terms of resources. Indeed, it has almost as many multipliers as the sequential method, but must also implement three FFT modules which requires specific amount of memory to store the coefficients and transform results. By observing only the resources used, the PFS is the most economical acquisition method. Considering other acquisition methods, BPS and DBZP correlation methods present a lowest complexity as the PCS. The details of the BPS technique will be presented in Chapter 5 where we propose the use of this technique to accelerate the calculation while increasing the sensitivity of the receiver using the CD approach. For details on the comparison of the PCS, BPS and DBZP, the reader is invited to read (Esteves, 2014b).

3.5 Summary

In this chapter, the basic principle of GNSS signal acquisition is presented. We have seen that acquisition problem can be treated as an estimation/detection problem in order to roughly estimate the code delay and the Doppler frequency, and therefore, to detect the satellites in

view. The acquisition module provides only a rough estimate of the Doppler frequency and the code delay.

GNSS signal acquisition can be seen as a two-step process: the detection metric is first calculated for all the unknown parameters combinations in the uncertainty search of interest and the highest detection metric is chosen as $\widehat{\boldsymbol{\theta}}_{ML}$ from the combination, corresponding to Equation (3.13); then the highest detection metric value is compared to a predefined threshold in order to make a decision if the signal is present or not, corresponding to Equation (3.14).

The Doppler frequency shift effect imposes a restriction on the length of the data. If a perfect correlation is done, the correlation peak decreases by half when a PRN code is changed by a half chip. The data size and coherent integration periods are important factors in FFT-based acquisition. As the coherent integration period increases, the data size becomes larger. On the other hand, the Doppler frequency resolution must become narrower because of the correlation peak roll-off. This requires higher Doppler frequency resolution, which induces larger number of FFT points. These effects should be carefully considered. Parallel methods can use two approaches: Discrete Fourier Transform or a faster Delay and Multiply method characterized by a low SNR (Tsui, 2005).

Despite the large reduction in the amount of computation of the PCS method, the implementation complexity of the algorithm is higher than that of the SS and PFS algorithms. This difference can be seen from the architecture of these different acquisition methods. The PCS acquisition is the method that forms the basis for the acquisition method used in this thesis. However, the basic model presented in the previous section needs some modifications in order to meet the requirements for the HS-CGR which is the main goal of this thesis. There is also a contribution in this thesis that proposes the use of the BPS acquisition method in CHAPTER 5.

The following chapter develops in depth the different techniques for acquiring low power GNSS signals which is the focus of this thesis.

CHAPTER 4

HIGH-SENSITIVITY ACQUISITION TECHNIQUES

This chapter will describe different techniques of GNSS signals acquisition in more detail by focusing on the most promising acquisition techniques with an investigation of the various sources of degradation of GNSS signals acquisition in deep urban environments. The chapter begins with a state of the art of high sensitivity techniques and their limitations. A presentation of the different architectures of high sensitivity GNSS receivers will then be carried out before developing assisted GNSS techniques and combined acquisition approaches. At the end, we will present some techniques proposed in order to reduce the complexity of computation during the acquisition of the secondary codes.

4.1 Existing works

Satellite positioning systems have been used for many years in the field of air, naval and automotive navigation, but their use in difficult environments, such as urban city, inside building, deep forest, under tunnel, is still very limited. Studies by (Melgard, Lachapelle et Gehue, 1994; Peterson et al., 1995; Seco-Granados et al., 2012) demonstrate the significant degradation of satellite signals when subjected to this type of environment. Methods developed over the last two decades to address this issue can generally be classified into three distinct categories: the use of complementary RF (radiofrequency) signals, the use of advanced signal processing techniques, and the use of external sensors.

Knowing that it is difficult to process satellite signals in GNSS-denied environments, here are some techniques proposed in the literature for navigation or positioning in challenging environments.

The proposed methods for the acquisition of weak signals share the same basic idea of increasing the integration time in order to increase the signal strength during the correlation and possibly at the end of the acquisition. The key idea for acquiring highly degraded GNSS

signals is the optimal combination between coherent integration and non-coherent accumulation to increase hold time for periods of up to several hundred milliseconds (Ioannides, Aguado et Brodin, 2006). The period of the coherent integration must be limited to 20 ms because of the length of the navigation bits with the residual frequency errors resulting from the relative movement of the satellite, the instability of the receiver clock and the Doppler effect (Macgougan, 2003). Without compensating for the effects of the data bits, a long coherent integration of more than 20 ms can cause a loss of power. In general, non-coherent integration refers to the accumulation of the square of the output of the coherent integration, so it may be longer than the period of coherent integration. Non-coherent integration, however, suffers from the phenomenon of squaring loss (Pany, 2010). In short, the acquisition and tracking of weak signals is a matter of maximizing the interval of coherent integration and minimizing residual frequency errors. The total hold time of an HS-GNSS receiver can be up to 100 milliseconds, whereas for conventional GNSS receivers the maximum coherent integration interval is 20 ms. The non-coherent processing increases the sensitivity of the receiver when the coherent integration reaches its limit (Borio, O'Driscoll et Lachapelle, 2009a). Unlike coherent integration, the advantage of non-coherent integration is that it is not affected by the transitions of navigation data bits.

To facilitate the complex task of searching for vulnerable satellite signals, (van Diggelen et Abraham, 2001) have introduced that the use of a parallel massive correlation is necessary while carrying out long period of coherent integration and non-coherent. On the other hand, in unaided mode, the HS receiver does not have the same capacity as the assisted receivers to acquire the vulnerable signals if it has no prior knowledge. However, they can have the same functional capabilities if the HS receiver is initialized with the same assistance data. In their work, (van Diggelen et Abraham, 2001) equipped the GPS chip with a real-time convolution processor with more than 16000 correlators, or more than 2000 correlators for each satellite, to calculate the correlation of all code phases in real-time. By providing accurate information through the assistance data frequency and using a total integration of 1 s, GNSS signals of -150 dBm can be detected inside buildings.

High sensitivity methods can be implemented either in assisted mode or unaided mode. Most of the techniques take advantage of the assisted GNSS (A-GNSS) system to have longer coherent integration intervals in order to increase receiver sensitivity (van Diggelen, 2009). It has been shown that it is possible to use both HS-GNSS and A-GNSS receivers together to overcome the problems of positioning in indoor environments such as unavailability and multipath effects. For example, (Watson et al., 2005) proposed a technique for detecting extreme sensitivity GPS signals inside buildings. The technique consists of evaluating the signal characteristics in a data pair collected inside with a C/N_0 ratio of 40 dB or more below the nominal level of the open signals. Their HS technique allowed for a maximum coherent integration time of 10 s offering up to 79 dB of processing gain for a static receiver with an 8 MHz bandwidth at the receiver RF front-end. Doppler modeling techniques lead to coherent integration greater than 10 s with minimal loss of signal strength. (Watson et al., 2005) have shown that a power signal of less than -202.4 dBW relative to the initial power can be detected, which shows the extreme sensitivity of the receiver despite the variation in noise level with better detection threshold accuracy in terms of C/N_0.

Most of the proposed methods in the literature are intended for software receivers (SDR), because of their flexibility for research and development. This choice is well-founded because the SDR receivers have many advantages: all-software control of signal processing algorithms (acquisition and tracking) and no need to change hardware when adding or modifying algorithms, frequency hopping, automatic communication link establishment, real-time processing, etc. In addition, several methods for processing weak signals are performed by signal block processing. This class of algorithms is based on the "store-and-process" procedure, which is why several software receivers use the FFT technique as an acquisition algorithm (Agarwal et al., 2002; Kim et Kong, 2013; Lin et Tsui, 1998; Psiaki, 2001; Sun-Jun, Jong-Hoon et Ja-Sung, 2006; Won, Pany et Hein, 2006; Ziedan, 2006). The principle idea in block processing is to be able to have a block of received signal samples that can be processed with any HS acquisition algorithm of choice.

BOC modulated signals are known for their best performance of multipath mitigation and potentially their best tracking characteristic, but they present multiple peaks for the autocorrelation function which can cause problems during the acquisition and tracking phase when the receivers use simple and conventional approaches. To mitigate the problems of ambiguities during tracking of the codes due to these secondary peaks, (Avellone, Frazzetto et Messina, 2007) proposed a new waveform family based on the Code Composite Ranging Waveform (CCRW), which is itself based on the work of (Dovis, Pini et Mulassano, 2004). This new waveform family is obtained by combining the local BOC modulated code phase with two shifted unmodulated code phase replicas, capable of alleviating the ambiguity problem related to the modulated BOC signals in the discriminators using the early minus late (EPL) code tracking scheme. Their approach consists in subtracting the cross-correlation between the received signal and the PRN code of the autocorrelation of the received signal.

Several BOC modulation techniques exist to treat different navigation signals. All techniques have common objectives: to mitigate the effects of multipath, to reduce interference between GNSS systems that can demotivate their combined use, and to eliminate lateral peaks due to BOC signal correlation functions during acquisition and/or tracking levels and to deal with ambiguities (Blunt, Weiler et Hodgart, 2007; Floc'H et Soellner, 2007; Julien et al., 2007; Li, Liu et Li, 2007). In 2008, (Avila-Rodriguez et al., 2008) worked on Multiplexed BOC (MBOC) modulation as a final touch to Galileo signals. The final touch of the Galileo signal plane has been completed thanks to studies on the compatibility and interoperability between GPS and Galileo, based on the new MBOC modulation of the E1/L1 common signals. The other techniques aim to minimize the complexity of the receivers by reducing the number of correlators used.

One of promising techniques for processing weak signals and for calculating the position of a receiver in difficult environments is the Assisted-GNSS approach (DiEsposti, 2007; van Diggelen, 2009). This approach will be developed in paragraph 4.5 with the concept of snapshot positioning (Axelrad et al., 2011; Cheong et al., 2012; Jiménez-Baños et al., 2006) and collective detection (Esteves, Sahmoudi et Ries, 2014; Omar et al., 2014). Collective

Detection can be seen both as a high sensitivity and a direct positioning method because it provides a coarse estimation of the user position using direct navigation solution. The basic principle of the CD approach with some concrete contributions on its practical use will be detailed in Chapter 5. These proposals present the innovations as well as the originality of the research carried out in this thesis (Andrianarison, Sahmoudi et Landry, 2015; 2016; 2017).

4.2 Limitations of high sensitivity techniques

First of all, weaker GNSS signals require a longer acquisition period. The use of a long period of coherent integration and non-coherent accumulation makes it possible to increase the sensitivity of the receivers. However, their use has some technical challenges and limitations (DiEsposti, 2001). First, there are unknown data bits of duration 20 ms in the received signal. Without compensating for the effects of unknown data bits, long coherent integration (> 20 ms) can cause a significant loss of signal strength. Then, the residual frequency error due to the Doppler effect and the instability of the clock of the receiver are also factors which limit the increase of the integration time. The residual frequency error causes the length of the code to drift and involves the loss of the signal in the coherent integration. In addition, the coherent integration period is limited by the transition of data bits and dynamics. They lead to narrow Doppler shift. Thus, the transitions in the navigation data and the Doppler effect on the code can degrade the acquisition performance, and limiting the integration period (Shayevits et al., 2002). But with the new GNSS signals, it is possible to have a longer integration time since the signal components are no longer modulated by the navigation message (Ioannides, Aguado et Brodin, 2006; Kaplan et Hegarty, 2006).

For the processing of weak GNSS signals, the size of the data increases as the integration time increases. The size of the data is equal to the product of the sampling period and the coherent integration time. In addition, the required memory size is proportional to the coherent integration time. Thus, the size of the data and the coherent integration time is limited by the available memory of the receiver. Similarly, in the tracking process of the GPS C/A signal, the long coherent integration time of 20 ms is limited by the 50 Hz navigation data over the

baseband CDMA signals. The coherent integration time is also limited by the length of the data bits since the memory may be insufficient because the data is first stored before being processed (Borio, O'Driscoll et Lachapelle, 2009b; Petovello, O'Driscoll et Lachapelle, 2008; Seco-Granados et al., 2012). The effect of the data bits on the coherent integration is shown in Figure 4.1 [Adapted from (van Diggelen, 2009)].

As the polarity of the data bits changes, the coherent summation with long intervals can lead to power loss and a failure of the acquisition process. In fact, coherent integration over several bits of data without knowing the exact bit values will imply loss of power.

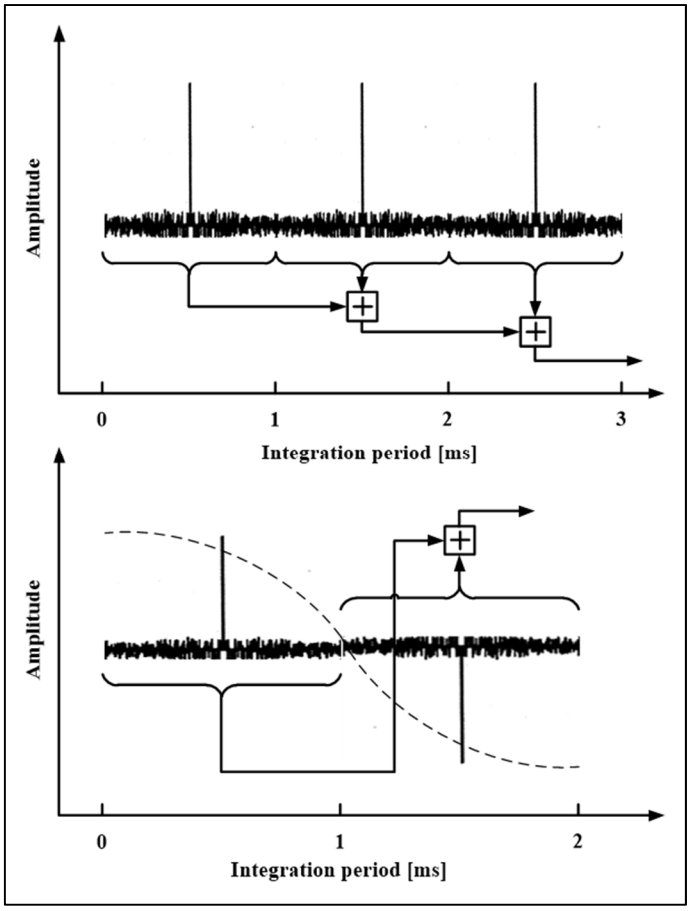

Figure 4.1 Effect of data bits on the coherent integration

The other problem associated with data bits is the alignment of the bits. Even though the bit values are known, but the starting point is unknown, the parts that do not overlap the flow of

data will result in negative values and loss of power (Ioannides, Aguado et Brodin, 2006; Yang et al., 2007). This phenomenon is illustrated in Figure 4.2.

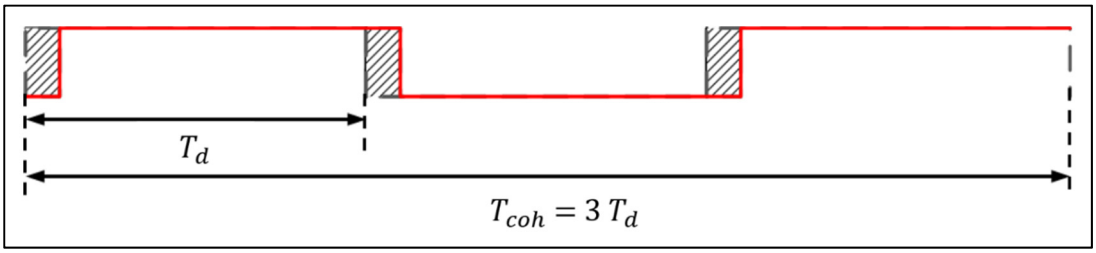

Figure 4.2 Effect of data bit misalignment on the coherent integration

Since the non-coherent integration refers to the accumulation of the square of the coherent integration output, then it may be longer than the period of coherent integration. However, with this accumulation of the square, the non-coherent integration suffers the loss phenomenon by squared or "*squaring loss*", as denoted SQ_{loss}. This phenomenon occurs because the squaring operation increases the mean value of the noise, then the standard deviation of the noise and the amplitude of the correlation peak change. For a fixed sampling rate, changing the period of coherent integration or non-coherent integration will not change the gain, but this will change the "*implementation losses*". Since squared loss has a non-linear behavior, the perfect combination of coherent and non-coherent integration cannot be easily determined because of its dependence on signal strength and implementation losses including the squaring loss (Yang, Ling et Poh, 2013). Long integration also averages out the noise because of the random nature of the noise. If N_s is the number of samples in one coherent integration interval, the ideal coherent gain for an uncorrelated noise is given by:

$$G_C = 10\log_{10}(N_s) \tag{4.1}$$

For M_{NC} non-coherent accumulations, the non-coherent gain, calculated as ideal coherent gain, is given by:

$$G_{NC} = 10\log_{10}(M_{NC}) \tag{4.2}$$

The total gain G_P (processing gain in dB) using coherent correlation and non-coherent accumulation is then given by:

$$G_P = 10\log_{10}(N_s) + 10\log_{10}(M_{NC}) \pm SQ_{loss} \tag{4.3}$$

It has been shown in (van Diggelen, 2001) that squaring loss varies with the SNR after coherent correlation as illustrated in Figure 4.3, in which we see that squaring loss is significant if the post coherent correlation SNR is low.

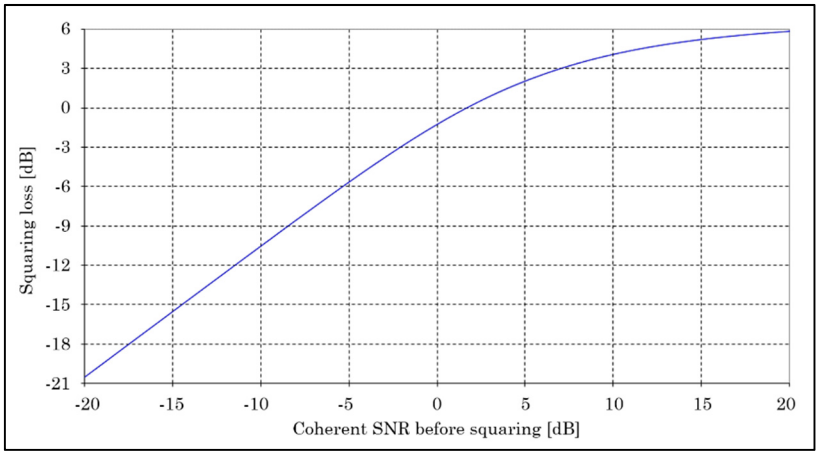

Figure 4.3 Squaring loss due to non-coherent accumulation

Several losses constitute the total loss of implementation, such as: IF filtering loss due to the filtering at IF and sampling, quantization loss due to analog to digital conversion in IF, frequency mismatch loss due to the difference between the frequency bin and correct Doppler frequency, code alignment loss due to the correlator spacing and bit alignment loss due to the increase in coherent integration period more than 1 ms (Tsui, 2005; Ziedan, 2006). According to the architecture of the algorithm, some other losses may be added. Among these losses, the most dominant are the code alignment and bit alignment losses. These losses can be removed from the coherent gain if data wipe-off is available.

Apart from the presence of data bits, frequency constraints also limit the increase of the coherent integration period. For an integration period T_{coh}, a mismatch of f_m Hz between the

reference frequency and the received signal frequency will result in a roll-off of the correlation response of:

$$\Delta_{f_d} = 20\log_{10}|\sin(\pi T_{coh} f_m) / (\pi T_{coh} f_m)| \quad (4.4)$$

Despite its simplicity of implementation and its computing performance, the FFT technique is limited by the size of the data and the coherent integration time. Indeed, increasing the coherent integration time involves increasing the size of the navigation data bits which is limited by the available memory of the receiver. The use of long coherent integration increases the sensitivity of the receiver assuming that there is this limitation available. The parallel code search acquisition method is the fastest method but is the most expensive in terms of resources since it implements three FFT modules. Its implementation is then very complex because of the need for a large number of resources. Moreover, depending on the hardware performance used and the importance of the number of computations to be performed, the use of FFT techniques presents a difficulty for a real-time implementation. That is why most of existing methods associate the FFT technique with the massive parallel correlation (Bardak, Adane et Kale, 2011).

Techniques using only GPS L1 C/A signals exclusively are limited a priori by the number of visible satellites to be acquired and to track, i.e. the number of navigation signals received at the reception antenna is already limited. Indeed, GPS constellations alone cannot cover the whole globe and the number of satellites visible to the receiver is limited according to the position of the receiver. In addition, with the various physical phenomena that can degrade the quality of the received signals, the receiver must be constraint to deal with these degraded signals. Moreover, the use of other GNSS signals, i.e. other than the GPS L1 C/A, can compensate for these limitations by combining several signals, for example.

Since snap-shot positioning is used to roughly estimate the position of the receiver, the horizontal positioning error is too great for some demanding applications in terms of accuracy. Similarly, the CD concept depends heavily on assistance information, provided by a fixed

reference station, which is given to the user in order to define a position and clock bias uncertainty range. In the case where no reference station is available to assist the receiver, it cannot calculate its position. It is precisely to overcome these limitations of HS techniques using A-GNSS techniques (snapshot positioning and collective detection) that this thesis has been carried out.

4.3 Challenges in weak GNSS signal acquisition

We have previously seen the limitations of high sensitivity techniques regarding the effect of increasing coherent and non-coherent integration, let us see in this section other challenges in acquisition of weak satellite signal such as the cross-correlation between strong and weak signals, the effect of code Doppler, and the effect of data message.

4.3.1 Cross-correlation between strong and weak signals

The presence of strong disturbing signals is one of the weak signal acquisition problems. The interfering signals may come from different GNSS frequencies or they may be on the same frequency from different transmitting satellites. The cross-correlation between these signals may result in higher peaks compared to the peaks expected to result from the correlation for an intended PRN code. According to (Mattos, 2001), it is very easy to misdetect the stronger GPS L1 C/A code because the cross-correlation between different GPS L1 C/A codes is only about 20 dB apart from their auto-correlation peak. This problem of misdetection becomes very important for very low power satellite signals. Similar to the true signal, the interfering signal also appears at its Doppler shift and Doppler bins spaced by multiples of 1 kHz. This also causes multiple correlation peaks at several code delays. (Ziedan, 2006) proposed a solution to exploit this property and discard the Doppler bin at which more than one peak exceeds the predetermined acquisition threshold. However, if the cross-correlation peak appears at the same Doppler shift as the autocorrelation peak of the expected signal, this method is no longer valid.

Similarly, (Madhani et al., 2003) proposed an alternative method where the strong GNSS signals found are subtracted from the input signal before correlating the weaker signals. However, the search for strong satellites requires a high computational load, which means that the acquisition times become impractical. Another method proposed by (Lopez-Risueno et Seco-Granados, 2007) consists in the cancellation by subspace projection as an efficient calculation technique for the attenuation of GPS cross-correlations in HS receiver.

4.3.2 Effect of code Doppler

One of the main degradation sources of weak signal is the effect of uncompensated code Doppler which implies a change in the received code period. The effect of Doppler shift on the code length has already been developed in section 2.2.2. Doppler shift is mostly known as the residual frequency error in the carrier frequency but it also affects the received signal by modifying the code frequency (chipping rate). Indeed, a frequency difference between the incoming and locally generated signals is also project itself as a difference in the code phase rate between the incoming and local codes.

The chipping rate, denoted $f_{c,d}$, is expressed as:

$$f_{c,d} = f_c\left(1 + \frac{f_d}{f_L}\right) = f_c + \delta f_{c,d} \tag{4.5}$$

where f_c represents the chipping rate without Doppler, f_d represents the Doppler frequency affecting the incoming signal, f_L represents the carrier frequency without Doppler, and $\delta f_{c,d}$ represents the Doppler shift and can be modeled as the amount of shift in samples every T_{coh} seconds (Ziedan, 2006), expressed by:

$$\delta f_{c,d} = f_{c,d} - f_c = f_c \times \frac{f_d}{f_L} = f_s T_{coh} \times \frac{f_d}{f_L} \tag{4.6}$$

where f_s represents the sampling frequency.

For the same amount of time, if the Doppler is negative, the incoming code is longer in length than the locally generated one, and the duration of the code cycles varies with time. Figure 4.4 shows the effect of the code Doppler on the spreading code period corresponding to a negative Doppler, in which $t_{c,d}$ represents the spreading code chip duration.

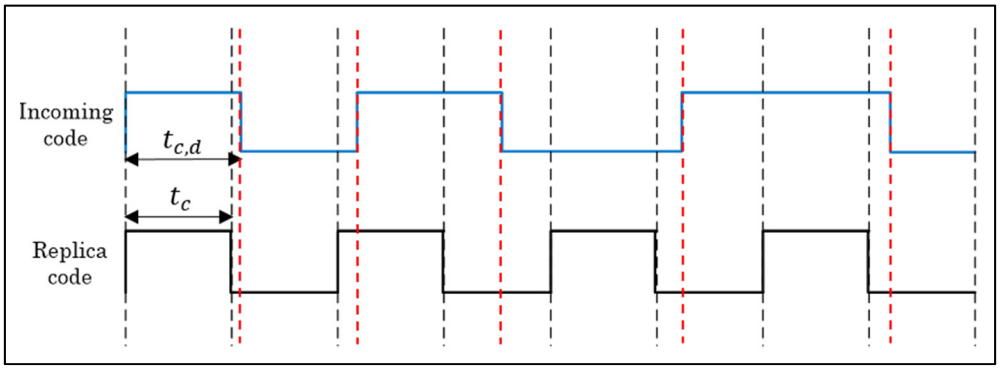

Figure 4.4 Code Doppler effect on the spreading code period

The spreading code chip duration is defined by:

$$t_{c,d} = \frac{1}{f_{c,d}} = t_c\left(\frac{f_L}{f_d + f_L}\right) \tag{4.7}$$

The spreading code duration expands if the Doppler is negative and shrinks if the Doppler is positive (Ziedan, 2006). So,

$$\begin{aligned} f_d > 0 \Rightarrow \delta f_{c,d} > 0 \Rightarrow f_{c,d} > f_c \Rightarrow t_{c,d} < t_c \\ f_d < 0 \Rightarrow \delta f_{c,d} < 0 \Rightarrow f_{c,d} < f_c \Rightarrow t_{c,d} > t_c \end{aligned} \tag{4.8}$$

Considering different incoming Doppler frequencies (2 kHz, 4 kHz, 6 kHz, 8 kHz, and 10 kHz) and assuming a synchronization at the beginning,

Table 4.1 shows the time after which a slip of one chip occurs for GPS L1 C/A and L5 signals, and Galileo E1 OS signal. Knowing that the code Doppler results in a change of the spreading code period, the time before the slip of 1 chip is really shorter for L5 signal (on the order of a

few tens of ms) compared to L1 C/A and E1 OS signals (on the order of a few hundreds of ms) due to their chipping frequency which is 10 times higher for L5 signal. The acquisition performance would suffer from the rapid slip of chips (van Diggelen, 2009).

Table 4.1 Time to get an offset of 1 chip w.r.t the received Doppler frequency

Signal		**Offset of 1 chip [ms]**				
		2 kHz	**4 kHz**	**6 kHz**	**8 kHz**	**10 kHz**
GPS	L1 C/A	770	385	257	193	154
	L5	58	29	20	15	12
Galileo	E1 OS	770	385	257	193	154

Thus, (Akopian, 2001; Jiao, Wang et Li, 2012; O'Driscoll, 2007b; Psiaki, 2001; Ziedan, 2006) proposed methods to compensate the effect of code Doppler. For example, (Ziedan, 2006) proposed to generate a code Doppler compensated replica for each Doppler bin, expressed as:

$$\begin{aligned} I_{cd}(t_l, \tau_m, f_{d_n}) &= c_{cd}\left([t_l - \tau_m]\left[1 + \frac{f_{d_n}}{f_L}\right]\right)\cos\left(2\pi\left[f_{IF} - f_{d_n}\right]t_l\right) \\ Q_{cd}(t_l, \tau_m, f_{d_n}) &= c_{cd}\left([t_l - \tau_m]\left[1 + \frac{f_{d_n}}{f_L}\right]\right)\sin\left(2\pi\left[f_{IF} - f_{d_n}\right]t_l\right) \end{aligned} \quad (4.9)$$

where τ_m and f_{d_n} represent respectively the possible code delay and the possible Doppler shift, with $m = 1, \cdots, N_\tau$ (N_τ is the number of code delays) and $n = 1, \cdots, N_{f_d}$ (N_{f_d} is the number of Doppler bins). Based on this compensation approach, the position of the local code samples at the same position as the incoming code will be guaranteed. The use of Doppler code compensation is mostly recommended for applications in which both weak signals (involving large integration period) and high dynamics (involving large Doppler frequency) are involved. Note that the code Doppler effect is negligible for small integration times. For example, there is approximately a code shift of one sample for a long integration time of 100 ms with a Doppler frequency of 4.5 kHz and a sampling frequency of 4 MHz.

4.3.3 Effect of data bit transitions

We have already seen in the limitations of HS techniques (section 4.2) that the presence of bit transition in the navigation data causes a deterioration in the acquisition of weak GNSS signals. A data bit transition is defined as the transition between two consecutive bits of the useful data sequence or secondary code (modernized GNSS signals). If a data bit sign transition occurs within the coherent integration interval, the amplitude of the auto-correlation function is attenuated since a part of the terms in the integration changes sign causing a subtraction in the correlation values. Assuming that the data sequence is random and each bit value is independent from the previous one, there is a probability of ½ that a sign change happens.

To understand this phenomenon, consider the example illustrated in Figure 4.5, in which 2 bit transitions are represented but there is only one bit sign transition (red dotted line). In this case, a bit sign transition occurs at t_0 with $0 \leq t_0 \leq T_{coh}$. The correlation duration T_{coh} is assumed to be shorter than or equal to the data bit duration T_d. Thus, during a correlation interval, which occurs in the interval $[0, T_{coh}]$, only a bit transition is possible.

The navigation data during the correlation interval where the transition occurs is expressed as:

$$d(t) = \begin{cases} +1, t \in [0, t_0] \\ -1, t \in]t_0, T_{coh}] \end{cases} \tag{4.10}$$

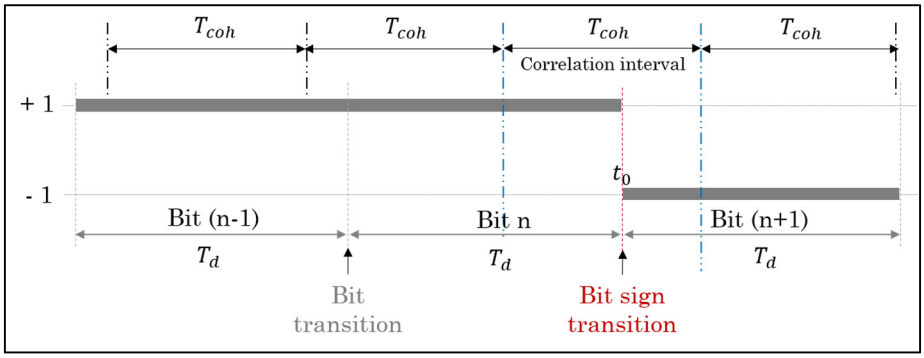

Figure 4.5 Illustration of bit sign transition

In presence of bit sign transition at t_0, the correlator outputs corresponding to the in-phase $I(t_0, k)$ and the quadrature-phase $Q(t_0, k)$ can be expressed as:

$$\begin{aligned} I(t_0,k) &= \frac{A}{2}R_c(\Delta\tau)\left(-\sin\left(\pi\Delta f_d T_{coh}+\varphi_0(k)\right)\frac{\cos(\pi\Delta f_d T_{coh})}{\pi\Delta f_d T_{coh}}\right. \\ &\left.+\frac{\sin\left(2\pi\Delta f_d t_0+\varphi_0(k)\right)}{\pi\Delta f_d T_{coh}}\right)+\eta_{I(t_0)}(k) \\ Q(t_0,k) &= \frac{A}{2}R_c(\Delta\tau)\left(\cos\left(\pi\Delta f_d T_{coh}+\varphi_0(k)\right)\frac{\cos(\pi\Delta f_d T_{coh})}{\pi\Delta f_d T_{coh}}\right. \\ &\left.-\frac{\cos\left(2\pi\Delta f_d t_0+\varphi_0(k)\right)}{\pi\Delta f_d T_{coh}}\right)+\eta_{Q(t_0)}(k) \end{aligned} \tag{4.11}$$

In cases where longer non-coherent integration is required to process very weak signals, the correlation interval may be larger than the period of the data. This implies that one can have more than one bit transition during the integration. The case where there are 1 or 2 transitions (with change of sign or not) is shown in Figure 4.6.

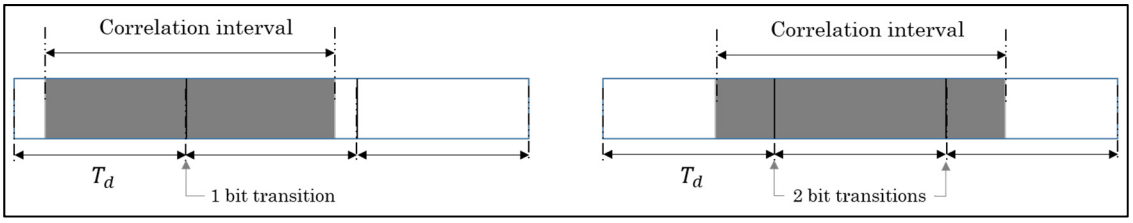

Figure 4.6 Illustration of data bit transition (1 and 2 transitions) during correlation

In order to overcome the effect of the data bit transition and avoid the losses due to the sign transitions, some acquisition methods have been proposed in literature. These approaches are proposed to solve the data bit transition problem and enable long coherent integration. The most natural way to deal with the problem of data bits randomly taking the value +1 or -1 is to perform squaring of the calculations performed over a few periods. Thus, let's take the example of the GPS C/A on a number N_c of code period C/A less than or equal to 20, starting at a time

t_m. The squaring is then carried out and the result obtained is summed with that performed for other instants t_n (n: delay index). This is mathematically translated by the following relation:

$$S_{long} = \sum_{m=0}^{M_{NC}-1} \left\{ \left[\sum_{I=I_m}^{I_m+N_c-1} I_I\left(n, \hat{f}_d\right) \right]^2 + \left[\sum_{I=I_m}^{I_m+N_c-1} Q_I\left(n, \hat{f}_d\right) \right]^2 \right\} \quad (4.12)$$

where I_m is the m-th period of the code (starting at time t_m) at which the partial summation is started. With this expression, we can envisage an integration of the GPS signal over a very long period, provided that the sequence $I_0, I_1, \cdots, I_{M-1}$ is chosen correctly. In particular, no data transition must take place between the period I_m and the period $I_m + N_c$. To ensure this, some methods have been proposed in literature. One of the well-known method has been proposed by (Psiaki, 2001). This approach, called an "*alternate half-bit method*", consists in integrating a half-period of data bits (10 ms) without a priori knowledge of the data bit transition. The basic idea is to make two independent acquisitions on two blocks of 10 ms each. Indeed, the integration is carried out separately on even blocks and odd blocks while dividing the data into blocks of 10 ms. The objective is to have at least one of the groups without bit transitions and will result in a higher acquisition peak. In the end, the choice of the block of sequence will be made by considering the best SNR. The simplicity of the algorithm remains the great advantage of this method. Despite its simplicity, the starting point of bit transitions remains unknown, whereas it is necessary for pseudorange calculations. Similarly, the coherent integration time is limited.

Note that performing integration without sufficient knowledge of the transition times results in loss of alignment of the data bits. In order to find the transition times of the data bits, (Psiaki, 2001) proposed another method, called *full-bits method*, in which the acquisition algorithm keeps track of 20 coherent integrations. Each integration begins with different chip and searches for the one that has the maximum results. This method of estimating the transition time is certainly more costly in time because of the important computational burden. On the

other hand, it allows an energy gain of the order of 2 with respect to the previous method: that is to say a gain of 3 dB on the partial summations and a gain of 6 dB during the squaring.

(Ziedan, 2006) has proposed another method for searching the combination of most probable data bits at each step of the acquisition. To do this, multiplication of the correlation results for N_T intervals of 20 ms by 2^{N_T-1} possible data bit combinations is performed. Then, the results are non-coherently summed and the most likely combination of data bits is chosen as the one that maximizes total non-coherent accumulation, and the other matrices are eliminated. Unfortunately this method is not very practical since it requires a large amount of memory to store and compare 2^{N_T-1} correlation and integration results when long coherent and non-coherent integration periods are used. (Ziedan, 2006) has also proposed another method that estimates bit alignments by maintaining N_{nc} arrays of non-coherent integrations in parallel, each starting with a possible bit edge position. To alleviate the complexity required in processing time and memory requirements, N_{nc} arrays less than 20 are selected by the algorithm, with the bit edges extending uniformly over all of the 20 possible edges. By choosing $N_{nc} \geq 4$, this method can limit to 10 % the maximum loss due to the use of only N_{nc} transition. Despite efforts to reduce complexity, the calculation amount is still high.

(Petovello, O'Driscoll et Lachapelle, 2008; Soloviev, van Graas et Gunawardena, 2009) have proposed other methods using maximum likelihood methods to estimate navigation data bits.

In order to manage the data bits, the assisted GNSS approach can be used to provide the information about the navigation data bits to the user. For example, (van Diggelen, 2009) has proposed a very useful method that consists in choosing odd-valued coherent integration times such that them or their compliments do not divide into data bit interval. The advantage is that, independently of the initial alignment, all possible overlap patterns can result from integration with these coherent intervals over the non-coherent correlation. This shows the simplicity of the algorithm based on assistance compared to other unaided methods, even though it still has a loss associated with this method.

The above methods can also be used in tracking level during baseband processing. Other data bit estimation methods are proposed in the literature, such as proposed in (Lin et Tsui, 2002), depending on the repetitive updating of the data bit estimation using the tracking loops.

After seeing the limitations of high sensitivity techniques, we will see in the next section the overall architecture of the HS receivers with specific blocks for HS techniques compared to conventional receivers.

4.4 Architecture of HS-GNSS receiver

HS-GNSS receivers allow satellite signals to be received in non-ideal environments where reception was not possible before with conventional receivers. In these locations, reliability and positioning accuracy are greatly degraded by multipath errors, satellite unavailability, noise associated with the low power received signal, etc. Several algorithms (acquisition and tracking algorithms) have been proposed for the processing of low-power navigation signals in GNSS receivers.

Weak GNSS signals are acquired and tracked by using long signal integration times which is accomplished by coherent correlation and further non-coherent accumulation. The difference between a high-sensitivity GNSS receiver and a conventional GNSS receiver is that HS receivers are capable of performing correlation for longer periods of time, and therefore, can process weaker GNSS signals than the conventional receivers. Similarly, compared with conventional receivers under the same conditions, HS receivers have a faster TTFF and a faster re-acquisition times. Some HS GNSS receivers can also benefit from massive parallel processing to facilitate the complex task of searching for the weaker GNSS signals while using long coherent integration periods and further non-coherent accumulation which increase receiver sensitivity (van Diggelen, 2001). The block diagram of the weak GNSS signal processing is illustrated in Figure 4.7 where we see the difference between the processing of strong signals in conventional receivers which requires only coherent integration and processing of weak signals where non-coherent accumulation is indispensable.

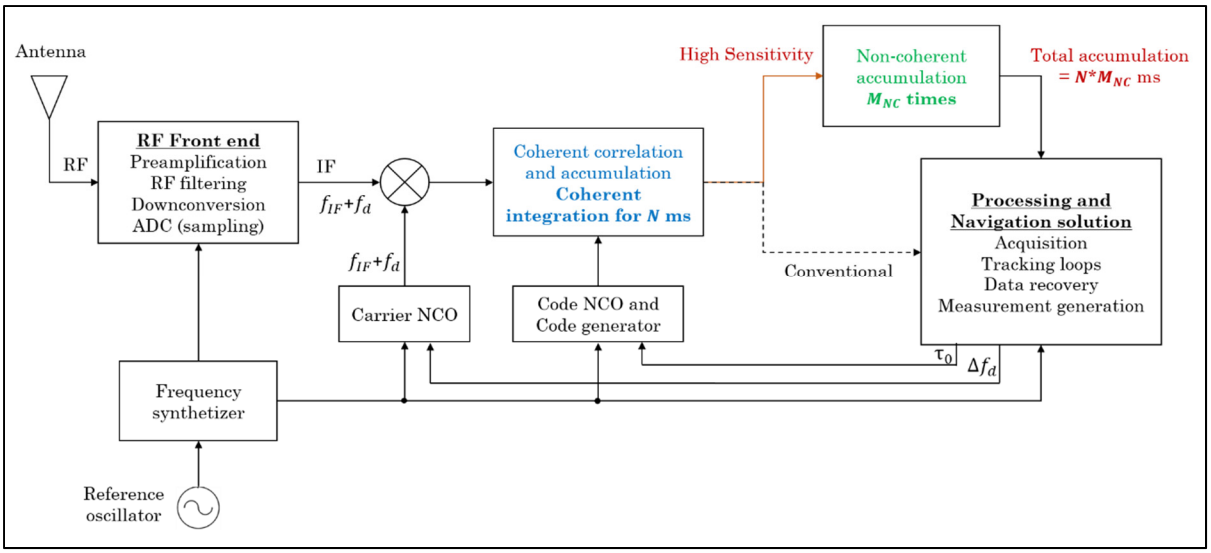

Figure 4.7 Generic high sensitivity receiver signal processing block diagram

To understand the processing of weak GNSS signals, examination of the coherent correlation process and non-coherent integration is useful.

If the calculation of the correlation over a period of 1 ms allows the detection of the GNSS signals at a nominal SNR (45-50 dB-Hz), this acquisition becomes impossible when dealing with weaker ratios such as those in urban environments where satellite signals are greatly attenuated. The correlation operation must therefore take place over a longer period of time. It is then naturally envisaged to calculate over several periods of the PRN code.

4.4.1 Coherent integration

This is the coherent summation over one (or more) period of the PRN code samples of the complex signal for fixed values of the Doppler f_d, correlation of these samples with those of the replica for different values of the code delay τ, coherent summation of the correlation signal over several navigation bit periods. It is possible to calculate in parallel several long integration sequences shifted by a certain number of periods, denoted n. In this phase, it is essential to use algorithms which serve to maximize the power of the correlation function. After calculating

these different sequences, a logical decision will be taken to determine the optimal sequence defined by the delay index n.

During the acquisition stage, the noise term is often assumed to be additive, stationary and zero-mean. While the signal itself is constant, its mean is equal to its amplitude. Thus, if the measurements are accumulated over a long period of time and the intensity is averaged, the value of the signal is approached and the noise is eliminated.

The correlation on the i-th period of the PRN code can be expressed by the following equation:

$$\begin{aligned} r_i(\hat{\tau}, \hat{f}_d) &= I_i + jQ_i \\ &= \sum_{n=N_{T_i}}^{N_{T_{i+1}}-1} s_b(nT_s)c(nT_s - \hat{\tau}_k)\, \mathrm{e}^{\{-\mathrm{j}2\pi(f_{IF}+\hat{f}_d)nT_s\}} \end{aligned} \tag{4.13}$$

Thus the coherent summation (index cs) over several periods gives:

$$\begin{aligned} r_{CS}(\hat{\tau}, \hat{f}_d) &= I_{CS} + jQ_{CS} \\ &= \sum_{i=0}^{N_c-1} r_i(\hat{\tau}, \hat{f}_d) \end{aligned} \tag{4.14}$$

Then the signal strength is calculated by $S_{CS} = I_{CS}^2 + jQ_{CS}^2$ which we seek to optimize as a function of f_d and τ. The calculation of this summation is done by the block processing method.

4.4.2 Non-coherent integration

In order to eliminate the restriction of coherent integration technique, non-coherent integration technique uses the sum of the squaring of the signal. This square operation in the non-coherent integration technique reduces the influence of data bit transition and inaccurate carrier phase (Borio et Lachapelle, 2009).

The change of the data bits every 20 ms leads to a phase change of the raw signal. To deal with this problem, we compute the squared quantities r_{cs} calculated previously. The number N_c of PRN code periods is chosen such that $N_c \leq 20$, while starting at time t_m. The same calculation is repeated for other instants t_n, and all the squared elements are summed at the end. This is expressed by the equation:

$$\begin{aligned} S_{NCS}(\hat{\tau}, \hat{f}_d) &= \sum_{m=0}^{M_{NC}-1} \left| r_{CS}(\hat{\tau}, \hat{f}_d) \right|^2 \\ &= \sum_{m=0}^{M_{NC}-1} \left\{ \left[\sum_{i=i_m}^{i_m+N_c-1} I_i(\hat{\tau}, \hat{f}_d) \right]^2 + \left[\sum_{i=i_m}^{i_m+N_c-1} Q_i(\hat{\tau}, \hat{f}_d) \right]^2 \right\} \end{aligned} \tag{4.15}$$

where i_m is the i-th period of the code, beginning at time t_m, at which we start the partial summation. M_{NC} represents the number of periods of 20 ms over which the long integration takes place.

However, non-coherent integration also amplifies the noise in the signal and introduces the "*squaring loss*". Then, the squaring loss increases when the period of non-coherent integration increases. Optimal combination between coherent and non-coherent operations is a strategy that depends on the signal power, available resources, and designer choice.

4.5 Assisted GNSS

4.5.1 Principle of Assisted GNSS

Assisted GNSS (A-GNSS) is one of the methods widely used in mobile location services to provide assistance data to GNSS receiver to help it in its position calculation. (Taylor et Sennott, 1984) proposed the first structure of A-GPS in 1984. They were able to show that TTFF can be significantly reduced by providing useful information (ephemeris, navigation data, timestamps, etc.) for processing GPS data. The assistance data can be transmitted by a

wireless reference station (may be a mobile base station) to the GPS receiver. In conventional GNSS receivers, the navigation message must be decoded by the receiver to obtain the ephemeris and the transmission time of the satellites only after the receiver acquires the signal, and the position can be calculated at the end. In addition, a conventional GNSS receiver needs at least 30 seconds, including the acquisition time, to calculate the position. Whereas, using the A-GNSS assistance approach, it is not necessary to decode the navigation data since they are already provided by the assistance network. Another advantage of A-GPS is the improvement of the bit error rate (BER), knowing that the BER related to decoding the navigation data and which increases as the signals are attenuated, this then implies a higher processing time and a greater error in conventional GNSS receiver (Agarwal et al., 2002). So, A-GNSS improves on standard GNSS performance by providing information to the user through an alternative communication channel (Harper, 2010; Li et al., 2011; Monnerat et al., 2004; van Diggelen, 2009). The basic principle of the A-GNSS technique is illustrated in Figure 4.8 where we see the assistance information sent by the reference station to reduce the frequency/code phase search space.

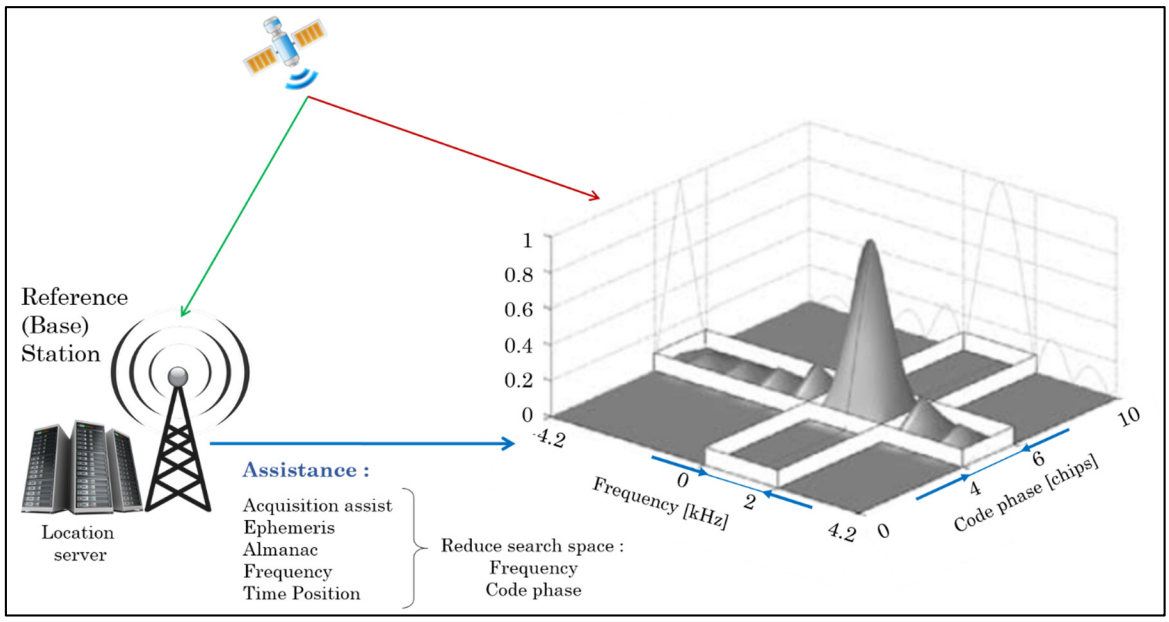

Figure 4.8 Basic principle of the Assisted GNSS approach
Adapted from (van Diggelen, 2009)

The reference station and the location server provide some subset of the assistance information such as ephemeris, almanac, frequency, time, position. A GNSS receiver without any a priori information has to search the entire frequency/code phase search space until it finds the correlation peak. However, using the pre-calculated ephemeris and other assistance data in A-GNSS, the frequency/code phase search space is reduced.

In the Figure 4.8, the white rectangular boxes indicates the search range, and the intersection of the two boxes represents the space where the desired satellite signal is found corresponding to the combination of frequency and code phase. The great advantage of the assistance approach is that the more precise the assistance data, the narrower the search range can be. Assistance always provides some reduction in the frequency search, but there is a reduction in the code phase search only if fine-time assistance is available (van Diggelen, 2009).

In A-GNSS approach, two major industrial approaches exist: MS-assisted and MS-based GNSS. The position is computed at a reference station or by a server in MS-assisted GNSS whereas it is computed by the receiver itself in MS-based GNSS. In MS-assisted GNSS, the receiver only performs the signal acquisition and sends the measurements to the reference station (RS) (van Diggelen, 2009). These two approaches naturally have different requirements in the type and amount of data to be shared between the MS and the RS. The MS requires more assistance data (coarse time and ephemeris, reference frequency and RS position) in MS-Based approach but also presents several advantages, such as better position accuracy, and possibility of integration of improved navigation filters (de Salas et van Diggelen, 2011; DeSalas et van Diggelen, 2010). The provided information data are also different according to the type of assistance: A-GNSS frequency assistance or A-GNSS time assistance for code delay as summarized in Table 4.2 (van Diggelen, 2009).

In this thesis, we focus exclusively on the MS-based GNSS approach, i.e. all calculations are carried out at the GNSS receiver, even though we will still do a comparison of the performance of the proposed algorithm according to the approach used.

Table 4.2 Summary of assistance data required according to assistance approach

Assistance type	Assistance approach	Including assistance information
A-GNSS frequency assistance	MS-based frequency assistance	- Time - Reference frequency - Position - Almanac and/or ephemeris
	MS-assisted frequency assistance	- Reference time - Reference frequency - Expected satellite Doppler and Doppler rate
A-GNSS time assistance for code phase	MS-based fine-time assistance	- Fine time - Position - Almanac and/or ephemeris
	MS-assisted fine-time assistance	- Fine time - Expected satellite Doppler and Doppler rate

So, let's see the description of the different components of assistance sent to the MS (van Diggelen, 2009).

- **Time:** It represents the date and time and may be delivered as GPS (week and seconds of the week) or UTC form. For frequency assistance purposes, the accuracy of time should only be good for a few seconds.
- **Reference Frequency:** It is used to calibrate the local oscillator of the receiver (mobile phone). It is sent by the signal received from the cell tower (reference station). This is an important assistance data to reduce the frequency search space. The frequency of the tower is generally known to within 50 ppb, and the carrier frequency of the mobile phone is known to be within 100 ppb.
- **Position:** This is the position of the reference station allowing the receiver to estimate its position. In mobile phones, the position assistance usually comes from a database of cell tower positions. Generally, the accuracy of this position would be about 3 km, although this could vary considerably.

- **Almanac and/or Ephemerides:** The almanac and the ephemeris can be provided to the user receiver, in the MS-based assistance data, in order to calculate the expected satellite motion. Note that the approximate correct time is needed to calculate the satellites position, and the approximate position is required to calculate the relative satellites motion, or the expected Doppler frequency expected for each satellite.

Note that the reduction of the frequency search space depends on the available assistance data and the receiver scenario. To see the contribution of the assistance technique in reducing the frequency search space, let us consider the example in Table 4.3 showing the typical values of coarse-time assistance parameters corresponding to a stationary receiver with a total search space of ± 400 ppb (van Diggelen, 2009).

Table 4.3 Typical values of A-GPS coarse-time assistance for a stationary receiver

Assistance data		**Search space**		**Percentage of Total (± 400 ppb)**
Parameter	**Value**	**[Hz]**	**[ppb]**	
Assistance time	± 2 s	± 1.6	± 1	0.3 %
Assistance position	3 km	± 3	± 2	0.5 %
Reference frequency	± 100 ppb	± 157	± 100	25 %
Maximum speed	160 km/h	± 468	± 297	74 %
Total		± 629.6	± 400	

(van Diggelen, 2009) has also proposed the use of massive parallel processing combined with A-GNSS in order to reduce the TTFF and increase the sensitivity of the receiver. The only problem with A-GNSS is the availability of the service, which is limited or non-existing in some locations.

The performance of A-GNSS system depends on the communication technology: CDMA, TDMA, OFDM, UMTS, etc. The performance also depends on the business model. In fact,

some industrials have difficulty to commercialize their technology since other concurrent offer the service with mobile or with a better OS for example.

Let us now look at the techniques that can benefit from this approach to assist in processing weak satellite signals in order to calculate the position despite the weak signal power.

4.5.2 Snap-shot positioning

An interesting technique that has become possible with the A-GNSS approach is known as Snap-shot Positioning, also called "Single-shot Positioning" or "One-shot Positioning" (Carrasco-Martos et al., 2010; Dötterböck et Eissfeller, 2009; Jiménez-Baños et al., 2006; López-Risueno et Seco-Granados, 2004; Schmid, 2007). The principle is simple, snap-shot receivers use the estimated code phase for each satellite in view to obtain a direct position solution, thus eliminating the need for tracking loops. This is why this approach is also called "Direct Positioning" (DP). This technique is particularly useful if we have strongly attenuated signals at the reception, i.e. in cases where it is impossible to extract the navigation messages. Snap-shot positioning technique allows to increase the sensitivity of the receiver thanks to the possibility of having a longer observation time for the positioning process. However, the single-shot positioning implies that each signal is acquired individually and then used in the navigation equation to calculate the estimated position of the receiver. An alternative consists of using this effective positioning technique in harsh environments and combine it with a collaborative approach to acquire all satellites signals collectively as a vector acquisition approach, not sequentially as in the standard or the Snapshot methods. This concept is called the "Collective Detection" or "Collaborative Detection" (CD) approach that will be introduced in the following section 4.5.3. This promising approach will be developed in CHAPTER 5 where we will see the various improvements made in order to use it effectively.

Several methods have been introduced for Direct Positioning Estimation (Cheong, Dempster et Rizos, 2011; Closas, Fernández-Prades et Fernández-Rubio, 2009). There are two steps in conventional position estimation: the receiver first estimates the synchronization parameters

of the visible satellites and then performs a position estimation with that information. In contrast to the conventional method, the DP introduced the concept of position-based synchronization in one step in which the synchronization parameters can be covered from a user position estimation. And ML estimator of position in the framework of GNSS can be obtained (Closas, Fernández-Prades et Fernández-Rubio, 2007). Despite the effectiveness of the DPE technique, its implementation within a GNSS receiver remains a great difficulty since the works are just theoretical and very general studies. However, we will still use the results obtained in these works to compare the results using our proposed CD algorithms in CHAPTER 5.

4.5.3 Collective Detection (CD)

The concept of A-GNSS was inspired to develop the new approach of positioning using GNSS signals called as “Collective Detection” (CD) which represents the focus of the contributions of this thesis. This new detection concept is intended to complement an existing assisted GNSS and positioning method. In fact, Collective Detection is an A-GNSS approach for direct positioning in which all information from satellites in view are combined in order to enable acquisition in harsh environments. For example, if the signal duration of one or two satellites signals among four are very weak or very short which cannot be detected, the CD method could compute a positioning solution by processing all signals in visibility together. This is a multi-satellite positioning method that processes the signals in the position domain instead of the standard receivers that perform an individual processing in the signal domain. One the one hand, conventional A-GNSS method is based on raw code phase measurements detected individually from multiple satellite channels to directly reconstruct the pseudorange measurement without waiting for all data navigation. Thus, the TTFF is significantly reduced by the a priori position provided in the assistance data. On the other hand, the Collective Detection approach uses Maximum Likelihood search over the uncertainty region of solution space instead of code phase measurement and least squares estimation. The basic idea has been introduced in (DiEsposti, 2001) where the proposal consists of coherently combining the

detection metrics from all visible satellites in order to improve the overall acquisition sensitivity.

The idea of direct estimation of the position in a single step without going through the tracking step and the decoding of the navigation data is the basis of the CD approach, which is why it is considered as a method of direct positioning (Axelrad et al., 2011). In fact, for weak satellite signals, the navigation messages cannot be decoded, hence we must find other alternatives to the determination of the navigation solution by following all the steps like the conventional receivers. Direct Positioning algorithms are based on a set of individual correlogram formed by code phase/Doppler for the satellites potentially visible. CD is able to provide for the MS a first coarse estimate of position and clock bias in situations where the individual satellite signal cannot be acquired and/or tracked. Note that the accuracy of parameter estimates is highly dependent on the available *a priori* information and especially the geometry of the satellites in view. It has been shown that the positioning error of the CD approach depends on the number of visible satellites, their geometry and signal power; and the CD metric is driven by the stronger signals (Bradley et al., 2010). Some CD works have shown that the mean horizontal positioning error is within a few tens of meters at best. The positioning error depends on the code phase resolution. For example, for an error of 0.5 chips in the code phase estimation (equivalent to 150 m in pseudorange for L1 C/A), a position error of 30 m may still be within the correct code phase estimation region (Bradley et al., 2010).

Conventional GNSS receivers process different satellite signals individually, sequentially one by one, since each signal is treated independently at the acquisition level. Indeed, satellite detection is based only on its own signal power and user's dynamics. In addition, acquisition process is performed in code phase and Doppler frequency domain in conventional GNSS receiver. However, in CD approach, the code phase search for all satellites in view is projected to a receiver position/clock bias grid and the satellite signals are not acquired individually but collectively, known as vector acquisition (DiEsposti, 2001; O'Driscoll, 2007b; van Diggelen, 2009). The projection of the code phase into position/clock bias domain is done differentially with respect to the pseudorange measurements provided by a reference station with known

location. The main idea of the use of CD is that the acquisition of satellite signals in harsh environments is a challenging task because the signals are highly attenuated and the conventional GNSS receivers are not able to acquire and track the satellite signals. In addition, it is known that the GNSS receiver antenna receives at least one or more strong signals and these strong signals are used to detect the weak GNSS signals in view as a sort of multi-satellites collaborative processing. Figure 4.9 shows the global difference between conventional acquisition and Collective Detection approach.

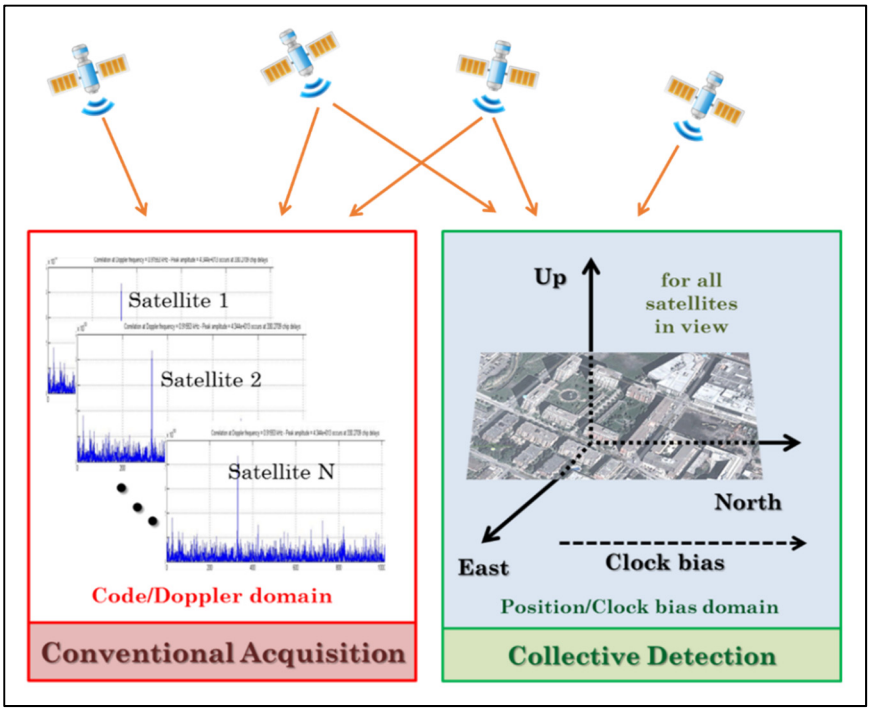

Figure 4.9 Comparison between conventional acquisition and Collective Detection

Despite the benefits of the CD approach, its practical implementation faces some challenges, including the need for a second static receiver and the high computational load that makes it difficult to implement. The main limitations of CD approach and proposed solutions will be detailed in CHAPTER 5.

4.6 Combined acquisition approaches

One of the very promising techniques for future generations of GNSS signals is their combination in order to increase the sensitivity of the receiver. Using multiple GNSS signals combined is motivated by the idea of removing the need for network support, which may not always be available. Several approaches exist for combining the different GNSS signals: channels combination, frequencies combination and satellites combination.

4.6.1 Combining channels

This approach involves both the combination of data/pilot components and the acquisition of signals from the same satellite at the same frequency band.

Knowing that the P(Y) code signal is limited to military use, there are nevertheless authorized users who can make use the two signals C/A and P(Y) to improve the detection performance of the signal on the L1 band. For example, (Macchi-Gernot, Petovello et Lachapelle, 2010; Macchi, 2010) proposed and evaluated the combined GPS L1 C/A and L1C acquisition scheme while showing its merits in weak GNSS signal acquisition. Similarly, (Yang, Hegarty et Tran, 2004) has proposed a method for acquiring the new GPS L5 signal using a coherent combination of I5 and Q5. Various mechanizations for coherently combining I5 and Q5 have been examined in this paper, and the proposed technique takes advantage of the synchronicity and orthogonality between signal-to-noise improvement compared to the usual method of non-coherently combining I5 and Q5 correlator outputs. As demonstrated in (Aguado et al., 2004), the combination of two coherent integrations across the single-frequency data and pilot channels allows an increase in sensitivity of 3 dB SNR in post-correlation. (Borio, O'Driscoll et Lachapelle, 2009a) have also shown that the combination of data and pilot channels for different GNSS signals increases sensitivity of the receiver. (Axelrad, Donna et Mitchell, 2009) have also proposed a non-coherent combination of C/A and P(Y) codes to have 1 to 2 dB greater than the C/A code alone.

4.6.2 Combining frequencies

Several GNSS signals are available and possible to be received on the receiver antenna thanks to the large number of visible satellites with the modernization of GNSS systems and all GNSS constellations (GPS, Galileo, Glonass and BeiDou). Therefore, the idea of combining the energy of all signals from the same satellite has been proposed to obtain an increased sensitivity of the receiver. Several proposals on the acquisition of multi-frequency GNSS signals can be found in the literature.

(Gernot, 2009; Gernot, O'Keefe et Lachapelle, 2011; Gernot et Shanmugam, 2007) have shown that the non-coherent combination of multiple transmissions from the same satellite on different GNSS frequencies, such as L1 C/A and L2C, is possible and can improve the sensitivity of a GNSS receiver. Moreover, (Ioannides, Aguado et Brodin, 2006) has demonstrated that the coherent combination of the L1 and L5 frequencies for both GPS and Galileo systems showed lower acquisition times and higher probability of detection than coherent combining on a single frequency. According to (Megahed, O'Driscoll et Lachapelle, 2009), the combination of L1 C/A and L5 GPS signals using a single Kalman filter to estimate tracking errors increased the tracking sensitivity by 4 dB. (Hurskainen et al., 2009) concluded that a combined E1/E5a scenario is the one that offers the most benefits in their studies on the investigation of the best candidates of Galileo signals for multi-frequency acquisition. Further studies on the combination of signals of different frequencies from the same satellite that can be seen in (Della Rosa et al., 2010; Ta et Ngo, 2011).

4.6.3 Combining satellites

This approach represents the basic principle of the Collective Detection (as presented in section 4.5.3 and described in more detail in CHAPTER 5) by combining the satellites at the acquisition level or by combining the satellite replicas to accelerate the acquisition process. This approach is also known as the "sum of replicas" (Al Bitar, 2007; Arribas, Closas et Fernández-Prades, 2010; Lin et Jan, 2010). The sum of replicas technique will be developed

in ANNEX I where the best satellites are non-coherently combined in order to propose the cognitive exploitation of high sensitivity receiver.

(DiEsposti, 2007) showed that it is also possible to combine satellites in a coherent way in order to increase the sensitivity of the receiver. Despite the potential gain obtained, this method has a disadvantage because of the maintenance of the phase shift due to the coherent processing. Moreover, the non-coherent combination of satellites for an A-GPS receiver was shown by (El Natour et Monnerat, 2006). This method accelerated the acquisition based on the FFT technique in an A-GPS receiver and made it possible to reduce the TTFF. Similarly, (Axelrad, Donna et Mitchell, 2009) proposed a non-coherent combination of satellite signal correlations. In this method, the user is assumed to have access to the a priori information about the satellite's position, ephemeris, and clock bias. The search is centralized in the reference position, the correlation values of the clock bias and the Doppler values are combined at the satellite level to construct the correlogram position domain. Acquisition of weak signals (20 dB-Hz) with coherent integration of 1 ms and 20 non-coherent accumulations of satellites was possible.

4.7 HS acquisition methods for GNSS signals with a secondary code

As we have seen previously, the presence of secondary codes in modern GNSS signals has a limitation at the processing level, particularly at the acquisition level because there is a potential sign transition between each period of the primary code and because of the long length of these codes. In addition, when long coherent integrations are used, i.e. if high sensitivity is required, synchronization with the secondary code is necessary. The simplest solution to synchronize with the secondary code is to combine the primary code correlation results with the secondary code chips, but this involves a significant computational load. Thus, several methods have been proposed in (Leclère et Landry, 2016) to reduce the complexity of the secondary code correlation, such as the decomposition of the local secondary code into two codes and the use of recursion. The optimal reduction with these methods is proposed in (Leclère, Andrianarison et Landry, 2017) by conducting an exhaustive search. These proposed

methods represent one of the main proposals to this thesis. The effectiveness of these techniques has been demonstrated for GPS L5, Galileo E1 and E5, as presented in ANNEX V.

4.7.1 Modernized GNSS signal acquisition

The characteristics of modernized GNSS signals have been presented in Section 2.1.3. The fact that modernized GNSS signals have two components (data and pilot), unlike the GPS L1 C/A, implies an adaptation of the acquisition methods to the signal structure. The presence of binary sequence on both components (navigation message on the data component and secondary code on the pilot component) is one of the characteristics of these signals. The bit durations are equivalent to the period of the spreading code. There are two kinds of acquisition method for modernized GNSS signals: coherent integration over a single spreading code period and over multiple spreading code periods (Esteves, 2014a). For integration over multiple spreading code periods, the sign recovery is required. The secondary code brings several benefits and can significantly improve the performance of a GNSS receiver. However, this complicates the acquisition because of a potential sign transition between each period of the primary code. If a high sensitivity is required this problem becomes more serious due to long coherent integrations, which requires synchronization with the secondary code. Thus, to solve this problem of complexity, some solutions have been proposed in (Leclère, Andrianarison et Landry, 2017) as efficient methods of GNSS secondary code correlations for high sensitivity acquisition.

4.7.2 Efficient GNSS secondary code correlations for HS acquisition

Among the solutions proposed in (Leclère, Andrianarison et Landry, 2017), two techniques consist of decomposing the local secondary code into two codes: a code with many zeros to avoid many operations when calculating the correlation; and the second code having a correlation which can be efficiently calculated. To enable this efficient calculation, the second code should contain a repeated pattern repeatedly. The other idea is based on recurrence, that is, by calculating a correlation result using a previously calculated result. Note that the

operations performed are not changed for the different methods but the difference lies only in how the operations are performed. These techniques have been tested for more signals such as GPS L5, Galileo E1 and Galileo E5 and we have been able to have better results. Details of these techniques are presented in ANNEX V but are not developed here. The proposed techniques show only an example of processing of modern GNSS signals with secondary codes but other techniques exist in literature. These approaches allow the HS-CGR receiver to minimize the calculation loads according to the received signals.

4.8 Summary

In this chapter, several techniques which can increase the sensitivity of the receiver have been developed with their advantages and disadvantages. The architecture of the HS GNSS receivers has also been shown. With regard to HS techniques and more particularly the acquisition of low-power GNSS signals, here are some essential points developed in this chapter. It is important to note that the effect of oscillator errors and multipath are ignored in this thesis even though they are paramount in real-world data. The multipath effect could be safely ignored during the acquisition stage since the coarse estimation of time delay is enough i.e., rough precision is enough to start the synchronization process.

Increasing coherent integration time will increase the sensitivity of the receiver but the limitations and effects of it should be carefully taken into account in a HS receiver. It was demonstrated that the code Doppler clearly needs to be dealt with for modernized GNSS signals since the auto-correlation function peak is attenuated and shifted. Acquisition of modernized GNSS signals is more complex because of the length of the modernized codes. So a proposed technique to reduce complexity in acquisition of secondary code will be developed in ANNEX V.

The main goal of the assistance data, in A-GNSS approach, supplied by a reference station is to improve the TTFF and sensitivity of the receiver. The assistance data allows the GNSS receiver to reduce the search space by providing information such as satellite ephemeris,

reference time and a priori position. There are lots of assistance methods that are based on providing time assistance or frequency assistance, and if the user position is calculated at the receiver or at the network server related to the reference station.

Since snap-shot positioning is used to roughly estimate the position of the receiver, the horizontal positioning error is too great for some demanding applications in terms of accuracy. Similarly, the CD concept depends heavily on assistance information, provided by a fixed reference station, which is given to the user in order to define a position and clock bias uncertainty range. In the case where no reference station is available to assist the receiver, it cannot calculate its position. It is precisely to overcome these limitations of HS techniques using A-GNSS techniques (snap-shot positioning and collective detection) that this thesis has been carried out. Contrary to the conventional technique, in CD approach all satellite signals are used even if they are strong or weak. In fact, the objective of CD as a vector acquisition approach is its ability to use stronger signals to facilitate the acquisition of the weaker ones. The number of satellite signals and the relation between their strengths are essential to analyze the performance of CD as an HS acquisition technique.

As we have said several times, the main focus of this thesis is the use of the CD approach to address the problem of positioning in GNSS-challenging environments, we will develop it in depth in the next chapter.

CHAPTER 5

COLLECTIVE DETECTION OF MULTI-GNSS SIGNALS

In the previous chapter, we have presented different techniques for processing GNSS signals in non-ideal locations. Among these techniques, the Collective Detection (CD) approach, was introduced as a promising technique of acquisition and positioning allowing to calculate the position of a receiver in difficult locations. This technique based on the assistance of a reference station is a recent approach proposed by researchers in the field of navigation and positioning in order to overcome the limitations of the different techniques used before. The basic principles of this approach will be developed in this chapter. Then, the limitations of CD approach will be addressed. The different solutions to overcome these disadvantages will be developed as original contributions which are the foundations of this thesis.

5.1 Introduction

The rapid evolution of mobile telephony, which is increasingly equipped by GNSS chips, as well as the reduction in the size and cost of cellular phones and their services, requires better operation of navigation systems in non-ideal environments (urban area, deep forest, canyon, under tunnels, etc.). Urban city is a place where the use of GNSS receivers has increased substantially recently with the integration of GNSS chips in cellular phones and tablets for different services forming a big market called the sector of location-based service (LBS). On the one hand, the user is waiting for a high positioning accuracy, because of the proximity to various points of interest. On the other hand, urban environment generates difficulties in the reception of GNSS signals. Indeed, GNSS signals cannot typically be well captured in urban areas. GNSS acquisition in harsh environment is a challenging task because the signal power is very low and it is almost impossible to acquire and track signals autonomously, because of the importance of obstacles which involve high signal attenuation. Received signals are affected by several sources (multipath problems, masking, interference and jamming). The receiver then delivers a position often affected by an error of several tens of meters, when there is not entirely impossible to calculate its position himself.

Collective Detection approach has been proposed recently to address positioning problems in non-ideal environments and there are not yet many researchers dealing with this subject compared to other positioning techniques. In fact, works on this interesting approach are not yet numerous. The vectorial acquisition concept has been developed in depth in (DiEsposti, 2007). This concept is mainly based on the use of assistance information from the reference station (or base station) to define the user position and clock bias uncertainty range. Then, many works using the vectorial approach were proposed for positioning and navigation. The main idea of this concept is to improve the overall acquisition sensitivity by combining coherently the detection metrics from all visible satellites (Axelrad et al., 2011; Bradley et al., 2010). Assistance information can be used to eliminate the requirement for GNSS data recovery and the receiver's ability to increase integration time (Axelrad et al., 2010). In CD, the detection of weak satellite signals is aided by the stronger ones. Using CD, position solution can be obtained with signals at 20 dB-Hz of C/N_0 (Axelrad et al., 2011). Various studies should be performed in the CD as reduce the complexity of the collaborative approach, increase the sensitivity by using deeply the assistance information and minimize as much as possible the assumed available information from the base station.

5.1.1 Existing works

In the proposition of original CD, the main idea was to conduct the acquisition by several iterations while refining the search spacing at each iteration until we can get an estimate of the position (Axelrad et al., 2011). It has been shown that the CD is able to enhance signal detection performance by several dBs (Axelrad et al., 2011; Cheong, 2012). However, the CD approach is computationally intensive because of the important number of candidate points which makes its practical implementation very difficult (Axelrad et al., 2010; Cheong, 2011).

So, various approaches have been proposed to solve this complexity problem. For example in (Axelrad et al., 2011), an averaged correlogram is used at the beginning of the search in order to accelerate the detection process. Indeed, (Axelrad et al., 2011) proposed first to evaluate the correlogram of all possible satellites, and subsequently project and combine the individual

satellite correlogram to the position/common clock bias (CCB) domain (corresponding to the correlator output) in order to construct a position domain projected correlogram (PDPC) corresponding to the CD metrics, which is then used to produce estimations of the parameters of interest. The correlation values are pre-stored which requires a larger memory database. This approach also facilitates CD by enabling the use of FFT technique to evaluate the correlogram of each visible satellite. Similarly, according to (Cheong et al., 2012), it should be noted that the discrete correlogram used in FFT can result in aliasing artefacts when the sampling frequency is not high enough.

Reduce the complexity by hybridizing the standard correlation with the CD in a multi-stage method has been proposed in (Cheong, Dempster et Rizos, 2011). It has been shown that the proposed technique could reduce the complexity of the receiver after several iterations. Another technique for reducing complexity has been proposed in (Narula, Singh et Petovello, 2014) by estimating roughly the clock bias in order to reduce the clock bias search range from 300 km to 100 m and estimating the coarse-time error as a fifth unknown in the navigation solution. This proposed method is called as Accelerated Collective Detection. In order to mitigate the large computational burden required by the traditional CD scheme related to the clock-bias uncertainty, this method is based on the hypothesis that there is at least one strong GNSS signal and it is known.

Otherwise, an improvement of the multi-resolution approach initiated in (Axelrad et al., 2011) is proposed in (Esteves, Sahmoudi et Ries, 2013) by using small clock bias spacing with large horizontal position step size to get a high time resolution and reduce the calculation load. According to (Li et al., 2014), a multi-resolution CD has been proposed to be a coarse-to-fine searching approach to solve for the position/common clock bias estimation. On the one hand, for a coarse search with large horizontal position step size, a smaller CCB step size has been proposed instead of an averaging correlogram to reduce computation complexity as well as to obtain high time resolution. On the other hand, for the fine search with small horizontal space step size, a 3-D dichotomous searching scheme has been designed and applied to reduce the

number of searching points on the grid. Similarly, dichotomous search of coarse time error in CD for GPS signal acquisition has been proposed in (Cheong, Wu et Dempster, 2015).
Since the first proposal of CD, all work in CD use a representation in cartesian coordinates (North-East referential) for the horizontal position search space, but a new representation in polar coordinates (Rho-Theta) is proposed in (Esteves, Sahmoudi et Ries, 2013; 2014). This coordinate transformation can decrease considerably the total number of points to evaluate. This proposal allowed authors to develop the method called Systematic and Efficient Collective Acquisition (SECA). Indeed, "systematic" because the resolution to be employed in the position/clock bias searches is determined according to a set of input parameters; and "efficient" because the search steps assure that the true signal code phase is not missed while avoiding excessively fine and computationally heavy search grids. The performance of the algorithm was verified by analyzing the impact of the search grid resolution in the maximum code phase estimation error while varying the geometry of the constellation of visible satellites.

All these works described treat the acquisition as a detection problem. Moreover, other works consider it as an estimation problem. For example, (Cheong, 2012) uses MLE (Maximum Likelihood Estimation) to get the position solution and (Axelrad et al., 2011) adopts the SAGE (Space Alternating Generalised Expectation-Maximisation) optimization algorithm to solve the problems. The MLE is approximated sequentially by dividing a multi-dimensional search into a sequence of single dimensional searches. In (Cheong, 2012; Cheong, Dempster et Rizos, 2011), in order to estimate the user position, a MLE is adopted by solving an optimization problem with sequential Monte Carlo methods. So, signal from different satellites are combined in the estimation process.

Furthermore, a new approach has been proposed in (Jia et Sahmoudi, 2016) to handle the CD problem. They consider the acquisition problem as an optimization problem and solve the problem using an improved Pigeon-Inspired Optimization algorithm. A Swarm Intelligence algorithm is adopted in order to obtain the user's relative position vector with good resolutions without searching the whole search space, and it considerably reduces the computational

burden. However, the sensitivity of the CD is compromised by this approach according to the results of the studied case.

5.1.2 Issues in Collective Detection

In view of the various publications previously cited, we can deduce that CD approach is simultaneously a high-sensitivity acquisition method, by application of vector acquisition, and a direct positioning method, providing a rough estimate of position/clock bias solution directly from acquisition without tracking process.

On the one hand, as a HS acquisition method, CD approach is characterized by:

1) Sensitivity, and
2) Complexity.

On the other hand, as a DP method, CD approach is characterized by:

1) Position error, i.e. accuracy,
2) Time to first fix (TTFF), i.e. availability,
3) Complexity (in certain cases, and can become a problem if it is excessively high).

These performance metrics are summarized in Table 5.1. They are all related to the search grid resolution. These metrics are the basis of the performance analyzes carried out in tests and simulations to verify the effectiveness of each algorithm proposed in this thesis.

The trade-off between complexity and sensitivity has always been critical in GNSS signal acquisition. Uncertainty in both code phase and Doppler search grid dimensions is the main reason for the difficulty in reaching this compromise. From Table 5.1 we can deduce that the largest issue to be resolved is the trade-off between the search grid resolution and the total number of candidate points to be analyzed. The search grid resolution must be fine enough to obtain a higher sensitivity and a lower position error. However, the number of candidate points has a direct effect on the TTFF and the complexity of the algorithm.

Table 5.1 Performance metrics of Collective Detection approach

Performance metric	**Corresponding parameter**	**Key point**
Sensitivity	Code delay search step size	Search grid resolution, integration period
Complexity	Number of candidate points	Search grid resolution
Position error (accuracy)	Code delay search step size	Search grid resolution
TTFF (availability)	Number of candidate points	Search grid resolution

The CD approach requires a very high calculation load because of the important number of candidate points which makes its practical implementation very difficult. For example, in (Axelrad et al., 2011) there are nearly 31 million candidate points to estimate the user position with ± 150 km clock bias search range and ± 3 km, ± 3 km, ± 600 m for the search range in north, east and down directions. Similarly, since the correlation values are pre-stored in (Li et al., 2014), part of the computation burden of CD is transformed into a tractable hardware issue, formulating and accessing a larger memory database.

With a view to practical use of the CD approach, the performance of the developed algorithms must be tested with real GNSS signals. Thus, in this case the Doppler frequency shift must be taken into consideration.

Until now, all the research on CD approach are based on the use of a fixed reference station and this approach requires that the RS must exist physically. This implies that it is impossible to apply CD technique in certain cases where there are no reference stations.

In addition, despite its effectiveness in treating satellite signals in non-ideal environments, the computed position comes with a large error compared to the conventional positioning method. Depending on the geometry of the satellites and the signal strength, the error can be up to

hundreds of meters, which is not interesting for certain applications that require positioning accuracy.

Thus, this thesis proposes some techniques to address these problems of the CD, while reducing the complexity, which is the main obstacle to its practical implementation, and increasing sensitivity as an efficient and innovative techniques for CD. This is done while ensuring not to degrade the performance in terms of accuracy, as a DP method, which is also a metric to be well considered.

Before developing the different contributions proposed to overcome these CD limitations, we will first describe the basic principle of this approach and illustrate its merits.

5.2 Working principle of Collective Detection

In this section we provide a detailed description of the working principle of the Collective Detection approach and its methodology of application where we will see the dependence on assistance data. The two facets of CD approach as a high sensitivity method and direct positioning method are then assessed.

5.2.1 Description of the Collective Detection approach

The basic idea of the use of Collective Detection is that the strong signals are used to detect the weak GNSS signals in view as a sort of multi-satellites collaborative processing. The principle of CD has been introduced in (DiEsposti, 2007). Then it was studied in depth and refined by different researchers, in particular in (Axelrad et al., 2011; Axelrad et al., 2010; Bradley et al., 2009; Cheong, 2011; 2012; Cheong, Dempster et Rizos, 2011; Cheong et al., 2011; 2012; Esteves, Sahmoudi et Ries, 2013; 2014; Jia et Sahmoudi, 2016; Li et al., 2014; Narula, Singh et Petovello, 2014).

In CD technique, the satellite signals are acquired collectively but not individually one by one, and the code delay search for all visible satellites is mapped into a receiver position/clock bias search space. The CD approach depends heavily on information data from assistance which is given to the MS with the way of defining a position and clock bias uncertainty range. The projection of the signal code phase to the position/clock bias domain is performed differentially with respect to the pseudorange measurements from the reference station. An exhaustive Doppler search may not be necessary, because components of Doppler sources can be eliminated with assistance data. The CD performs the search in the space of receiver position relative to RS position and clock bias. In fact, the search of the position solution is carried out around the reference station with a known position.

In conventional acquisition, the input signal is correlated with a local replica and the correlation power of a GNSS receiver corresponding to satellite k is expressed as:

$$S_{conv}(\tau_k) = |\mathbf{s}_{\boldsymbol{\tau}} \cdot \hat{\mathbf{v}}(\hat{\tau}_k)|^2 = |a_k \mathbf{v}_k(\tau_k) \cdot \hat{\mathbf{v}}(\hat{\tau}_k) + \mathbf{n}_k \cdot \mathbf{v}_k(\tau_k)|^2 \tag{5.1}$$

with $\mathbf{s}_{\boldsymbol{\tau}}$ is the input signal and represents the complex baseband signal such as :

$$\mathbf{s}_{\boldsymbol{\tau}} = \sum_{k=1}^{N_k} a_k \mathbf{v}_k(\tau_k) + \mathbf{n} \tag{5.2}$$

where $\mathbf{v}_k(\tau_k)$ is the signal vector of the satellite k, τ_k is the code phase, N_k is the number of visible satellites, $\mathbf{n}$ represents the noise component as an AWGN. In equation 5.1, $\hat{\mathbf{v}}(\hat{\tau}_k)$ and $\hat{\tau}_k$ represent respectively the signal local replica and the hypothesised code delay of satellite k. Note that the notation $\sum_k$ means $\sum_{k=1}^{N_k}$ (sum of all visible satellites) throughout the manuscript.

First, in conventional acquisition the peak position of the correlation is estimated as the code delay of each acquired satellite. Then, the estimation of position and others parameters defined as a vector $\hat{\gamma}$ is carried out. This vector includes three parameters of the estimation of receiver

position (e_r, n_r, u_r) and one parameter of the estimation of common clock bias b. $\hat{\gamma}$ can include other factors according to the parameters to be studied. The navigation solution can be obtained effectively if the number of parameters to be estimated is less than the number parameters of satellites measurements. The fourth parameter of $\hat{\gamma}$, the common clock bias b, represents the timing difference between the local clock of the receiver and the synchronized clock of the satellite. An uncertainty space Γ is used to define the parameter $\hat{\gamma}$.

Based on this point of view, in CD approach the estimation of parameters is carried out by non-coherently summing the correlation power of all satellites in view computed for conventional acquisition and it is performed in position and clock bias domain. Then,

$$S_{CD}(\tau_k) = \sum_{k=1}^{N_k} |\mathbf{s}_{\boldsymbol{\tau}} \cdot \hat{\mathbf{v}}(\hat{\tau}_k(\hat{\boldsymbol{\gamma}}, \boldsymbol{\psi}))|^2 \tag{5.3}$$

where $\boldsymbol{\psi}$ represents the satellite position vector.

The ECEF (Earth-Centered Earth-Fixed) coordinates of the satellite k provided by the reference station are (e_k, n_k, u_k). Then, the pseudorange corresponding to the satellite k can be obtained by the non-linear relationship between the receiver's position and the code delay.

$$\rho_k = \sqrt{(e_k - e_r)^2 + (n_k - n_r)^2 + (u_k - u_r)^2} + c \cdot \Delta b \tag{5.4}$$

where c is the speed of the light and Δb is the user clock bias w.r.t the GNSS constellation time.

Rather than requiring each satellite signal to be acquired and tracked before it can be used in the navigation solution, CD approach combines the received signal power from all satellites in view in a direct-to-navigation-solution.

5.2.2 Dependence on Assistance Data

We have introduced in the previous chapter (section 4.5.3) that the concept of A-GNSS was inspired to develop the CD approach. The concept of CD is intended to complement an existing assisted GNSS and positioning method. In fact, Collective Detection is an A-GNSS approach for direct positioning in which all information from satellites in view are combined in order to enable rapid acquisition, i.e. to reduce the TTFF and increase the sensitivity of the receiver.

The assistance data allows the GNSS receiver to reduce the search space by providing assistance information. Two major approaches to A-GNSS exist: MS-assisted and MS-based GNSS. The position is computed at a server (reference station) in MS-assisted GNSS whereas it is computed by the receiver itself in MS-based GNSS. In MS-assisted GNSS, the receiver only performs the signal acquisition and sends the measurements to the reference station. The MS requires more assistance data in MS-based approach but also presents several advantages, such as better position accuracy, and possibility of integration of improved navigation filters (van Diggelen, 2009).

Since one of the objectives of this thesis is to minimize dependence on support, then the MS-based approach will be exclusively used in all algorithms developed. In addition, the assistance information to be sent to the MS will vary according to the proposed algorithm and corresponding to the type of assistance (A-GNSS frequency assistance or A-GNSS time assistance for code phase) according to Table 4.2.

In most cases studies in the literature, in order to put the CD approach into practice, the required assistance data to be supplied to the MS for the application of the MS-based A-GNSS approach are:

- **Coarse time:** may be delivered as GPS or UTC form. For example, time synchronization within few milliseconds (± 0.5 ms to ± 2 ms) should permit direct despreading on secondary code sequences;

- **Ephemeris:** for computation of the expected satellite position and velocity from azimuth and elevation angles which are themselves calculated from the parameters sent. The velocity is used for compensation of the Doppler offset component due to satellite motion;
- **Reference Frequency:** for calibration of the MS oscillator. It allows compensation of most of oscillator Doppler offset component;
- **RS position:** for reducing the initial MS spatial uncertainty; and,

Apart from the assistance data listed here, it should be noted that for the application of the CD principle, a new assistance parameter is required, which is the *pseudorange measurements* for all visible satellites as seen from the reference station. This is used in the problem formulation of the CD to link the difference between RS pseudorange and rover pseudorange to the relative position of the user to be estimated. As it will be explained, the RS measurements are used in the code phase estimation of each candidate point in position domain in order to estimate the user position.

As we have introduced at the beginning of this chapter, some CD algorithms are proposed in this thesis in order to achieve the great objectives such as increasing the sensitivity of the GNSS receiver and reducing the complexity while maintaining a good margin of positioning accuracy, and especially to minimize reliance on assistance information. Thus, according to the hypothesis for each proposed algorithm, an exhaustive Doppler search may not be necessary, because the main Doppler sources can be eliminated with assistance data. Indeed, the Doppler search is not even required since both oscillator and satellite-motion Doppler offset components are compensated. The user motion, the source which most impacts the residual satellite Doppler, is typically the least significant source from the three (van Diggelen, 2009).

According to (van Diggelen, 2009), the receiver can also receive fine timing information (less than 1 ms accuracy) from the reference station, which can considerably reduce its uncertainty in clock bias. But it is not necessarily the general case.

With the assistance data, the TTFF of A-GNSS receivers can be reduced and becomes the equivalent of a standalone GNSS receiver in a “hot start” where acquisition occurs only a few minutes after the receiver was last switched off. In fact, depending on the power levels of the received signal, a “cold start” requires a TTFF of 1 min in the case where there is no a priori information, whereas the TTFF can be reduced to 1 s using assistance information (Li et al., 2011).

5.2.3 Methodology of application

In CD technique, the acquisition search grid is set in a space defined by 3D position coordinates $(\Delta N, \Delta E, \Delta D)$ and clock bias (ΔB). The 3D position coordinates represent the algebraic distances between the receiver and the RS in North, East and Down directions, and the ΔB represents the relative clock bias of receiver to the RS. In fact, the equation (5.4) is used to project the code delay in the individual detection metric (correlator output) corresponding to a given point in the position/clock bias domain for each satellite. Figure 5.1 shows the mapping of the signal code delay to the position/clock bias domain of the user (MS) is done differentially with the respect to the pseudorange measurements $\rho_{RS,k}$ provided by the reference station (RS) for the satellite k.

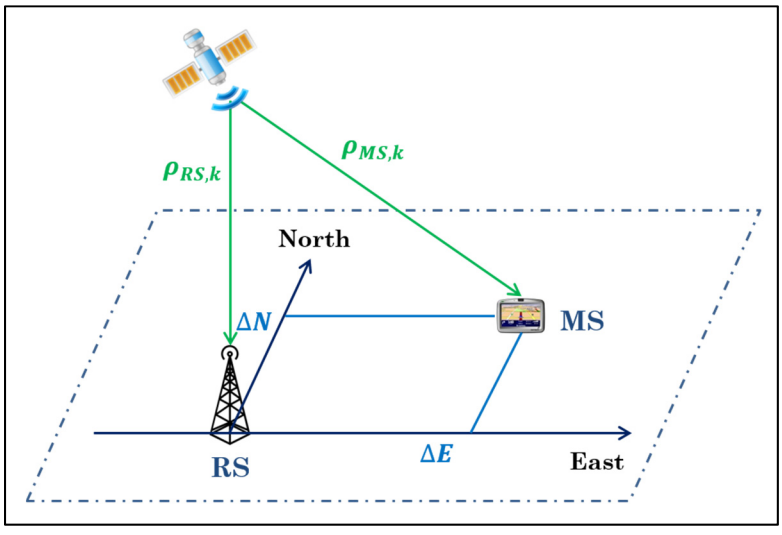

Figure 5.1 Projection to position/clock bias domain in Collective Detection of each satellite

For the satellite k, the pseudorange seen by the MS can be calculated by:

$$\rho_{MS,k} = \rho_{RS,k} + \Delta\rho_k \tag{5.5}$$

For CD, the uncertainty space Γ is centered on the initial position and clock bias. The accuracy of the initial knowledge is essential in the definition of the uncertainty space. If the pseudorange seen by the RS, at the center of the search space, is $\rho_{RS,k}$ for the satellite k, then the range-offset at a location separated by $(\Delta N, \Delta E, \Delta D, \Delta B)$ from the RS is expressed in terms of the position and the clock bias:

$$\Delta\rho_k = f(\Delta P_{MS}, \Delta B_{MS})$$

$$\begin{aligned}\Delta\rho_k(\Delta N, \Delta E, \Delta D, \Delta B) \\ = -\cos(az_k)\cos(el_k)\,\Delta N - \sin(az_k)\cos(el_k)\,\Delta E + \sin(el_k)\,\Delta D \\ +c\cdot\Delta B\end{aligned} \tag{5.6}$$

where az_k is the azimuth of the satellite k and el_k is the elevation of the satellite k as seen by the RS (usually the same as for the MS). The coordinates ΔN, ΔE and ΔD represent the 3D position displacement of the MS with respect to the RS in a North-East-Down (NED) local coordinate frame. The term $c\cdot\Delta B$ represents the pseudorange variation due to the clock bias of the MS, and c being the speed of light.

Then, the pseudorange can be converted to an equivalent code phase, at a hypothetical location $\Delta N_i, \Delta E_j, \Delta D_m$ and a clock bias ΔB_n, as :

$$\hat{\tau}_k = \frac{\left[\rho_{RS,k} + \Delta\rho_k\left(\Delta N_i, \Delta E_j, \Delta D_m, \Delta B_n\right)\right]_{c\cdot T_c}}{c\cdot T_c}\cdot N_c \tag{5.7}$$

where $\hat{\tau}_k$ is the estimated code phase for the satellite k, T_c is the signal spreading code period (i.e. 1 ms for GPS L1 C/A code), N_c is the number of code chips per period, and $[.]_{c\cdot T_c}$

represents the modulo $c \cdot T_c$ operation such that $\hat{\tau}_k \in [0, N_c - 1]$ chip. Note that $\hat{\tau}_k$ corresponds to a hypothetical delay that is varied via the four delta variables.

Then, the individual detection metric, i.e. the correlator output value, corresponding to this satellite for these 4D coordinates can thus be effectively projected from code phase domain to the position/clock bias domain and calculated by:

$$D_{ind}(\hat{\tau}_k) = |S(\hat{\tau}_k)|^2 \tag{5.8}$$

where $S(\hat{\tau}_k)$ corresponds to the correlation output at the code phase $\hat{\tau}_k$ for the satellite k. It should be better to specify that this detection metric is simply used as an example to represent the correlation output, so other detection metrics can be used whether they use non-coherent or differential integrations. For all satellites in view, the individual detection metrics obtained for these 4D hypothetical coordinates $(\Delta N_i, \Delta E_j, \Delta D_m, \Delta B_n)$ are then summed in order to obtain a single Collective Detection metric as:

$$D_{CD}(\Delta N_i, \Delta E_j, \Delta D_m, \Delta B_n) = \sum_k D_{ind}(\hat{\tau}_k) \tag{5.9}$$

Once the Collective Detection metric is carried out for all candidate points, many approaches can be followed to decide which set of values represents the best estimation of the true MS position coordinates and clock bias. If the Collective Detection metric exceeds a pre-defined threshold, the satellite signal could be detected. It is also important to specify that different decision techniques exist in the literature and can be used, but most studies use the typical maximum likelihood estimation and what we also use in our algorithms. Then, the method developed in (Esteves, Sahmoudi et Ries, 2013) is used to obtain the code phase and Doppler frequency corresponding to the detected signal.

Input/output of CD process

According to equation (5.7), the estimation of the code delay for each satellite requires several information from the reference station, such as the RS position for setting the initial MS spatial uncertainty, the pseudorange measurements for all satellites in view as seen from the RS, ephemeris to extract the necessary parameters in order to compute the expected satellite azimuth and elevation angles. The implementation of the CD requires other information provided by the reference station, such as the reference frequency to calibrate the MS oscillator and compensate the oscillator Doppler offset component. A summary of the inputs and outputs of Collective Detection is shown in Figure 5.2.

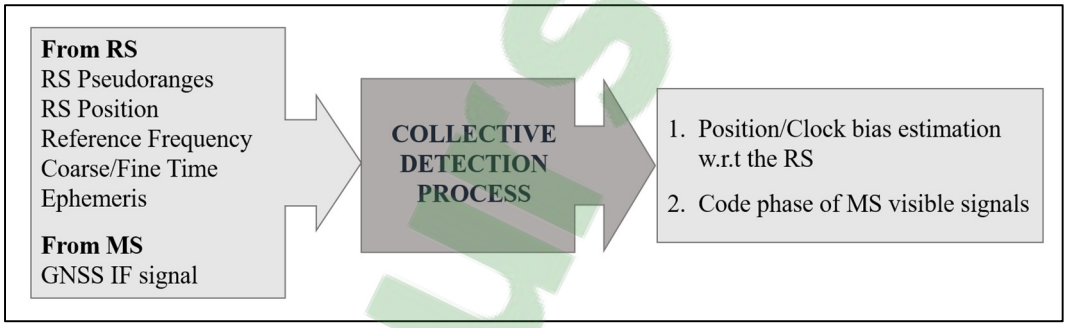

Figure 5.2 Input/output bloc diagram of Collective Detection process

Algorithm of CD process

The benefit of the application of the CD approach is shown in equations (5.8) and (5.9). In fact, weak signals may not be detectable in conventional receivers with only individual correlator output value given by the equation (5.8). Nevertheless, the accumulation of all individual correlation values for each satellite in view can increase the receiver sensitivity using equation (5.9), in position domain, in which the summation operator represents the term “Collective” in the Collective Detection.

The implementation of the Collective Detection algorithm can be described by the following six steps (Esteves, Sahmoudi et Ries, 2014):

1) Establish an appropriate search space of position/clock bias uncertainty range for the MS with respect to the RS and define a grid to overlay this uncertainty;
2) For all satellites in view, compute the estimated code delay corresponding to each of the 4D candidate point in the position-time search grid;
3) Perform the correlation between the incoming signal and the signal locally generated for all satellites in view using the estimated code delay;
4) Sum non-coherently the correlation values corresponding to the estimated code delay of each satellite;
5) Perform an iterative refinement of the search grid's resolution in order to reduce successively the uncertainty range in both domains with each execution of the algorithm;
6) Determine the MS position/clock bias estimate based on the results obtained in step 4, this value corresponds to the highest power.

The function block diagram of the Collective Detection approach is shown in Figure 5.3. It is composed mainly of two components, the satellite detection (acquisition) and the position estimation part.

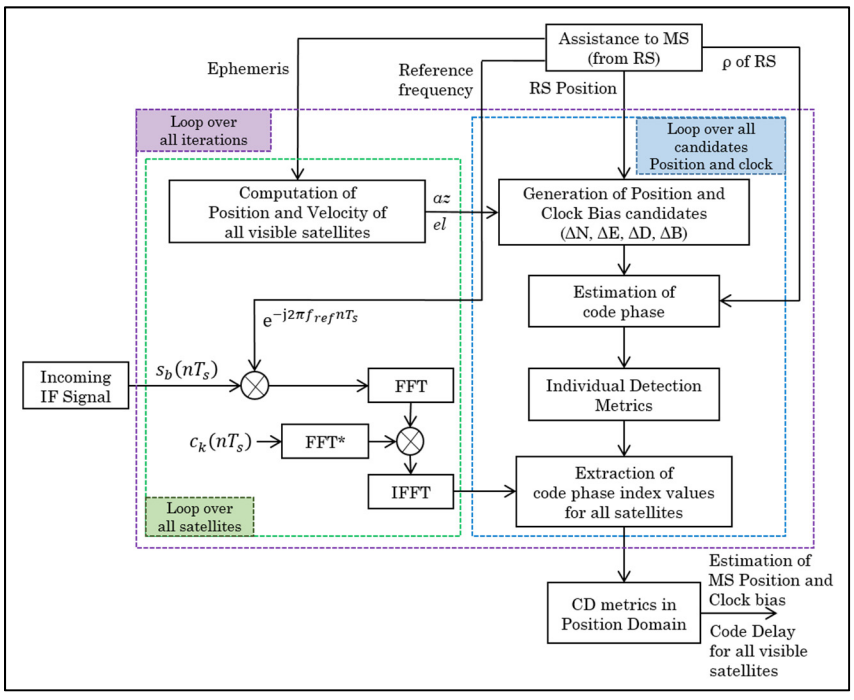

Figure 5.3 Basic block diagram of Collective Detection process

In order to verify the effectiveness of the CD approach to process low power GNSS signals, consider the following example. We simulate four satellite signals with different C/N_0 level: PRN 3 (45 dB-Hz), PRN 6 (43 dB-Hz), PRN 12 (42 dB-Hz), PRN 23 (30 dB-Hz). In traditional sequential acquisition, we are not able to detect the peak of PRN 23 (weaker signal) for 1 ms integration period as we can see in the fourth curve (bottom) of Figure 5.4. In collective acquisition process, the signal was sampled at a rate of 16 samples per chip. In this scenario, we assume that the receiver and satellites clocks are stable. Figure 5.4 shows the correlations for each satellite, corresponding to individual detection metric generated as function of the expected user position and clock bias, and then shows how the correlation peak results are cumulated in order to have the CD metric. In Figure 5.4, the operator $\sum$ represents the sum of the different correlation values and also the projection in the position domain.

In this case, the traditional acquisition cannot estimate the code phase of PRN 23, no PVT solution could be then provided to the MS in this scenario which needs 4 nominal satellites to be able to calculate the PVT solution. However, by applying the CD approach a PVT solution can be computed within an error of 20 meters.

Thus, the 3D correlogram constructed from these individual detection metrics corresponding to 1 ms integration period, after three iterations, are shown in Figure 5.5. Figure 5.5 illustrates clearly the benefit of using CD approach. PRN 23 cannot be acquired individually with conventional receivers using the same integration time but it profits the presence of several satellites even if it is weak. According to this basic principle, the positioning error of the CD depends on the number of satellites in view, their geometric configuration, and the signals power.

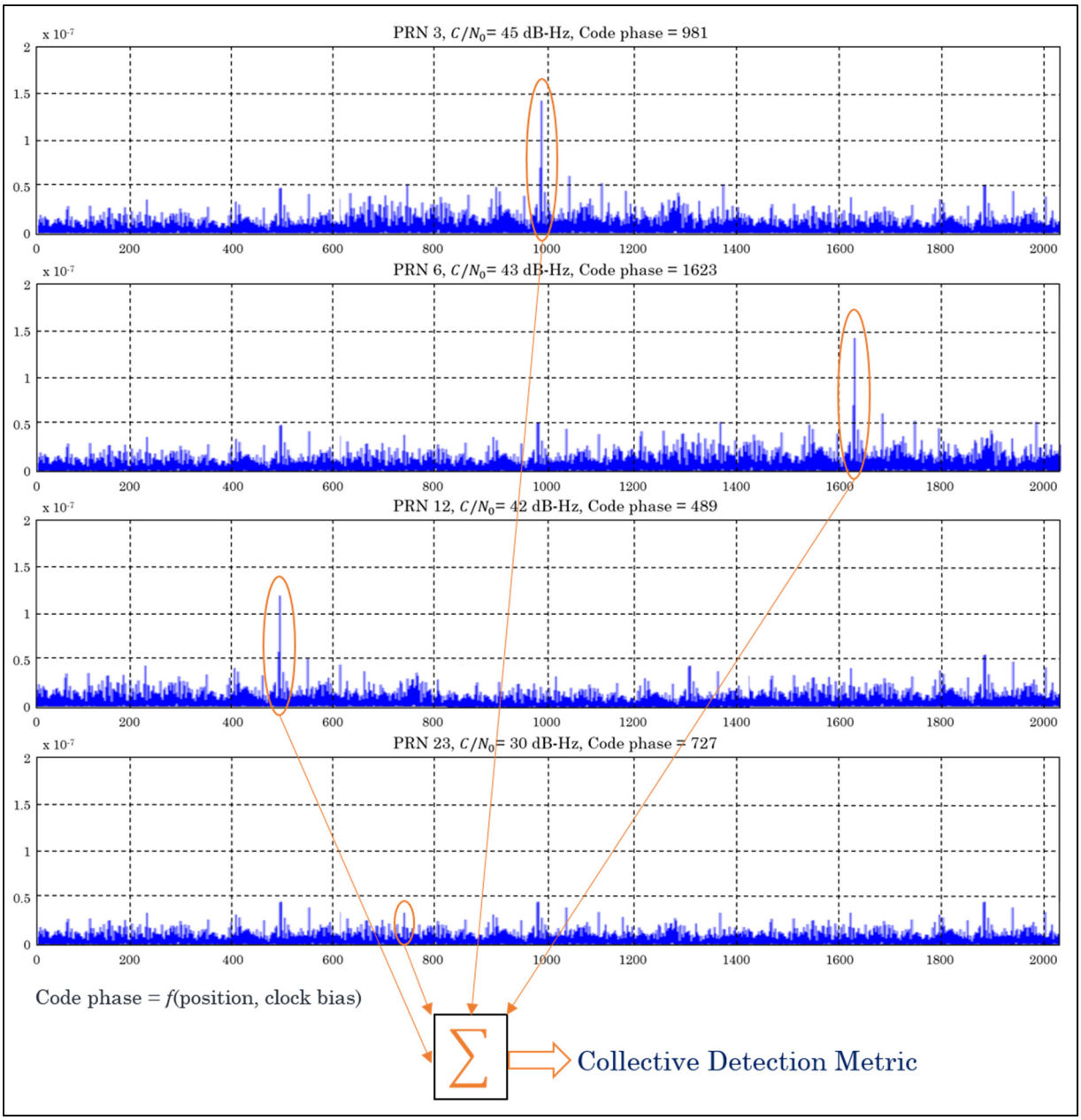

Figure 5.4 Generation of Collective Detection metric by combining GNSS signals from multiple satellites

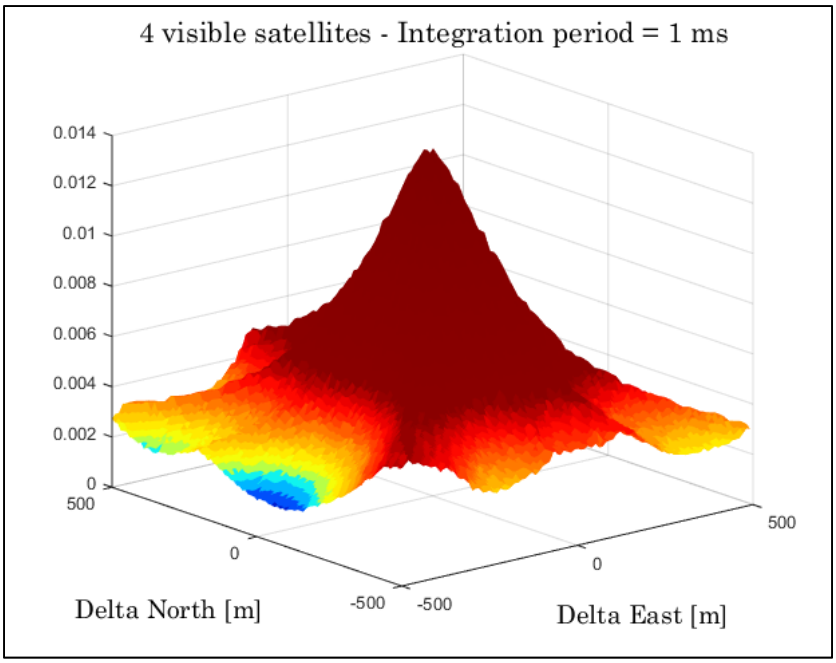

Figure 5.5 3D correlogram of Collective Detection metric after the 3rd iteration (4 satellites: 3 nominal + 1 weak)

5.2.4 CD as a Direct Positioning and High Sensitivity method

The idea of direct estimation of the position in a single step without going through the tracking step and the decoding of the navigation data is the basis of the CD approach, which is why it is considered as a method of direct positioning. In fact, for weak satellite signals, the navigation messages cannot be decoded, hence we must find other alternatives to the determination of the navigation solution by following all the steps like the conventional receivers. Direct Positioning algorithms are based on a set of individual correlogram formed by code delay/Doppler for the satellites potentially visible. CD is able to provide for the MS a first coarse estimate of position and clock bias in situations where the individual satellite signal cannot be acquired and/or tracked. From what we have seen in the previous section, the accuracy of parameter estimates is highly dependent on the available *a priori* information and especially the geometry of the satellites in view. It has been shown that the positioning error of the CD approach depends on the number of visible satellites, their geometry and signal power; and the CD metric is driven by the stronger signals (Bradley et al., 2010). Some CD

works have shown that the mean horizontal positioning error is within a few tens of meters at best. The positioning error depends on the code phase resolution. For example, for an error of 0.5 chips in the code phase estimation (equivalent to 150 m in pseudorange for L1 C/A), a position error of 30 m may still be within the correct code phase estimation region (Bradley et al., 2010).

Contrary to the conventional technique, in CD approach all satellite signals are used even if they are strong or weak. In fact, the objective of CD as a vector acquisition approach is its ability to use stronger signals to facilitate the acquisition of the weaker ones. The number of satellite signals and the relation between their strengths (C/N_0) are essential to analyze the performance of CD as an HS acquisition technique.

As a technique used in harsh environments, the CD can also play the role of a HS receiver by varying the coherent integration period and non-coherently which are key parameters to process weak signals. The CD approach becomes more interesting if there are several satellite signals available, but it is even better if the signal strength can be increased and process stronger signals in order to increase the sensitivity of the receiver as shown in Figure 5.6. Thus, it can be noted that the period of integration is very important in this approach in order to increase the sensitivity. Figure 5.6 shows the comparison of the probability detection for 1 ms and 100 ms coherent integration of 4 and 9 GPS L1 C/A signals in Collective Detection approach. The sensitivity curves show that, as expected, more the integration period increases, more weak signals can be detected.

The second output of CD process is the code phase for all satellites in view which exploits the stronger signal to facilitate the acquisition of the weaker ones. This is expected to be achieved by adding up energy from each individual satellite in the CD metric. According to (Esteves, Sahmoudi et Ries, 2014), for the same C/N_0 value of 35dB-Hz, the detection probability for one satellite is less than 3 % and it becomes more than 30 % when processing 4 satellites collectively.

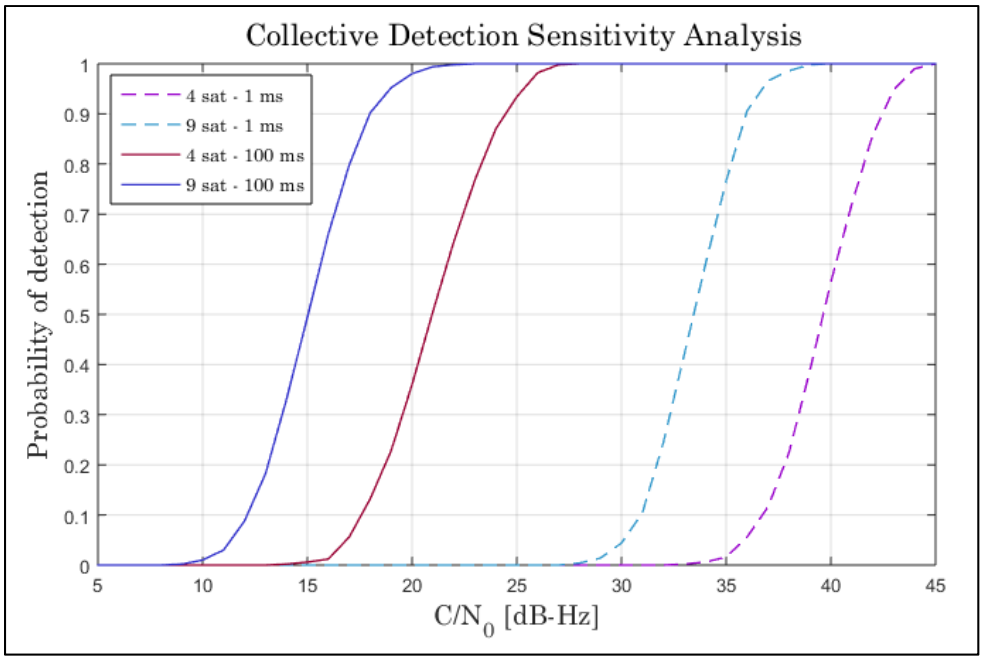

Figure 5.6 Sensitivity enhancement from collective acquisition

5.3 Proposed contributions in CD approach

From what has been introduced in Section 5.1.2, despite the effectiveness demonstrated by the CD approach, this technique has some limitations. Indeed, the complexity caused by the large number of computations is a serious challenge. Sensitivity is an opportunity and not a limitation since CD uses weaker signals than standard receivers. Similarly to the positioning error caused by the DP technique, the precision of existing CD algorithms is not enough for most of urban application requiring meter level of application. The last not least is the dependence on the existence of a fixed RS.

We have already seen in the Section 5.1.1 the different works carried out on CD approach which deal with the reduction of the complexity, the increase of the sensitivity and the reduction of the position error. In this thesis, several techniques are proposed to overcome these problems of the CD approach. All these contributions will be developed. Two case studies of CD application are also developed in this work such as the use of a mobile reference station and the use of an IGS station in order to overcome the dependence of a fixed RS. All

current literatures about collective acquisition are based on the use of a static reference station assigned to a well-known position for assisting the user receiver with its measurements. We would like to extend the applicability of this approach by using a mobile reference station and exploring all the impacts of its mobility.

5.4 Mobile receiver as a reference station in CD approach

Collective Detection approach is a very interesting technique, because of its better performance to detect weak signals in challenged environments, in which the code phase search for all visible satellites is mapped into a receiver position/clock bias grid and the satellite signals are not acquired individually but collectively (Axelrad et al., 2011). This concept depends heavily on assistance information, which is given to the user in order to define a position and clock bias uncertainty range. All studies about CD are based on the use of a fixed reference station, jointly with a communication link, that provides sets of data assistance to the user receiver so that it can estimate roughly its position. Thus, the practical implementation of the CD is still facing the challenge of applications including the need of a second static receiver. To relax the need of such material, the possibility of using a mobile reference station has been studied. A new algorithm about cooperative positioning using a mobile reference station will be presented. This way shows that we are not limited to a static reference station and allows a mobile receiver in challenging reception conditions to get help from another mobile station or other cooperative user in a good reception situation. This new approach has not yet been investigated in published articles about Collective Detection. This scenario is motivated by modern applications in the field of cooperative vehicles and drones.

5.4.1 RS motion effect analysis

For a fixed RS, the code delay is calculated within the MS according to the calculated pseudorange to each satellite in view from RS and the distance between the RS and the mobile user. However, with the use of a mobile RS, these parameters may change if we process a long GNSS signal over many periods of the spreading code, and it is necessary to calculate them

before calculating the code delay within each candidate test point. The sensitivity of the receiver will also be enhanced with increasing integration period.

Let us consider the context in Figure 5.7 to explore the issue of using a mobile reference station instead of a fixed RS. Distance variations may occur due to the reference station motion. Figure 5.7 shows the study context if a mobile reference station is used with the various important parameters to be taken into account such as the change of the position of the satellite and of the reference station during the signal processing time, the difference of the instants when the acquisition of the signal was started and the next instant corresponding to the actual position, which implies a new pseudorange value.

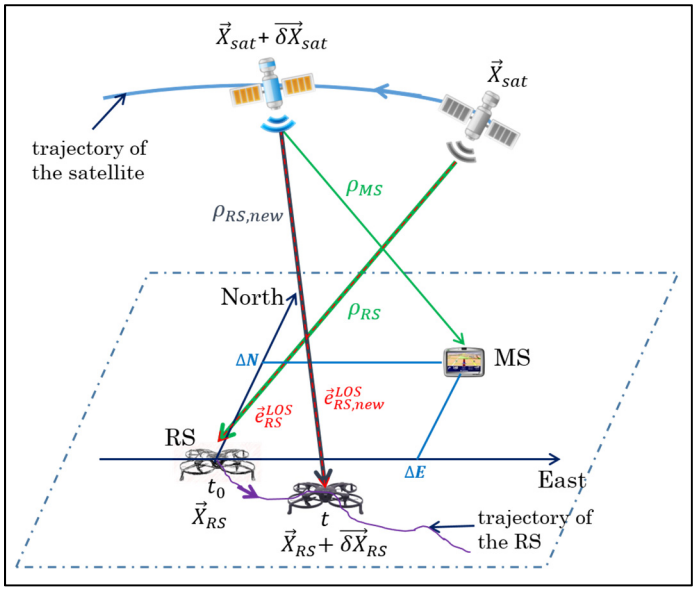

Figure 5.7 Context of mobile reference station in Collective Detection

We assume that the position of the RS changes during the reception of the satellite signals and an uncertainty in the RS position causes a Doppler variation. The effects of this position change of the reference station should be investigated on several sides. Knowing that these impacts are function of the integration period and the dynamics of the RS, Table 5.2 shows the relationship between the integration period and the position change of the reference station according to three types of dynamic (low dynamics, medium dynamics and high dynamics).

Table 5.2 RS motion according to integration period of GNSS signal

Dynamics		**Low dynamics**	**Medium dynamics**	**High dynamics**
Example of application		Pedestrian, robot	Car in urban city, drone	Car in a highway
Velocity [km/h]		5	50	120
Displacement for different integration periods [m]	1 ms	0.00138	0.01388	0.03333
	10 ms	0.01388	0.13888	0.33333
	20 ms	0.02776	0.2776	0.66666
	100 ms	0.13888	1.38888	3.33333
	1 s	1.388	13.88	33.33
	5 s	6.94	6.94	166.6
	10 s	13.88	138.8	333.3
	100 s	138.8	1388	3333.3

We can see in the Table 5.2 the effect of high dynamics on the change of RS location. For example, in 1 s the uncertainty of RS will increase with 33.33 m and by 3.3 km in 100 s.

According to (van Diggelen, 2009), if the receiver is moving, i.e. the reference station in our case, then this affects the observed GPS Doppler by up to 1.46 Hz for each 1 km/h of speed. Thus, the carrier Doppler effect caused by the mobility of the RS, corresponding to the signal L1, is summarized in Table 5.3.

Table 5.3 Carrier Doppler due to the RS motion

Dynamics	**Example of application**	**Velocity [km/h]**	**Doppler shift [Hz]**
Low dynamics	Pedestrian, robot	5	7.3
Medium dynamics	Car in urban city, drone	50	73
High dynamics	Car in a highway	120	175.2

5.4.2 Motion effect on code phase error

The main aim is to analyze the impacts of the RS motion on the code delay estimation. Two main issues must be resolved: Is the value of pseudorange change acceptable for sending a proper measurement to the MS? What is the limitation of this value compared to the code delay resolution $\Delta\tau$? In our case, we have chosen $\Delta\tau$ = 0.5 chips = 150 m. However, if the code delay resolution is reduced, the limitation value becomes an issue.

According to (van Diggelen, 2009), the Doppler change is not very sensitive to small changes of user location, so can we use the *a priori* RS location and the satellites velocity (estimated from RS) to predict the user Doppler.

Thus, to demonstrate the feasibility of the proposal, i.e. to validate the performance of the technique using a mobile RS, we have simulated the change of RS position during signal acquisition. This involves the change of the pseudorange for each satellite in view. We propose to perform the analysis for the following changes: $\delta\vec{X}_{RS}$ = 5 m, 10 m, 100 m, 500 m, 1 km and 2 km. The relationship between the signal processing duration and each RS position change corresponding to each dynamic type can be seen in Table 5.4.

Table 5.4 Limitation of signal processing duration corresponding to each RS position change

Dynamics	**Velocity [km/h]**	**Integration period limitation for each $\delta\vec{X}_{RS}$ [ms]**					
		5 m	**10 m**	**100 m**	**500 m**	**1 km**	**2 km**
Low dynamics	5	3602	7204	72046	362318	720461	1440922
Medium dynamics	50	360	720	7204	36231	72046	144092
High dynamics	120	150	300	3000	15001	30003	60006

The effect of the RS mobility depends mainly on the coherent integration period. If we restrict ourselves to small signal integrations (1 ms) for signals with nominal powers, the impact of the RS motion is negligible because during 1 ms of integration, the reference station moves only by 1.38 mm if it is moving in low dynamic. So even if the RS moves, the estimation of the code phase is not affected during the integration period. However, this effect can be more significant if the integration period increases, as shown in Table 5.2.

Foremost, in CD, the code delay is calculated within the MS from the computed pseudoranges ρ_{RS} corresponding to all the satellites in view from the RS, and from the difference of pseudoranges seen by the RS and the MS for the same satellite, $\Delta\rho$. However, with the displacement of the reference station, these parameters would change. Thus, by applying the CD process with 10 visible satellites, the code error expressed as a function of the difference of pseudoranges value is shown in Figure 5.8. These results are obtained using simulated GPS L1 C/A signals and correspond to a particular geometry of the GPS constellation at a given moment.

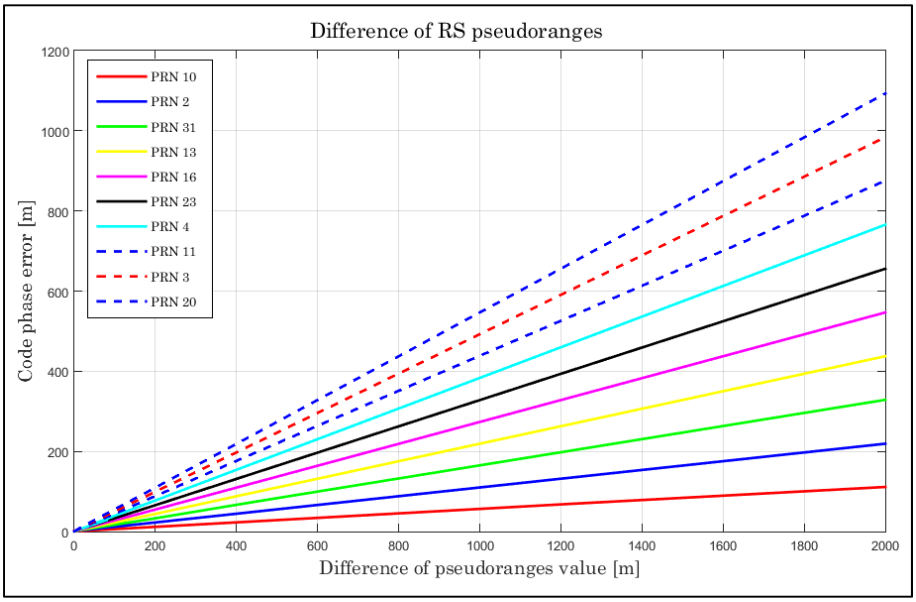

Figure 5.8 Code phase error as a function of pseudorange change

We can find that more the RS moves away, i.e. the value of the relative distance of RS from its initial position increases, the impact on the estimation of the code phase becomes larger. This statement can be validated by Figure 5.9 showing the increase of the code phase error with the evolution of the difference of pseudoranges.

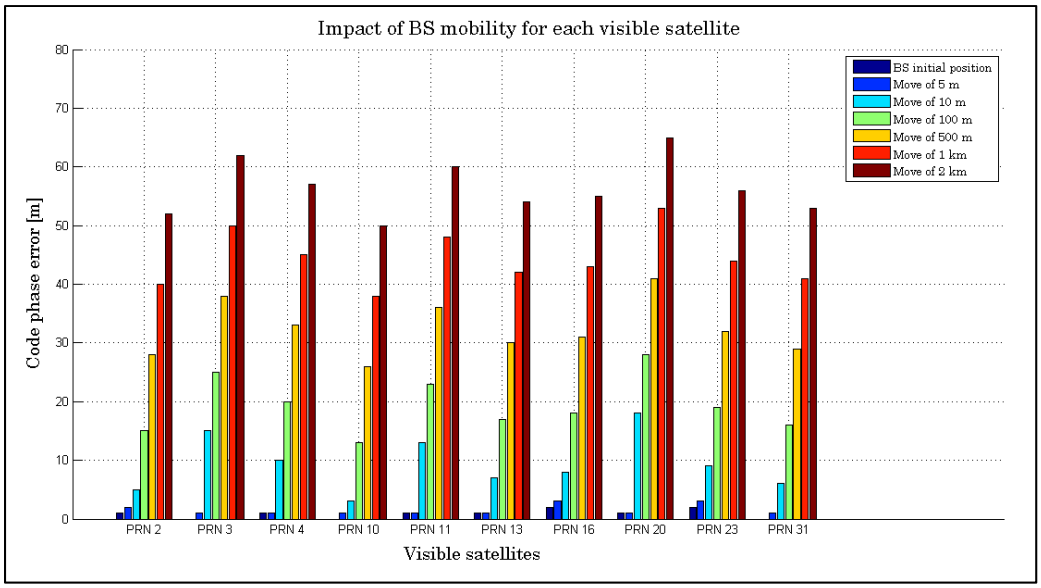

Figure 5.9 Effect of the position change $\delta\vec{X}_{RS}$ on code delay estimation for all visible satellites

In this case, pseudorange change is the difference between the pseudorange in the new position of the RS, $\rho_{RS,new}$ (move of 5 m, 10 m, 100 m, 500 m, 1 km and 2 km) and the pseudorange calculated in the initial position of the RS, ρ_{RS}. Note that the code phase error is calculated by the difference between the true code phase and the estimated code phase. In Figure 5.9, it is important to clarify that the code phase error corresponding to the initial position of RS is not zero, may be zero but not necessarily.

Note that the code delay estimation error depends on the grid step resolution chosen to search for the correlation peak. And given that the maximum estimation error in the code phase is under half chip for every satellite ($\Delta\tau \leq T_c/2 \approx 150$ m), a low dynamic user (as reference station) may have an impact on the estimation of the code delay when we perform an acquisition during 108.069 s. Similarly, a medium dynamic user may affect the code delay

estimation if it moves during 10.806 s of integration period. Finally, the impact may be significant for a high dynamic RS if we perform signal acquisition during 4.5 s.

We can also see that the difference of code phase error value of each satellite in view depends on its elevation angle. For example, PRN 10 is the less affected satellite because corresponds to an elevation of 10.33°. Whereas, PRN 20 has 81.47° of elevation which is very high. The same case for PRN 3 (elevation of 51.08°) and PRN 11 (elevation of 49.99°) which have high elevation. The elevation angles corresponding to all the visible satellites are summarized in Table 5.5.

Table 5.5 Elevation angle corresponding to each satellite in view

PRN	2	3	4	10	11	13	16	20	23	31
Elevation [°]	12.34	51.08	32.73	10.33	49.99	16.64	18.62	81.47	24.99	16.43

In addition, the code phase error is also affected by the line-of-sight vector because it is a function of the position of the satellites and the reference station which are variable parameters. According to the moving direction of the RS, the RS may be positioned at a location where the geometry of the satellites is poor, which implies that the displacement of the reference station can also affect the number of visible satellites. Knowing that the pseudoranges computed in several positions of the RS corresponding to all satellites in view are different. Thus, the mobility of the reference station can impact the estimation of the code phase, as shown in Figure 5.9. We can find that, for all satellites in view, this effect is not significant when the RS moves during 100 ms.

If the maximum code phase error is exceeded due to the combination of integration period, position change and dynamic of the reference station, the impact of the mobility should be compensated in the estimation of the code delay performed within the user receiver in order to obtain an estimation of its position with acceptable value.

5.4.3 Compensation of the mobility impact

In order to compensate the impact of the mobility of the reference station, pseudorange corrections (PRC) and range rate corrections (RRC) should be transmitted to the MS (Hofmann, Lichtenegger et Collins, 2001). Given that the estimation of the code phase depends on the pseudorange seen by the RS and also the difference in pseudorange calculated from the MS w.r.t to the one measured by the RS for the satellite k, $\Delta\rho_k$. Then, $\rho_{RS,k}$ and $\Delta\rho_k$ vary according to the displacement of the RS. Note that the correction is added to the measurement.

Let's assume that t_0 is the reference epoch for the correction. The pseudorange correction at the MS for the measurement epoch t may then be calculated by (Hofmann, Lichtenegger et Collins, 2001; RTCM-SC104, 2001):

$$PRC(t) = PRC(t_0) + RRC(t_0) \cdot (t - t_0) \tag{5.10}$$

The interval $(t - t_0) = \Delta t$ represents the age of the corrections (is also the integration period). Then, the pseudorange measured by the MS $PRM(t)$ is corrected as follows:

$$PR(t) = PRM(t) + PRC(t) \tag{5.11}$$

The pseudorange correction PRC(t_0) can be diverged from its proper value, so it will be updated and transmitted to the MS as often as possible.

Thus, the new expression of the code delay estimation is :

$$\hat{\tau}_k = \frac{\left[\rho_{RS,k} + \Delta\rho_k\left(\Delta N_i, \Delta E_j, \Delta D_m, \Delta B_n\right) + \rho_{corr,k}\right]_{c.T_c}}{c.T_c} \times N_c \tag{5.12}$$

where

$$\rho_{corr,k} = \rho_{RS,k}^{update} + \dot{\rho}_{RS,k}^{update} \cdot \Delta t \tag{5.13}$$

where $\rho_{corr,k}$ represents the pseudorange corrections (PRC) and the range rate corrections (RRC) sent to the MS; $\rho_{RS,k}^{update}$ is the pseudorange computed by the RS in its initial position at the measurement epoch, and $\dot{\rho}_{RS,k}^{update}$ is the range rate corresponding to the actual position; and Δt corresponds to the integration period of the signal.

Note that as the distance between the RS and the MS grows, the number of satellites in common view at the two sides is reduced, and also the available differentially corrected pseudoranges are reduced to estimate the position (Misra, Burke et Pratt, 1999). Since the velocity of RS is assumed constant, i.e. not time varying, we do not need to carry out analyzes on the variation of the RS velocity and acceleration on their impact into the code calculation and the estimation of the MS position.

With a mobile RS, the range rate has to be considered, which is defined as a timely variation of the geometric distance between the satellite located at $\vec{X}_{sat}$ and the receiver at $\vec{X}_{RS}$. The velocity of the satellite and of the reference station are respectively $\vec{V}_{sat}$ and $\vec{V}_{RS}$. So the range rate $\dot{\rho}_{RS}$ is given as the velocity difference projected into the line of sight:

$$\dot{\rho}_{RS} = \vec{e}_{RS}^{LOS,k} \cdot (\vec{V}_{sat} - \vec{V}_{RS}) \tag{5.14}$$

where $\vec{e}_{BS}^{LOS,k}$ is the unit vector pointing to the RS position from the *k*-th satellite.

If the RS position changes by an amount of $\delta\vec{X}_{RS}$, the range rate changes will be in amount of $\delta\dot{\rho}_{RS}$:

$$\dot{\rho}_{RS}^{new} = \dot{\rho}_{RS} + \delta\dot{\rho}_{RS} = \vec{e}_{RS,new}^{LOS,k} \cdot (\vec{V}_{sat} - \vec{V}_{RS}) \tag{5.15}$$

with

$$\vec{e}_{RS,new}^{LOS,k} = \frac{\vec{X}_{sat}^{new} - \vec{X}_{RS}^{new}}{\left\|\vec{X}_{sat}^{new} - \vec{X}_{RS}^{new}\right\|} = \frac{\vec{X}_{sat} + \delta\vec{X}_{sat} - \vec{X}_{RS} - \delta\vec{X}_{RS}}{\left\|\vec{X}_{sat} + \delta\vec{X}_{sat} - \vec{X}_{RS} - \delta\vec{X}_{RS}\right\|} \tag{5.16}$$

Thus, equation 5.15 becomes:

$$\dot{\rho}_{RS}^{new} = \frac{\vec{X}_{sat} + \delta\vec{X}_{sat} - \vec{X}_{RS} - \delta\vec{X}_{RS}}{\left\|\vec{X}_{sat} + \delta\vec{X}_{sat} - \vec{X}_{RS} - \delta\vec{X}_{RS}\right\|} \cdot (\vec{V}_{sat} - \vec{V}_{RS}) \tag{5.17}$$

According to (Leick, Rapoport et Tatarnikov, 2015), line-of-sight accelerations caused by the satellite are below 0.2 m/s^2 for GPS satellites which causes line-of-sight variations below 2 cm over an interval of 1 second. Thus, for a processing time of 1 ms, line-of-sight variation caused by the satellite is negligible.

By applying a first-order Taylor series expansion in the position change of the geometric distance, we can obtain a first order approximation of the range rate change as:

$$\begin{aligned}\dot{\rho}_{RS} + \delta\dot{\rho}_{RS} \approx{}& \left\|\vec{X}_{sat} - \vec{X}_{RS}\right\|^{-1} \\ &\times \left(1 - \frac{\left(\vec{X}_{sat} - \vec{X}_{RS}\right) \cdot \delta\vec{X}_{RS}}{\left\|\vec{X}_{sat} - \vec{X}_{RS}\right\|^2}\right) \\ &\times \left(\vec{X}_{sat} + \delta\vec{X}_{sat} - \vec{X}_{RS} - \delta\vec{X}_{RS}\right) \cdot \left(\vec{V}_{sat} - \vec{V}_{RS}\right)\end{aligned}$$

$$\begin{aligned}\dot{\rho}_{RS} + \delta\dot{\rho}_{RS} = \dot{\rho}_{RS} &- \left\|\vec{X}_{sat} - \vec{X}_{RS}\right\|^{-3} \cdot \left(\left(\vec{X}_{sat} - \vec{X}_{RS}\right) \cdot \delta\vec{X}_{RS}\right) \\ &\times \left(\left(\vec{X}_{sat} - \vec{X}_{RS}\right) \cdot \left(\vec{V}_{sat} - \vec{V}_{RS}\right)\right) \\ &- \left\|\vec{X}_{sat} - \vec{X}_{RS}\right\|^{-1} \cdot \delta\vec{X}_{RS} \cdot \left(\vec{V}_{sat} - \vec{V}_{RS}\right)\end{aligned} \tag{5.18}$$

The reference station velocity (a few km/h) can be ignored with the respect to the satellite velocity (few km/s). Then, the maximum absolute value of the range rate change can be bounded by some minimum or maximum values in equation 5.18, as follows,

$$\|\delta\dot{\rho}_{RS}\| \leq \left\|\vec{X}_{sat} - \vec{X}_{RS}\right\|^{-1}\left\|\delta\vec{X}_{sat}\right\|\left\|\delta\vec{X}_{RS}\right\|\left\|\vec{V}_{sat} - \vec{V}_{RS}\right\| + \left\|\vec{X}_{sat} - \vec{X}_{RS}\right\|^{-1}\left\|\delta\vec{X}_{sat}\right\|\left\|\delta\vec{X}_{RS}\right\|\left\|\vec{V}_{sat} - \vec{V}_{RS}\right\|$$

Then,

$$\|\delta\dot{\rho}_{RS}\| \leq 2\left\|\vec{X}_{sat} - \vec{X}_{RS}\right\|^{-1} \cdot \left\|\delta\vec{X}_{sat}\right\| \cdot \left\|\delta\vec{X}_{RS}\right\| \cdot \left\|\vec{V}_{sat}\right\| \tag{5.19}$$

So, we take into account $\delta\vec{X}_{RS}$ to upper bound the range rate change. For example, if the reference station moves at a distance $\delta\vec{X}_{RS} = 500$ m from its origin. Assuming a satellite-RS distance of 20000 km and a satellite velocity of 4 km/s, then the maximum range rate error is $\delta\dot{\rho}_{RS} \approx 0.2$ m/s. This means that the pseudorange ρ_{RS} changes about 20 cm (1/5 m) over 1 s. This is equivalent to a Doppler error of 1.05 Hz. So the change is not significant.

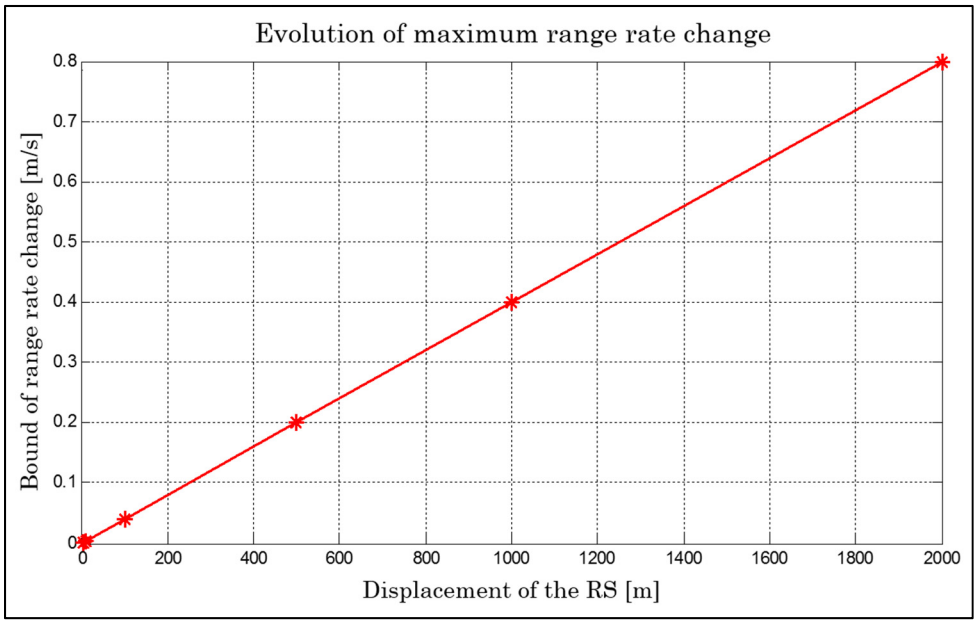

Figure 5.10 Evolution of the maximum range rate change

The range rate change increases gradually as RS moves, as shown in Figure 5.10, but its value is very low and does not affect the estimation of the code delay.
Thus, as compared to the resolution of the code delay $\Delta\tau \leq \frac{T_{code}}{2} \approx$150 m, the effect of $\delta\dot{\rho}_{RS} \approx$ 0.2 m/s on the code delay τ_k is negligible.

So, taking into account the mobility of the RS, the new expression of the code delay estimation in function of the pseudorange correction and the range rate correction in equation 5.12 is:

$$\hat{\tau}_k = \frac{\left[\rho_{RS,k}^{t_0} + \Delta\rho_k\left(\Delta N_i, \Delta E_j, \Delta D, \Delta B_n\right) + \dot{\rho}_{RS,k}^{new} \cdot \Delta t\right]_{c \cdot T_c}}{c \cdot T_c} \times N_c \tag{5.20}$$

where $\rho_{RS,k}^{t_0}$ is the initial RS pseudorange, and $\Delta t = t - t_0$, t is the instant when the new pseudorange measurement is calculated according to the displacement $\delta\vec{X}_{RS}$ of the RS; and t_0 represents the instant where the pseudorange has been measured before the move of the RS.

5.4.4 Performance analysis of the CD algorithm using a mobile RS

To analyze the performance and verify the possibility of using the CD approach with a mobile RS, two tests will be used: with signals simulated under Matlab and with signals simulated by Spirent. The performance metrics to be analyzed are: sensitivity, TTFF, complexity and positioning error.

Using simulated signals in Matlab, AWGN is injected into the raw complex baseband samples to simulate various C/N_0 conditions. Thus, the injection of AWGN uniformly reduces the C/N_0 of all satellite channels.

Knowing that the motion effect of the reference station depends mainly on the integration period, its variation should be analyzed. Moreover, the sensitivity of the receiver will also be enhanced with increasing integration period. Figure 5.11 shows the comparison of the

probability detection for 1 ms and 100 ms coherent integration of GPS L1 C/A signal in Collective Detection approach using a mobile reference station moving at 50 km/h. In this case, four satellites are used for collective acquisition. As seen in this figure, the trend of the curves is similar to the sensitivity curves using a static base station, i.e. more the integration period increases, more weak signals can be detected.

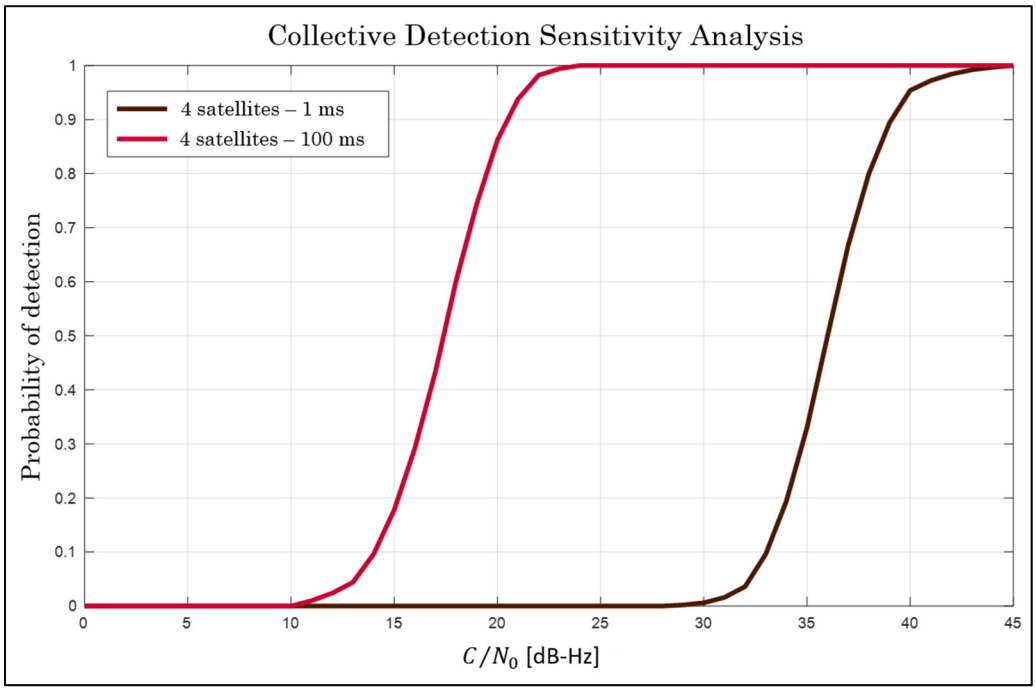

Figure 5.11 Sensitivity enhancement drawn from Collective detection
(T_c= 1 ms vs 100 ms, V_{RS} = 50 km/h)

According to the concept of Collective Detection as a High-Sensitivity acquisition method, the aim in Collective Detection is to make use of the stronger signals to ease the acquisition of weaker ones. So, in order to investigate the effect of the reference station mobility on the Collective Detection sensitivity, test in harsh environment has been performed: reference station moving at high dynamic (120 km/h) during a very long integration period of 450 ms. In this severe scenario, the sensitivity curves corresponding to RS initial position and position changes (5 m, 10 m, 100 m and 1 km) are superposed, as shown in Figure 5.12. It means that the different position changes of the reference station, within the limit of 1 km, do not impact the probability of detection of weak signals. Indeed, despite the fact that the effect depends on

dynamic level and integration time, there is no effect on probability of detection if we still below the limit of 1 km.

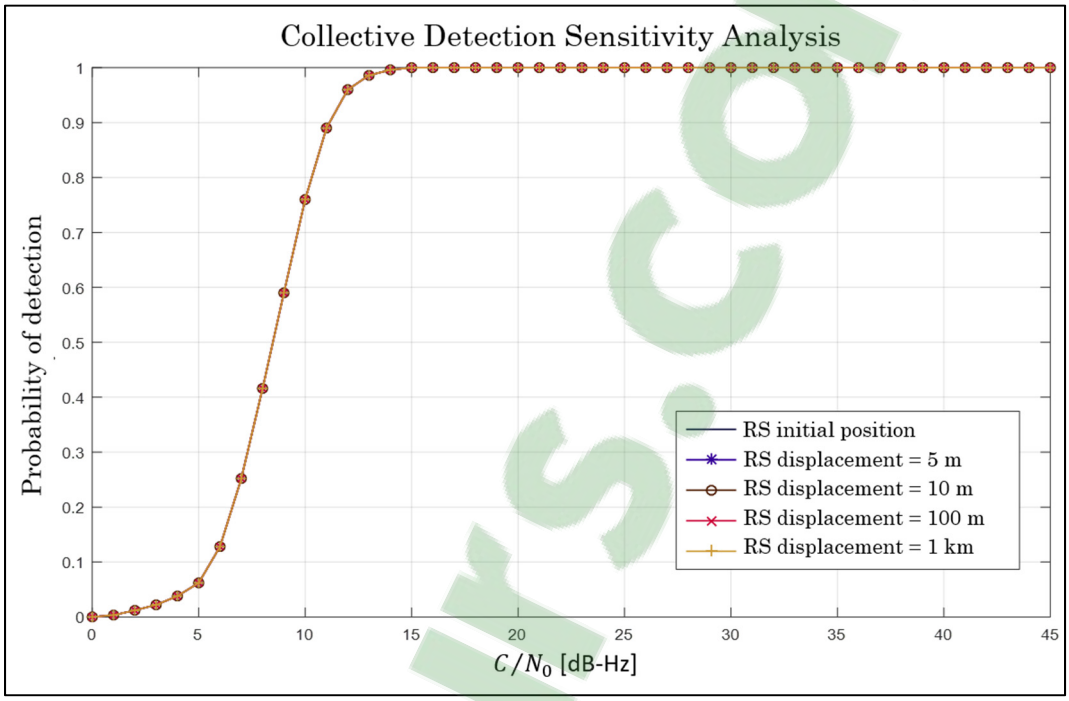

Figure 5.12 Comparison of sensitivity analysis for different position change of RS (T_c = 450 ms and V_{RS} = 120 km/h)

Due to the lack of resources, a test with a very long integration period of tens of seconds or hundreds of seconds has not been performed. We can say that with simulated signals, the RS mobility does not impact the estimation of the code delay within the MS and also in the estimation of its position.

It is well noted that the mean horizontal error is the same as using a static reference station in Collective Detection approach.

In terms of complexity, since the Doppler and motion effect are compensated, the computational load is the same as with static RS. Similarly, the TTFF is the same as with static RS.

5.5 IGS station as a reference station in CD approach

This section is intended to show another way to calculate the user mobile position based on reference points that exist somewhere as a network reference point with a known position. The idea is to apply the concept of positioning with IGS (International GNSS Service) in Collective Detection process.

In that case, we are no longer limited by the fact of having at all times a second receiver to assist the mobile user, it is sufficient to use existing IGS reference stations to provide assistance to the mobile user with all measurement data as pseudoranges and satellites positions for estimating the user position. This proposal is original since no studies have been done on this way.

5.5.1 Working principle

In this proposal, we can exploit the IGS data through the internet to update the data sets in the user mobile in order to compute its position using collective acquisition of all visible satellites. Reference stations locations are already known. Satellites coordinates and angles of elevation and azimuth can be extracted from downloaded ephemeris (Dow, Neilan et Rizos, 2009).

The IGS global system of satellite tracking stations were deployed to put high-quality GNSS data on line in near real time to achieve its objectives in support of Earth science research, engineering applications and studies. The long-term goals of the IGS are to provide the highest-quality, reliable GNSS data and products openly and readily available to all users, and to promote universal acceptance of IGS products as the world standard (Leick, Rapoport et Tatarnikov, 2015).

The various parameters that can be found in the ephemeris sent are summarized in Table 5.6 (Navstar, 2000). These parameters are specific to GPS and Galileo ephemeris.

Table 5.6 GPS and Galileo ephemeris parameter definitions

Parameters	Description	Unit
M_0	Mean anomaly at reference time	rad
Δn	Mean motion difference from computed value	rad/s
e	Eccentricity	-
$A^{1/2}$	Square root of the semi-major axis	$m^{1/2}$
Ω_0	Longitude of ascending node of orbit plane at weekly epoch	rad
i_0	Inclination angle at reference time	rad
ω	Argument of perigee	rad
$\dot{\Omega}$	Rate of right ascension	rad/s
i_{dot}	Rate of inclination angle	rad/s
c_{uc}	Amplitude of the cosine harmonic correction term to the argument of latitude	rad
c_{us}	Amplitude of the sine harmonic correction term to the argument of latitude	rad
c_{rc}	Amplitude of the cosine harmonic correction term to the orbit radius	m
c_{rs}	Amplitude of the sine harmonic correction term to the orbit radius	m
c_{ic}	Amplitude of the cosine harmonic correction term to the angle of inclination	rad
c_{is}	Amplitude of the sine harmonic correction term to the angle of inclination	rad
t_{oe}	Reference time ephemeris	s
Δt_{oe}	Issue of data (ephemeris)	s

5.5.2 Results with downloaded ephemeris from internet

To analyze the feasibility of using IGS reference station as a RS in CD approach, tests with simulated signals are carried out. We assume the nearest reference station in Ottawa with a well-known position, as shown in Table 5.7 (from National Resources Canada - NRC) (Canada, 2015). Assistance data (observations in sp3 files in order to get precise ephemeris) have been downloaded through the internet to update the data sets in the MS in order to estimate roughly its position. Given that reference station position and ephemeris can be obtained with IGS service, the MS can estimate its position. Downloaded ephemeris contains necessary parameters to compute all visible satellites coordinates, azimuth and elevation angles.

Table 5.7 Coordinates of the IGS reference station in Ottawa

Latitude	**Longitude**	**Altitude**
N 45°27'14.985792"	W 75°37'25.784497"	83.601 m

In this scenario, there are seven visible satellites: three nominal satellites (C/N_0 > 40 dB-Hz) and four weak satellites ($C/N_0 \leq$ 35 dB-Hz), as shown in Table 5.8.

Table 5.8 Visible satellites during observation period

PRN	2	5	13	15	20	21	29
$\boldsymbol{C/N_0}$ **[dB-Hz]**	35	46	35	32	41	31	44

With these parameters, Figure 5.13 shows the Collective Detection metric using the IGS reference station in Ottawa (left).

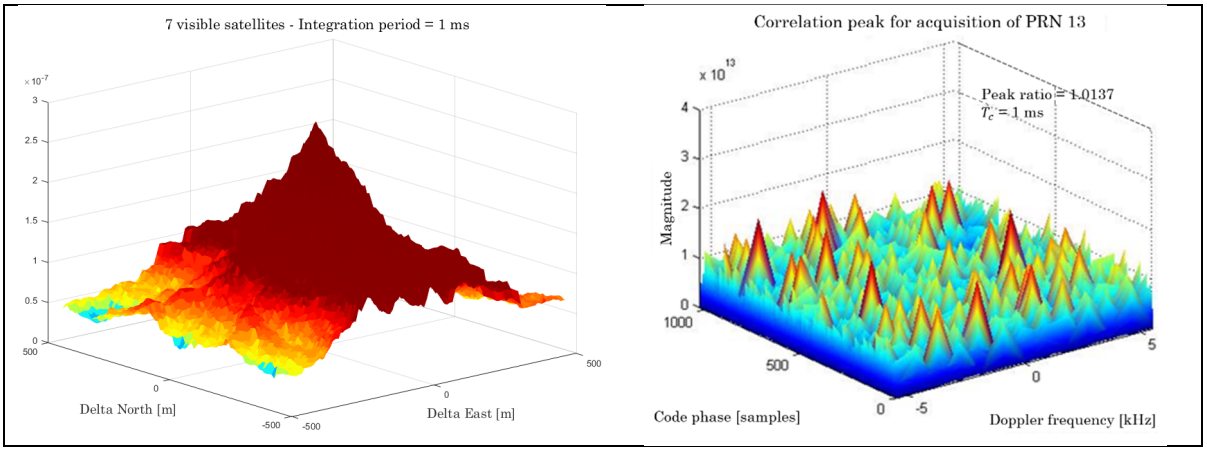

Figure 5.13 Collective Detection metric using an IGS reference station vs Sequential Acquisition at C/N_0 = 35 dB-Hz

According to this correlogram and the mean positioning error value (31 m), using an IGS station is a better alternative in Collective Detection technique implementation. For one millisecond coherent integration of signals, a clear peak around the user true location $(\Delta N, \Delta E) = (0,0)$ can be seen in the Collective Detection metric plot. Furthermore, with the conventional FFT individual acquisition, we cannot find a clear correlation peak with signals at 35 dB-Hz and the individual signals are undetected on their own even if there is 7 visible satellites. Then, it is quite probable of not having a stable PVT. Figure 5.13 (right) shows that it is impossible to detect the real correlation peak for the same C/N_0 level (35 dB-Hz).

To conclude, it has been demonstrated that it is possible to use IGS stations as a reference station in Collective Detection approach to estimate the user position in position/clock bias domain. IGS represents a better alternative in the case that there is no other reference receiver to assist the user receiver. Knowing that there is a network of over 350 continuously operating dual-frequency GPS stations in the world, we do not have the constraint of using our own reference station in areas where there is IGS stations.

5.6 New method for efficient Doppler estimation in CD algorithm

In order to minimize dependence on the assistance, if the reference frequency is not available, the Doppler shift caused by the movement of the satellite and the receiver must be estimated and included in the individual and collective detection process. The fact to estimate the Doppler and do it effectively can also enhance receiver sensitivity.

5.6.1 Proposed Doppler estimation method for CD acquisition

For increasing sensitivity of the GNSS receiver, several approaches have been developed in literature. For conventional sequential acquisition, increasing the coherent integration period and non-coherent accumulation is the basic key. For the multi-satellite approach, different techniques have been proposed. For example, (Kong, 2014) proposed a correlator-based fast multi-satellite maximum likelihood algorithm to achieve fast acquisition and provides higher sensitivity for weak signals.

It has been shown in (Esteves, 2013) and (Sahmoudi et al., 2010) that it is possible to enhance the receiver's sensitivity by using the frequency offset correction to compensate for the Doppler shift during the correlation process. The acquisition method proposed in (Esteves, 2013) aimed to improve the performance of computationally efficient GNSS acquisition in the presence of unknown Doppler shifts. This method is based on the signal processing technique developed in (Jacobsen et Kootsookos, 2007). Similarly, (Sahmoudi et al., 2010) proposed a new frequency offset correction loop architecture to compensate the Doppler of each sample of the input signal while using the estimated frequency offset during the previous coherent integrations in a feedback scheme in order to extend the coherent integration period. Still regarding this problem, two innovative techniques are proposed in (Linty et Presti, 2016) in order to further increase the accuracy of the frequency estimate as the FFT zero forcing and the double FFT (DFFT) method. These methods are focused on reducing the complexity and the computational load of the estimation algorithm.

In this proposal, we are exploiting the signal processing technique developed in (Jacobsen et Kootsookos, 2007) to estimate the Doppler frequency within the acquisition process in CD approach. In fact, the frequency estimation technique developed in (Jacobsen et Kootsookos, 2007) demonstrated its efficiency in the acquisition of GNSS signals in (Esteves, 2013). The proposed acquisition method, adapted from signal processing studies, allows improving the accuracy of the Doppler estimation through FFT. This approach aims to apply the spectral peak location (SPL) delta-correction technique in the acquisition of degraded satellite signals within the CD algorithm. The new method for GNSS signal acquisition approach consists to determine a fine estimate of the spectral peak location located at the cyclic frequency.

Knowing that the two major performance metrics (sensitivity and complexity) of CD approach greatly depends on the search grid resolution, the objective of this proposal is to achieve a better estimate (fine estimation) of Doppler frequency and also can reduce the dimension of uncertainty area.

5.6.1.1 Direct vector processing

Based on CD architecture, the ephemeris from reference station allow to calculate satellite velocity. (He et al., 2013) developed a way to measure the Doppler frequency and work in velocity domain, in which the velocity and Doppler are estimated by using direct vector receivers, similarly as performed in position domain within CD approach.

The measured Doppler frequency has the following relationship with the satellite and user velocity:

$$f_{d_k}(\mathbf{v}) = \frac{1}{\lambda}\Big[\Big(u_{x,k}\big(v_{MS,x} - v_{sat,x}\big) + u_{y,k}\big(v_{MS,y} - v_{sat,y}\big) + u_{z,k}\big(v_{MS,z} - v_{sat,z}\big)\Big) + c\dot{d}t\Big] \tag{5.21}$$

where k represents the satellite number (k = 1,2,…,N_{sat}), λ represents the wavelength of transmitted satellite signal, $(v_{MS,x}, v_{MS,y}, v_{MS,z})$ and $(v_{sat,x}, v_{sat,y}, v_{sat,z})$ are respectively the user and the satellite ECEF velocities, $\mathbf{u}_k = [u_{x,k}, u_{y,k}, u_{z,k}]$ represents the direction unit vector from the satellite to the receiver, and $c\dot{dt}$ represents the receiver clock drift. The user velocity vector includes also the clock drift term: $\mathbf{v}_{MS,xyz} = [v_{MS,x}, v_{MS,y}, v_{MS,z}]$. From the Equation 5.21, the Doppler frequency and the velocity are linearly related. Thus, a small offset in the Doppler will cause a small offset in the velocity.

$$\Delta f_{d_k} = \left[\frac{1}{\lambda}u_{x,k}, \frac{1}{\lambda}u_{y,k}, \frac{1}{\lambda}u_{z,k}, \frac{1}{\lambda}\right]\Delta\mathbf{v}_{MS,xyz} = \boldsymbol{a}_i^T C_n^e \Delta\mathbf{v}_{MS,\boldsymbol{enu}} = \boldsymbol{e}_i^T \Delta\mathbf{v}_{MS,enu} \tag{5.22}$$

where Δf_{d_k} represents the Doppler frequency offset for the satellite k, $\Delta\mathbf{v}_{MS,enu}$ represents the user velocity offset w.r.t the velocity searching centre in navigation frame, C_n^e represents the rotation matrix from navigation frame to the earth frame, $\boldsymbol{e}_i^T$ represents the projection from velocity to the Doppler for the satellite k.

Note that the main sources of performance degradation of the GNSS acquisition are the uncertainty on the acquisition search grid (code phase and Doppler frequency), the non-compensation of the code Doppler and the presence of bit sign transition (for the modernized GNSS signals: data bit transition on the data component and secondary code bit transition on the pilot component). In this proposal, we especially focus on the choice of the Doppler search grid value in order to have a better estimate of the Doppler. In fact, the wrong choice of the cell width in acquisition search grid can cause residual estimation errors there. Knowing that the Doppler shift increases with the coherent integration period, it does not change too much in the case of low dynamics or short integration times. An integration interval of 1 ms (1023 chips) requires a residual frequency of less than 500 Hz, and for 20 ms of coherent integration the residual frequency must be less than 25 Hz. Thus, there is a big challenge with a very long integration period, nevertheless it is the best way to enhance the acquisition sensitivity. The main sources of frequency offset for GNSS receivers are the satellite motion (± 4880 Hz), the

uncompensated user motion (± 190 Hz) and the oscillator deviation (± 440 Hz for ± 0.28 ppm) are shown in Table 2.7.

5.6.1.2 Correlation process and search grid definition

If Δf_{d_k} and $\Delta\tau_k$ are respectively the uncertainty width in the frequency search space and the uncertainty width in the code delay search space for the satellite k and assuming that the sign of the navigation data bit does not change throughout the period of coherent integration, then the correlation output can be approximated as:

$$S_k\left(\hat{\tau}_k, \hat{f}_{d_k}\right) = A \cdot N \cdot R(\Delta\tau_k) \cdot \mathrm{sinc}\left(\Delta f_{d_k} T_{coh}\right) \cdot e^{j\varphi_k} + \hat{\eta}_n \tag{5.23}$$

where N represents the data length, $R(\Delta\tau_k)$ is the autocorrelation function of the signal spreading code evaluated at the code phase offset $\Delta\tau_k$ between the true and candidate code phase ($\Delta\tau_k = \tau_k - \hat{\tau}_k$), Δf_{d_k} is the offset between the true and candidate carrier frequencies ($\Delta f_{d_k} = f_{d_k} - \hat{f}_{d_k}$), T_{coh} represents the coherent integration time and $\hat{\eta}_n$ represents the resulting noise component, assumed as an AWGN characterized by a variance $\sigma^2 = \mathcal{N}_0 B$, $\mathcal{N}_0$ being the power spectral density of the noise and B is the front-end filter bandwidth as $B \simeq 1/T_s$.

The code phase and Doppler offsets on the correlation process are used to establish the search grid resolution. So, the grid resolution for the code is:

$$\delta\tau = \frac{\Delta \mathrm{T}}{N_\tau} = \frac{N_c}{N_s} \tag{5.24}$$

where ΔT represents the code phase uncertainty dimension, N_τ represents the number of search bins and usually equals to the number of samples per code N_s, and N_c represents the length of the code in chips. As seen in Section 3.3, the possibility of having a better estimate of the Doppler frequency can address the trade-off between sensitivity and complexity of the

receiver; and it concerns the setting of the grid resolution for the frequency dimension. In fact, the maximum tolerable loss for the sensitivity performance and the number of search bins to be tested for the complexity problem. These parameters have to be considered. So, the resolution of the FFT search grid is:

$$\delta f_d = \frac{f_s}{N} = \frac{1}{NT_s} = \frac{1}{T_{coh}} \tag{5.25}$$

where f_s represents the signal sampling frequency and N represents the data length. δf_d is chosen according to the loss to be accepted. For example, if $\delta f_d = 1/2 \cdot T_{coh}$, a maximum of 3.92 dB sensitivity loss may be incurred due to the inflexibility of the FFT frequency search grid. Knowing that the maximum frequency offset is half the spacing between cells, so the maximum frequency estimation error is:

$$\Delta f_{d,max} = \frac{\delta f_d}{2} = \frac{1}{2T_{coh}} \tag{5.26}$$

Based on the functions $R(\cdot)$ and $\mathrm{sinc}(\cdot)$ in (5.23), the coherent processing gain is defined as (Kaplan et Hegarty, 2006):

$$G_{coh_{dB}} = 10\log_{10}(N) - L_{\Delta\tau_k} - L_{\Delta f_{d_k}} \tag{5.27}$$

where losses due to misalignment of code phase and Doppler frequency are respectively defined as (Kaplan et Hegarty, 2006):

$$\begin{aligned} L_{\Delta\tau_k} &= 10\log_{10}[R(\Delta\tau_k)] \\ L_{\Delta f_{d_k}} &= 10\log_{10}\left[\left|\mathrm{sinc}\left(\Delta f_{d_k} T_{coh}\right)\right|\right] \end{aligned} \tag{5.28}$$

5.6.1.3 Efficient correlation method in CD acquisition

We have seen in Section 3.4 the various correlation methods used for acquisition of GNSS signals with their advantages and disadvantages. In this proposal, the idea is to apply a technique to better estimate the Doppler, more precisely to have a fine estimation of the Doppler frequency. This requires a technique capable of accelerating the correlation processing because of the importance of the number of points to be scanned (flexibility in the frequency search). Since in the position domain, where the CD process is performed, the code is estimated as a function of the RS pseudorange and the difference with those of RS and MS, then the ideal technique for reconciling the intention to estimate the Doppler frequency as well as scanning all the possible positions to estimate the code is the Bi-dimensional Parallel Search (BPS) acquisition method which makes it possible to make a parallel search in both dimensions, code and frequency. BPS acquisition method is then used to compute the target set of $S_k(\hat{\tau}_k, \hat{f}_{d_k})$ values.

The BPS acquisition method presents a great optimization because it allows simultaneous parallel search in code and frequency dimensions. As described in Section 3.4.4 and Figure 3.16, the BPS correlation method is defined as (Pany, 2010):

$$S_k(\hat{\tau}_k, \hat{f}_{d_k}) = \text{IFFT}\left\{\text{FLIP}\{\text{FFT}\{l_c\}\} \cdot \text{SHIFT}_j\{\text{FFT}\{s\}\}\right\}_k \tag{5.29}$$

where l_c represents the local code replica, s is the incoming signal, FLIP is a function inverting that inverts the last index into the first place, and SHIFT is a function performing an index shift according to the index j of the candidate Doppler frequency. (Akopian, 2005; Pany, 2010) have demonstrated that the BPS correlation method is able to effectively reduce the number of computations to a minimum of $\mathcal{O}(N_\tau)$ by eliminating redundant calculations and taking advantage of the FFT properties. In fact, the frequency step depends on the integration time used. In general this step is so large and it is not better for high sensitivity.

5.6.1.4 Spectral Peak Location algorithms with delta-correction

In this proposal, Spectral Peak Location (SPL) algorithms are proposed because of its ability to better estimate the Doppler frequency. The capacity of the SPL algorithm to improve the accuracy of FFT frequency estimation has been demonstrated in (Esteves, 2013). Indeed, SPL technique can reduce the FFT-derived losses in the coherent processing output. The basic principle of SPL estimators is to correct the estimate of the spectral peak index, i_{peak}, which is based on three consecutive FFT samples: $S(i_{bin}-1)$, $S(i_{bin})$ and $S(i_{bin}+1)$. If $S(i)$ is the FFT output at index i, and i_{bin} represents the frequency bin which produces the highest magnitude FFT output, for a given signal $s_b(nT_s) = A \cdot e^{j2\pi f_d nT_s}$, the spectral analysis of the three consecutive FFT samples are expressed as:

$$\begin{aligned} S(i_{bin}-1) &= A \cdot \sum_{n=0}^{N-1} s_b(nT_s) e^{-j2\pi(i_{bin}-1)\frac{n}{N}} \\ S(i_{bin}) &= A \cdot \sum_{n=0}^{N-1} s_b(nT_s) e^{-j2\pi i_{bin}\frac{n}{N}} \\ S(i_{bin}+1) &= A \cdot \sum_{n=0}^{N-1} s_b(nT_s) e^{-j2\pi(i_{bin}+1)\frac{n}{N}} \end{aligned} \tag{5.30}$$

In order to determine the fine i_{peak} estimate, a fractional correction term, δ, is calculated and added to the i_{bin} index. This technique is called "delta-correction technique" because of the "delta" term which is applied in FFT acquisition. Then, i_{peak} can be expressed as:

$$i_{peak} = i_{bin} + \delta \tag{5.31}$$

Several SPL estimator algorithms exist. The delta-correction term chosen for the SPL estimator in this proposal is the one of the best-performing algorithms compared by (Jacobsen et Kootsookos, 2012; Jacobsen et Kootsookos, 2007) as:

$$\delta = -\mathrm{Re}\left\{\frac{S(i_{bin}+1) - S(i_{bin}-1)}{2S(i_{bin}) - S(i_{bin}-1) - S(i_{bin}+1)}\right\} \tag{5.32}$$

The accuracy of frequency estimation using SPL with delta-correction has been demonstrated by using a 1 ms-long GPS C/A signal with a 500 Hz Doppler offset, corresponding to the middle between two consecutive FFT bins (1 kHz). In this proposal, SPL algorithm is used in order to improve the detection capabilities of the acquisition methods. Two ways can be employed if SPL algorithms are used: 1) if the detection is achieved, do refinement of the frequency estimation; or 2) if detection is not achieved, execute acquisition process with the fine frequency. In the second case, the serial correlation chain is used to perform the posterior acquisition attempt with the fine frequency, in which the code phase $\hat{\tau}_k$ and the delta-corrected frequency $\hat{f}_d$ corresponding to the peak location which produced the highest output in the initial execution is employed. The delta-corrected frequency is expressed as:

$$\hat{f}_d = \hat{f}_{d_k} + \hat{f}_\delta \tag{5.33}$$

where $\hat{f}_\delta$ is the frequency correction term as calculated by $\hat{f}_\delta = \hat{\delta} \cdot \delta f_d$, and $\hat{\delta}$ obtained by Equation 5.32.

Thus, the delta-corrected coherent output is defined as:

$$\begin{aligned} S_\delta(\hat{\tau}_k, \hat{f}_d) &= S(\hat{\tau}_k, \hat{f}_{d_k} + \hat{f}_\delta) \\ &= \sum_{n=0}^{N-1} s(nT_s) \cdot c(nT_s - \hat{\tau}_k T_s) \cdot e^{-j2\pi(\hat{f}_{d_k} + \hat{f}_\delta)nT_s} \\ &= A \cdot N \cdot R(\Delta\tau_k) \cdot \mathrm{sinc}(\Delta f_\delta T_{coh}) \cdot e^{j\varphi_k} + \hat{\eta}_n{}' \end{aligned} \tag{5.34}$$

5.6.1.5 Individual and Collective Detection metrics

The individual detection metric (correlator output) becomes:

$$D_{ind}\left(\hat{\tau}_k, \hat{f}_{d_k}\right) = \left|S_\delta\left(\hat{\tau}_k, \hat{f}_d\right)\right|^2 \tag{5.35}$$

Finally, the CD metric for all visible satellites is expressed as:

$$D_{CD}\left(\Delta N_i, \Delta E_j, \Delta D_m, \Delta B_n\right) = \sum_k D_{ind}\left(\hat{\tau}_k, \hat{f}_{d_k}\right) \tag{5.36}$$

5.6.1.6 Proposed CD architecture

To accelerate the CD process, the combination of the Bi-dimensional Parallel Search (BPS) acquisition method and the delta correction in SPL method of Doppler frequency estimation is proposed. This proposed idea allows having a better result in terms of sensitivity and complexity for the CD approach. The proposed way to better estimate the Doppler frequency within the CD approach is performed according to the architecture in Figure 5.14.

In this diagram (Figure 5.14), for the application of the BPS acquisition method, characterized by parallel search of both frequency and code phase as shown in Figure 3.16, the FFT_c block consists of the FFT of the elements in columns and then index flip after having generated the matrix $N_c \times N_\tau$, and the CS_p block corresponds to circular shift over code samples p.

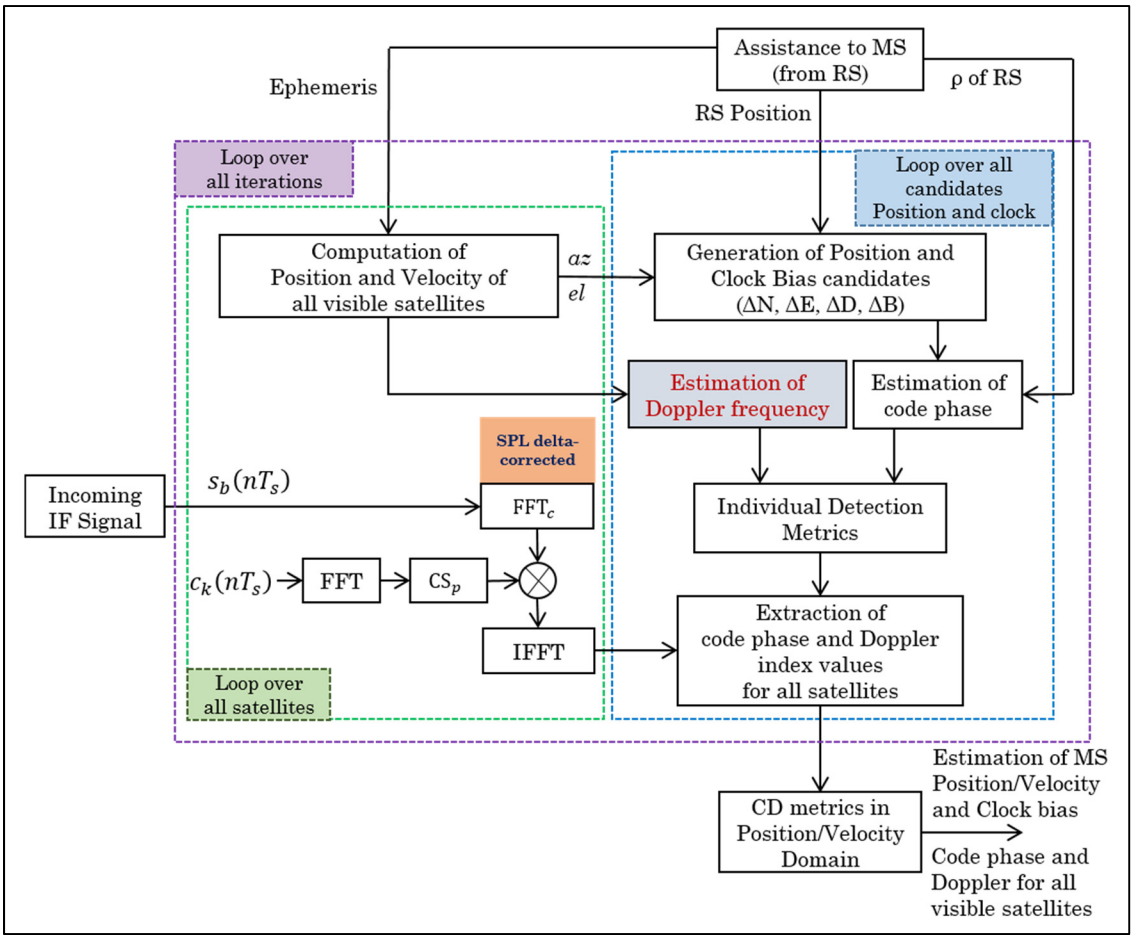

Figure 5.14 Proposed CD architecture using an efficient Doppler estimation technique

5.6.2 Performance analysis using real signals

To demonstrate the feasibility of this proposal in the Collective Detection approach, its performance is tested in indoor conditions with real GPS L1 C/A signal. The Doppler frequency shift must be taken into consideration in the case of real GNSS signals.

5.6.2.1 Live data setup

A series of measurements collected with a Septentrio PolaRx3e TR Pro receiver was carried out. This receiver was setup as RS, with antenna fixed on the roof of the French Institute of Aeronautics and Space (ISAE). And a NordNav R30 was used as a Front-End to collect the

RF GPS signals inside the building of the navigation lab at ISAE wherein the acquisition of the weak GNSS signals is very difficult. Then, the recorded data were post-processed to perform the collective detection process. The horizontal uncertainty range was set to 20 km to reflect a realistic application scenario. Figure 5.15 shows the setup used to test the effectiveness of the algorithm with real signals and measurements using good quality receivers.

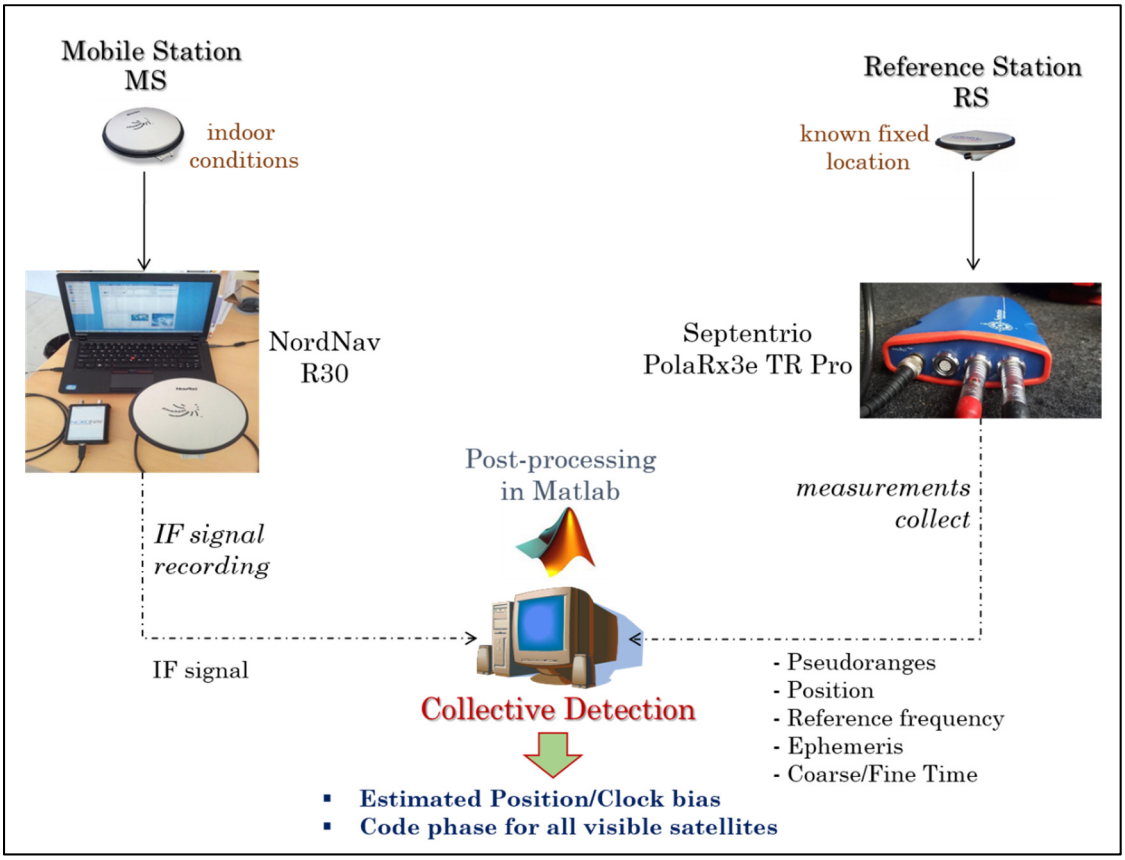

Figure 5.15 Setup of CD process and real signal acquisition
(NordNav as MS & Septentrio as RS)

The experimental parameters used for this test are:

- Sampling frequency: 16.36 MHz
- Intermediate frequency: 4.13 MHz
- Centre frequency of antenna:1575.42 MHz
- Quantization: 4 bits per sample
- Initial receiver position: 43.565084°, 1.477004°, 205.146 m

An SPL delta-corrected FFT for a middle-bin offset is used to analyze the performance of the proposed algorithm. In this proposal, another loop of frequency search is added in CD correlation process to conduct the search on Doppler frequency and then to better estimate it. In this case, the carrier is not eliminated in the processed satellite signal.

Let's consider a Doppler range of ± 10 kHz and 1 ms of signal observation. The number of samples per code period is $N_\tau = f_s \cdot T_{coh}$ = 16368. This is equivalent to the number of code bins to be searched. So, for each satellite, there are a total of approximately 1.8E5 cells to be searched. Table 5.9 summarizes the values we used for the range and spacing of each component for rough, medium and fine search level during three iterations.

Table 5.9 Description of search space for CD process

Item		**Rough 1st iteration [m]**	**Medium 2nd iteration [m]**	**Fine 3rd iteration [m]**
Horizontal dimension	North/East Uncertainty	±10,000	±2,000	±500
	North/East Step Size	1,000	100	10
Vertical dimension	Down Uncertainty	0	0	0
	Down Step Size	0	0	0
Clock Bias	Clock Bias Uncertainty	±150,000	±1,200	±300
	Clock Bias Step Size	1,000	100	30

5.6.2.2 Real data results

To better test the performance of the proposed CD algorithm, the comparison with the original CD approach (Bradley et al., 2010) is carried out in term of sensitivity, complexity and accuracy. Note that the reference approach does not take into account the Doppler effect by comparison with the proposed approach.

Sensitivity analysis

The first test involves comparing the values at the correlator output based on the ratio of the maximum peak over the average of remaining peaks. Figure 5.16 shows that the values of the ratio between the maximum peak and the remaining peaks of the new algorithm are higher than the ratio value of the reference approach. The difference between values depends on some parameters. We can see that the difference of the ratio value is noticeable for the PRN 7 which is the lowest satellite signal with 37.25 dB-Hz mean C/N_0 level. This difference shows clearly the effect of the delta-corrected approach on the improvement of the detection of satellite signal.

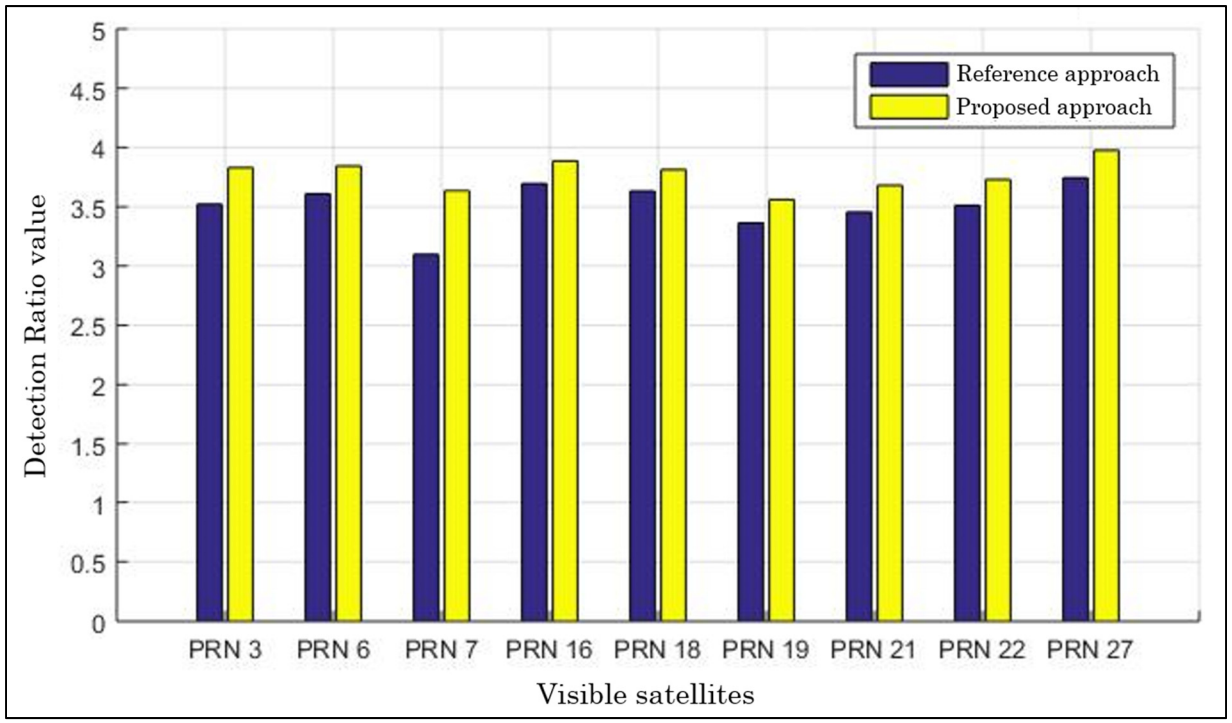

Figure 5.16 Ratio of maximum peak/average of remaining peaks

Table 5.10 shows the mean C/N_0 and the mean Doppler offset for all visible satellites of the collected data. These values are obtained with the Septentrio PolaRx3e TR Pro as a reference receiver.

Table 5.10 Mean C/N_0 and Mean Doppler offset for all satellites in view

PRN	Mean C/N₀ [dB-Hz]	Mean Doppler Offset [Hz]
3	45.75	4710
6	46.75	3210
7	37.25	4480
16	46.00	2160
18	43.50	3010
19	41.25	4990
21	42.75	240
22	44.50	4930
27	47.25	3930

As seen in Table 5.10, PRN 7 is in a good condition to profit from the delta-corrected acquisition application. In fact, its mean Doppler offset is close to a mid-bin frequency value despite its low power.

To see the effectiveness of the proposal from the application of the delta-correction methodology using BPS acquisition method compared to the simple BPS acquisition method, the correlation peak corresponding to the SV PRN 19 ($C/N_0 < 42$ dB-Hz) is shown in Figure 5.17. This curve shows that using the proposed algorithm (SPL algorithm with delta-corrected frequency), the receiver is able to obtain a good correlation peak in order to detect the weak satellite signal.

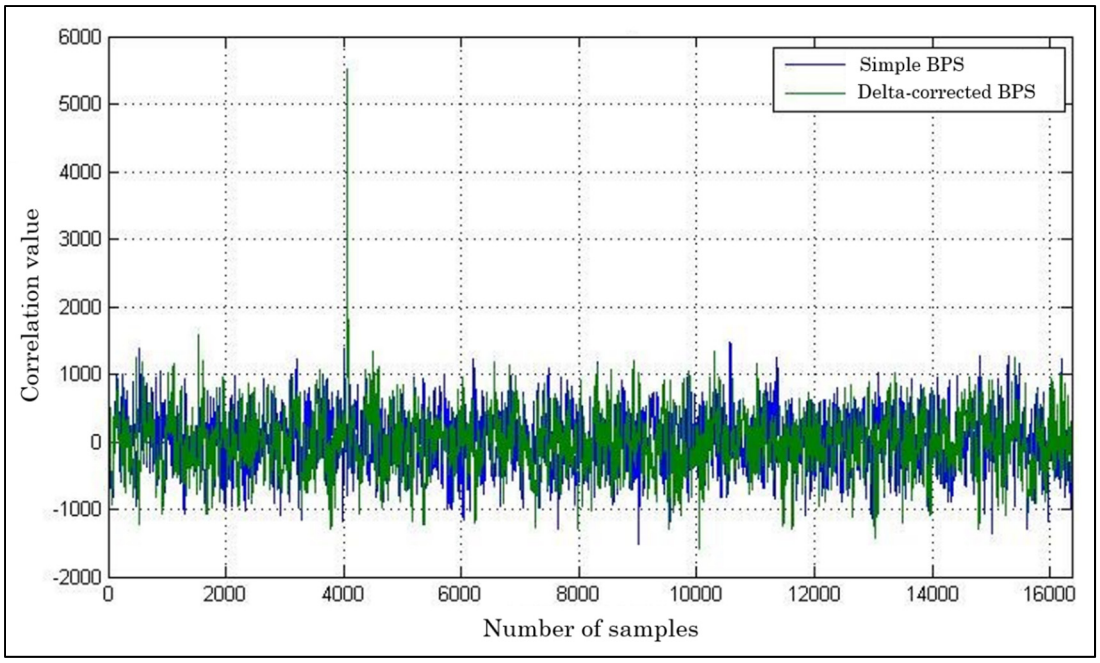

Figure 5.17 Correlation peak of SV PRN 19 for simple and delta-corrected FFT

According to the concept of the Collective Detection as a High-Sensitivity acquisition method, the principal objective of the collective acquisition is to make use of the stronger signals to facilitate the acquisition of weaker ones. So, to investigate a bit more the receiver sensitivity, the probability of detection in function of C/N_0 level has to be explored. For this purpose, let's consider two different scenarios depending on the number of detected satellites and their power. In these two scenarios, we consider four satellites with different C/N_0 level:

- Scenario 1: 3 strong satellites (PRN 3, PRN 6, PRN 16) and 1 weak satellite (PRN 7)
- Scenario 2: 2 strong satellites (PRN 3, PRN 18) and 2 weak satellites (PRN 7, PRN 19)

Each scenario is tested other 1000 independent blocks of 1 ms and 10 ms GPS L1 C/A. The increase of the coherent integration time to 10 ms is carried out in order to increase the sensitivity of the receiver. Figure 5.18 shows the collective detection sensitivity analysis corresponding to the scenario 1 and scenario 2.

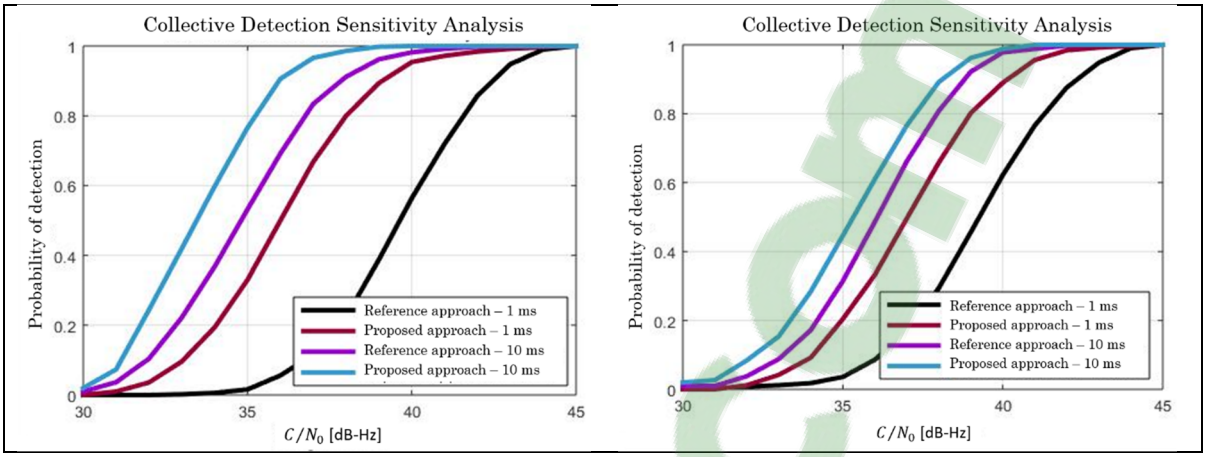

Figure 5.18 Sensitivity enhancement drawn from the new CD algorithm corresponding to scenario 1 (left) and scenario 2 (right)

Two clear conclusions can be drawn from Figure 5.18. First, if the integration time is longer the probability of detection increases. Next, for an interval of 1 ms, the application of the new CD algorithm allows to have a better improvement in term of sensitivity compared to the result obtained by the reference approach. Similarly, the proposed approach has a better probability of detection when using a longer integration time of 10 ms. However, the sensitivity improvement for 1 ms and 10 ms signals are not the same, the difference is most noticeable for an integration time of 1 ms. This shows that the use of the proposed technique is more beneficial for short signals.

Complexity analysis

Considering again a Doppler uncertainty of ± 10 kHz and the frequency resolution is set to be the same for the PCS acquisition method used in the reference approach and the BPS acquisition method with SPL delta-corrected FFT used in the proposed approach as $\delta_{f_d} = f_s/N = 1/(N_{code}T_c)$. The execution time of the reference approach using the PCS method is much higher compared to the new approach using BPS acquisition method with SPL delta-corrected FFT. For example, to process 1 satellite (PRN 3), the reference approach takes 625 ms to perform whole acquisition process for 10 code periods of GPS L1 C/A signal, whereas the proposed approach treats these 20 code periods for only 150 ms. Likewise, the execution

time of 20 code periods is 2500 ms for the reference approach and only 500 ms for the proposed approach. The processing time of the reference approach becomes noticeable from $N_{code} > 3$. To process all satellites in view (9 satellites), the proposed approach takes 1600 ms to execute acquisition process of 20 code periods whereas 7000 ms is required for the PCS acquisition method within the reference approach. These results show that the application of the BPS acquisition method and the SPL delta-corrected FFT method within the CD approach allows to have a better performance in terms of complexity without compromising the sensitivity acquisition.

According to the computational burden of acquisition operation in the CD algorithm developed in (Bradley et al., 2009) and the acquisition process using PCS method in (Pany, 2010), comparison of the total number of FFT-based operations is shown in Table 5.11.

Table 5.11 Comparison of computational load between some acquisition approaches

Approach developed by	**Number of multiplications**
T. Pany (Pany, 2010)	4909944
P. Axelrad (Bradley et al., 2009)	3453301
Proposed CD algorithm	339592

We can see that the proposed algorithm has a computational load 10.17 times lower than the CD algorithm developed in the reference approach (Bradley et al., 2009), and 14.46 times lower than the FFT acquisition presented in (Pany, 2010).

Accuracy analysis

To analyze the performance of the new CD algorithm in terms of accuracy, the comparison of the horizontal positioning error (HPE) between the proposed CD algorithm and the reference one is conducted. In our case, a mask angle of 10 degrees is applied, and the geometric dilution

of precision (GDOP) was around 2.8. Despite this good GDOP, the final positioning error obtained is on the order of tens of meters. According to the initial uncertainty of 20 km radial, we can see that the position uncertainty is greatly decreased. To investigate in details the accuracy performance, test with simulated 1 ms GPS L1 C/A signal has been carried out. Table 5.12 presents the comparison of the horizontal positioning error (95 %) between the proposed CD algorithm and the reference approach. Satellite geometry (GDOP of 2.4, 10.5 and 18.5) and signal power (20 dB-Hz and 30 dB-Hz) are varied to investigate the effect. Results show that we obtain the same performance in term of accuracy for the reference approach and proposed one.

Table 5.12 Horizontal Positioning Error - 95% [meters]

GDOP	**20 dB-Hz**		**30 dB-Hz**	
	Reference	**Proposed**	**Reference**	**Proposed**
Good (2.4)	376.5	375.7	32.7	31.7
High (10.5)	301.8	300.9	115.1	114.3
Weak (18.5)	375.7	374.8	219.1	218.6

These results of accuracy of the position solutions are obtained using 1000 acquisitions for varying signal levels and satellite geometries. Result values correspond to the position solution achieved 95 % of the time using 1 ms of data.

In spite of the inaccuracy of the solution, it is possible to increase the integration time for collective detection in order to reduce the positioning error. For example, for a high configuration of four satellites (GDOP = 10.5), with 1 ms of data, the horizontal position errors is 300.9 m for 95% of the time, while we can have a position accuracy of 97.6 m if we use 10 ms of non-coherent integration for a very weak signal (20 dB-Hz).

5.7 A new scheme of hybrid CD with standard correlation method

Still with a view to reduce the complexity in the implementation of the CD process, another contribution to reduce the computational load is proposed. The idea of this proposal consists of hybridizing the standard correlation approach with CD in a multi-stage method with different code phase and position resolution.

5.7.1 Hybrid CD schemes in literature

The idea of using a hybrid method of CD with conventional acquisition has already been proposed in some works (Cheong, 2012; Cheong et al., 2012; Esteves, 2014a), but each approach treats the subject differently. Note that one or more strong signals can be present in challenged environments. The number of strong signals depends on the user location but the presence of these signals greatly helps the performance of CD process. Then, the idea is to take advantage of the strong signals to improve CD performance.

In (Cheong, 2012) and (Cheong et al., 2012), the proposed hybrid method is used to reduce the search space of CD by employing singular value decomposition (SVD) of the geometry matrix in order to subtract the contribution of the strong signals. A better position solution and lower computation load are achieved with this approach. Otherwise, works in (Esteves, 2014a) consist of taking advantage of the fact that it is desirable to make use strong signals in order to optimize the CD search process. Compared to the full CD method, (Esteves, 2014a) has shown that the hybrid detection methods can detect much weaker signals and significantly reduce the final positioning error using the same signal integration time, number of signals, and satellite geometry. He showed the improvement in the search grid resolution in the presence of one, two or three strong signals among the received satellite signals.

5.7.2 Proposed hybrid scheme of CD with conventional acquisition

The main idea of this proposal is to take advantage of a hybrid scheme of CD with conventional acquisition for its ability to dramatically reduce the number of operations throughout the position estimation process. The concept of multi-resolution is adopted and it requires a down sampling of the received signal before calculation of individual detection metric for each iteration.

5.7.2.1 Motivation of the proposed hybrid scheme

As seen previously, the computational load of the CD implementation is caused essentially by the correlation step and the candidate points of the position-time domain. In the sequential acquisition, the correlation of a 1/4 chip resolution is enough in the most cases so no more than 2.5 dB are lost for weak signals detection. Otherwise, in CD approach, the correlation's resolution depends on the position grid resolution search of the last iteration. For example, with a resolution of 10 meters in the last iteration, the change of the estimated code phase between the two closest candidates will be 1/16 of the chip (150 m ÷ 16 = 9.375 m). In PCS acquisition method, 1023 x 16 points have to be considered which is highly complex to be implemented on current mobile receivers.

As mentioned previously, the correlation process contributes highly to the computational load of CD approach. So, in the correlation operation of the local code with the incoming signal, the required resolution in the third iteration should be less than 1/16 chips, because the estimated code phase between two closest candidate points in the position domain is more than 1/16 chips. Thus, in this case, the number of multiplications needed for the parallel code correlation is:

$$Total\_ops = \mathcal{M}[\mathrm{FFT}(N)] + \mathcal{M}[\mathrm{FFT}(N)] + N + \mathcal{M}[\mathrm{IFFT}(N)] \tag{5.37}$$

where the function $\mathcal{M}[x]$ represents the number of multiplication needed for the operation x, N represents the number of samples, i.e. N = 1023 x 16 in our case. The FFT and inverse FFT operation is obtained by (Pany, 2010):

$$\mathcal{M}[\mathrm{FFT}(N)] = \mathcal{M}[\mathrm{IFFT}(N)] = 5 \cdot N \cdot log_2(N) \tag{5.38}$$

So, the total number of operations required during the step of correlation is:

$$Total\_ops = 3 \cdot 5 \cdot N \cdot log_2(N) + N \tag{5.39}$$

Thus, with a sampling factor of 16, the correlation process in CD approach needs a total number of operations of 3437957, which is a very high value and makes the computation process of CD very heavy.

To deal with this problem, a new scheme of collective acquisition is proposed to reduce the computational load. This proposal consists of a hybrid scheme between correlation blocks and collective detection which is referred to a High-Sensitivity Collective Detection method.

5.7.2.2 Architecture of the proposed hybrid scheme

Note that CD approach requires a high resolution in the correlation block in the last iteration. Thus, there is no need for a better resolution in the first iteration in order to avoid the high computational load, a correlation of 1 sample per chip is enough with a position domain resolution of 1 km. Individual detection metric for all satellites in view and CD metric are computed in order to have a rough estimate of the user position and an estimated code phase of each visible satellite. Then, a new correlation around the estimated code phase is performed using a window w with 4 samples per chip resolution, i.e. $w/2$ on both sides of the estimated code phase and shifted by a sample period T_s at each correlation. In the same way, it carries out the calculation of individual detection and CD metrics, then a new code phase is estimated for each satellite (second iteration). A new correlation around the estimated code phase is

performed, with a resolution of 16 samples per chip in the third iteration to obtain a final position accuracy of 10 m. The architecture corresponding to this proposed hybrid scheme of CD and conventional correlation is shown in Figure 5.19.

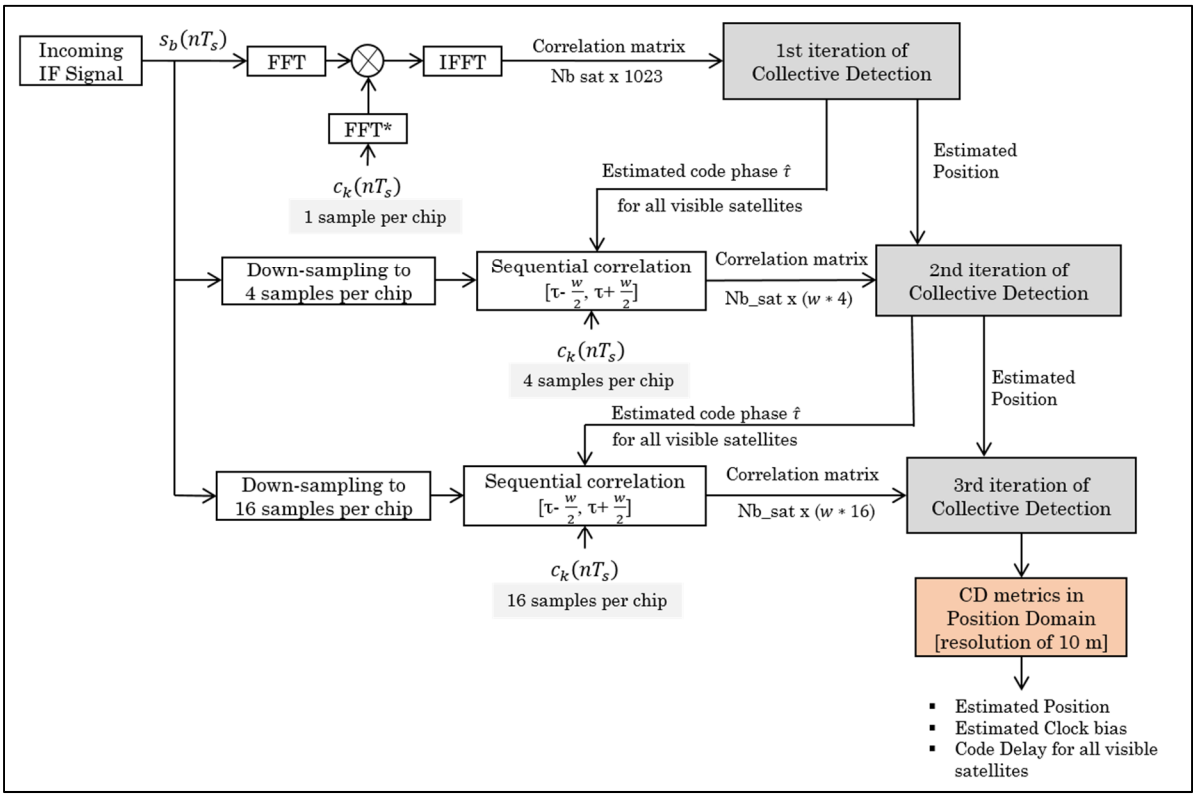

Figure 5.19 Proposed hybrid scheme of conventional correlation and collective detection

5.7.2.3 Results of the hybrid CD method

Since this resolution is needed just in the last iteration, we propose in the beginning a correlation with a resolution of 1 sample per chip which is enough for the first iteration, with a resolution of 4 samples per chip for the second iteration to calculate a new correlation around the estimated code delay, and finally with a resolution of 16 samples per chip for the last iteration to achieve the final position accuracy of 10 meters.

Complexity analysis

The key point is then the choice of the value of window w to have a good estimate of the code during the correlation process but also to optimize the computational load. This method may considerably reduce the number of calculations compared to different approaches developed in literature. Let's consider the work in (Axelrad et al., 2011) which initiated the use of the multi-iterations approach and compare the computational load with the proposed scheme.

The detail of operations in the hybrid scheme is analyzed. The complexity in this proposed CD scheme is divided in three stages:

1) A stage that calculates the correlation matrix in first iteration of CD, using PCS method with a code phase resolution of 1 sample per chip. The number of operations in this stage is:

$$\begin{aligned} Ops\_first\_stage &= \mathcal{M}[\mathrm{FFT}(N)] + \mathcal{M}[\mathrm{FFT}(N)] + N + \mathcal{M}[\mathrm{IFFT}(N)] \\ &= 3 \cdot 5 \cdot N \cdot log_2(N) + N \end{aligned} \tag{5.40}$$

2) A stage that calculates the correlation matrix in second iteration of CD, using the sequential search around the code phases τ that have been estimated in the first iteration, with a resolution of 4 samples per chip. The sequential search around the estimated code phase is performed in order to be sure to not lose the correct true code phase. The number of operations depends on the window value w. So the correlation output will be the result of multiplication of the incoming signal by the generated code shifted by $\tau - \frac{w}{2}$, $\tau - \frac{w}{2} + T_s$, $\tau - \frac{w}{2} + 2T_s$, … , and $\tau + \frac{w}{2}$. The number of operations in this stage is:

$$Ops\_second\_stage = w \cdot 4 \cdot N \tag{5.41}$$

3) A stage that calculates the correlation matrix in last iteration of CD, using the sequential search around the code phases τ that have been estimated in the second iteration, with a resolution of 16 samples per chip. Similarly, the number of operations in this stage is:

$$Ops\_third\_stage = w \cdot 16 \cdot N \tag{5.42}$$

The total number of operations in this proposed hybrid scheme is then:

$$Total\_ops = 3 \cdot 5 \cdot N \cdot log_2(N) + N + w \cdot 4 \cdot N + w \cdot 16 \cdot N \tag{5.43}$$

For $w = 1$ and N = 1023, the total number of operations is:

$$\begin{aligned} Total\_ops &= 3 \cdot 5 \cdot 1023 \cdot log_2(1023) + 1023 + 4 \cdot 1023 + 16 \cdot 1023 \\ &= 174911\ operations \end{aligned} \tag{5.44}$$

Thus, the hybrid CD scheme has a computational load 19.6 times lower than the previous result calculated in Equation 5.39 which corresponds to collective acquisition process in (Axelrad et al., 2011). Tests results show that the proposed hybrid CD scheme requires less computational resources compared to the approaches described in (Axelrad et al., 2011) and (Cheong, 2012).

Sensitivity analysis

The sensitivity performance of the proposed hybrid CD scheme is compared to the approach developed in (Bradley et al., 2010) as a reference approach. Figure 5.20 shows the comparison between the proposed method and the reference approach during 3 iterations depending on the number of detected satellites according to the C/N_0 level. The average number of satellite is obtained by launching 100 times the CD process with w = 1.

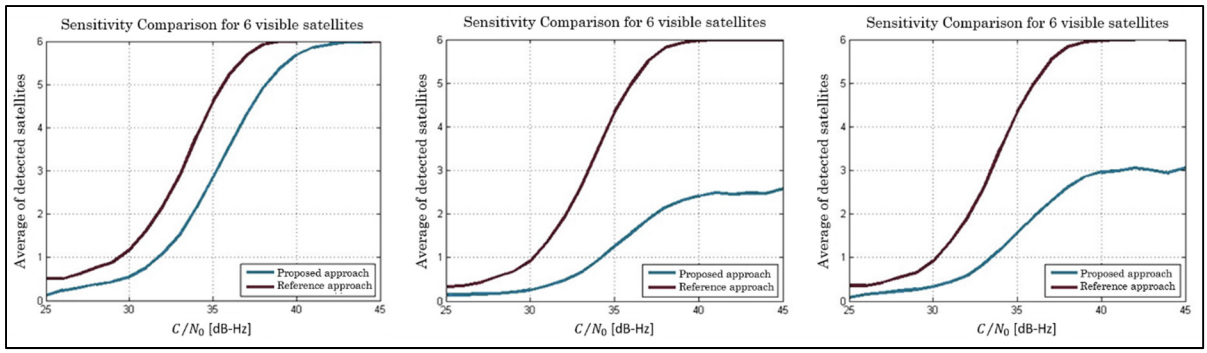

Figure 5.20 Comparison of sensitivity performance of the proposed CD hybrid scheme and the reference approach during 1st iteration (left), 2nd iteration (center) and 3rd iteration (right)

According to Figure 5.20, there are some losses in terms of sensitivity comparing to the reference approach during the first and the second iterations due to the choice of correlation resolution proposed with the new approach. However there are fewer operations performed in this method compared to the reference one. The performance curve of the reference approach in the last iteration seems to remain the same as in the first iteration because of the chosen position in the simulation ($\Delta N = 0, \Delta E = 0$), also used for the proposed algorithm. In the position $(\Delta N, \Delta E) = (0,0)$, the position error in each iteration could be zero because the chosen position is perfectly aligned with a candidate point in the grid position in all iterations. However, the sensitivity loss for the proposed approach from one iteration to another could be explained by the use of certain window *w* performed around the estimated code phase instead of zooming just in position as performed in the reference approach. Thus, if any of the estimated code phases are not close enough to the true code phases (by maximum of 1 chip in first iteration), the zoom in the next iteration will not include the true code phase.

In terms of computational load, it has been shown that the proposed hybrid CD approach is very efficient in terms of reducing complexity and has significant gain compared to other approaches. However, it presents some losses in terms of sensitivity. Hence another proposal of hybrid CD approach combined with other methods is necessary to overcome the various limitations for the implementation of the CD technique as well as to reach the objectives fixed for these works.

5.8 Improved CD algorithm: EITHSCD method

It has been shown that the sensitivity decreases after several iterations using the hybrid method developed previously. So we propose a new approach to solve the problem of sensitivity into the CD process which is the implementation of a better technique of Doppler estimate as developed in Section 5.6. Indeed, this method also reduces the computational burden by reducing the frequency search space. Its ability to combine high sensitivity and low complexity has been demonstrated. And also in order to minimize as much as possible the assumed available assistance information, we also propose a new architecture where the MS would be able to calculate its position with the minimums of assistance data. The combination of all these techniques is called "Efficient and Innovative Technique of High-Sensitivity Collective Detection" (EITHSCD). The main idea is to apply the proposed EITHSCD approach to process GNSS signals in deep urban environments while minimizing reliance on assistance.

5.8.1 Architecture of the new EITHSCD scheme

5.8.1.1 New hybrid CD scheme

It is proved in that the hybrid CD method developed in Section 5.7 has higher efficiency in terms of complexity compared to traditional CD (Axelrad et al., 2011), but the disadvantage of this method is that the sensitivity decreases after several iterations according the value of w. Thus, to overcome the sensitivity problem, the new hybrid CD scheme combines the idea of hybridizing the sequential correlation with CD approach as shown in Section 5.7 and the use of the SPL delta-corrected technique to better estimate the Doppler frequency using BPS acquisition method as shown in Section 5.6. In fact, the proposed BPS acquisition method allows improving the accuracy of the Doppler estimation through FFT, and therefore enhancing the correlation energy.

5.8.1.2 Minimizing assistance information

According to the basic block diagram of Collective Detection process in Figure 5.3, the information required to assist the user receiver (MS) are satellite ephemeris, RS position, RS pseudoranges, and reference frequency. As seen in Section 5.2.2, the works in this thesis focus on the MS-based GNSS, i.e. all calculations are carried out at the MS GNSS receiver.

With respect to A-GNSS, in our architecture, called EITHSCD, we use 2 assistance data from RS, such as the satellites ephemeris and the position of the reference station. In this proposal, the pseudoranges seen from the RS are not sent to MS but extracted within the MS from the RS ephemeris. In addition, the reference frequency does not have to be sent since the proposed technique makes it possible to estimate the frequency within the MS.

5.8.1.3 Multi-iteration method

In the state of the art on the CD using the multi-iteration method for solving the position, we notice that there are solution that is based on 3 iterations (Axelrad et al., 2011) and there are others that use 4 iterations (Narula, Singh et Petovello, 2014). In this proposal, in order to get a better estimate of the position, we use a resolution of 10 m in the 3rd iteration, so the change of the estimated code phase between two closest candidates is located in 1/16 chips, i.e. 18.75 m (9.375 m from each side of search). This is enough as a fine resolution to estimate the user position. However, using such a resolution with the search dimensions used in the literature requires a very high computational load. For example, (Axelrad et al., 2011) uses a resolution of 30 m in the last iteration, which requires 3 times less research on this latest iteration compared to the proposed method performance. Thus, some techniques must be implemented to reduce this large number of operations so that we can apply our proposal in order to have a better solution estimate.

5.8.1.4 Proposed EITHSCD architecture

In order to reduce operation costs in CD approach, a new scheme of hybrid method of Collective Detection with conventional high-sensitivity correlation is proposed. The concept of high sensitivity is ensured by the use of a better Doppler estimation technique and the variation of coherent integration periods and non-coherent accumulation. This technique of frequency estimation makes it possible to reduce the information required from the reference station, which minimizes the dependency on assistance. So, Figure 5.21 shows the architecture of the proposed EITHSCD algorithm which is a new scheme of hybrid CD with conventional acquisition in 3 iterations, coupled with a technique to better estimate the Doppler frequency. The ability to properly estimate the Doppler offset allows for having a sensitivity gain and reduces the algorithm computational load because of the reduction of the frequency uncertainty area. The proposed hybrid CD algorithm makes it possible to solve the problem of sensitivity, complexity, positioning accuracy and the minimization of assistance dependence.

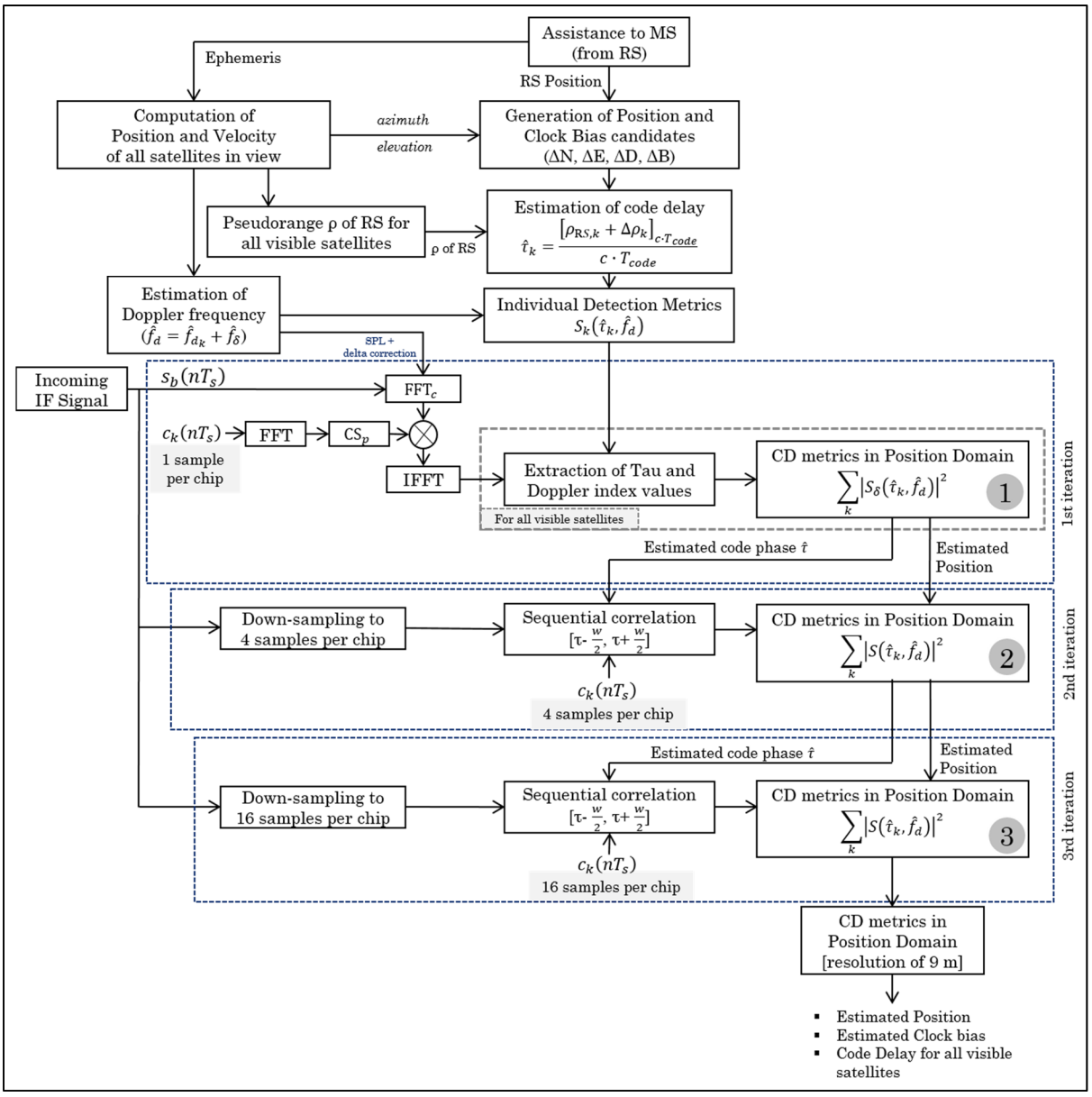

Figure 5.21 New scheme of hybrid CD with HS conventional acquisition (EITHSCD)

The implementation of the proposed EITHSCD algorithm presented in Figure 5.21 involves three steps, corresponding to the following three iterations:

1) In the first iteration, there is no need for a better resolution in order to avoid the high computational burden, a correlation of 1 sample per chip is enough with a position domain resolution of 1 km. Individual detection metric for each visible satellite is the correlation

value corresponding to the estimated code phase and Doppler frequency. Then, the CD metric for all satellites in view is computed to have a coarse estimate of the user position and an estimated code phase of each visible satellite. It is calculated by summing non-coherently all individual metrics corresponding to the estimated code phase and Doppler. The distinct peak is identified and is used to center the solution process for medium search in the second iteration.

2) In the second iteration, a new correlation using sequential search around the estimated code phase is performed using a window w with 4 samples per chip resolution. The correlation process is carried out in an interval between $\tau - w/2$ and $\tau + w/2$ and shifted by a sample period T_s at each correlation. The individual detection corresponds to the estimated code phase within $w/2$ on both sides and the fixed Doppler frequency estimated in the first correlation. Then, CD metric is computed by summing all correlation values for all visible satellites. A position domain resolution of 100 m is established in order to have a medium grid resolution search. A new code phase can be estimated for each satellite from the correlogram of CD metric which is required in the third iteration process. The search space is re-center on the location where a distinct peak is identified and it is used to perform fine search in the last iteration.

3) In the last iteration, a new correlation using sequential search around the estimated code phase in second iteration is performed. In order to have a fine estimate, a resolution of 16 samples per chip is used to obtain a final position accuracy of 10 m. The rest of the process remains the same as in the second iteration, i.e. individual detection and CD metrics are calculated with the estimated code phase resulting by correlations around the last iteration around estimated code phase during the second iteration and the Doppler frequency estimated in first iteration. Position and clock bias of the MS (user) is estimated with regard to the RS. Code phase of the MS for each visible satellite can be obtained.

5.8.2 Performance analysis of the EITHSCD technique

To analyze the performance of the proposed EITHSCD algorithm, tests with simulated signals and real signals are performed. For a better comparison of the proposed algorithm with algorithms developed in the literature, performance analysis in terms of sensitivity, complexity and accuracy is carried out, and we will be limited in the case of a fixed reference station, which is used in all works on Collective Detection. In most cases, the CD approach developed in (Axelrad et al., 2011) is used as a reference approach since it is one of the earliest works on the collective detection concept.

5.8.2.1 Simulated signals experiments

To study the performance of the new scheme of hybrid CD with conventional acquisition presented in the proposed architecture in Figure 5.21, simulated satellite signals in Matlab are used.

The reference station is located at ETS Montreal, its geodetic coordinates are shown in Table 5.13. To facilitate the simulation conditions, the true position of the MS in 4D coordinates $(\Delta N, \Delta E, \Delta D, \Delta B)$ w.r.t. the RS is set to be (0,0,0,0), which is centered at RS. The other simulation parameters used for this test are:

- Mask angle: 10°
- GDOP: 1 (in order to have a better constellation geometry)
- Signals: GPS L1 C/A
- Coherent integration: 1 ms
- Search grid description: defined in Table 5.9
- Window w value: 1 chip
- AWGN noise injected

Table 5.13 Reference station coordinates

Latitude	Longitude	Altitude
N 45°49'40.350527"	W 73°56'27.701694"	73.899 m

The values used for the range and spacing of each component for rough, medium and fine search level during three iterations are summarized in Table 5.9. After launching the algorithm, there are 10 satellites in view. This means that there are 10 code phase to estimate. In the algorithm, a satellite is declared visible if the difference between the estimated code phase and the true code phase is less than half the sampling factor which is 16 in our case.

To better analyze the performance of the proposed technique EITHSCD, the conventional CD approach proposed in (Axelrad et al., 2011) is used as a reference. First, in order to get and compare the statistical characteristics of results obtained from both algorithms, each algorithm is executed 100 times. For C/N_0 = 35 dB-Hz, both approaches find 10 visible satellites. Table 5.14 shows the mean error and the standard deviation of the difference between the estimated code phase and the true code phase. This makes it possible to analyze the number of correctly estimated code phases. The calculated statistical values are based on all visible satellites that are all detected.

Table 5.14 Comparison of statistical results between EITHSCD and reference approach

SV	**EITHSCD approach**		**Reference approach**	
	Mean Error [m]	**Std. Dev. [m]**	**Mean Error [m]**	**Std. Dev. [m]**
PRN 1	2.3000	1.6364	3.6000	1.5776
PRN 2	2.5000	1.5092	3.8000	1.8738
PRN 14	2.7000	1.9465	4.0000	2.3094
PRN 15	2.2000	1.3166	3.5000	1.4337
PRN 18	2.6000	0.9661	3.9000	1.1005
PRN 21	3.0000	2.9059	4.3000	3.0569
PRN 23	2.7000	2.5841	4.0000	2.2608
PRN 25	3.8000	1.8738	5.1000	1.8529
PRN 27	2.9000	2.3310	4.2000	1.8135
PRN 31	1.6000	1.1738	2.9000	1.1972

From this table it can be seen that the value of the mean of the difference between the estimated code phase and the true code phase corresponding to the proposed algorithm is always lower than the value of reference approach. Even if the values obtained for the reference approach are still below the threshold and involves the detection of the satellite, it shows that the proposed technique offers a better accuracy.

Sensitivity analysis

According to the concept of the Collective Detection as a High-Sensitivity acquisition method, the aim of CD approach is to facilitate the acquisition of weak signals by using strong signals. So, to analyze the receiver performance in terms of sensitivity, the probability of detection in function of C/N_0 level has to be explored. Thus, three different scenarios are analyzed for both approaches depending on the number of satellites and their power as seen in Table 5.15.

Table 5.15 Scenarios used in simulation tests

	Scenario 1		**Scenario 2**		**Scenario 3**	
	Satellite	$\boldsymbol{C/N_0}$	**Satellite**	$\boldsymbol{C/N_0}$	**Satellite**	$\boldsymbol{C/N_0}$
Weak signals	PRN 1	30 dB-Hz	PRN 1	30 dB-Hz	PRN 1	30 dB-Hz
	PRN 2	30 dB-Hz			PRN 2	30 dB-Hz
					PRN 14	30 dB-Hz
Strong signals	PRN 25	45 dB-Hz	PRN 25	45 dB-Hz	PRN 25	45 dB-Hz
	PRN 27	45 dB-Hz	PRN 27	45 dB-Hz	PRN 27	45 dB-Hz
			PRN 33	45 dB-Hz	PRN 33	45 dB-Hz

Each scenario is tested with 1000 independent blocks of 1 ms and 10 ms GPS L1 C/A. Coherent integration during 10 ms is performed in order to increase the receiver sensitivity. Figure 5.22 shows the CD sensitivity analysis corresponding to the three scenarios for both approaches. These curves represent the probability of detection in function of C/N_0 level after the third iteration. The more powerful satellites are available, the more the CD sensitivity increases.

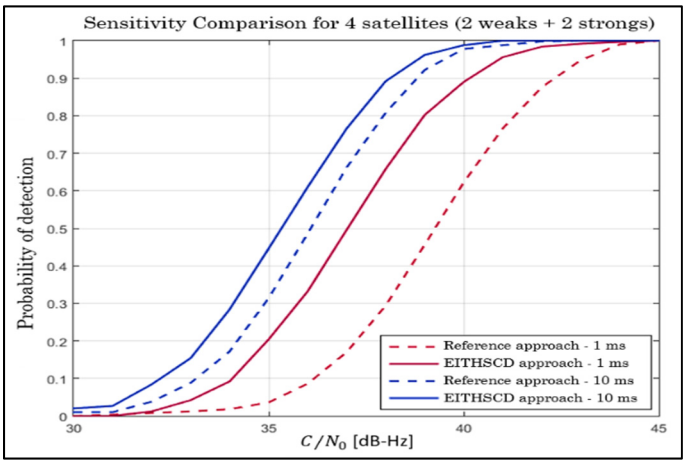

(a) Scenario 1

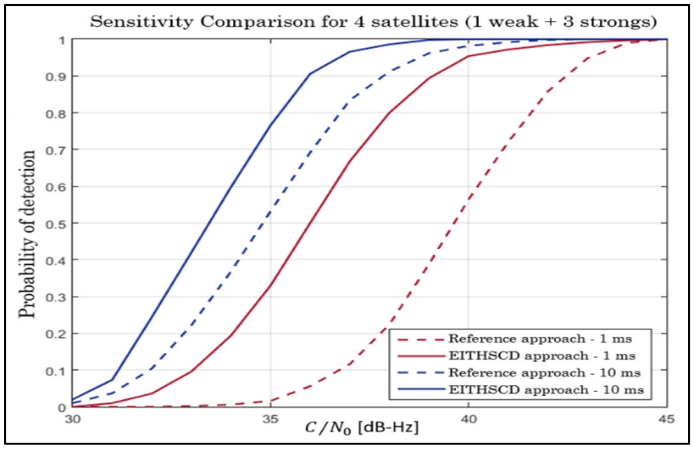

(b) Scenario 2

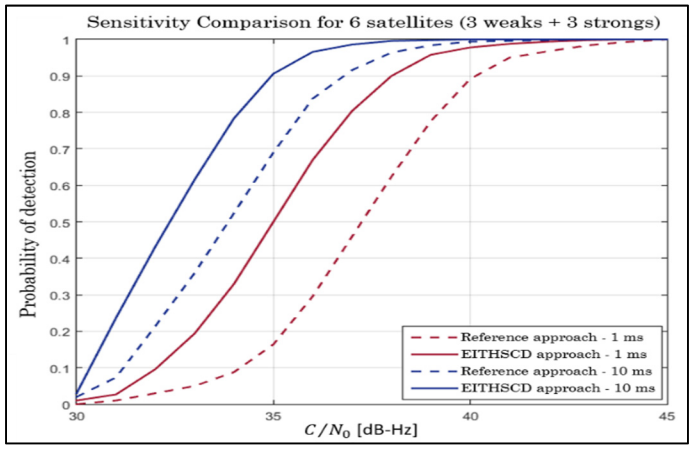

(c) Scenario 3

Figure 5.22 EITHSCD and reference CD approach in sensitivity performance

We can see that using the EITHSCD algorithm the receiver is able to get out a good correlation peak in order to detect the weak satellite signal. EITHSCD approach is very beneficial for short signals of 1 ms in which the difference is very noticeable.

Consider now the 3D correlogram that represents the CD metric to analyze the effect of the variation of coherent integration and non-coherent accumulation. Figure 5.23 show the importance of increasing the period of coherent integration for the same parameters (mask angle = 10º, C/N_0 = 30 dB-Hz).

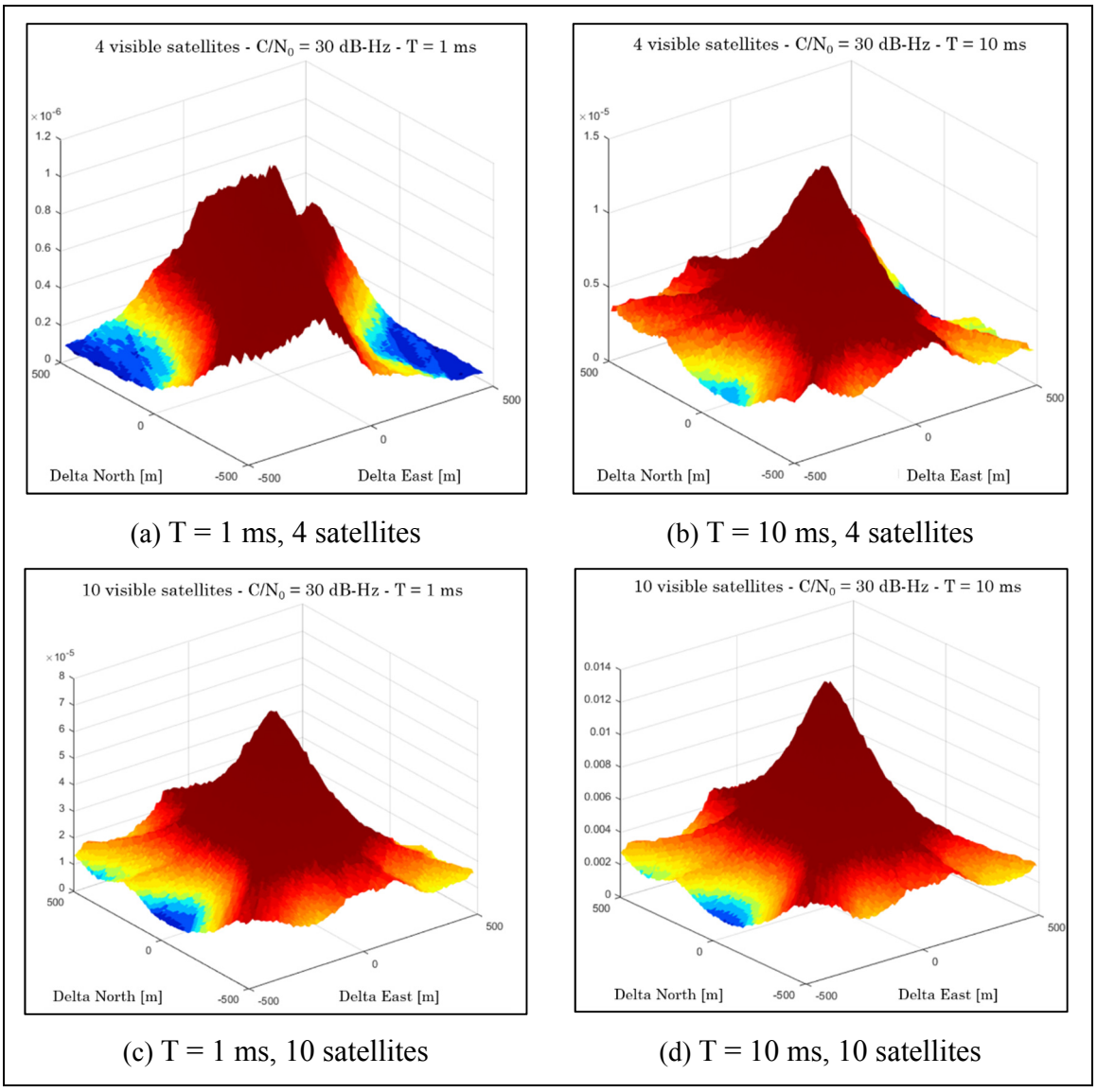

Figure 5.23 CD metrics with different periods of coherent and non-coherent integration

These curves confirm that extending the integration period results in a good correlation peak for CD metrics computation even with weak signals received at 30 dB-Hz. In Figure 5.23(a), all detected satellites (4) are very weak (30 dB-Hz), and the signals are acquired during only 1 ms, it is normal that we do not get a good correlation peak. These signals cannot be acquired individually with the sequential correlation, but we can still have a rough estimate of the user's position using EITHSCD approach, i.e. with a large horizontal positioning error.

Accuracy analysis

The best way to compare the proposed EITHSCD approach and the reference approach in terms of accuracy is to analyze the horizontal position error which is an important metric in the CD technique. Very weak signals of 20 dB-Hz and 30 dB-Hz are simulated to test the algorithms. For the reference approach, the signal-limited threshold method is used as described in (Axelrad et al., 2011). To investigate in details the accuracy performance, three values of geometric dilution of precision (GDOP) are tested given that the geometric configuration of satellites is essential in the receiver position estimation, such as Good (GDOP = 1), High (GDOP = 10), Weak (GDOP = 18). A mask angle of 10° is applied for each of the 10 satellites. The size of the initial uncertainty range is set to of 20 km. After the first iteration, the position uncertainty is greatly decreased. Test with simulated 1 ms GPS L1 C/A signal has been carried out. Table 5.16 shows the comparison of the horizontal positioning error (95%) between the EITHSCD algorithm and the reference approach. Signal power of 20 dB-Hz and 30 dB-Hz are varied to investigate the effect.

Table 5.16 Horizontal Positioning Error – 95 % [m]

GDOP	**20 dB-Hz**		**30 dB-Hz**	
	EITHSCD	**Reference**	**EITHSCD**	**Reference**
Excellent (1)	106.1	304.4	9.3	23.6
Moderate (10)	137.9	325.1	31.7	110.7
Fair (18)	201.3	397.3	87.2	216.3

Results show that we obtain a better estimate of the position of the MS compared to that obtained by the reference approach. These results of position accuracy are obtained using 1000 acquisitions for varying signal levels and satellite geometries.

In spite of this inaccuracy of the solution, it is possible to increase the integration time for CD in order to reduce the positioning error. For example, for a high configuration of four very weak satellites (GDOP = 10, C/N_0 = 20 dB-Hz), with 1 ms of GPS L1 C/A, the HPE is 243.6 m for 95% of the time, but a position accuracy of 53.2 m can be obtained by using 10 ms of non-coherent integration. We can deduce that with the proposed EITHSCD algorithm, the final positioning error obtained in the best case is 9.3 m, i.e. a PVT solution can be computed within an error of 10 m, which is a better result compared to other results in literature.

Complexity analysis

The last comparison to both approaches is the complexity of the algorithm. Ten satellite signals of 35 dB-Hz are simulated to compare some CD approaches such the proposed EITHSCD, the reference basic CD approach (Axelrad et al., 2011), the ECPIOCD approach developed in (Jia et Sahmoudi, 2016) and the HSCD approach developed in (Narula, Singh et Petovello, 2014). Table 5.17 presents the performance comparison in terms of computational burden.

Table 5.17 Computational load between some CD approaches

CD Approach	Execution time [s]	Number of points evaluated
Traditional CD (Axelrad et al., 2011)	26.09	388987
ECPIOCD (Jia et Sahmoudi, 2016)	5.78	180100
Accelerated CD (Narula, Singh et Petovello, 2014)	7.31	236517
Proposed EITHSCD	5.36	175032

We can see that the number of candidate points of the proposed EITHSCD approach is lower than the reference approach. EITHSCD algorithm has a computational load 4.84 times lower than the CD algorithm developed in the reference approach, 1.37 times faster than the Accelerated CD approach developed in (Narula, Singh et Petovello, 2014), and 1.07 times lower than the ECPIOCD approach developed in (Jia et Sahmoudi, 2016).

5.8.2.2 Real signal experiments

To analyze the performance of the EITHSCD algorithm, tests with real signals were also performed as shown in Figure 5.15. The horizontal uncertainty range (North/East) was set to 20 km to reflect a realistic application scenario as shown in Table 5.18. The various parameters used to perform the test with real signal are summarized in Table 5.18.

Table 5.18 Parameters used for real signal tests

BS receiver	Septentrio PolaRx3e TR Pro
MS receiver	NordNav R30
Sampling frequency	16.3676 MHz
Intermediate frequency	4.1304 MHz
Centre frequency of antenna	1575.42 MHz
Data	4 bits per sample
Computer configuration for post-processing	Intel Core i7-3770 CPU 3.40 GHz, RAM 12 Go, 64 bits
Horizontal uncertainty range	20 km
Initial position	43.565084°, 1.477004°, 205.146 m

Real data results

Using the previous configurations and settings in Table 5.18, all satellites in view during the setup (above 10° elevation) are shown in the skyplot in Figure 5.24. The sky plot represents the geometry of the nine tracked satellites, with a GDOP around 2.5.

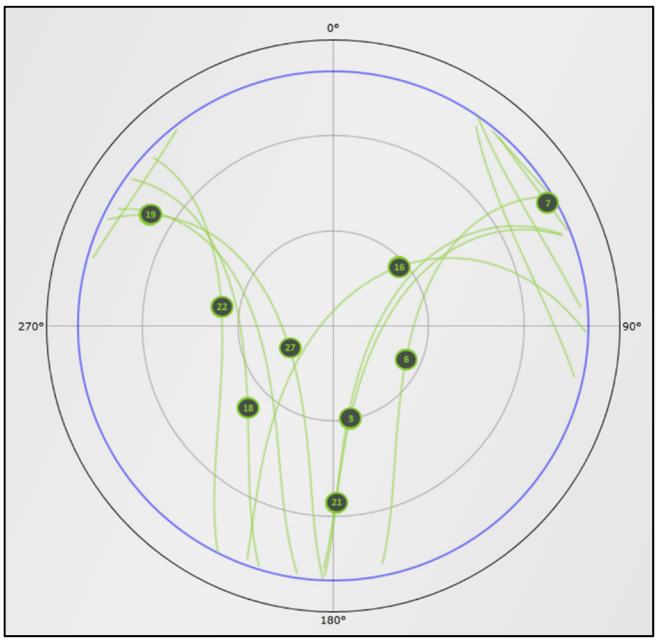

Figure 5.24 Satellite geometry of the indoor scenario test

Table 5.19 shows the mean C/N_0 for all satellites in view obtained by the RS receiver during the setup as shown in Figure 5.24.

Table 5.19 Power level for all visible satellites

PRN	3	6	7	16	18	19	21	22	27
Mean C/N₀ [dB-Hz]	45.75	46.75	37.25	46.00	43.50	41.25	42.75	44.50	47.25

In the EITHSCD algorithm, an SPL delta-corrected FFT for a middle-bin offset is used. Consider a Doppler range of ± 10 kHz. 1 ms of signal observation is used, i.e. the number of samples per code period is $N_\tau = f_s \cdot T_{coh}$ = 16368. This is equivalent to the number of code bins to be scanned and there are a total of approximately 1.8E5 cells to be scanned in code domain for each satellite in view.

Sensitivity analysis

To better analyze the performance of algorithm in terms of sensitivity, it is important to see the ratio between the maximum peak and the average of the remaining peaks for each detected satellite. This makes it possible to see the ability of the algorithm to get out the weak signals among the different peaks formed because of the noises. Figure 5.25 shows the value of the ratio between maximum peak and median CAF of the EITHSCD approach and the reference approach (Axelrad et al., 2011).

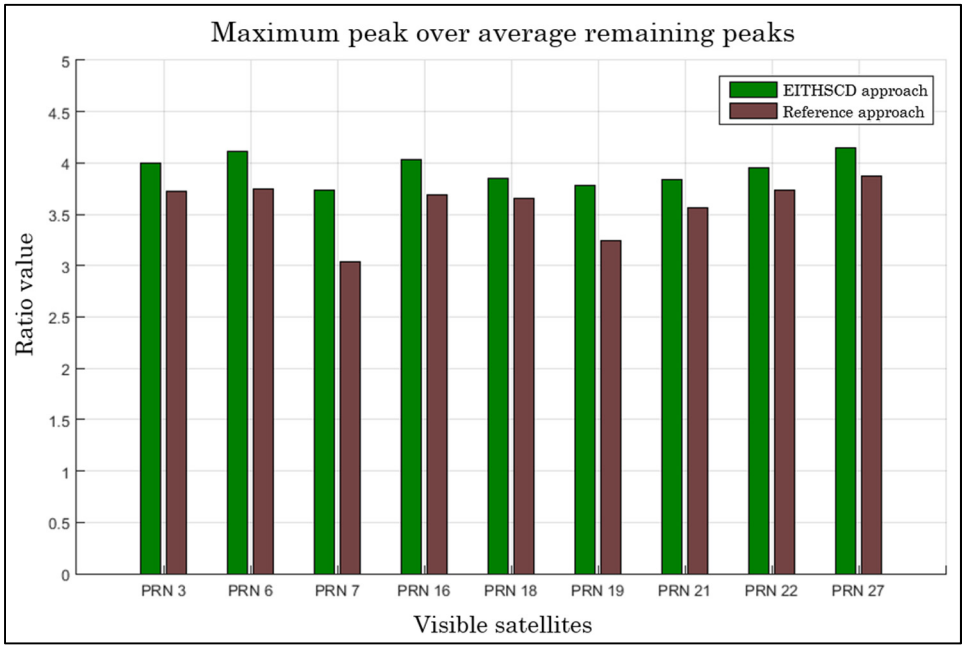

Figure 5.25 Ratio of maximum peak over average remaining peaks

The curves in Figure 5.25 show that the values of the ratio between the maximum peak and the remaining peaks of the EITHSCD algorithm are higher than the ratio value of the reference approach. The sensitivity gain for this parameter is summarized in Table 5.20 for each satellite.

Table 5.20 Sensitivity gain for EITHSCD algorithm w.r.t the reference approach

SV	PRN 3	PRN 6	PRN 7	PRN 16	PRN 18	PRN 19	PRN 21	PRN 22	PRN 27
Sensitivity gain [%]	7.52	9.62	23.10	9.51	5.47	16.67	7.86	5.61	6.97

It can be seen that the gain is always positive for all satellites. Furthermore, the difference of the ratio value is noticeable for weak signals such as PRN 7 and PRN 19. Note that the highest gain corresponds to the PRN 7 which is the lowest satellite signal with 37.25 dB-Hz mean C/N_0 level (orange part in Table 5.20). This result shows clearly the effect of the delta-corrected technique on the improvement of the detection of GNSS signal. On the other hand, PRN 21 has also low C/N_0 level but the difference is not very great because of the elevation angle which is not favorable for this satellite.

The minimum gain value (5.47 %) corresponds to PRN 18 because of its position. Thus, some parameters can affect the result. The average value of gain for all satellites is 10.26 %. There is a better gain of 23.1 % for the PRN 7 since it is in a good condition to profit from the delta-corrected acquisition method because its mean Doppler offset is close to a mid-bin frequency value despite its low C/N_0 level.

Complexity analysis

The comparison between EITHSCD algorithm and some CD approaches in literature that address the complex problem is shown in Table 5.21. The algorithms corresponding to each compared technique have been run with the same parameters and test conditions.

Table 5.21 Computational load between some CD approaches

CD Approach	Execution time [s]	Number of points evaluated
Traditional CD (Axelrad et al., 2011)	98.03	388987
ECPIOCD (Jia et Sahmoudi, 2016)	24.65	180100
Accelerated CD (Narula, Singh et Petovello, 2014)	32.37	236517
Proposed EITHSCD	21.98	175032

The number of point to be scanned is 175032. Compared to others methods in literature, this value is lower. Note that the number of candidate points is the same as using simulated signals, the difference is in the execution time of the algorithm. The execution of the algorithm is 4.46 times faster compared to the reference approach with real GPS signals, therefore reduces the complexity. These results show that the application of the SPL delta-corrected FFT method within the hybrid CD approach allows to have a better performance in terms of complexity and sensitivity acquisition. The CD approaches developed in (Narula, Singh et Petovello, 2014) and (Jia et Sahmoudi, 2016) appear to have good performance compared to the reference approach in (Axelrad et al., 2011) in terms of complexity, but the advantage of EITHSCD is related in the fact that it is also capable of increasing the sensitivity of receiver.

Accuracy analysis

Apart from the performance metrics mentioned above, the EITHSCD also makes it possible to have a better accuracy of the position solution. Table 5.22 summarizes the results obtained by both approaches to compare their performance.

Table 5.22 Performance comparison between EITHSCD and reference approach

Performance metrics		**EITHSCD**	**Reference approach**
HPE [m]	North (50/95 %)	10.32/18.57	35.21/97.03
	East (50/95 %)	9.97/17.72	37.64/101.15
Candidate points		175032	388987

It can be seen that the accuracy is improved because of the increased sampling rate, but complexity is increased. This compromise is precisely solved by the multi-iteration hybrid approach of conventional correlation with CD approach. The cumulative histograms of HPE (North and East) for all visible satellites obtained with mask angle of 10° is shown in Figure 5.26. The maximum pseudorange error is 9.3 m.

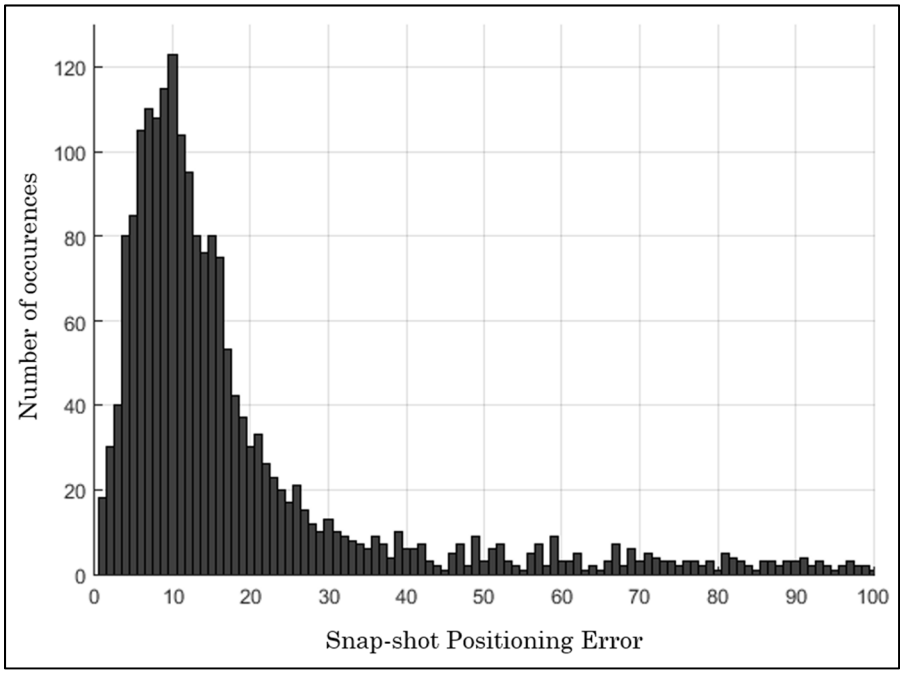

Figure 5.26 Histogram of snap-shot horizontal positioning error for all satellites in view

The histogram in Figure 5.26 is limited to 100 m positioning error but it is possible to obtain HPE of several hundreds of meters for very poor constellation configurations. Note that the worst results could be obtained with poor geometric configurations of satellites, i.e. when the satellites are very close to each other which is the case of positioning in challenged environments (urban, indoor, etc.). In fact, there is just a small part of the sky is visible to the user. The error of the solution accuracy on the ISAE map at the end of the recording scenario is shown in Figure 5.27.

This result shows that the position solution obtained is not poor in view of the technique used for direct positioning knowing that the other CD approaches in literature provides less accurate solutions using the same simulation and test parameters.

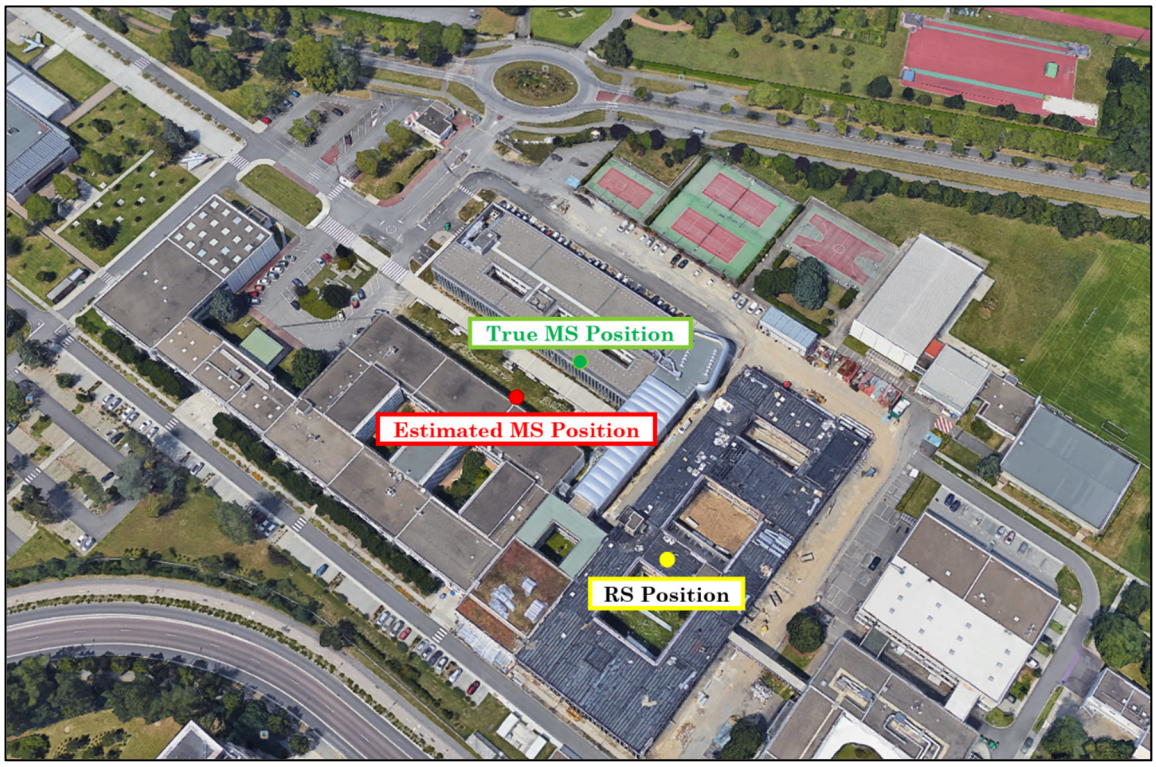

Figure 5.27 Position error obtained from EITHSCD algorithm at ISAE campus

5.9 Summary

This chapter was devoted to the CD approach where we introduced the state of the art of the various works carried out on this promising approach to solve the limitations of positioning systems in difficult environments. The basic principles of this approach were presented as well as its advantages and disadvantages. Then, different techniques have been proposed to overcome these limitations which are part of the original contributions of this thesis. The different proposals are summarized in Figure 5.28.

By proceeding step by step the different propositions in Figure 5.28, the core problems of the CD approach can be solved. It has been demonstrated that the final proposed EITHSCD algorithm offers better gain in terms of complexity reduction and increased sensitivity with respect to the traditional CD approach. Similarly, a good improvement of the position solution was obtained by this algorithm.

The minimization of reliance on assistance information sent by the RS is also addressed. In the EITHSCD algorithm, a new hybrid scheme of collective detection with the conventional correlation approach in multi-stage coupled with a better technique for Doppler frequency estimate is proposed to address the high computational burden, the low sensitivity, the large positioning error and the deep dependence on assistance data. SPL technique with delta-correction is used for frequency estimate within the hybridization CD scheme in order to have a better performance of the proposed algorithm. Applying this concept also minimizes reliance on assistance and helps to reduce costs associated with the installation of additional positioning equipment in GNSS denied environments.

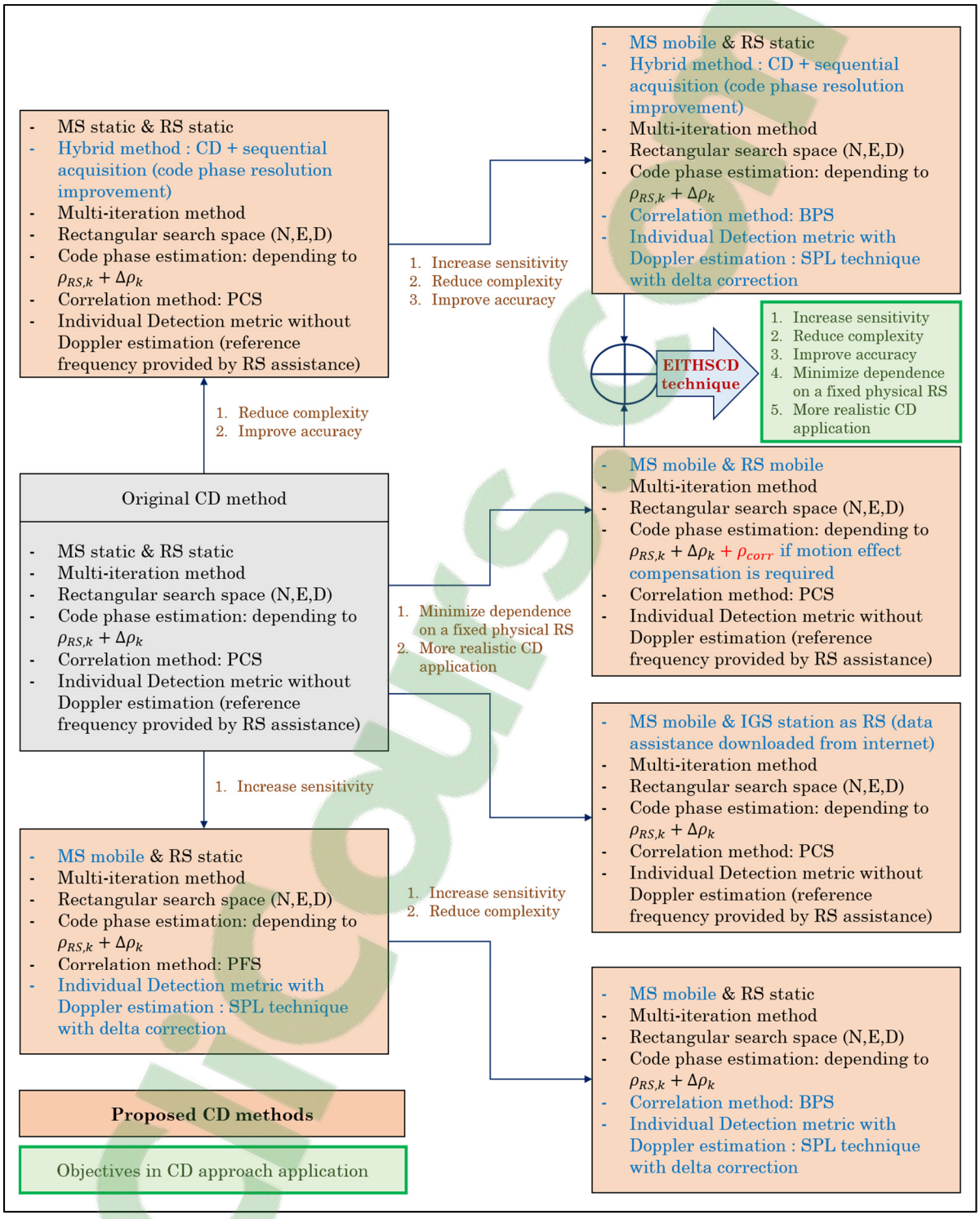

Figure 5.28 Summary of proposed methods in CD approach and part of main contributions in this thesis

The possibility of using a mobile reference station instead of fixed RS as well as an IGS station as an alternative to the requirement of a fixed physical RS has been demonstrated in order to have a more realistic application of the CD approach and achieve a great goal of this thesis. Variation of coherent integration and non-coherent has been conducted to show the receiver sensitivity. Applications of the EITHSCD with mobile RS and IGS service have been presented in (Andrianarison, Sahmoudi et Landry, 2017) to show its efficiency and feasibility.

With these good results, practical use of the CD approach will become increasingly feasible. In addition, we will be able to make good use of the various GNSS satellites to create a multi-frequency/multi-constellation receiver. Using cognitive radio technology to exploit the best satellites within CD approach will be the focus of the next chapter and it will lead to new lines of research in the CD and GNSS signal processing field.

CHAPTER 6

COOPERATIVE GNSS POSITIONING CONCEPT USING COLLECTIVE DETECTION APPROACH

In the previous chapter, the Collective Detection (CD) approach has been developed in details. CD technique can be considered as one of the promising approaches to meet the requirements of signal processing in GNSS challenging environments. Original contributions developed in the previous chapter of this thesis have been developed to improve the performance in terms of complexity, sensitivity and accuracy. This chapter is dedicated to apply the CD technique to Cooperative GNSS Positioning for modern navigation in harsh environments as a practical application of this interesting approach. In deep urban environments, a receiver that is unable to calculate its position may require assistance from one or more other nearby receivers that are able to receive good satellite signals to help it estimate its position. The architecture of the GNSS receiver should be then redesigned so that it is flexible and reconfigurable according to certain criteria (environment, parameters of the received signals, etc.). For that, the concept of cognitive radio (CR) is used in order to give some intelligence to the receiver so that it operates optimally according to the given criteria.

6.1 Need for a hybrid architecture

As we have seen in Section 2.1, by using different GNSS signals, GNSS receivers should be able to improve the main weaknesses of navigation systems such as availability (increasing the number of visible satellites to determine the receiver position), integrity (more reliable navigation messages), accuracy (several frequencies allowing better correction of certain errors) and electromagnetic vulnerability (use of different modulation techniques).

GNSS signals are heterogeneous because of some differences in principles on signal components, spectra, modulation type, navigation messages, time references, etc. Each system has its advantages and limitations depending on the application and the environment. Moreover, it is really interesting to make combination of measurements from the three

operating systems (GPS/Galileo/Glonass), and then a technique of combining all GNSS systems (GPS/Galileo/Glonass/BeiDou) when the BeiDou will be global and fully operational. It will make the GNSS receivers more robust and more accurate than the current receivers. That's why the developments of new and modern GNSS signals have been done with the need of interoperability in mind between the different systems.

The aim of this thesis is to be able to use all future GNSS signals in addition to the GPS signal L1 (the mostly used in current market) in order to have a more sensitive hybrid receiver in hostile environments or especially inside buildings. Indeed, the receiver will be able to acquire several navigation signals even broadband signals such as GPS L5 and Galileo E5. The characteristics of these different signals including the modernized GNSS signals have been presented in Section 2.1.3. The main idea is to propose architectures of hybrid GNSS receiver capable of operating in challenging environments by optimally exploiting the various GNSS signals (current and future). So, interoperability is one of the most important criteria to be taken into account which refers to the ability of making systems work together (Fernandez-Prades, Arribas et Closas, 2015). In fact, we have to consider all parameters such as the possibility to exchange information with other software, devices and systems, including external assistance, GNSS signals, RF front-ends, and all sort of information-displaying or sensor data fusion applications via standard outputs.

6.2 Need for a cognitive receiver

A very interesting idea for a practical application of the CD approach is the assistance request as needed. For example, a user does not necessarily require full-time assistance to a receiver from a service provider (Novatel, Bell, Qualcomm, Broadcom, Orange, etc.) but rather a subscription to the service type *"pay as you need"*. Another example, a user in bad condition of reception can be helped by two or several receivers nearby which are able to receive good satellites. These concepts require an intelligent function of the GNSS for the need of assistance according to the conditions. The CR technology applied to navigation and GNSS positioning

is a better solution for that. Thus, a new architecture of the receiver, called as “High Sensitivity Cognitive GNSS Receiver (HS-CGR)” based on CD concept, should be designed.

To design the architecture of an intelligent HS GNSS receiver, we will begin by defining its basic operation according to the number of satellites detected as shown in Figure 6.1. Indeed, if there are enough satellites (greater than or equal to 4) to calculate the position of the receiver, the conventional sequential acquisition is carried out. Otherwise, the CD process is used. Then, the intelligence of the receiver must consider other parameters according to the acquisition method used to process the received satellite signals.

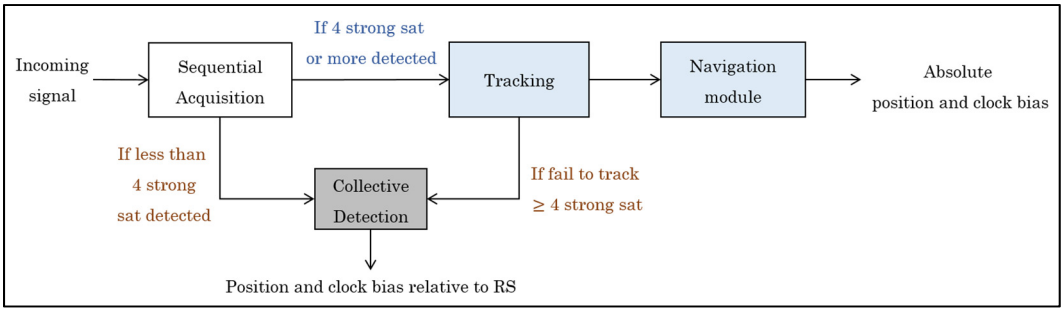

Figure 6.1 Smart functional operation of HS GNSS receiver

6.2.1 Relationship between Cognitive Radio and Software Defined Radio

In order to take advantage of the new GNSS signals, the use of a technique allowing them to be exploited optimally is the ideal solution. The SDR concept was introduced to meet this expectation. Furthermore, given the performance and success of CR technology in telecommunications field, we propose its use in satellite navigation in addition to the SDR approach already used in the current GNSS receivers. A comparison of the radio properties between SDR and CR technologies is presented in Table 6.1, which shows that cognitive radio technology has more flexibility than software radio that is why its use is proposed. In fact, an additional cognitive layer is needed to provide an even more flexible and intelligent system to the SDR platform. Moreover, the radio properties in the last four lines of Table 6.1 are essential for the design of the cognitive GNSS receiver.

Table 6.1 Properties of SDR and CR
Adapted from (Bruce, 2006)

Radio property	Software Defined Radio	Cognitive Radio
Frequency hopping	X	X
Automatic link establishment (channel selection)	X	X
Programmable crypto	X	X
Networking capabilities	X	X
Multiple waveform interoperability	X	X
In-the-field upgradable	X	X
Full software control of all signal processing, crypto, and networking functionality	X	X
Modification of radio parameters as function of sensors inputs		X
QoS measuring/channel state information gathering		X
Learning about environment		X
Experimenting with different settings		X

According to (Polson, 2004), we talk about a CR when a radio is aware, adaptive, and learns. In our case, we will exploit the awareness and adaptability of the GNSS receiver. The notions of "learning" are not further elaborated in this thesis. To know more about the machine learning applied to SDR, interested readers are invited to read (Mitola III, 2006).

6.2.2 Cognitive Radio technology for navigation and positioning

Somewhat similar to the software radio technology SDR, CR technology has become the attraction of researchers in navigation field, and many researchers are now investing in it. This is really a very promising alternative for future generations of GNSS signals from different

constellations and transmitted over different frequencies. Currently, there is a growing discussion of cognitive positioning systems (CPS) in the field of satellite navigation. The greatest advantage of the CPS is its ability to dynamically manage the bandwidth.

CPS was initiated in (Celebi et Arslan, 2007b) in which the bandwidth determination is derived from the Cramer-Rao Lower Bound (CRLB) equation for AWGN noise and multipath channels. The CPS is able to achieve a precise adaptation of indoor and outdoor environments on the basis of cognitive radio technology (Celebi et Arslan, 2007a). For example, the CR uses the waveform of the GSM system with an accuracy level of 100 m outside. If the user enters inside, the CR directly recognizes the WLAN wireless network using its interoperability capability and changes its WLAN waveform with an accuracy level of 5 m indoors. Compared to the standard GPS or UWB positioning, the CPS approach has the ability to recognize location using CR technology.

Similarly, (Celebi et Arslan, 2007a) proposed an adaptive CPS technique that uses hybrid bandwidth (lower/upper-spectrum, H-EDSM) and an adaptive TOA method (A-TOA) to determine the band required to estimate the location information. Basically, the CR is used for its intelligence to know the free bands and to be able to transmit information there. But the evolution of CR technology has shown that this ability to recognize spectra can be used to improve SDR receivers. In a reconfigurable CR, there are some components that work together to emit and receive waveforms, there are analog components like PLL, and there are also digital components like FPGA processors. The CR operation is based on three principles: reconfigurable hardware, embedded software and radio management (Jian et al., 2009).

SDR and CR technologies are very promising since they can be used to alleviate the problem of spectrum shortages, but also to overcome problems of interoperability in various fields of application (Baldini et al., 2008). Moreover, (Luise et Zanier, 2009) demonstrated that the use of multi-carrier signals is very advantageous for the cognitive positioning system.

A few years before, the design of multi-frequency GNSS receivers was the center of research in the field of satellite navigation. But recently, the design of a new receiver architecture called as Cognitive GNSS Receiver (CGR) was born. Given the advantages of using cognitive radio technology in the field of positioning, this idea of CGR, which is the latest technology, will bring solutions to several research problems that arose before and will open a new axis of research. Recently, (Shiravaramaiah et Dempster, 2011) studied the concept and the challenges to be faced on the design of this new type of receiver.

Decision-making is one of the major criteria for the use of this type of receiver. In order to make a decision, three reasoning methods are possible: case based reasoning (for new cases, search for a similar case by finding in data stored within the cognition functional layer with updates based on previous situations), rule based reasoning (based on if-then-else reasoning), temporal knowledge (stores interesting data as the CGR works) (Shiravaramaiah et Dempster, 2011). The decision-making process is often multi-objective oriented and this is the point where the cost functions help make the decision, which is why it is modeled as:

$$\begin{aligned} &\min/\max\{y\} = f(\bar{x}) = [f_1(\bar{x}), f_2(\bar{x}), \dots, f_n(\bar{x})] \\ &\bar{x} = (x_1, x_2, \dots, x_n) \in X, \bar{y} = (y_1, y_2, \dots, y_n) \in Y \end{aligned} \tag{6.1}$$

The biggest constraint for using CR technology in satellite navigation is the decision-making time that is too long, not in real time.

(Sahmoudi, Yang et Calmettes, 2010) proposed a technique exploiting the spectral characteristic (cyclo-stationarity) of GNSS signals and using cognitive radio technology to develop a new CGR to process the acquisition and tracking of GNSS signals in navigation environments. Their technique is to exploit the cyclo-stationarity of BOC signals for interference mitigation, multiple correlator design, extended coherent integration and robustness to frequency variations. The use of CR technology in a GNSS receiver requires some important features of the CR module such as recognition of the navigation environment to detect interference, multipath and multiple GNSS signals via a cognitive decision,

(characteristics from signal analysis and decision); ease of reconfiguration and adaptation using optimal signal processing corresponding to the current case (combination of all possible scenarios with the corresponding algorithms implemented); and resource optimization based on complexity and effectiveness compromise (use of statistical or metric information computed by the cognitive module in the receiver, or conversely records the feedback values from the receiver to predict the change by the cognitive module) .

CR technology offers a good alternative solution for future generations of GNSS systems, especially with the modernization of GPS and Glonass systems as well as the new Galileo and BeiDou systems. In addition to increasing the number of signals with different characteristics, the number of channels will also increase, which justifies the use of high-performance GNSS receivers in terms of data processing. Despite some challenges to overcome, several benefits are offered by this technology. Since the CR technology is still very recent, research on its use for the design of a GNSS receiver is not yet numerous, tracks are still open such as the design of a high sensitivity cognitive GNSS receiver, acquire and track weak C/N_0 signals in challenging environments.

6.2.3 Basic architecture of HS-CGR

In general, the idea is to add cognitive ability to GNSS receivers in order to have smarter receivers. The design of the CGR can be seen as the use of CR technology in the design of GNSS receivers. The purpose of adding cognitive capacity is to have a self-adaptive and autonomous system. For this, different levels must be taken into account: "programmability" to modify the behavior of the system by changing the design parameters; "reconfigurability" to modify the behavior of the system by changing the design itself; "cognitive capacity" allowing the adaptability of the system behavior according to the situation (environment) in which the system is operating, that is to say that the system observes the actions and then learns from these actions (Shiravaramaiah et Dempster, 2011).

The block diagram of the HS-CGR is illustrated in Figure 6.2 which shown the SDR receiver as a platform for CR. The gray part (bottom part) is the typical HS-GNSS receiver. The yellow part (upper part) consists of the cognitive layer where the intelligence of the receiver resides. It is this part which commands the receiver to what it must do according to certain situations (operating environment, type of starting, power of received signals, etc.).

The implementation of cognitive ability can be done in all the different levels of GNSS receiver processing: RF front-end, baseband module (acquisition and tracking) and navigation solution. There are many opportunities to implement it. The cognitive capacity implementation then depends on what we want to have, i.e. the objective set. For example, if we want to save energy when the battery is low, the CGR receiver uses a simple GPS L1 C/A signal to find the positioning solution, and the receiver avoids acquiring several signals at the same time whose processing requires enormous energy consumption.

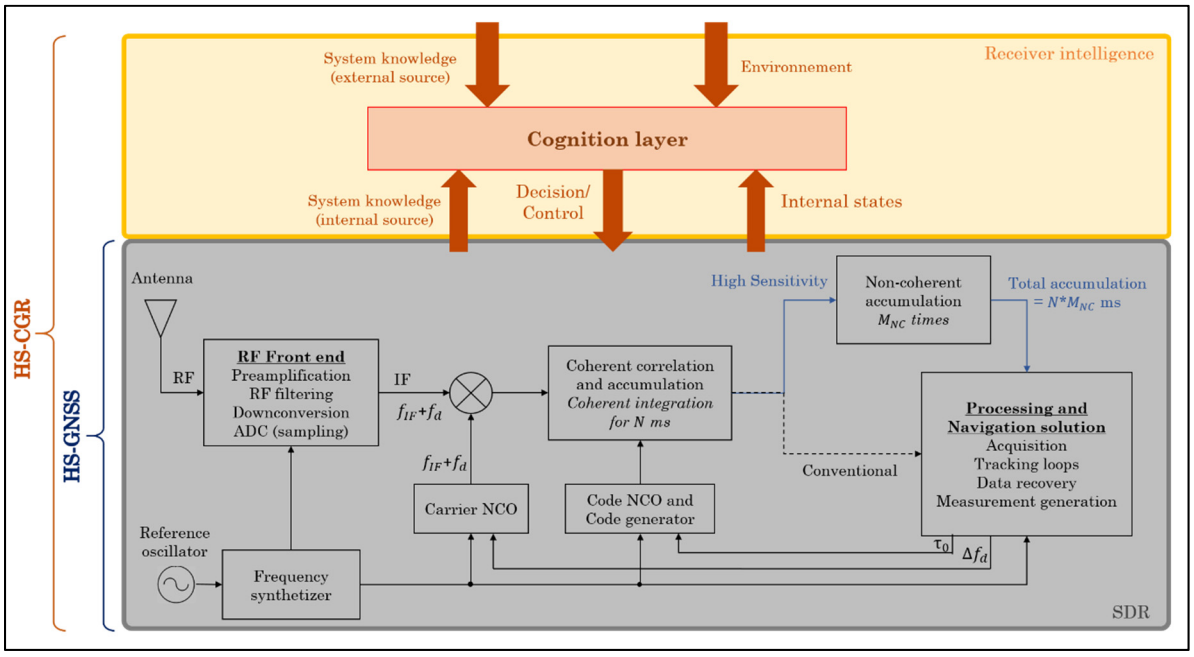

Figure 6.2 Block diagram of the proposed HS-CGR

Similarly, if the aim is to have a high positioning accuracy, then at least two satellites will be used by the CGR to reduce the positioning error. From another point of view, several cases are

possible for the same objective. For example, if one does not want to waste resources, two decisions can be made: the CGR receiver will not use additional signals if the additional measurements are not necessary to find a precision of the solution, or the CGR receiver will not use very weak signals that require complex algorithms while in an ideal environment. Referring to the functional diagram block of the HS-CGR, several configurations can be made at several levels. For example, for positioning inside buildings or in challenging environments, the baseband algorithm may select the appropriate pre-correlation integration time (longer integration period). Examples of the cognitive functioning of the receiver in different situations (according to the environment, internal status of the receiver, available assistance information, number of received satellites with different powers, etc.) will be presented in Section 6.2.5.

6.2.4 Some configurations according to intended objectives

To implement the CR technology in the design of the HS-GNSS receiver, several parameters can be considered and several solutions can be proposed according to the desired objectives. Input parameters and configurations are always based on the set objectives.

For example, depending on the signal received on the antenna, spectrum management is done intelligently. Since four satellites are required to calculate the position of the receiver, several cases are possible: the best combination is to have 4 GPS satellites (the most used system) and the worst case is the use of the four GNSS systems such as 1 GPS satellite + 1 Galileo satellite + 1 Glonass satellite + 1 BeiDou satellite. An optimization method will then be applied to minimize the use of resources. The effectiveness of the GPS combination with Galileo has already been shown by several studies in Section 4.6, which means that we can limit ourselves to these two systems if the case presents itself instead of using other systems that will just increase the calculation load knowing that the signals of all GNSS systems have different characteristics. For more information, principles of satellites combining are presented in ANNEX I.

The cognitive module makes it possible to optimally choose the best signal processing technique to use in order to process the received signal according to a few parameters: number of visible satellites, received signal level, navigation environment, number of available channels, microprocessor load, etc. This module contains only the intelligent selection algorithm of best technique to use: conventional HS-GNSS acquisition method or CD approach by exploiting the best reference station for assistance and processing the best satellites. The techniques proposed to increase the sensitivity of the receiver are: coherent integration over a long period and non-coherent accumulation, use of FFT technique by parallel code search or bi-dimensional parallel search, combination of several GNSS signals, SPL delta corrected technique for Doppler estimation, etc.

The motivation idea is to carry out the minimum of calculation while having a good margin of precision of position. Indeed, this can reduce the complexity of implementation but especially minimize the energy consumption as part of a multi-GNSS receiver where tens of signals are present in the receiver antenna. For example, the core baseband of receiver based on a twelve channel two constellation (civil/open service signal) would consume about 35 times the power consumption of a receiver receiving GPS L1 C/A only (Shiravaramaiah et Dempster, 2011).

It is through the cognitive layer of the HS-CGR that the receiver processes the navigation signals intelligently. In order to optimize the use of resources (minimum number of channels during acquisition), decision-making is based on several data (signal level, GNSS system used, selected filter, modulation type, navigation environment, receiver internal status, existing scenarios, etc.). In fact, cognitive decisions are made to drive the hardware receiver through switching to select techniques, signals, channels, etc. This layer makes it possible to make the optimum decision on the HS-GNSS receiver. According to various parameters, to make a decision, a decision table which is stored in the database can be consulted.

Several scenarios can be described with the corresponding decisions. For example, in our case, the goal is to increase the sensitivity of the HS-CGR receiver while optimizing its operation (maximize performance by minimizing resource use). Thus, the scenarios described in the table

should take into account previous navigation information such as ephemeris and almanacs, the last stored position in order to minimize the TTFF and the MTTA has new satellites to acquire or in the case of a cold start of the receiver which will take a long time to initialize and have stable navigation solutions. Indeed, the principle of GNSS receivers is based on the type of start (cold, warm or hot) depending on the availability of relevant information in the receiver, and it is also the idea of the internal state in CR. Similarly, knowledge of the system refers to the satellite selection algorithm that helps the receiver to find the first satellite to acquire.

In addition, knowledge of the navigation environment also helps the receiver to optimally manage the selection of signal processing techniques. For example, if the receiver passes from the outside to the inside, the baseband algorithms can choose an appropriate pre-correlation integration time in order to effectively increase signal energy. Similarly, if the receiver knows that it is operating in an urban environment, it can choose the CD approach.

While CD can be considered as a high sensitivity acquisition method because it combines all satellites in a single detection measure, it increases the detection performance of weak signals. This final application proposal presents the idea of exploiting to the maximum the advantages of the CD approach depending on the working environment of the receiver.

6.2.5 Use case 1 of HS-CGR: Exploitation of the navigation environment

If there is no receiver (RS) capable of assisting the user, here is an example of information that will be described in the HS-CGR decision table:

- Depending on the type of receiver start-up (cold/warm/hot): use relevant information in the receiver or perform the normal process;
- According to level C/N_0: use high sensitivity techniques (long coherent integration with non-coherent accumulation);
- Depending on the number of signals received: track more powerful signal or combine stronger signals.

In order to facilitate a new processing method and to be more efficient, the receiver should remember the last known success tracking parameters such as: Did the receiver track this satellite just a few seconds before? What was the power of the signal? Is it the use of this satellite had led to have a good position solution? How long was that satellite in tracking mode? Was it still used in the solution during the last tracking? How many times the signal of this satellite had to be re-acquired? etc.

Listening to the environment is done by answering several questions such as: What systems are available (GPS/Galileo/Glonass/BeiDou)? How many visible satellites? Which fixed satellite (PRN number)? What is its power (SNR)? What is the elevation mask angle? What kind of assistance is available?

In addition to the decision table, the cognitive layer must be able to act on the receiver even if the current case does not exist in the scenarios described in the table based on machine learning. All this shows a possible proposition to the application of CR in HS-CGR but are not studied in depth in this thesis.

The flow chart of the proposed HS-CGR can be simplified as shown in Figure 6.3. In summary, according to the data taken into account (navigation parameters: C/N_0, elevation angle, GDOP), the cognitive layer is used to decide whether the receiver is able to carry out the standard processing of satellite signals, i.e. the HS acquisition techniques (long coherent integration and non-coherent accumulation); otherwise, it makes use of assistance and proceed to the CD process. If the CD approach is used, the objectives of minimizing dependence on assistance should always be considered such as: RS position is calculated within MS via ephemeris, Doppler estimation is performed within MS (reference frequency not provided), and only ephemeris and RS pseudorange are provided from RS. The functioning of the "Assistance" block is based on the proposals developed in Sections 6.3 and 6.2.4 (Andrianarison et Landry, 2018).

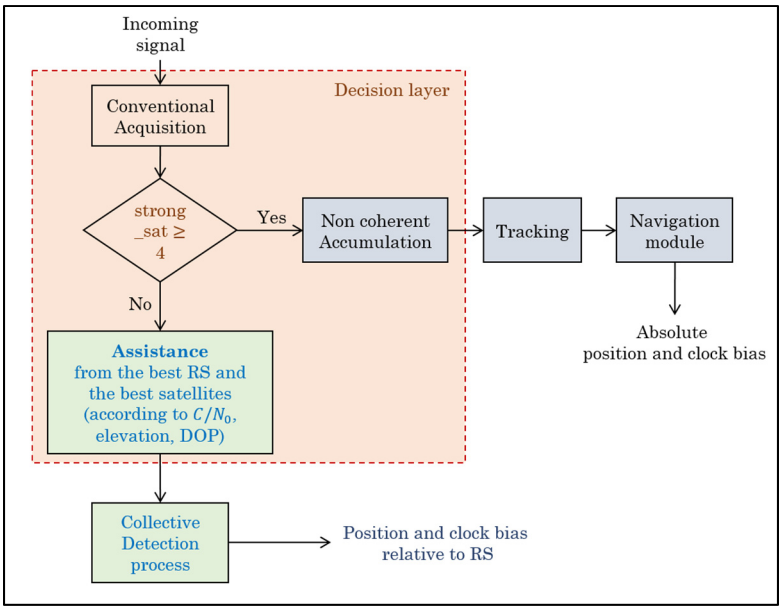

Figure 6.3 Flow chart of the use case 1 of HS-CGR

6.2.6 Use case 2 of HS-CGR: Working with optimum number of parameters

To illustrate the benefit of operating the CR in the HS-GNSS design, let's see an example of optimal use of certain parameters. This example shows the influence of the signal strength in the position estimation accuracy in the context of the CD approach. In Figure 6.4, we compare 6 weaker satellites [PRN 2, PRN 3, PRN 11, PRN 13, PRN 20, PRN 31], 6 satellites (3 weaker [PRN 3, PRN 11, PRN 13] + 3 stronger signals [PRN 10, PRN 16, PRN 23]) and 10 satellites (3 weaker [PRN 3, PRN 11, PRN 13] + 7 stronger signals) as shown in Table 6.2.

Table 6.2 Visible satellites during observation period

PRN	C/N_0 [dB-Hz]	Elevation [°]	PRN	C/N_0 [dB-Hz]	Elevation [°]
2	40.25	10.33	13	30.50	24.99
3	35.75	49.99	16	43.50	32.73
4	42.25	16.43	20	40.75	12.34
10	45.00	81.47	23	44.75	46.08
11	37.75	18.62	31	38.50	14.64

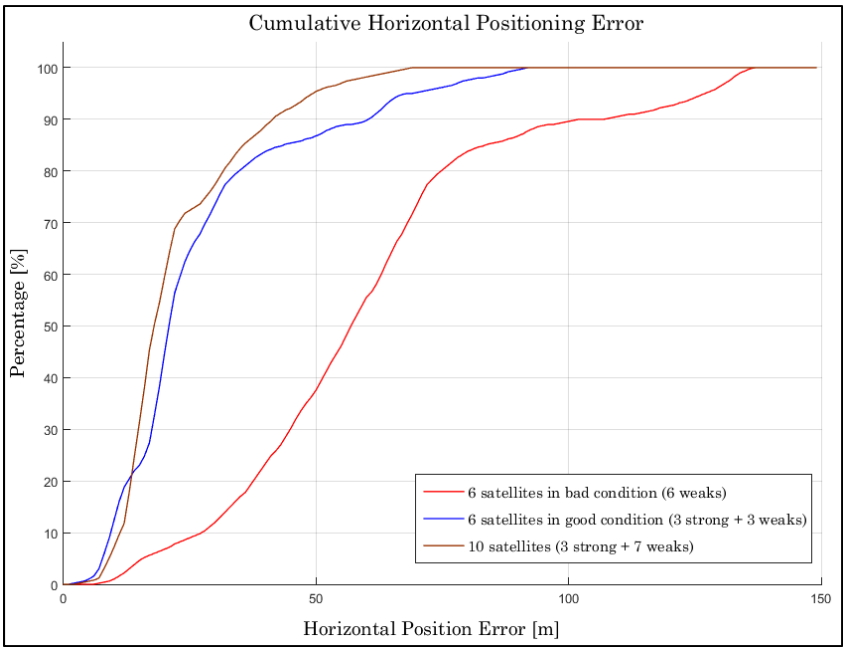

Figure 6.4 Comparison of HPE between 6 satellites and 10 satellites w.r.t SNR

By observing these curves, we can see that there is no great difference between HPE using only 6 satellites including 3 strong and that of 10 satellites including 3 strong too. This can be explained by the weak influence of the weak signals exploitation (difference of 4 weak satellites) which come to collaborate to the collective detection metrics. We can deduce from this that we can limit to process only 6 satellites in order to minimize the computational load. The idea is to use the minimum number of satellites while keeping a precise positional solution.

6.3 Some applications of CD approach Cooperative GNSS Positioning

We will see some applications of the CD approach based on cognitive functioning according to various parameters such as working environment, satellite parameter (C/N_0 level, elevation angle and geometry configuration), intern state of the receiver, etc. (Andrianarison, Sahmoudi et Landry, 2018)

6.3.1 Application with real signals

To see the effectiveness of these applications in practice (Cooperative Positioning based on CD approach and selection of best reference and best satellites), a scenario in downtown Montreal was carried out. A bit grabber USRP B210 as used as MS, and two uBlox LEA-6T are used as RS1 and RS2 to assist the MS. Raw GPS L1 C/A signal data was collected from the test setup where signals were attenuated by building structure. The position of RS1 and RS2 that assist the MS in downtown Montreal is shown in Figure 6.5 Figure 6.6 shows the location of the data acquisition where the GPS L1 C/A signals are degraded because of the high buildings around.

Figure 6.5 Location of receivers during GPS L1 C/A signals recording

Positions of MS and both RSs are shown in Table 6.3, and the satellites received by each reference station are summarized in Table 6.4.

Table 6.3 Main coordinates and distances from both RSs to MS

Station	Latitude	Longitude	Altitude	Distance to MS
MS	N 45°29'35.6"	W 73°33'48.4"	83.60 m	n/a
RS1	N 45°29'39.2"	W 73°34'08.1"	83.61 m	412.03 m
RS2	N 45°29'30.5"	W 73°33'37.0"	83.59 m	424.66 m

Figure 6.6 Location of MS in downtown Montreal (GPS antenna placed inside a car)

Table 6.4 Visible satellites during observation period

RS1		**RS2**		**MS**	
Satellite	C/N_0 [dB-Hz]	Satellite	C/N_0 [dB-Hz]	Satellite	C/N_0 [dB-Hz]
PRN 2	40.25	PRN 2	40.75		
PRN 3	35.75	PRN 3	36.75	PRN 3	35.25
PRN 4	42.25	PRN 4	41.00	PRN 4	38.75
PRN 10	45.00	PRN 10	45.75	PRN 10	45.25
PRN 11	37.75	PRN 11	37.50	PRN 11	35.50
PRN 13	30.50	PRN 13	30.50	PRN 13	30.50
PRN 16	43.50	PRN 16	42.75	PRN 16	42.75
PRN 20	40.75	PRN 20	40.50		
PRN 23	44.75	PRN 23	44.25	PRN 23	42.75
PRN 31	38.50	PRN 31	37.50		

6.3.2 Application 1: Use of multiple receivers in CD as a Cooperative Positioning

Cooperative Positioning or Collaborative Positioning (CP) is known as a better localization technique used to locate a user in challenged environments, which is driven by the increasing

presence of cellular phones and mobile devices in urban area. The basic idea is that the mobile devices can cooperate with each other to improve their ability to determine position. In this concept, a network of GNSS receivers can collectively receive available satellite signals, and each receiver can receive signal measurements from other receivers via a communication link. This application shows how to use the Collective Detection approach to deal with the concept of collaborative or cooperative positioning. Specifically, this application proposal develops new techniques allowing a receiver in deep urban environment to perform its positioning using the CD approach (Andrianarison, Sahmoudi et Landry, 2018). The focus in this proposal was strongly motivated by the idea of some devices equipped by GNSS chips connected to help each other as shown Figure 6.7 in which the application scenario is presented by two drones in good conditions helping a drone in difficult situation.

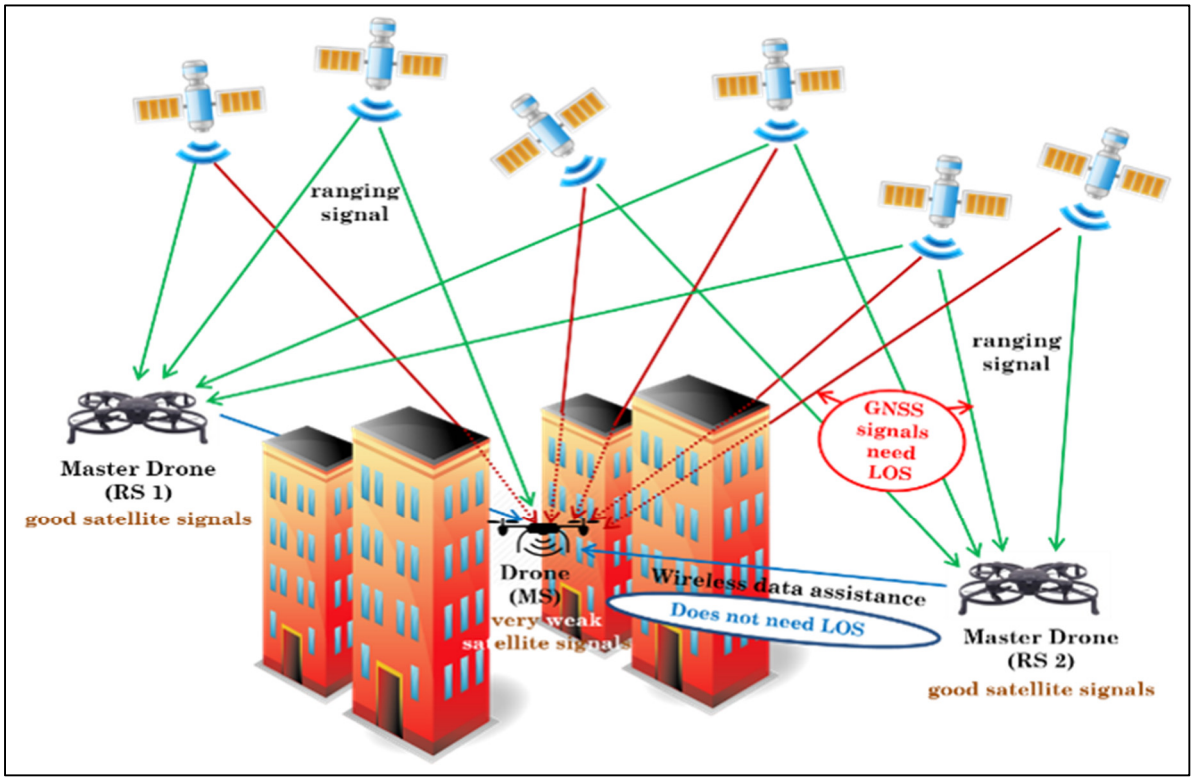

Figure 6.7 An application scenario of the proposed approach

6.3.2.1 Concept of Collaborative Positioning

There are different ways of addressing the Collaborative Positioning problem. For example, in (Soloviev, Dickman et Campbell, 2013) the collaboration between receivers is performed in both signal processing and measurement level, and each receiver processes the incoming satellite signal (1 ms signal) with a correlation engine before sending its data to others to perform CP in the measurements domain. The concept of a multi-platform signal and trajectory estimation receiver (MUSTER) is introduced in (Soloviev, Dickman et Campbell, 2013) where relative navigation states between individual receiver nodes contain large uncertainties (100 m position uncertainty). In (Kealy et al., 2013), CP techniques are analyzed for robust GPS positioning in vehicular ad-hoc networks (VANET) based on the range communications infrastructure. In fact, an algorithm that support CP across a VANET is developed in (Kealy et al., 2013): a Cramer Rao Lower Bound analysis is carried out to demonstrate the performance of the CP architecture where standalone GPS positions and inter-node distances are combined in a loosely coupled integration architecture. A new paradigm around how some devices (smartphones, cameras, gaming devices, etc.) can cooperate with each other to improve their ability to compute position and navigate is developed in (Waters, Pande et Balakrishnan, 2011). In fact, the cooperation is performed at the position-engine level and on the case when measurements are not synchronized in time. The basic idea in (Waters, Pande et Balakrishnan, 2011) is to demonstrate two ways: a receiver with “strong” measurement data (good condition) can assist a receiver with “weak” measurement data (in difficulty) to compute its location and two receivers with “weak” measurement data (poor condition) can cooperate to improve their positioning accuracy and reliability. They have demonstrated that receivers can cooperate to compute their GNSS positions in some challenging environments where non-cooperative GNSS receivers fail. Other sensors with extended Kalman filter are used in (Grejner-Brzezinska et Toth, 2013) to assure continuous, accurate and reliable PNT even in GNSS-challenged environments, and enable robust cooperative navigation including seamless transition between different types of navigation platforms that navigate together. Some statistical network-based collaborative navigation algorithms are proposed and compared to Kalman filter in (Lee, Grejner-Brzezinska et Toth, 2012).

The benefit of the CD application is shown in Equations 5.8 and 5.9. The accumulation of all individual detection metrics for each visible satellite can increase the sensitivity of the receiver.

Taking into account the ability of the CD approach to process very weak GNSS signals, the following points were the main reasons that led us to apply the CD principle, as a tight fusion of multi-satellites signals, in the concept of collaborative/cooperative positioning:

- **Position of satellites:** study of the best methods for calculating the approximate positions of satellites without decoding the navigation message using the available ephemerides from a previous epoch or received via the internet;
- **Multi-user collaboration:** several users share the information (signal, measurements, ephemeris, etc.) to calculate the PVT of each one that they cannot calculate without cooperation (Kassas et Humphreys, 2014; Soloviev et Dickman, 2013);
- **Selection of satellites:** select the best satellites to be detected in order to eliminate those which will contribute little to the sensitivity of the receiver and to reduce the search space in the position/clock-bias domain. This process is performed after the correlation but before the calculation of the collective metric in (E, N, clock-bias).

Knowing that the use of a mobile reference station in the CD approach is indeed possible, demonstrated in Section 5.4, in this application proposal all the considered receivers can be fixed or mobile. We have seen the possibility of using a mobile reference station instead of static base station in order to expand the availability of assistance for the mobile user in GNSS-challenged environment. Despite the great advantage of being able to use a mobile RS, there is nevertheless a limit of its mobility which has been presented as a limitation value according to the coherent integration period, the dynamic of the reference station and the resolution of the code delay. If the limitation threshold of dynamic is reached, the error should be compensated by transmitting the pseudorange correction and the range rate correction to the MS in order to add theses parameters within the code phase estimation which is function of the RS pseudorange and the geometric difference of each candidate point with regard to the RS. In this application proposal, the mobile RS context is applied with the CD/CP approach.

6.3.2.2 Uncertainty range reduction using multi-receivers

Taking into account the three points mentioned in the previous section, let's consider the case of two receivers (RS1 and RS2) assisting a receiver (MS) in difficulty so that it calculates its position. Depending on the position of RS1 and RS2 relative to the user, some cases can be considered. Anyway, MS is still in the intersection area of RS1 and RS2. In other words, the intersection of RS1 and RS2 (assumed initial uncertainty area of RS1 and RS2) is the new search grid area to determine the position of the MS.

In CD, by carrying out the projection to position domain, two representations of horizontal position search can be used: Cartesian coordinates (rectangular search area) (Axelrad et al., 2011; Cheong, 2012) or polar coordinates (circular search area) (Esteves, Sahmoudi et Ries, 2014). When polar coordinates are used, it has been shown that the total number of points evaluated decreases considerably (Esteves, Sahmoudi et Ries, 2014). This is why, in this application proposal, we chose to adopt the technique developed in (Esteves, Sahmoudi et Ries, 2014) in order to minimize the uncertainty area where the MS position search is performed. For circular search, the uncertainty area is even smaller compared to rectangular search. Both cases are shown in Figure 6.8.

In this scenario, RS1 is further than the RS2 compared to the MS, i.e. the distance between RS1 and MS is greater than MS and RS2.

In the case where RS1 and RS2 are going to assist MS as a CP concept, the implementation of the CD requires some information provided by both reference stations, such as their pseudoranges, positions, ephemerides and reference frequencies to compensate the oscillator Doppler offset component.

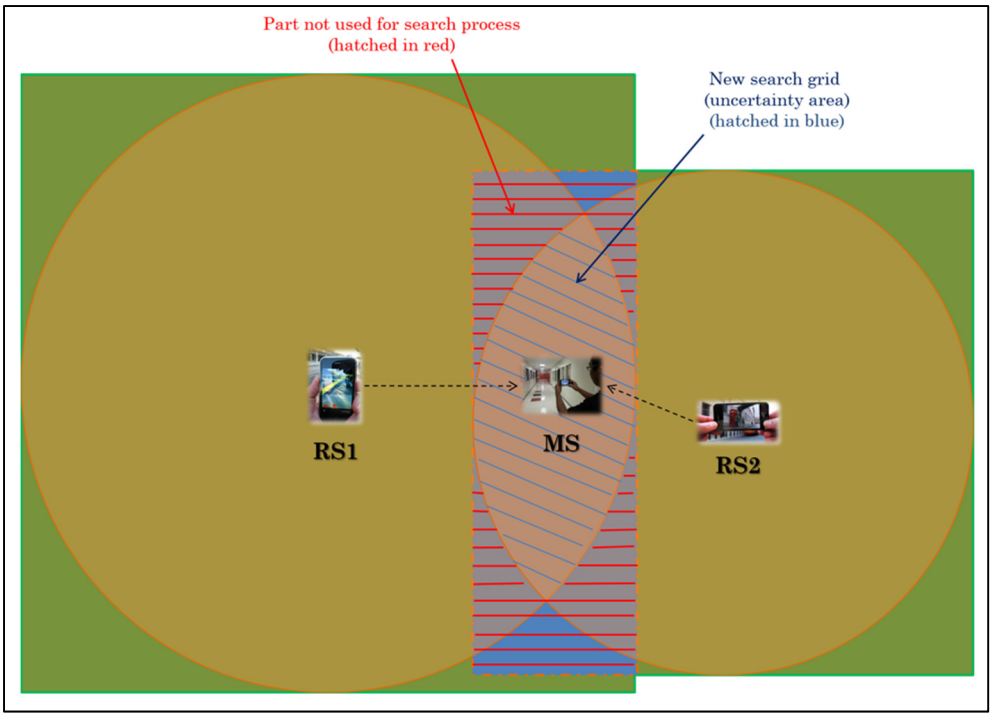

Figure 6.8 Scenario of CD approach used in CP concept

The CD process for estimating the position of the MS can be performed in two ways:

Case 1: Both RSs are used to define the search area but only one in the CP/CD algorithm. RS1 is used to determine the initial uncertainty area and the RS2 is used only to reduce the search space, and a single RS is used to calculate the delay $\hat{\tau}_k$. In this case:

- Both circles are used to calculate the uncertainty area in which the MS position is estimated;
- A single circle is used in the following two iterations using the CD approach in (Esteves, Sahmoudi et Ries, 2014) based on the polar coordinates by limiting only the variation values of R and θ according to the defined uncertainty area to reduce the number of calculations to be performed, in order to have a complexity gain.
- At each iteration, the grid resolution is reduced (values of R and θ).

Case 2: Both RSs measurements are used in the CP/CD algorithm. RS1 and RS2 are used to reduce the search space and each receiver sends their information to the MS to calculate the delay $\hat{\tau}_k$. Based on the code delay calculated according to the position of each reference station,

it is necessary to choose the best operation within MS. We must just assume that the two RS receivers are well synchronized in good satellites visibility. In this case:

- The estimation of the code delay is calculated according to the position of both reference station; and the computation of the individual and collective detection metrics are performed by merging the measurements of the two reference stations.
- At each iteration, the grid resolution is reduced (values of R and θ).

Case 1:

The assistance of RS1 and RS2 are only necessary during the first iteration. This is to take advantage of a high probability of better satellites existence, knowing the higher numbers of mobile receivers in urban areas, in order to reduce the search space of the MS position.
Thus, the CD process used to determine the MS position is as follows. Each candidate point coordinate (potential position and clock bias) is mapped to the code delay and Doppler space for each visible satellite. Figure 6.9 shows the projection of the signal code delay to the position/clock bias domain of the MS w.r.t the pseudorange measurements provided by the RS (Esteves, Sahmoudi et Ries, 2014).

In our case, the local horizontal search is a polar Rho-theta coordinates instead of North-East coordinates. In this way, ΔN and ΔE are expressed in terms of R and θ:

$$\begin{cases} \Delta N = R.\cos(\theta) \\ \Delta E = R.\sin(\theta) \end{cases} \tag{6.2}$$

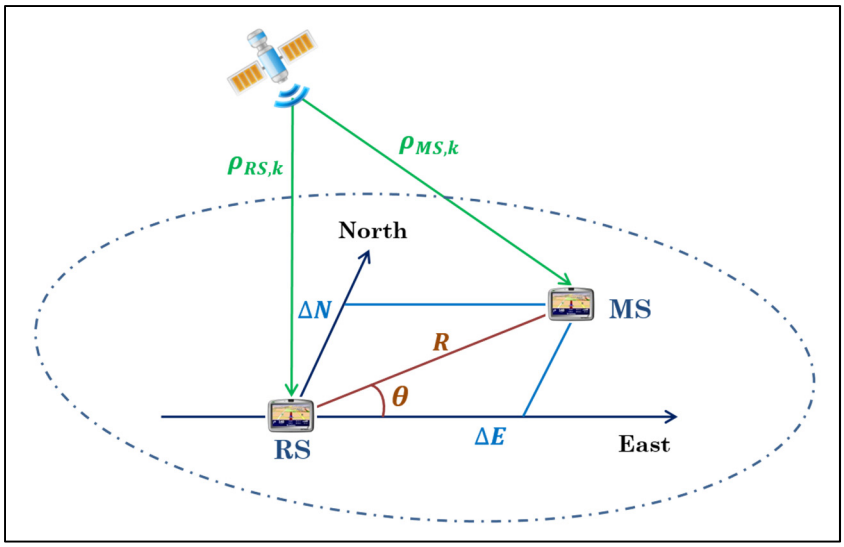

Figure 6.9 Mapping of the MS code delay search to position/clock-bias and pseudorange domains

So, from Equation 5.6 we yield (Esteves, Sahmoudi et Ries, 2014):

$$\begin{aligned}\Delta\rho_k(R,\theta,\Delta D,\Delta B) &= -Rcos(el_k)[\cos(az_k)\cos(\theta)+\sin(az_k)\sin(\theta)] \\ &\quad +\sin(el_k)\,\Delta D + c.\Delta B \\ &= -Rcos(el_k)\cos(az_k-\theta)+\sin(el_k)\,\Delta D + c.\Delta B\end{aligned} \tag{6.3}$$

In order to simplify operations, we neglect the vertical component for the time-being, then:

$$\Delta\rho_k = -Rcos(el_k)\cos(az_k-\theta)+c.\Delta B \tag{6.4}$$

Thus, the estimated code delay for satellite k for a hypothetical location $(\mathrm{R}_i,\theta_j,\Delta D_m,\Delta B_n)$ is given by:

$$\hat{\tau}_k = \frac{\left[\rho_{RS,k}+\Delta\rho_k\left(R_i,\theta_j,\Delta D_m,\Delta B_n\right)\right]_{c\cdot T_c}}{c\cdot T_c}\cdot N_{code} \tag{6.5}$$

where $\rho_{RS,k}$ and $\Delta\rho_k$ could be those of RS1 or RS2.

In order to reduce the number of candidate points in the search area, let's consider β as the maximum code phase error in chips that can be acceptable in CD process. Based on the relation between the code phase and the differential pseudorange, we have:

$$\pm\beta = \frac{\pm\Delta\rho_{err,max}}{c \cdot T_c} \cdot N_{code} = \frac{\pm\Delta\rho_{err,max}}{c \cdot T_{chip}} \tag{6.6}$$

Then, the estimated code delay can be expressed as:

$$\hat{\tau}_k = \frac{\Delta\rho_k\left(R_i, \theta_j, \Delta B_n, \beta\right)}{c \cdot T_c} \cdot N_{code} \tag{6.7}$$

Finally, if the estimated code delay can be within $\pm\beta$ chips of the true code delay, then the correlation output is expressed as:

$$D_{ind}\left(R_i, \theta_j, \Delta B_n, \beta\right) = \sum_{\tau=\hat{\tau}_k-\beta}^{\tau=\hat{\tau}_k+\beta} |S(\hat{\tau}_k)|^2 \tag{6.8}$$

CD metric is then obtained by the sum of individual detection metric for all visible satellites.

Consider the scenario of Figure 6.10 to show how the position of MS is calculated by considering the assistance of RS1 and RS2 which are located at the centers of the blue and orange circles respectively.

A mathematical model of the intersecting surface of the two horizontal search areas should be defined. The collective detection metric, which is a function of R and θ, is calculated as follows. Instead of varying R and θ over all possible values, in order to have a gain in terms of calculation number, we will proceed to:

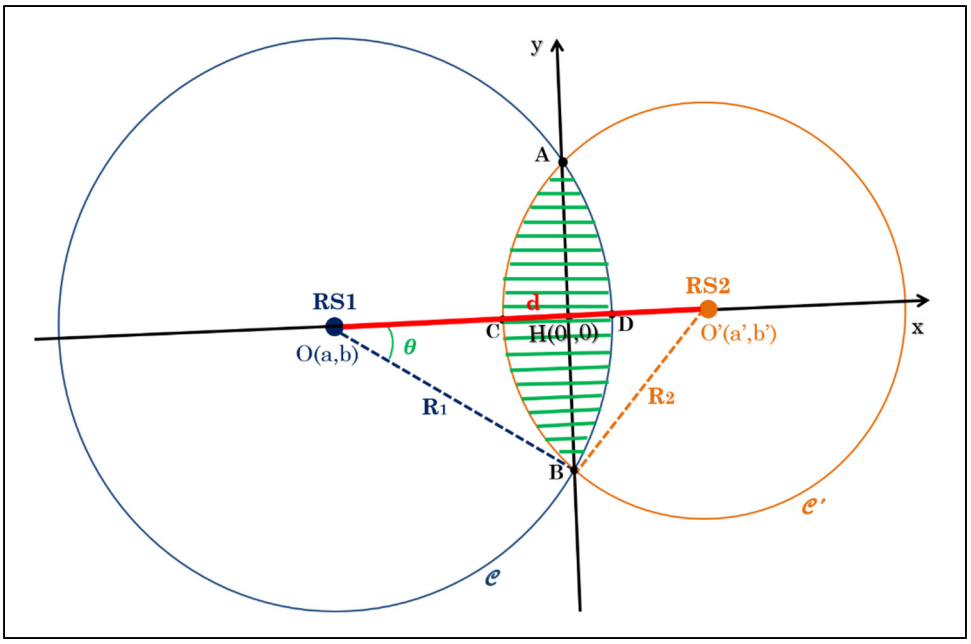

Figure 6.10 Uncertainty range reduction using two reference receivers

- R is delimited by the hatched region (ACB and ADB arcs) instead of scanning all the values of R;
- θ varies between the angle $\widehat{HOB}$ and $\widehat{HOA}$ instead of scanning all the angles in $[0,2\pi]$.

Thus, the collective detection metric should be calculated under the following conditions:

$$\begin{aligned} -C < x < D \\ -B < y < A \\ (x-a)^2 + (y-b)^2 < {R_1}^2 \\ (x-a')^2 + (y-b')^2 < {R_2}^2 \end{aligned} \tag{6.9}$$

Note that in our case: $b = 0$ and $b' = 0$. The surface of the intersection zone where the values of R and θ vary, i.e. where the search of the MS position is carried out, is equivalent to:

$$I_{RS} = {R_1}^2\cos^{-1}(({d^2} - {R_2}^2 + {R_1}^2)/2dR_1) + {R_2}^2(\cos^{-1}(({d^2} + {R_2}^2 - {R_1}^2)/2dR_2) - \tfrac{1}{2}\sqrt{([2dR_1 + ({d^2} - {R_2}^2 + {R_1}^2)][2dR_1 - ({d^2} - {R_2}^2 + {R_1}^2)])} \quad (6.10)$$

where d is the distance between RS1 and RS2.

In the case where $R_1 = R_2$, i.e. the distance between RS1 and MS is equal to that between RS2 and MS, I_{RS} becomes:

$$I_{RS} = 2{R_1}^2\cos^{-1}(d/2R_1) - \tfrac{1}{2}\, d\sqrt{(4{R_1}^2 - {d^2})} \quad (6.11)$$

Then, after performing the 1st iteration in the surface delimited I_{RS}, the 2nd and 3rd iteration is carried out using Equations 6.7 and 6.8 while reducing the uncertainty area and the resolution search grid in order to have a finer estimate. Note that the use of two reference stations is interesting only if $d \leq R_1 + R_2$. In practice, the intersection of RS1 and RS2 areas is not empty, and it means that both areas of each RS confirm that the MS is around it.

Case 2:

In the case where there are several reference receivers (*n* references), which the MS can use as suppliers estimate its position using their respective measurements. This can be done in several ways. In our case, we propose a very simple combination approach which is described as follows. The range-offset at a position separated by $(\mathrm{R}, \theta, \Delta B)$ from each RS (RS1, RS2, …, RSn) is expressed in terms of the position and the clock bias:

$$\begin{aligned} \Delta\rho_{k,1} &= -R_1 cos(el_{k,1})\cos(az_{k,1} - \theta_1) + c.\Delta B_1 \\ \Delta\rho_{k,2} &= -R_2 cos(el_{k,2})\cos(az_{k,2} - \theta_2) + c.\Delta B_2 \\ &\cdots \\ \Delta\rho_{k,n} &= -R_n cos(el_{k,n})\cos(az_{k,n} - \theta_n) + c.\Delta B_n \end{aligned} \quad (6.12)$$

Thus, the estimated code delay for satellite k for a hypothetical location $(R_i, \theta_j, \Delta D_m, \Delta B_l)$ corresponding to each RS is:

$$\begin{aligned}
\hat{\tau}_k^1 &= \frac{\left[\rho_{RS1,k} + \Delta\rho_{k,1}\left(R_i, \theta_j, \Delta D_m, \Delta B_l\right)\right]_{c \cdot T_c}}{c \cdot T_c} \cdot N_{code} \\
\hat{\tau}_k^2 &= \frac{\left[\rho_{RS2,k} + \Delta\rho_{k,2}\left(R_i, \theta_j, \Delta D_m, \Delta B_l\right)\right]_{c \cdot T_c}}{c \cdot T_c} \cdot N_{code} \\
&\cdots \\
\hat{\tau}_k^n &= \frac{\left[\rho_{RSn,k} + \Delta\rho_{k,n}\left(R_i, \theta_j, \Delta D_m, \Delta B_l\right)\right]_{c \cdot T_c}}{c \cdot T_c} \cdot N_{code}
\end{aligned} \tag{6.13}$$

So, the correlation output is function of the code delay estimated by using both RS, and is expressed as:

$$D_{ind}\left(R_i, \theta_j, \Delta B_l, \beta\right) = \sum_{\tau=\hat{\tau}_k-\beta}^{\tau=\hat{\tau}_k+\beta} \left\{ \left| \sum_{n=1}^{RS_n} S\left(\hat{\tau}_k^n, \hat{f}_{d_k}^n\right) \right|^2 \right\} \tag{6.14}$$

The CD metric is then calculated in the intersection area of all the search grid corresponding to each reference station, i.e. $S_1 \cap S_2 \cap \cdots \cap S_n$, and defined as:

$$D_{CD}\left(R_i, \theta_j, \Delta B_l, \beta\right) = \sum_k \left[\sum_{\tau=\hat{\tau}_k-\beta}^{\tau=\hat{\tau}_k+\beta} D_{ind}\left(\hat{\tau}_k^n, \hat{f}_{d_k}^n\right) \right] \tag{6.15}$$

In order to improve the results, we can also consider assigned weights for each code delay according to the better code delay estimation of each RS, w_1, w_2, …, w_n corresponding respectively to RS1, RS2, …, RSn. In this case, the code delay used for the individual detection is calculated as a function of the n calculated delays corresponding to each RS. We assign a

higher cost for RS that has more accurate code delays, i.e. which has the slightest error between the true value and the estimated value. So,

$$\hat{\tau}_k = w_1\hat{\tau}_k^1 + w_2\hat{\tau}_k^2 + \cdots + w_n\hat{\tau}_k^n \tag{6.16}$$
$$\hat{\tau}_k = \sum_{n=1}^{RS_n} w_n\hat{\tau}_k^n$$

where the values of w_n vary according to the estimated phase code for each RS, such that $\sum_{n=1}^{RS_n} w_n = 1$.

Knowing that the information coming from different reference stations may have different levels of reliability, weighting coefficients are useful to merge the estimated code delay corresponding to each RS in the individual and collective detection metrics. Thus, the weights related to the aiding quality (accuracy of code delay), inspired by (Garello et al., 2012), can be expressed as:

$$w_n(\tau) = z \cdot \frac{1}{\sigma_n(\tau)} \tag{6.17}$$

where $w_n(\tau)$ represents the proper weights for the code delay estimate corresponding to each RS, $\sigma_n(\tau)$ is the standard deviation of the estimated code delay corresponding to each RS, and the coefficient z is used to obtain a unitary sum of all weights. Indeed, according to the values of $\sigma_n(\tau)$, weighting coefficients inversely proportional to them can be used as:

$$z = 1 \Big/ \sum_{n=1}^{R_n} \frac{1}{\sigma_n(\tau)} \tag{6.18}$$

Note that the MS computes the code delay estimate corresponding to each RS (expressed in equation 6.13) and combine them during the collective acquisition (expressed in equation 6.14 and equation 6.15). The choice of the assigned weight costs may depend on several criteria on

the quality of the corresponding reference station (low cost or professional receivers, acceptable margin of error, receivers that know their position with very high precision, etc.).

In the case where the values of the code delay errors are almost the same for all reference stations, another simpler approach can be used by using constant weights while performing the arithmetic average of the code delay corresponding to all reference stations i.e. $w_n(\tau) = w = \frac{1}{n}$.

In practice, we can also assign costs according to the quality of the receivers. For example, various receivers of different ranges such as Novatel, uBlox, or smartphones are present around, the receiver having the best quality of reception can help the MS to estimate its position. Note that this example is not considered in this thesis.

6.3.2.3 Experimental results and performance analysis

According to in Table 6.4, RS1 and RS2 are in good reception condition and they are used to assist MS, which is placed in an environment where the satellite signals are very weak (7 visible satellites vs 10 visible satellites). Collective acquisition is performed by 3 iterations while refining the search space at each iteration until an accurate estimate of the MS position can be obtained as we shown in Table 6.5. Note that the real distances between the receivers are: RS1-RS2 = 816.46 m, RS1-MS = 412.03 m, and RS2-MS = 424.66 m.

Table 6.5 Parameters of CP/CD process

Item		**Rough 1st iteration**	**Medium 2nd iteration**	**Fine 3rd iteration**
Horizontal dimension	Radial Uncertainty [m]	±10000	±2922	±146
	Radial Step Size [m]	2922	292	14.6
	Angular Step size [°]	14.4	5.7	5.7
Clock Bias	Clock Bias Uncertainty [m]	±150000	±220	±22
	Clock Bias Step Size [m]	440	44	4.4

First, CD process is performed for each of RS1 and RS2 as an assistant to MS. In order to choose the best reference to be used to help the MS to roughly estimate its position, let's compare the statistical characteristics of results obtained in code phase estimation from both RS. For that, each CD algorithm is executed 100 times and a mask angle of 10° is applied. At each algorithm execution, 10 satellites are found. Table 6.6 shows the mean error and the standard deviation of the difference between the estimated code phase and the true code phase. This result makes it possible to analyze the number of correctly estimated code phases.

Table 6.6 Statistical results of the code phase during CP/CD process

SV	**RS1**		**RS2**	
	Mean error [m]	**Std. Dev. [m]**	**Mean error [m]**	**Std. Dev. [m]**
PRN 2	2.50	1.33	2.80	1.47
PRN 3	3.70	2.00	3.90	2.17
PRN 4	2.40	1.74	2.30	1.64
PRN 10	4.30	2.31	3.90	2.13
PRN 11	2.50	0.89	2.70	0.79
PRN 13	3.20	2.99	3.20	3.05
PRN 16	2.70	2.58	2.70	2.66
PRN 20	3.20	1.28	3.70	1.85
PRN 23	3.90	3.13	4.50	3.21
PRN 31	1.50	0.95	1.80	0.84
Mean value	2.99	1.92	3.15	1.98

The goal is to show whether the presence of two reference stations to help calculate the user's position is beneficial in the practical case. To do this, the two ways (case 1 and case 2), presented in Section 6.3.2.2, can be used. So, if we compare the statistical results of the parameters received by each reference, it can be seen from Table 6.6 that RS1 provides good results compared to RS2. In this case, RS2 is used only to determine the search area reduced

at the intersection of RS1 and RS2. Then, RS1 sends its position and ephemeris to the MS so that it can calculate its position. By performing the CD process, the results of the iterative method are illustrated in Figure 6.11 in which the resolution and the uncertainty are reduced at each iteration.

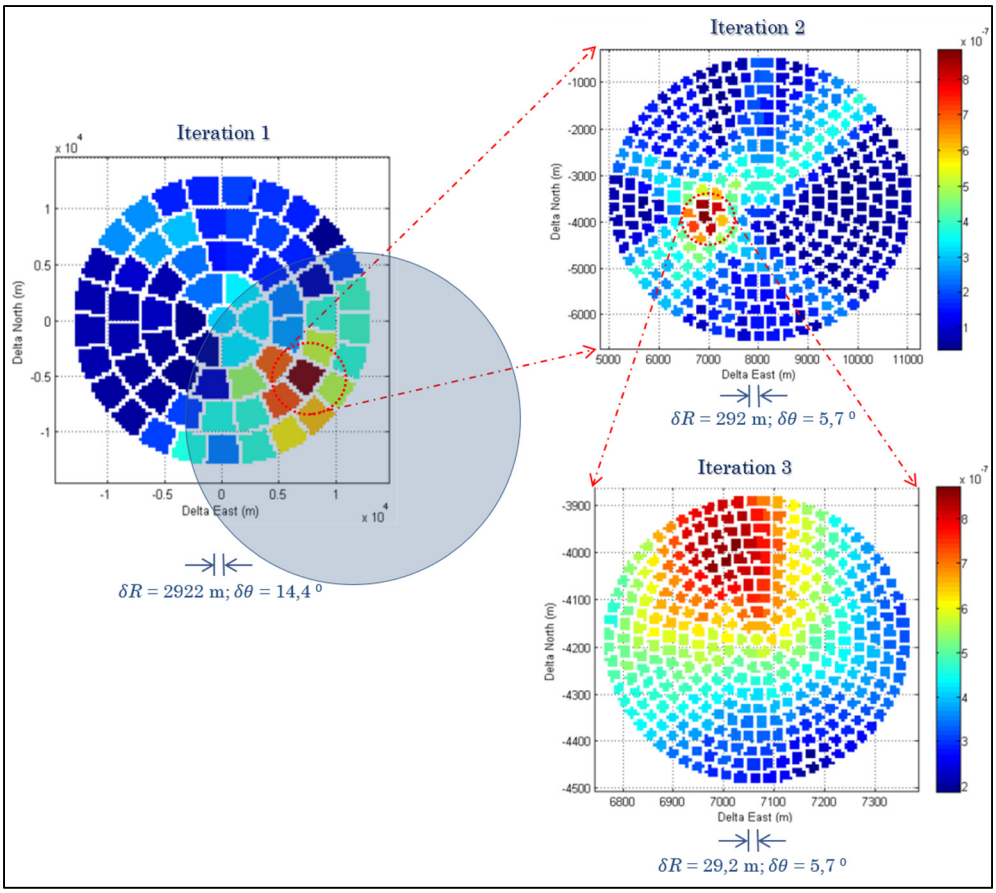

Figure 6.11 Application of CD with 2 RS as a CP approach

To analyze the performances of the developed techniques, we will compare two algorithms in terms of sensitivity, complexity and accuracy. Knowing that RS1 is the best reference station, the two algorithms are: “CP/CD with RS1-RS2 in 1st iteration and RS1 (i.e. best RS) in the last two iterations”, called “CP/CD-RS1-RS2”; and “CD with RS1 (i.e. best RS) during three iterations”, called “CD-RS1”.

CP/CD sensitivity analysis

Comparing the probability of detection in function of C/N_0 level between the algorithms of "CP/CD-RS1-RS2" and "CD-RS1", both algorithms have the same sensitivity performance. The sensitivity is almost the same since we use the two RS measurements in the first iteration only, which corresponds to a large resolution of R and θ as well as the clock-bias. Using two or more references does not affect enough the sensitivity of the receiver considering the case 2 proposed in this work, i.e. the reference stations are only used in the first iteration in order to reduce the uncertainty area to search the candidate points, then a single reference (the best) is used for the last 2 iterations.

CP/CD complexity analysis

As we have seen in Section 6.3.2.2, it is quite normal that the search area of the candidate points in the positional domain decreases considerably by using two or more reference stations. In the horizontal dimension, we observe at the first iteration a reduction of 2.03 times of the number of scanned points using the algorithm of "CP/CD-RS1-RS2" compared to the algorithm of "CD-RS1". Indeed, there are 21142 points to scan unlike the 42966 points in "CD-RS1". There is the same number of candidate points for the second and third iterations (3390 points). Taking into account the clock-bias, there are a total of 27922 points to scan, i.e. a much smaller number compared to 52030 points in "CD-RS1".

CP/CD accuracy analysis

If we compare "CP/CD-RS1-RS2" and "CD-RS1", there is no difference in accuracy performance since both algorithms use the same parameters for the resolution of R, θ and clock-bias as described in Table 6.5. With a smaller resolution at the 3rd iteration, a smaller horizontal positioning error (HPE) is obtained compared to another work in literature such as (Cheong, 2012) that is a good reference since it is part of the first detailed work on the CD approach. So, the resulting HPE of MS is 13.97 m (50 %) and 22.36 m (95 %) with a GDOP of 1.5. Result

values correspond to the position solution achieved 50 % and 95 % of the time using 1 ms of data in 1000 acquisitions. Note that the fact of having a good precision with respect to (Cheong, 2012) is not due to the technique of CP/CD itself but rather to the approach already proposed in (Andrianarison, Sahmoudi et Landry, 2017). Figure 6.12 represents the CD mean positioning error of the CD process with RS1 and the one in (Axelrad et al., 2011).

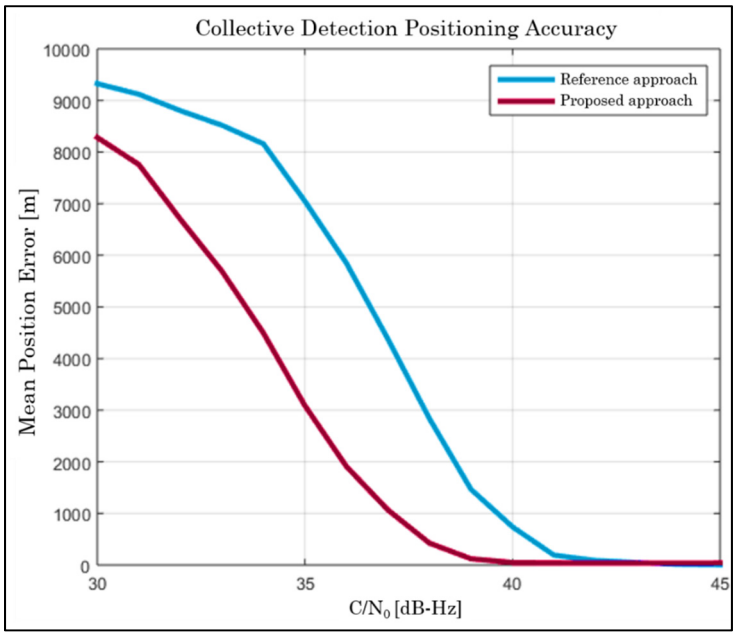

Figure 6.12 Comparison of CD positioning accuracy with RS1 as reference (10 satellites)

6.3.3 Application 2: Exploitation of best satellites

In this proposal, the receiver that is in good reception condition sends its data (position, pseudorange, ephemerides) to the other receivers in difficulty to allow them to estimate their positions. Costs will be allocated to the visible satellites in order to be able to optimally choose the best receiver chosen as a reference station. The new cognitive CD algorithm will be able to choose intelligently the best satellites. Finally, to calculate the position, the CD metric will be calculated as a function of time and Doppler. More precisely, the direct positioning algorithm is used to estimate the position according to the best chosen satellites, since in the case of a pure CD, all the available satellites are used. In fact, the algorithm consists of the

optimal use of the best satellites to take advantage of the CD's capability to increase sensitivity with fewer satellites and at the same time reduce the complexity of the operation as shown in Figure 6.14.

6.3.3.1 Influence of key parameters on CD positioning ambiguity

Knowing that the developed algorithm will be able to operate the receiver optimally according to the various parameters considered in choosing the best satellites or the selection of the best reference stations to assist the user, the influence of some parameters on the CD positioning ambiguity is shown in Figure 6.13. In this example, we compare the 3D correlogram by calculating the CD metrics corresponding to 6 best satellites and 10 satellites (all visible satellites) by varying some parameters (C/N_0, elevation mask angle, GDOP). It is based on the presence of 3 strong signals and the remaining satellites are weak to justify the use of the CD approach instead of the conventional acquisition. So, 3 weak + 3 strong for 6 best satellites and 7 weak + 3 strong for 10 satellites. Weak signals correspond to the strongest signals below the set threshold. And strong signals correspond to the strongest signals among all visible satellites.

According to the curves in Figure 6.13, we can see that the positioning ambiguity varies according to the change of certain parameters. For example, the position solution becomes less accurate when the mask angle increases. Similarly, the position error becomes larger when the geometrical configuration is poor. Moreover, it should be noted that, for the same parameters, the curves corresponding to the 6 best satellites and 10 satellites are approximately the same, i.e. do not present a great difference. Thus, we can deduce that using the best satellites may be sufficient to process the position solution instead of performing a process on all visible satellites, which can reduce the required computational burden.

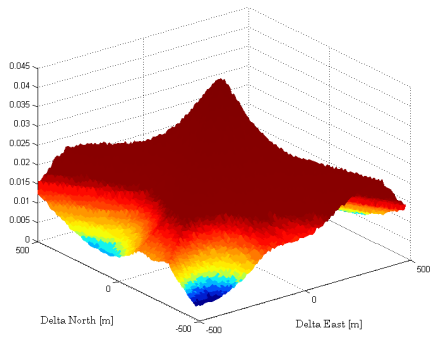

(a) 6 satellites, mask = 10º, GDOP = 1

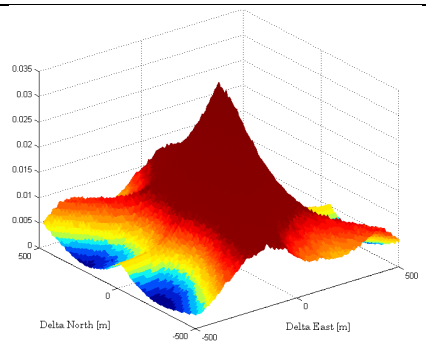

(b) 10 satellites, mask = 10º, GDOP = 1

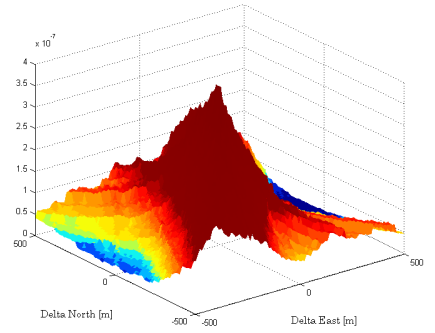

(c) 6 satellites, mask = 10º, GDOP = 2.5

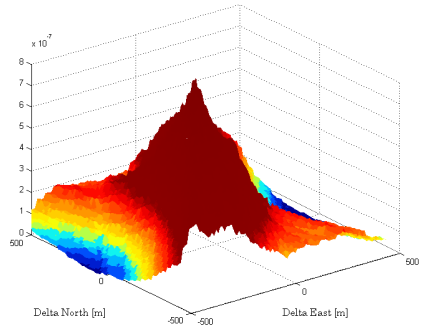

(d) 10 satellites, mask = 10º, GDOP = 2.5

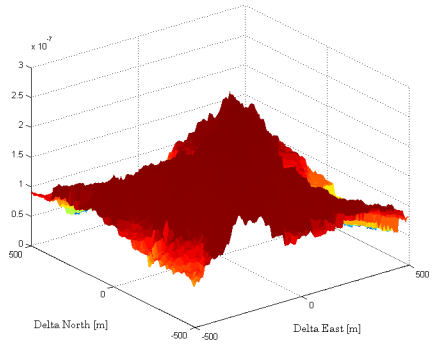

(e) 6 satellites, mask = 30º, GDOP = 2.5

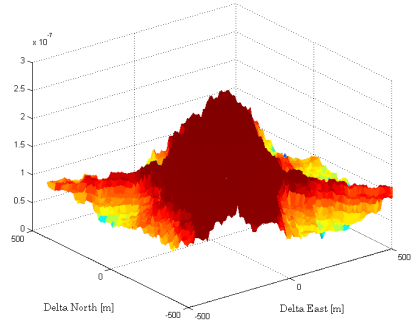

(f) 10 satellites, mask = 30º, GDOP = 2.5

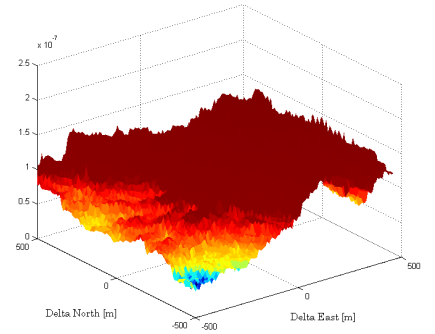

(g) 6 satellites, mask = 30º, GDOP = 10

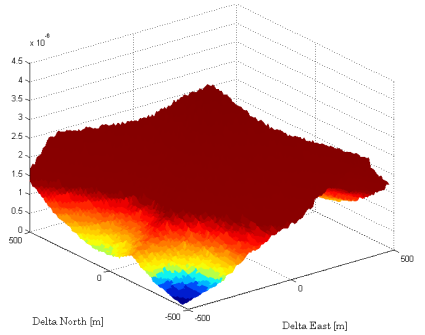

(h) 10 satellites, mask = 30º, GDOP = 10

Figure 6.13 Influence on CD positioning ambiguity

6.3.3.2 New metrics of CD with optimal weighting satellites

In this application idea, the CD algorithm is optimized by intelligently choosing the best satellites in the direct positioning technique instead of all visible satellites to reduce the number of computations. To implement this idea, the CD algorithm is based on several parameters, the most important of which are the C/N_0 level, the elevation angle and the satellites forming the best DOP.

To obtain a better performance of the algorithm, with these parameters taken into account in the selection of the best satellites in the CD process, we will also estimate the Doppler frequency using the SPL technique with the delta correction in the detection metric individual, then the correlation output is expressed as:

$$D_{ind}\left(\hat{\tau}_{k_{bs}}, \hat{f}_{d_{k_{bs}}}\right) = \left|S_{\delta}\left(\hat{\tau}_{k_{bs}}, \hat{f}_{d}\right)\right|^2 \tag{6.19}$$

where k_{bs} represents some satellites selected by the algorithm, which are considered the best (according to C/N_0 level, elevation angle and forming better DOP), but not all visible satellites.

CD metric is then obtained by the sum of the correlations of some satellites selected by the algorithm as the best satellites. So,

$$D_{CD}\left(R_i, \theta_j, \Delta B_l, \beta\right) = \sum_{k_{bs}} D_{ind}\left(\hat{\tau}_{k_{bs}}, \hat{f}_{d_{k_{bs}}}\right) \tag{6.20}$$

where D_{CD} is calculated by the sum of the correlations of all satellites selected by the algorithm, which are considered the best (satellites with higher C/N_0 and with higher elevation angles, and in some cases satellites forming the best GDOP), but not all visible satellites. That is why we have the k_{bs} index with the sum operator, which refers to the best satellites.

Briefly, the smart CD algorithm involves an optimization method allowing the use of the best satellites as follows:

1) For each RS that can assist the user:
   a) Get the elevations and azimuths of all satellites in view and sort them with their elevations in ascending order;
   b) Select the better satellites with higher C/N_0 :

      It is necessary to choose a certain value as a threshold for the selection of strong and weak satellites. For example, we can choose the nominal value of 45 dB-Hz as the threshold value. This can be changed according to the objectives set for the receiver design;
   c) Select the best satellites with higher elevation angles :

      It is necessary to choose a certain value as a threshold for the selection of satellites as good or bad according to their angle of elevation. To have good satellites, the threshold can be set at 10°, i.e. exclude satellites with elevation lower than 10°, even it is very common to define an elevation mask of 5°. The algorithm will just choose the satellites having the best angles, i.e. which have the highest angles.
2) Assign weights to each satellite in view corresponding to both parameters, $z_{1,k}$ for C/N_0 and $z_{2,k}$ for the elevation angle.
3) Compute the cost function according to assigned weights and select the best satellites.

   If the satellites selected by each RS have the same parameters by calculating the cost function, then select the satellites that make up the best GDOP among the satellites, i.e. look up the optimal geometry according to the number of available satellites.
4) Choose the best RS, which has optimal results, among the available RS which can assist the MS. If all RS have the same costs (almost impossible in reality), choose one RS randomly.

   Otherwise, an interesting alternative is to combine the measurements of all RSs in the calculation of individual and collective detection metrics to estimate the user position.
5) Send assistance data from the best RS or from both RS according to step 4.
6) Perform CD process:

- Correlation as a function of code phase and Doppler estimated by SPL method with delta correction;
- Based on polar coordinates in 2 or 3 iterations;
- CD metric is calculated as the sum of the best satellites chosen in step 1, 2 and 3, while combining measurements from all RS.

7) Estimate the user MS position.

This description of the best satellite selection algorithm applied in the CD process is shown in Figure 6.14.

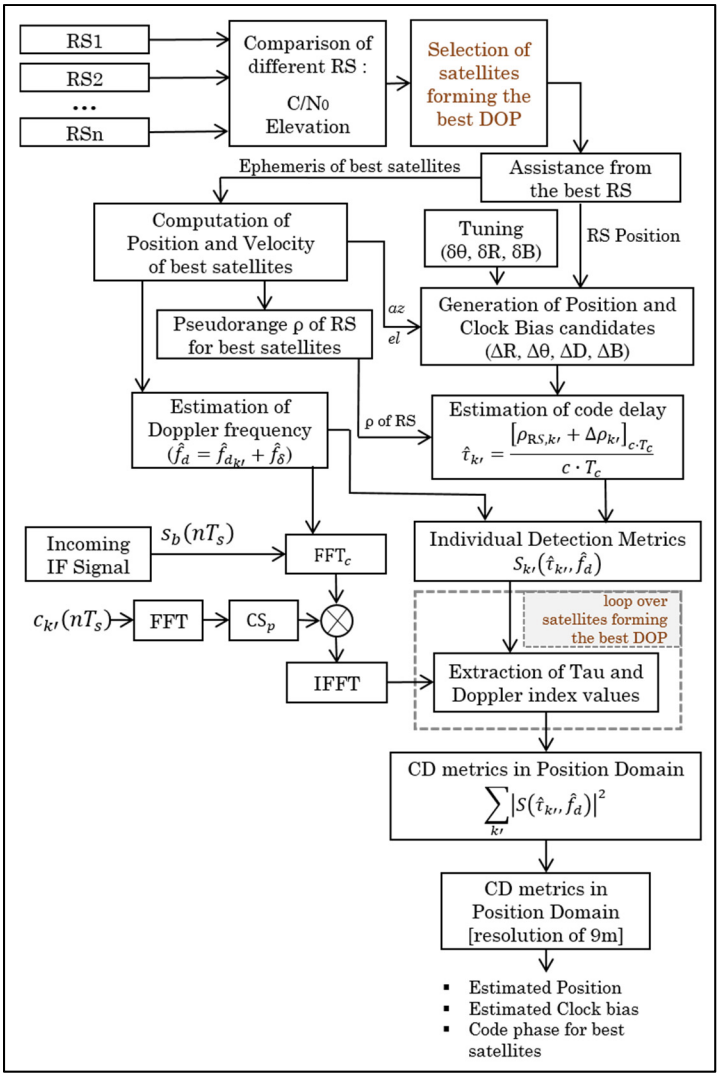

Figure 6.14 Flow chart of proposed smart cooperative positioning using CD

To select the best RS having better parameters, the decision-making process is multi-objective oriented where the cost functions help making the decision and it is modeled as:

$$\max\{y\} = f(\bar{z}) = \left[f\left(\bar{z}_{1,k}\right), f\left(\bar{z}_{2,k}\right)\right] \tag{6.21}$$

where $\bar{z}_{1,k} = \left(z_{1,1}, z_{1,2}, \dots, z_{1,k}\right) \in Z_1$ correspond to the C/N_0 for all satellites in view and $\bar{z}_{2,k} = \left(z_{2,1}, z_{2,2}, \dots, z_{2,k}\right) \in Z_2$ correspond to the elevation angle for all visible satellites; and $\bar{y} = (y_1, y_2, \dots, y_n) \in Y$ correspond to the step 3 and 4 of the above procedure.

In case we need to use more than one reference station, we can merge the measurements obtained from the different RS and then calculate the metrics for individual and metric detection of CD as follows:

$$D_{ind}\left(R_i, \theta_j, \Delta B_l\right) = \sum_{n=1}^{RS_n} w_n \left|S_\delta\left(\hat{\tau}_k^n, \hat{f}_{d_k}^n\right)\right|^2 \tag{6.22}$$

where n represents the number of reference station, $w_n = f(\bar{z})$ represents the weight of each RS corresponding to its parameters such as:

$$w_n[(C/N_0)_k, el_k] = w_{n,1}[(C/N_0)_k] w_{n,2}(el_k) \tag{6.23}$$

For C/N_0, weighting cost is calculated as:

$$w_n(x) = \begin{cases} 10^{\frac{x-45}{\alpha}} \left(\left(V_f \times 10^{\frac{P-45}{\alpha}} - 1 \right) \dfrac{x-45}{P-45} + 1 \right)^{-1}, & x < 45 \text{ dBHz} \\ 1, & x \geq 45 \text{ dBHz} \end{cases} \tag{6.24}$$

where x represents the value of C/N_0 [dB-Hz], α is a parameter to adjust the curve of the weighting function $w_n(C/N_0)$ as defined in (Lesouple et al., 2017), V_f controls the value of

the weighting function w_n for $x = P$, i.e. $w_n(P) = \frac{1}{V_f}$, P is the value of C/N_0 for which the weighting function w_n is forced in order to obtain the weight defined by parameter V_f, and γ is the threshold value is defined (step 1) a) of the algorithm description). According to (Lesouple et al., 2017), the optimal values obtained for the different parameters of the function w_n are: $(\alpha, V_f, P) = (80, 30, 20)$.

The second criteria is the satellite selection method based on maximal elevation angle during the observation period. For the elevation angle parameter, the weighting function is defined as (Lesouple et al., 2017):

$$w_n(x) = \begin{cases} \dfrac{\sin^2(x)}{\sin^2(10^\circ)}, & x < 10^\circ \\ 1 \quad , & x \geq 10^\circ \end{cases} \tag{6.25}$$

where x represents the value of elevation angle [°].

According to step 3 in the best satellite selection algorithm, if the satellites selected by each RS have the same parameters by calculating the cost function, then select the satellites that make up the best GDOP among the selected satellites as:

$$\min\{\mathrm{GDOP}(x)\} \leq 6 \tag{6.26}$$

Finally, the collective detection metric can be expressed in function of the best satellites as:

$$D_{CD}(\mathrm{R}_i, \theta_j, \Delta B_n) = \sum_{k_{bs}} D_{ind}\left(\hat{\tau}^n_{k_{bs}}, \hat{f}^n_{d_{k_{bs}}}\right) = \sum_{k_{bs}} \left\{ \sum_{n=1}^{RS_n} w_n \left| S_\delta\left(\hat{\tau}^n_k, \hat{f}^n_{d_k}\right) \right|^2 \right\} \tag{6.27}$$

where k_{bs} represents the number of the best satellites, and $\hat{\tau}^n_{k_{bs}}$ represent the estimated code delay corresponding to the best satellites k_{bs} for a hypothetical location $(\mathrm{R}_i, \theta_j, \Delta D_m, \Delta B_l)$ w.r.t each RS.

Thus, the acquisition problem is to search for the optimal vector $X = (R, \theta, \Delta B)$ in the search space $R \in [0\ m, 10000\ m]$, $\theta \in [0°, 360°]$, and $\Delta B \in [-150000\ m, 150000\ m]$ which maximizes the criterion function:

$$\begin{aligned} J &= \mathrm{fun}\left(D_{CD}\left(\mathrm{R}_i, \theta_j, \Delta B_l\right)\right) \\ &= \mathrm{fun}\left(\sum_{k_{bs}} D_{ind}\left(\hat{\tau}^n_{k_{bs}}, \hat{f}^n_{d_{k_{bs}}}\right)\right) \\ &= \mathrm{fun}\left(\sum_{k_{bs}} \sum_{n=1}^{RS_n} w_n \left|S_\delta\left(\hat{\tau}^n_{k_{bs}}, \hat{f}^n_{d_{k_{bs}}}\right)\right|^2\right) \end{aligned} \tag{6.28}$$

where « *fun* » is an increasing function in which the decision of detection is made with the surpass of a threshold determined by a pre-defined false-alarm probability.

6.3.3.3 Tests results and analysis

In the practical case, the measurements of RS1 and RS2 are almost identical if they are close to each other. The idea is that the CD algorithm is able to choose the best RS using the best satellites to optimize the CD process while reducing complexity with fewer satellites. Two criteria are used to choose which of RS1 and RS2 will be used to assist MS: C/N_0 and elevation angle.

In equation 6.24 and equation 6.25, the thresholds used for C/N_0 and elevation angle are 45 dB-Hz and 10°, respectively. Tests performed using the setup in Figure 6.5 and Figure 6.6 gave us: 11 satellites are received by RS1 and RS2 (PRN 1, PRN 3, PRN 6, PRN 11, PRN 17, PRN 18, PRN 19, PRN 22, PRN 24, PRN 28, PRN 30) and 9 satellites are received by MS (PRN 1, PRN

3, PRN 6, PRN 11, PRN 17, PRN 19, PRN 22, PRN 28, PRN 30). On the 11 visible satellites, 7 satellites received by RS1 are stronger than those received by RS2 (PRN 1, PRN 6, PRN 11, PRN 17, PRN 18, PRN 22, PRN 28), 1 satellite received by RS1 is weaker than those received by RS2 (PRN 30), and the remains have the same C/N_0 level. This means that the satellites received by RS1 are stronger than those received by RS2 in terms of C/N_0. Then, among these 7 strong satellites received by RS1, there are 6 satellites which have elevation angles lower than those of RS2 (PRN 1, PRN 6, PRN 11, PRN 17, PRN 22, PRN 28). This leads to the logical choice of RS1 as an assistant to MS in the smart CD algorithm.

In this case, since we have been able to distinguish the satellites to be taken according to the key parameters, we do not need to see which satellites form the best GDOP among those chosen. In addition we have a single satellite at more than 45 dB-Hz (strong) and the remaining satellites are considered weak satellites. Hence, based on the principle of CD, the algorithm will not be limited to the minimum of satellites, but will extend to use the best possible satellites.

To properly analyze the impact of using the best satellites or the best RS in the CD algorithm, compare the following 4 functions and evaluate the performance in terms of sensitivity, complexity, and accuracy:

1) CD in function of best satellites and best RS “CD/Best_Sat/Best_RS”,
2) CD in function of best satellites and all RS “CD/Best_Sat/All_RS”,
3) CD in function of all visible satellites and best RS “CD/All_Sat/Best_RS”, and
4) CD in function of all visible satellites and all RS “CD/All_Sat/All_RS”.

For the CD process using the best RS and/or the best satellites, the algorithm described in Section 6.3.3.2 is used. In cases where all RSs are used, the CD algorithm described in equation 6.27 is used, in which the measurements of RS1 and RS2 are combined in the CD algorithm. The best RS is RS1, the best satellites are: PRN 1, PRN 6, PRN 11, PRN 17, PRN 22, PRN 28; and all visible satellites are: PRN 1, PRN 3, PRN 6, PRN 11, PRN 17, PRN 19, PRN 22, PRN 28, PRN 30.

Smart CD sensitivity analysis

SPL with delta correction technique is used for Doppler estimation in all 4 CD algorithms described previously. Knowing that the CD is advantageous if we have as many satellites as possible, but we will compare if there is a big difference between the operation of the best satellites and the exploitation of all available satellites. Considering the previous analysis, the algorithm will compute the CD metric using 6 satellites (best satellites) instead of 9 satellites (all visible satellites). Figure 6.15 shows the comparison of the sensitivity analysis curves of all 4 CD algorithms: "CD/Best_Sat/Best_RS" (6 satellites/RS1), "CD/Best_Sat/All_RS" (6 satellites/RS1-RS2), "CD/All_Sat/Best_RS" (9 satellites/RS1) and "CD/All_Sat/All_RS" (9 satellites/RS1-RS2).

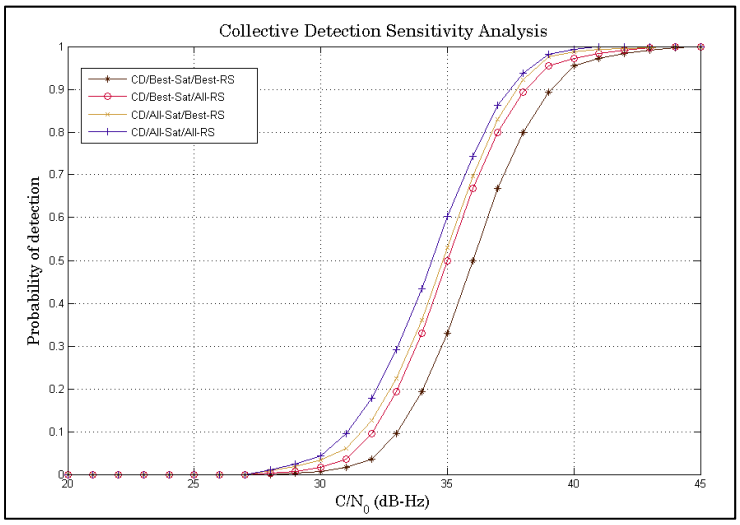

Figure 6.15 Sensitivity performance comparison between all 4 CD algorithms

It can be seen that the "CD/All_Sat/All_RS" algorithm is the best algorithm in terms of sensitivity. The idea of combining all available satellites is the basic principle of the CD approach to increase sensitivity as much as possible. The algorithms of "CD/Best_Sat/All_RS" and "CD/All_Sat/Best_RS" have almost the same performance. "CD/Best_Sat/Best_RS" has the lowest performance among all the algorithms (-2 dB-Hz compared to "CD/All_Sat/All_RS"). This is due to the use of some selected satellites instead of all available

satellites. On the other hand, the difference between “CD/All_Sat/All_RS” and “CD/Best_Sat/All_RS” is not very remarkable, which could be interesting if we look at the compromise between sensitivity (±0.7 dB-Hz) and complexity (9 satellites vs 6 satellites). Thus, using the best satellites makes it possible to have a reasonable sensitivity performance whereas there is a gain in complexity since there is less computation, which makes this proposed strategy interesting.

To better analyze the sensitivity performance of the all CD algorithms and to demonstrate these discussions, it is also important to see the ratio between the maximum peak and the average of the remaining peaks for each detected satellite. It is shown in Figure 6.16.

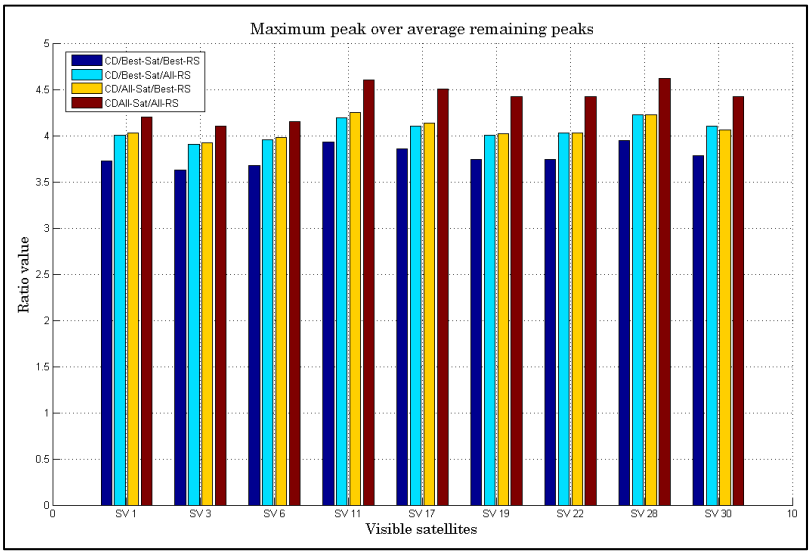

Figure 6.16 Ratio of maximum peak/average of remaining peaks of all 4 CD algorithms

Curves in Figure 6.16 show the better performance using all the satellites (the basic idea of CD) and combine the two RS compared to other algorithms. We can also notice that the algorithms of “CD/Best_Sat/All_RS” and “CD/All_Sat/Best_RS” have almost the same performance. We can even see that “CD/Best_Sat/All_RS” is better than “CD/All_Sat/Best_RS” for PRN 30, which may be due to the fact that RS2 receives a higher signal power than RS1 even if the difference is smaller.

To better choose the right algorithm, complexity is a very important performance metric that needs to be studied.

Smart CD complexity analysis

According to the CD process parameters in Table 6.5, there are 42142 candidate points in the execution of the "CD/All_Sat/All_RS" algorithm. The CD algorithm takes 2880 ms to execute the acquisition process of 20 code periods to process all satellites in view (9 satellites) and combining the RS1 and RS2 measurements whereas 1860 ms to process all satellites in view with only RS1 measurement (best RS). For "CD/Best_Sat/All_RS" algorithm, the execution time takes 1920 ms whereas 1240 ms if RS1 only is used. We can see that the execution of "CD/Best_Sat/All_RS" algorithm is 1.5 times faster than "CD/All_Sat/All_RS". Table 6.7 shows some overall conclusion of the performance of algorithms based on the criteria used.

Table 6.7 Parameters of CD process

Sat / **RS**	**Best RS**	**All RS**
Best Satellites	less sensitive less complex	less sensitive more complex
All Satellites	more sensitive less complex	more sensitive more complex

To better see the tradeoff between these two important performance metrics, Figure 6.17 shows the 4 CD algorithms compared in this study. The choice to use all visible satellites or to select the best ones as well as all the reference stations or the best one depends on the desired application. Here we can choose to use the best satellites while combining all reference stations that meets the criterion "not very complex but allows to have a good sensitivity".

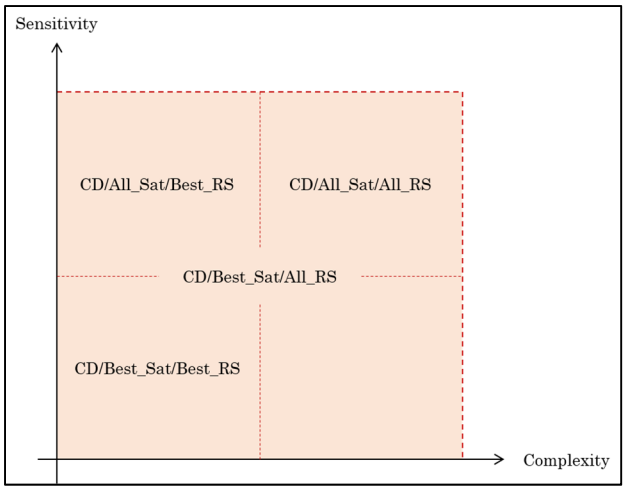

Figure 6.17 Compromise Sensitivity-Complexity of all 4 CD algorithms

Smart CD accuracy analysis

Apart from the complexity and sensitivity, the performance of the 4 CD algorithms in terms of accuracy has to be analyzed. To illustrate the benefit of using best satellites instead of all satellites in view (complexity vs sensitivity), let's compare the cumulative horizontal positioning error (HPE) of each CD algorithm, as shown in Figure 6.18.

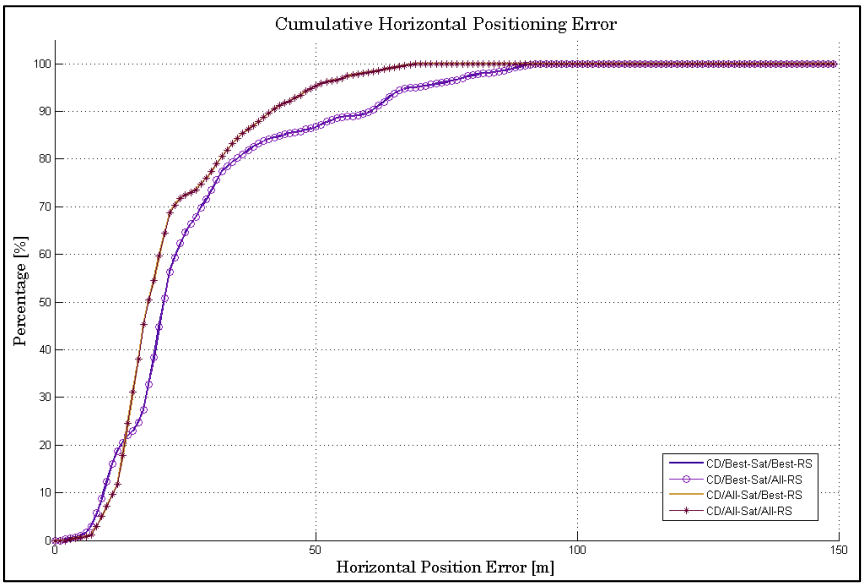

Figure 6.18 Comparison of HPE between the 4 CD algorithms

By observing these curves, we can see that the fact of combining 2 reference stations in the CD process has no impact on accuracy. We can see that the CD algorithm using all visible satellites has less positioning error than the others. Despite this, there is no significant difference between the HPE using only 6 best satellites and 9 satellites (all satellites in view). This can be explained by the low influence of the weak signals exploitation, which come to collaborate to the collective detection metrics.

We can deduce from this that we can limit the processing to only 6 satellites in order to minimize the computational load, with the goal being to use the minimum possible number of satellites while retaining a precise positional solution. The motivation idea is to carry out the minimum of calculations while retaining a good margin of precision of position.

6.4 Summary

This chapter has been devoted to the proposal and development of architectures of high sensitivity as a cooperative GNSS positioning while designing new algorithms integrated in a hybrid GNSS receiver capable of operating in deep urban environments. In order to achieve the objectives of GNSS receiver design (availability, integrity, accuracy and electromagnetic vulnerability), the smart module proposed in this work allows an optimal selection of the best signal processing technique to use. The idea is to allow the receiver to process the received signal according to certain parameters: number of visible satellites, received signal level, elevation angle, geometric configuration of available satellites, navigation environment, etc. This module contains only the intelligent algorithm for selecting the best technique to use, namely, conventional HS-GNSS acquisition method or CD approach, while exploiting the best reference station for assistance and processing the best satellites.

We have seen how the receiver processes the satellite signals according to the environment in which it is located, and it works optimally according to certain parameters or w.r.t its internal state. Indeed, if the receiver is in good receiving conditions, it operates as a standard HS receiver with basic HS techniques, otherwise the receiver switches to assisted mode using the

best satellites and the best(s) reference station(s). In assisted mode where the CD approach is used, the correct combination of the correlation values of several satellites can reduce the required C/N_0 level of the satellite signals that cannot be acquired individually but contribute constructively to a collective positioning solution. This work helps reduce costs associated with the installation of additional positioning equipment in GNSS challenging environments.

The principle of CR technology is not studied in depth in this thesis. For example, the faculty of learning that the receiver can do is not even addressed. The idea of using CR technology was to propose an adaptable architecture design and possible cognitive functioning for a high sensitivity GNSS receiver. The results presented in this chapter show the efficiency of the optimal exploitation of the navigation parameters.

From the different obtained results, we can deduce that using the best satellites while combining all reference stations measurements may be sufficient to process the position solution instead of performing a process on all visible satellites. It can reduce the required computational burden (1.5 time faster) and at the same time have a good receiver sensitivity (loss of ±0.7 dB-Hz), and also stay in a good margin of positioning accuracy. Indeed, this can reduce the complexity of implementation, but especially, it can minimize the energy consumption as part of a multi-GNSS receiver where tens of signals are present in the receiver antenna.

It has been shown that the CP is a viable solution if a ‘neighbourhood’ of users is positioned together and one of them is in good condition to receiver GNSS signal and help the other one to estimates its position, as it increases the accuracy, integrity, availability, and continuity of the PNT information for all users in challenging environments. Internet of Things (IoT) technology will also accelerate this possibility in the future.

The choice of the assigned weight costs may depend on several criteria on the quality of the corresponding reference receiver (low cost or professional receivers, acceptable margin of error, receivers that know their position with very high precision, etc.).

CONCLUSION

Innovation has always been the heart of GNSS, which continues to evolve with the coming of new satellite navigation Galileo and BeiDou systems and the modernization of GPS and GLONASS systems, with new satellites, new frequencies and modern signals that are making their appearance. Due to this modernization and the growing interest in navigation and positioning in challenging environments, the development of techniques and methods for weak GNSS signal processing is on the rise. Significant techniques and technologies making mobile phones capable of determining their position have been developed recently in positioning and navigation research field. And it is in this direction that this thesis has been carried out. The studies carried out in this thesis have focused on the acquisition process, which is one of the most difficult part of the signal processing chain within a GNSS receiver. To achieve the objectives set in this thesis, here is the summary of the different works carried out as well as the developed contributions.

The limitations on the reception of satellite signals in difficult environments have been introduced in CHAPTER 1. The characteristics of the GNSS signals (current and future) of the various constellations as well as the basic operations of a GNSS receiver have been presented in CHAPTER 2. The basic principles of acquisition of GNSS signals as well as the different acquisition methods are discussed in CHAPTER 3. Then, the various high sensitivity techniques for processing low-power satellite signals with their limitations have been described in CHAPTER 4. Similarly, architectures of HS-GNSS receivers have been presented. Several HS techniques have been proposed by researchers to solve the problem of research on positioning in difficult environments, but these techniques all have their limitations.

Thus, the last two chapters present our proposals of techniques and methods to overcome these problems of positioning in environments where the received signals are very weak. The major contributions of this thesis are summarized as follows.

CHAPTER 5 presents the developed Collective Detection approach, starting with the basic principles and then the different contributions are developed such as:

- **Section 5.4***:* Use of a mobile reference station instead of a fixed reference station as in all studies on CD approach. In this work, it can be demonstrated that we are not limited with a static reference station and it is possible for a mobile receiver in challenging reception condition to get help from another mobile station or other cooperative user in a good reception situation.
- **Section 5.5***:* Use of an IGS station in the CD approach. The idea consists in calculating the user mobile position based on reference points that exist somewhere as a network reference point with a known position. Knowing that there is a network of over 350 continuously operating dual-frequency GPS stations in the world, we do not have the constraint of using our own reference station in areas where there is IGS stations.
- **Section 5.6***:* Computation of CD metrics in function of both the code phase and the Doppler frequency for all satellites in view by applying an efficient technique to estimate the Doppler frequency. The idea consists of applying the Spectral Peak Location delta-correction technique within the CD algorithm. The proposed algorithm allows improving the accuracy of the Doppler estimation through FFT, and therefore enhancing the correlation energy.
- **Section 5.7***:* A new hybrid CD scheme with sequential acquisition method. This method reduces the complexity without compromising the sensitivity of CD while hybridizing the standard correlation approach with the CD in a multi-stages method with different code delay and position resolution.
- **Section 5.8**: Improved EITHSCD (Efficient and Innovative Techniques for High Sensitivity Collective Detection) scheme. The method consists of hybridizing the CD approach with some correlation techniques and coupling it with SPL delta-correction technique for Doppler frequency estimate. A new CD scheme with less computational load has been proposed in order to accelerate the detection and location process. HS acquisition techniques using long coherent integration and non-coherent integration have been used in order to improve the performance of the proposed EITHSCD algorithm. Its ability to combine high sensitivity and low complexity has been proven.

CHAPTER 6 presented the proposed design and architecture of the high sensitivity cognitive GNSS receiver. The cognitive functioning of the receiver has brought some contributions such as:

- **Section 6.2.5***:* The application of the cognitive radio technology to navigation and GNSS positioning in order to make the receiver more intelligent has been developed. The architecture of the new high sensitivity cognitive GNSS receiver has been proposed. This work treats the exploitation of the best satellites and the working environment by the receiver in order to achieve a certain level of intelligence and making it capable of operating even in harsh environments like indoor.
- **Section 6.3.2**: CD approach as a Cooperative Positioning. The idea consists in showing how to use the CD approach to deal with the concept of collaborative or cooperative positioning. In CP concept, a network of GNSS receivers which are interconnected may collectively receive any available satellite signals, and each receiver can receive signal measurements from other receivers via a communication link. We developed new techniques allowing a receiver in deep urban environment to locate using the CD approach while overcoming its complexity problem. The idea consists in applying the CD method in the case of two or more receivers to assist a receiver in a difficult situation.
- **Section 6.3.3**: Smart CP algorithm. The idea is to propose an algorithm which consists in choosing one receiver (or more) from several connected receivers to be a reference station to assist the other receivers in difficulty, as smart cooperative navigation. New metrics of CD with optimal weighting of visible satellites are exploited. Analyze of optimization method in order to use better satellites in CD process according to some defined parameters (elevation angle, C/N_0, satellites forming the best DOP, etc.) is carried out.

The application of the solutions proposed in this chapter makes it possible to reduce costs associated with the installation of additional positioning equipment in GNSS denied environments.

All the techniques proposed in this thesis have been analyzed and their performance assessed by real tests and simulations in order to evaluate their gain in terms of sensitivity, complexity and accuracy (positioning error).

Here are two essential issues on the current GNSS receivers with the use of cellular devices that have not been treated in this thesis but still need to be made explicit.

In some applications, the alternate reference station can be in a condition of high mobility and reception of multipaths. In this case, there are several techniques for reducing the effect of multipaths at the receiver level, measurements level and by hybridization with other sensors. The effect of multipath is not a real problem for the Collective Detection approach as we are in acquisition mode and the precision we are looking for is of the order of a few meters. On the contrary, the reception of the multipaths can simplify the detection of the global peak in the position domain by accumulating more energy of the signals being processed.

The quality of the front end (the hardware part) is an important factor in the sensitivity of the receiver and the antenna. However, my thesis work focuses on the processing of strongly degraded signals by the environment or the reception equipment itself (poor antenna and front-end quality). Indeed, this thesis work can be applied very well to low-cost receivers: the more the couple "front-end/antenna" is of bad sensitivity, the more the adoption of CD approach is beneficial. Unfortunately, the quantification of the gain per type of receiver was not carried out but conceptually what counts for the CD is the C/N at the output of the correlator (power of the satellite signal combined with the effect of the environment and equipment).

RECOMMENDATIONS AND FUTURE WORK

For companies and research centers working in GNSS receiver, the coming of any new open service GNSS system has to be considered as an opportunity for new integration as it improves the user experience with a need for assistance from time to time. Based on the results presented in the research carried out in this thesis, and based on the achievement of the objectives of practical use of the ideas set out in the motivations of this thesis, many points need to be studied further in depth:

- Real-time tests must be performed by implementing the algorithms developed in mobile receivers to fully benefit from the extraordinary growth of mobile devices equipped with GNSS chips. Some proposals in the thesis should be tested in real-time:
  - To test the effectiveness of using a mobile reference station in the CD approach, the variation of the dynamics of the receivers would be interesting to see the real limit of this proposition;
  - To test the effectiveness of the use of 2 or more receivers assisting a receiver in difficulty as a CP concept;
  - To verify the effectiveness of using an optimum number of parameters for the cognitive functioning of the receiver;
  - To verify the practical feasibility of smart CD application: the assistance data update, switch of reference station according to environment and measurement quality, taking into account the evolution of the MS-RS distance.
- The proposal for the use of CD in a CP context with 2 or more RSs should be studied in depth. For example, a proposal for ideas to merge measurements from different RSs if they are all able to assist the user. In addition, it is necessary to optimize its use in order to manage the compromise complexity/sensitivity/accuracy such as: number of RS, distance between RSs and between RS and MS, assistance information, etc.
- In the design of the HS-CGR, the use of signals of opportunity (SoOP) would also be useful in cases where satellite signals are not available. Indeed, the receiver should be able to use signals other than GNSS signals or other sensors that can help it calculate its position (RF signals that are not intended for navigation such as : Digital TV, AM/FM, UWB, GSM

and 3G/WCDMA mobile telephony, WiFi, infra-red, bluetooth, etc.). Similarly, existing signals can be used as a communication link between the user and the RSs.

- Finally, the application of the machine learning in HS-CGR design should be exploited in depth knowing its many advantages. The receiver would be able to learn during its prior phases of operations, then it would be able to operate easily in case it is in poor conditions.

ANNEX I

PRINCIPLE OF SATELLITES COMBINING

At acquisition level, satellites combining approach can take the form of Collective Detection. This combined acquisition approach is known as “sum of replicas” by combining satellites replicas in order to accelerate the acquisition process.

The principle of combined satellites acquisition through sum of replicas is shown in Figure A.I.1.

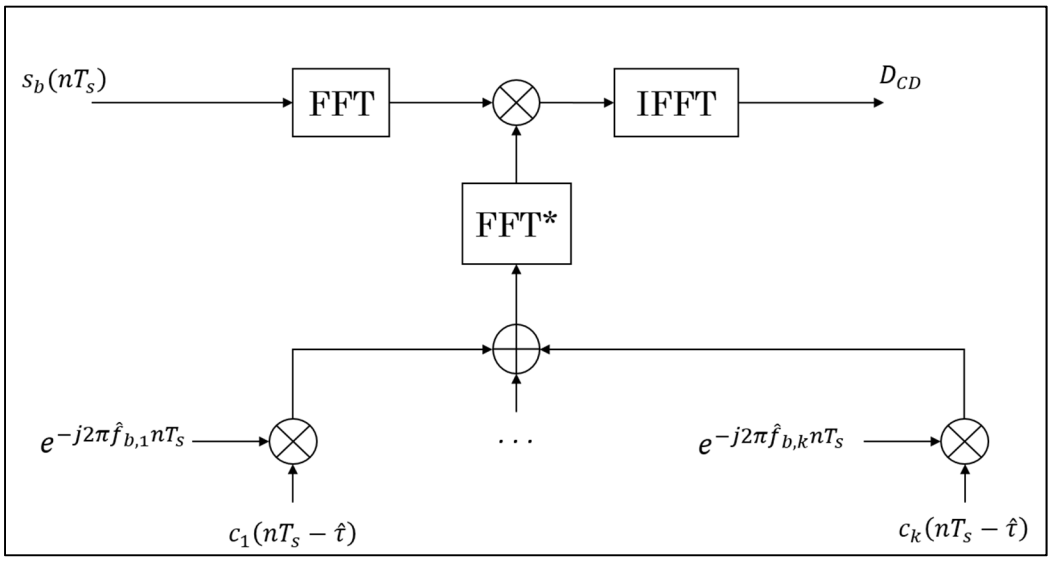

Figure-A I-1 Principle of combined satellites acquisition through sum of replicas

ANNEX II

POSITION AND VELOCITY COMPUTATION OF GPS SATELLITES

The trilateration principle is used to calculate the position of a GPS receiver. For this, it is first necessary to calculate the position of the different visible satellites. The orbit of GPS satellites meets Kepler's laws, that is,

1. The orbit of each of the satellites is an ellipse having as focal point the center of mass of the earth.
2. Each of the lines connecting a satellite to the center of mass of the earth sweeps an equivalent surface in a given time.
3. The square of the orbital period of a satellite is proportional to the cube of its mean distance to the center of mass of the earth.

It is possible to calculate the instantaneous position of each of the GPS satellites along their respective orbit using 6 orbital parameters, called as Kepler elements. Among these elements, the semimajor axis a as well as the eccentricity e define the size and the shape of the orbit of a satellite while the true anomaly v, the argument of perigee ω, the inclination angle i and the longitude of the ascending node Ω define the orientation of the orbital plane and the position of the satellite in that orbit. Knowing that the orbit of a GPS satellite can be disrupted and may deviate somewhat from its optimal trajectory, Kepler's parameters cannot be considered constant but rather need to be monitored and recalculated in real time. The GPS control segment performs this task by performing ground-level calculations and retransmitting the necessary corrections to the different satellites. The corrected orbital parameters are then transmitted to the users by means of ephemeris which form an integral part of the navigation message. Table-A.II.1 shows the orbital parameters from GPS ephemeris. It is from ephemeris that the position and velocity of the satellites at the emission time can be calculated inside the GPS receiver. Table-A.II.2 and Table-A.II.3 summarize the equations used to perform the calculations of position and velocity of the satellites. (Kaplan)

Table-A II-1 GPS ephemeris data definitions

Parameters	Description	Unity
t_{0e}	Reference time of ephemeris	[s]
Δt_{0e}	Validity period of the ephemeris	[s]
$\sqrt{a}$	Square root of semimajor axis	$[\sqrt{\mathrm{m}}]$
E	Eccentricity	-
i_0	Inclination angle (at time toe)	rad
Ω_0	Longitude of the ascending node (at weekly epoch)	rad
ω	Argument of perigee (at time toe)	rad
M_0	Mean anomaly (at time toe)	rad
di/dt	Rate of change of inclination angle	rad/s
$\dot{\Omega}$	Rate of change of longitude of the ascending node	rad/s
Δn	Mean motion correction	rad/s
C_{uc}	Amplitude of cosine correction to argument of latitude	rad
C_{us}	Amplitude of sine correction to argument of latitude	rad
C_{rc}	Amplitude of cosine correction to orbital radius	m
C_{rs}	Amplitude of sine correction to orbital radius	m
C_{ic}	Amplitude of cosine correction to inclination angle	rad
C_{is}	Amplitude of sine correction to inclination angle	rad

Table-A II-2 Computation of a satellite's ECEF position vector

Equation	**Description**
$a = \left(\sqrt{a}\right)^2$	Semimajor axis
$n = \frac{\mu}{a^3} + \Delta n$	Corrected mean motion, $\mu = 3.986005 \times 10^{14}$ m^3/s^2
$t_k = t - t_{0e}$	Time from ephemeris epoch
$M_k = M_0 + n(t_k)$	Mean anomaly
$M_k = E_k - e \sin E_k$	Eccentric anomaly (must be solved iteratively for E_k)
$\sin \nu_k = \frac{\sqrt{1-e^2}\sin E_k}{1 - e\cos E_k}$ $\cos \nu_k = \frac{\cos E_k - e}{1 - e\cos E_k}$	True anomaly
$\phi_k = \nu_k + \omega$	Argument of latitude
$\delta\phi_k = C_{us}\sin(2\phi_k) + C_{uc}\cos(2\phi_k)$	Argument of latitude correction
$\delta r_k = C_{rs}\sin(2\phi_k) + C_{rc}\cos(2\phi_k)$	Radius correction
$\delta i_k = C_{is}\sin(2\phi_k) + C_{ic}\cos(2\phi_k)$	Inclination correction
$u_k = \phi_k + \delta\phi_k$	Corrected argument of latitude
$r_k = a(1 - e\cos E_k) + \delta r_k$	Corrected radius
$i_k = i_0 + (di/dt)t_k + \delta i_k$	Corrected inclination
$\Omega_k = \Omega_0 + \left(\dot{\Omega} - \dot{\Omega}_e\right)(t_k) - \dot{\Omega}_e t_{0e}$	Corrected longitude of node, $\dot{\Omega}_e = 7.2921151467 \times 10^{-5}$ rad/s
$x_p = r_k \cos u_k$	In-plane *x* position
$y_p = r_k \sin u_k$	In-plane *y* position
$x_s = x_p \cos\Omega_k - y_p \cos i_k \sin\Omega_k$	ECEF *x*-coordinate
$y_s = x_p \sin\Omega_k + y_p \cos i_k \cos\Omega_k$	ECEF *y*-coordinate
$z_s = y_p \sin i_k$	ECEF *z*-coordinate

Tableau-A II-3 Computation of a satellite's ECEF position vector

Equation	**Description**
$\dot{E}_k = \frac{n}{1 - e\cos E_k}$	Variation of eccentric anomaly
$\dot{\phi}_k = \frac{\sqrt{1-e^2}}{1 - e\cos E_k}\dot{E}_k$	Variation of argument of latitude
$\dot{u}_k = (1 + 2C_{us}\cos(2\phi_k) - 2C_{uc}\sin(2\phi_k))\dot{\phi}_k$	Variation of argument of corrected latitude
$\dot{r}_k = 2(C_{rs}\cos(2\phi_k) - C_{rc}\sin(2\phi_k))\dot{\phi}_k + ae\sin E_k \dot{E}_k$	Variation of corrected radius
$\dot{X}_k = \dot{r}_k \cos u_k - r_k \sin u_k \dot{u}_k$	Variation of in-plane *x* position
$\dot{Y}_k = \dot{r}_k \sin u_k + r_k \cos u_k \dot{u}_k$	Variation of in-plane *y* position
$\frac{di_k}{dt} = 2(C_{is}\cos(2\phi_k) - C_{ic}\sin(2\phi_k))\dot{\phi}_k + \frac{di}{dt}$	Variation of corrected inclination
$\dot{\Omega}_k = \dot{\Omega} - \dot{\Omega}_e$	Variation of corrected longitude of node
$\dot{x}_s = \dot{X}_k \cos\Omega_k - \dot{Y}_k \cos i_k \sin\Omega_k + Y_k \sin i_k \sin\Omega_k \frac{di_k}{dt} - y_s\dot{\Omega}_k$	ECEF x-velocity
$\dot{y}_s = \dot{X}_k \sin\Omega_k + \dot{Y}_k \cos i_k \cos\Omega_k - Y_k \sin i_k \cos\Omega_k \frac{di_k}{dt} + x_s\dot{\Omega}_k$	ECEF y- velocity
$\dot{z}_s = \dot{Y}_k \sin i_k + Y_k \cos i_k \frac{di_k}{dt}$	ECEF z- velocity

ANNEX III

DILUTION OF PRECISION PARAMETERS COMPUTATION OF GNSS SYSTEM

The final accuracy of the absolute GNSS positioning is highly related to the configuration or geometry of the constellation (Geometric dilution of precision - GDOP). The GDOP, which is a dimensionless scalar, is a function of the diagonal elements of the covariance matrix of the instantaneous error on the observables. The GDOP is also a measure of the robustness of satellite geometry. This parameter is even better than the number of visible satellites is large. It is thus a criterion of choice of the satellites to be used in the calculation of the position. The best distributed satellites in space give the best geometry and therefore the best accuracy. In contrast, the nearest satellites give the bad geometry and therefore poor accuracy. This representation of the satellite geometry is shown in Figure-A III-1.

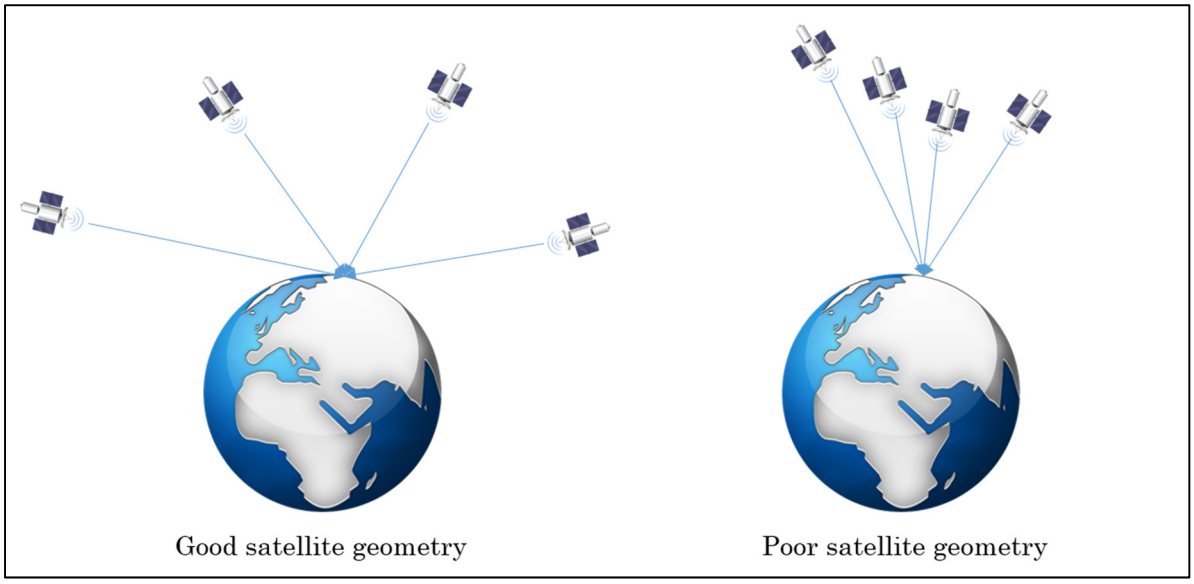

Figure-A III-1 Criterion of satellites distribution in space-GDOP

The GDOP is calculated in real-time within GNSS receivers and is used as an indicator of the quality of the position calculation. It is defined as the square root of the sum of squares of the standard deviations of the error of the spatial coordinates and the time, as:

$$GDOP = \sqrt{\sigma_E^2 + \sigma_N^2 + \sigma_U^2 + (c\sigma_T)^2} \quad \text{(A III-1)}$$

where σ_E and σ_N are respectively the standard deviation to the East and to the North [m], σ_U is the radial standard deviation [m], σ_T is standard deviation of receiver oscillator [s], and c is the speed of the light (299 792 458 m/s).

These standard deviations are obtained from the covariance matrix of the error on the position. Note that the geometry is good when the GDOP is less than 6.

The dilution of precision can be expressed as a number of separate measurements: GDOP, PDOP (Position DOP), TDOP (Time DOP), VDOP (Vertical DOP), HDOP (Horizontal DOP), EDOP (East DOP) and NDOP (North DOP).

PDOP is the measurement of 3D accuracy. This is the GDOP calculated without considering the error in time. The positioning accuracy is very good when $4 \leq PDOP \leq 5$. On the other hand, accuracy is poor when the PDOP exceeds 10. It is defined by:

$$PDOP = \sqrt{\sigma_E^2 + \sigma_N^2 + \sigma_U^2} \quad \text{(A III-2)}$$

HDOP is the measurement of horizontal positioning accuracy in 2D. Its typical value is $2 \leq HDOP \leq 3$. It is defined by:

$$HDOP = \sqrt{\sigma_E^2 + \sigma_N^2} \quad \text{(A III-3)}$$

VDOP is the measurement of vertical positioning accuracy. Its typical value is $3 \leq VDOP \leq 4$. In most cases, the VDOP is close to the PDOP. It is generally larger than the HDOP because the receiver can only see the satellites in the upper half-space bounded by the plane tangent to

the ground at the point where the receiver is, which makes it impossible to have a better satellite distribution from the earth. VDOP is defined by:

$$VDOP = \sigma_U \quad \text{(A III-4)}$$

TDOP is the measurement accuracy over time. It is expressed as:

$$TDOP = c\sigma_T \quad \text{(A III-5)}$$

Descriptions of the different values that the DOP can take are summarized in Table A.III.1.

Table-A III-1 Description of DOP values

DOP value	**Rating**	**Description**
< 1	Ideal	Recommended for applications requiring the highest possible precision at all times.
1 - 2	Excellent	Position measurements are considered accurate enough to meet all applications except the most sensitive.
2 - 5	Good	Position measurements could be used for in-route navigation suggestions.
5 - 10	Moderate	Position measurements could be used for various calculations, but the fix quality could be further improved for more accuracy.
10 - 20	Fair	Position measurements should be used only to indicate a very rough estimate of the current position.
> 20	Poor	Position measurements must be rejected as they are imprecise up to 300 meters of error with an accurate device of 6 meters.

ANNEX IV

DEFINITION OF RMS ERRORS

First, errors are usually considered as stationary and ergodic statistical process, i.e. their statistical distribution and mean remain invariable over time. It is also assumed that they are Gaussian distributed with zero mean. This is why we talk about normal and centered probability distributions as shown in Figure-A IV-1.

When referring to the positioning accuracy of a receiver, the term “error at 1σ, 2σ or 3σ” (1, 2 or 3 standard deviation" is often used. This notation relates directly to the area under the normal distribution curve presented in Figure-A IV-1 and indicates the confidence level assigned to a measurement. Thus, 1σ is equivalent to 68.3% probability, 2σ to 95.5% probability, 3σ to 99.7% and so on. For example, a receiver with a 2D accuracy of 3 m at 1σ means that the latitude and longitude measurements given by this receiver remain 68.3% of the time within a radius circle of 3 m.

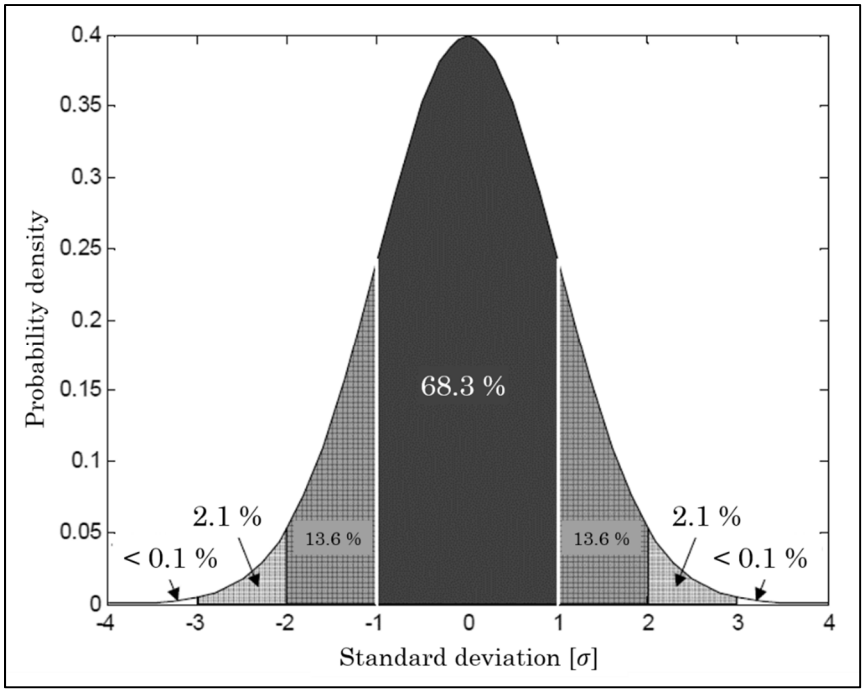

Figure-A IV-1 Centered normal distribution

The term RMS (Root Mean Square) error is also often used to describe the accuracy of measurements. Since we are referring to a normal centered distribution, this term has exactly the same meaning as 1σ. In fact, the RMS operation is the definition of the standard deviation for a centered normal distribution. We also use the RMS operator when it comes to adding two or more errors distributed in a normal way. For example, for M independent RMS errors $err_1, err_2, \dots, err_M$, the total RMS error, err_{tot}, is expressed by:

$$err_{tot} = \sqrt{\sum_{m=1}^{M} err_m} = \sqrt{err_1^2 + err_2^2 + \cdots + err_M^2} \qquad \text{(A IV-1)}$$

Other notations exist to describe the accuracy of a positioning receiver such as CEP (Circular Error Probable) and 2DRMS. The CEP is defined as the radius of a circle within which one has a 50% probability of being located. The 2DRMS error (twice the RMS distance), equivalent to a 2D error at $2\boldsymbol{\sigma}$ (not to be confused with the error RMS 2D, that is a 2D error with $1\boldsymbol{\sigma}$). The different notations cited in this section are summarized in Table-A IV-1.

Table-A IV-1 Most frequent precision measurements

Accuracy measurement	**Probability**
$1\boldsymbol{\sigma}$	68.3 %
$2\boldsymbol{\sigma}$	95.5 %
$3\boldsymbol{\sigma}$	99.7 %
RMS	68.3 %
CEP	50 %
2DRMS	95.5 %

It is also possible to have conversion factors to move from one notation to another as shown in Table-A IV-2.

Table-A IV-2 Conversion between CEP, 1σ, 2σ, 3σ, RMS, 2DRMS

From \ **To**	**CEP**	**1σ / RMS**	**2σ / 2DRMS**	**3σ**
CEP	1.0	1.2	2.4	4.8
1σ / RMS	0.83	1.0	2.0	3.0
2σ / 2DRMS	0.42	0.5	1.0	1.5
3σ	0.28	0.33	0.67	1.0

ANNEX V

EFFICIENT GNSS SECONDARY CODE CORRELATIONS FOR HS ACQUISITION

Most of the modern GNSS signals include a secondary PRN code. Although a secondary code brings some advantages and allows a significant improvement of the performance of a positioning receiver. However, it complicates the signal acquisition, because it introduces a potential sign transition between each period of the primary code. This problem is even more important when high sensitivity is required, because long coherent integrations are needed which necessitates the synchronization with the secondary code.

To overcome this problem, several methods to reduce the complexity of the secondary code correlation are proposed, namely decomposing the local secondary code in two codes, and using recursion. The first idea is to decompose the local secondary code in two codes: one code having a lot of zeros to avoid many operations when computing the correlation; and the second code having a correlation that can be computed efficiently. To allow this efficient computation method, the second code should contain a pattern that repeats several times. The second idea is based on recursion, i.e. computing a correlation result using a result previously computed. It is important to note that these methods do not change the operations performed; only the way the operations are performed differs.

The new efficient method proposed in (Leclère, Andrianarison et Landry, 2017) consists of performing an exhaustive search over all the possible decompositions. Indeed, we search the minimum complexity of the correlation of the second code within the decompositions that give a maximum of zeros in the first code. Since these correlations are relatively simple (product of a matrix and a vector with 4 or 5 rows), the goal is that the complexities found are the minimal ones.

After the correlation with the primary code we have:

$$r_i = a\, s_{i-n} r_{\mathrm{p}} + \eta_i \tag{A V-1}$$

where a is the amplitude, s_{i-n} is the $N-n$th secondary code chip (n is unknown), r_{p} is the correlation with the primary code of length N_{p}, and η_i is the noise. Then the correlation with the secondary code is:

$$y_k = \sum_{i=0}^{N_{\mathrm{S}}-1} s_{i-k}\, r_i \tag{A V-2}$$

with $k = 0, 1, \ldots, N_{\mathrm{S}} - 1$, and where the subscript of s is modulo N_{S}. Using matrix notation, Eq. (A.V.2) can be expressed as

$$\begin{bmatrix} y_0 \\ y_1 \\ \vdots \\ y_{N_{\mathrm{S}}-1} \end{bmatrix} = \begin{bmatrix} s_0 & s_1 & \cdots & s_{N_{\mathrm{S}}-1} \\ s_{N_{\mathrm{S}}-1} & s_0 & \cdots & s_{N_{\mathrm{S}}-2} \\ \vdots & \vdots & \ddots & \vdots \\ s_1 & s_2 & \cdots & s_0 \end{bmatrix} \begin{bmatrix} r_0 \\ r_1 \\ \vdots \\ r_{N_{\mathrm{S}}-1} \end{bmatrix} \tag{A V-3}$$

$$y = S\, r$$

where S is a right circular matrix with s^{T} as first row.

The secondary code can be expressed as the sum of two codes: $s = s_{\mathrm{z}} + s_{\Delta}$, where s_{z} contains a lot of zeros, and s_{Δ} has a correlation simple to compute. For this, s_{Δ} has typically a pattern that repeats and the length of this pattern should be a divisor of the secondary code length. The correlation can thus be expressed as:

$$\begin{aligned} y &= S\, r \\ &= (S_{\mathrm{z}} + S_{\Delta})\, r \\ &= S_{\mathrm{z}}\, r + S_{\Delta}\, r \\ &= y_{\mathrm{z}} + y_{\Delta} \end{aligned} \tag{A V-4}$$

where S is a right-circulant matrix with s as first row.

Let's check the effectiveness of this technique with GPS L5 and Galileo E1 OS signals. The L5 secondary code has a length of 20 chips. The divisors of 20 are 1, 2, 4, 5 and 10, we will thus consider pattern with these lengths for this code. The E1 secondary code has a length of 25 chips. The only divisors of 25 are 1 and 5, we will thus consider pattern with these lengths for this code.

Therefore, for all the possible codes s_Δ of different pattern lengths, the number of zeros obtained in s_z will be checked, and then for the most interesting codes s_Δ we will check the computation of their correlation to see how efficiently it can be done. The codes s_Δ maybe composed of 0, 1 and –1 since the goal is to remove 1 or –1 from the secondary code, others values would not make sense. Binary codes will be first checked (composed of two different values only among 0, 1, –1), and then ternary codes.

Search of optimal s_Δ codes is performed for all binary patterns of different length, i.e. length 1, 2, 4, 5, and 10 for GPS L5, and length 1 and 5 for Galileo E1 OS. To see the details of these different binary pattern, please refer to (Leclère, Andrianarison et Landry, 2017). The most interesting codes shown with different pattern for s_Δ codes are summarized in the following tables, Table-A V-1 for GPS L5 and Table-A V-2 for Galileo E1 OS.

Table-A V-1 Selected codes s_Δ and s_z for the GPS L5 signal

#	Pattern length	Pattern for s_Δ	Codes s_Δ and s_z	Number of zeros in s_z
1	1	1	1 1 1 1 1 1 1 1 1 1 1 1 1 1 1 1 1 1 1 1 0 0 0 0 0 -2 0 0 -2 -2 0 -2 0 -2 0 0 -2 -2 -2 0	12 (60 %)
2	2	1 –1	1 –1 1 –1 1 –1 1 –1 1 –1 1 –1 1 –1 1 –1 1 –1 1 –1 0 2 0 2 0 0 0 2 -2 0 0 0 0 0 0 2 -2 0 -2 2	12 (60 %)
3	4	1 –1 1 1	1 –1 1 1 1 –1 1 1 1 –1 1 1 1 –1 1 1 1 –1 1 1 0 2 0 0 0 0 0 0 -2 0 0 -2 0 0 0 0 -2 0 -2 0	15 (75 %)
4	4	–1 –1 1 1	–1 –1 1 1 –1 –1 1 1 –1 –1 1 1 –1 –1 1 1 –1 –1 1 1 2 2 0 0 2 0 0 0 0 0 0 -2 2 0 0 0 0 0 -2 0	14 (70 %)
5	4	1 0 1 1	1 0 1 1 1 0 1 1 1 0 1 1 1 0 1 1 1 0 1 1 0 1 0 0 0 -1 0 0 -2 -1 0 -2 0 -1 0 0 -2 -1 -2 0	11 (55 %)
6	5	1 1 1 –1 1	1 1 1 –1 1 1 1 1 –1 1 1 1 1 –1 1 1 1 1 –1 1 0 0 0 2 0 -2 0 0 0 -2 0 -2 0 0 0 0 -2 -2 0 0	14 (70 %)
7	5	1 –1 1 –1 1	1 –1 1 –1 1 1 –1 1 –1 1 1 –1 1 –1 1 1 –1 1 –1 1 0 2 0 2 0 -2 2 0 0 -2 0 0 0 0 0 0 0 -2 0 0	14 (70 %)
8	10	1 1 1 1 1 1 1 1 –1 1	1 1 1 1 1 1 1 1 –1 1 1 1 1 1 1 1 1 1 –1 1 0 0 0 0 0 -2 0 0 0 -2 0 -2 0 -2 0 0 -2 -2 0 0	14 (70 %)
9	10	1 1 1 1 1 –1 –1 –1 –1 –1	1 1 1 1 1 –1 –1 –1 –1 –1 1 1 1 1 1 –1 –1 –1 –1 –1 0 0 0 0 0 0 2 2 0 0 0 -2 0 -2 0 2 0 0 0 2	14 (70 %)

Table-A V-2 Selected codes s_Δ and s_z for the Galileo E1 OS signal

#	Pattern length	Pattern for s_Δ	Codes s_Δ and s_z	Number of zeros in s_z
1	1	1	1 1 1 1 1 1 1 1 1 1 1 1 1 1 1 1 1 1 1 1 1 1 1 1 1 1 0 0 -2 -2 -2 0 0 0 0 0 0 0 0 -2 0 -2 0 -2 -2 0 -2 -2 0 0 -2 0	15 (60 %)
2	5	1 1 –1 1 –1	1 1 -1 1 -1 1 1 -1 1 -1 1 1 -1 1 -1 1 1 -1 1 -1 1 1 -1 1 -1 0 0 0 -2 0 0 0 2 0 2 0 0 0 0 0 0 -2 0 0 0 -2 0 2 -2 2	17 (68 %)
3	5	1 1 1 1 –1	1 1 1 1 -1 1 1 1 1 -1 1 1 1 1 -1 1 1 1 1 -1 1 1 1 1 -1 0 0 -2 -2 0 0 0 0 0 2 0 0 -2 0 0 0 -2 -2 0 0 -2 0 0 -2 2	16 (64 %)
4	5	1 1 –1 1 1	1 1 -1 1 1 1 1 -1 1 1 1 1 -1 1 1 1 1 -1 1 1 1 1 -1 1 1 0 0 0 -2 -2 0 0 2 0 0 0 0 0 0 -2 0 -2 0 0 -2 -2 0 2 -2 0	16 (64 %)
5	5	1 1 –1 –1 –1	1 1 -1 -1 -1 1 1 -1 -1 -1 1 1 -1 -1 -1 1 1 -1 -1 -1 1 1 -1 -1 -1 0 0 0 0 0 0 0 2 2 2 0 0 0 2 0 0 -2 0 2 0 -2 0 2 0 2	16 (64 %)

BIBLIOGRAPHY

Agarwal, N., J. Basch, P. Beckmann, P. Bharti, S. Bloebaum, S. Casadei, A. Chou, P. Enge, W. Fong, N. Hathi, W. Mann, A. Sahai, J. Stone, J. Tsitsiklis et B. Van Roy. 2002. « Algorithms for GPS operation indoors and downtown ».

Aguado, L. E., G. J. Brodin, J. A. Cooper et I. D. Alston. 2004. « Combined GPS/Galileo Highly-Configurable High-Accuracy Receiver ». *Proceedings of the 17th International Technical Meeting of the Satellite Division of The Institute of Navigation (ION GNSS 2004)*.

Akopian, D. 2001. « A fast satellite acquisition method ». In *14 th International Technical Meeting of the Satellite Division of the Institute of Navigation(ION GPS 2001), Salt Lake City, UT*. p. 2871-2881.

Akopian, D. 2005. « Fast FFT based GPS satellite acquisition methods ». *IEE Proceedings-Radar, Sonar and Navigation,* vol. 152, nº 4, p. 277-286.

Al Bitar, H. 2007. « Advanced GPS signal processing techniques for LBS services ».

Andrianarison, M., et R. Jr. Landry. 2018. « New Approach of High Sensitivity Techniques Using Collective Detection Method with Multiple GNSS Receivers ». *Sensors,* vol. 18, nº 11, p. 3690.

Andrianarison, M., M. Sahmoudi et R. Jr. Landry. 2015. « Cooperative Detection of Multiple GNSS Satellite Signals in GNSS-Challenged Environments ». In *ION GNSS+ 2015*. (Tampa, Florida, USA), p. 370-380.

Andrianarison, M., M. Sahmoudi et R. Jr. Landry. 2016. « Innovative Techniques for Collective Detection of Multiple GNSS Signals in Challenging Environments ». In *IPIN*. (Alcala de Henares, Madrid, Spain).

Andrianarison, M., M. Sahmoudi et R. Jr. Landry. 2017. « Efficient and Innovative Techniques for Collective Acquisition of Weak GNSS Signals ». *Journal of Computer and Communications,* vol. 5, nº 06, p. 30.

Andrianarison, M., M. Sahmoudi et R. Jr. Landry. 2018. « New Strategy of Collaborative Acquisition for Connected GNSS Receivers in Deep Urban Environments ». *Journal of Positioning,* vol. 9, nº 03, p. 23-46.

Arribas, J., P. Closas et C. Fernández-Prades. 2010. « Joint acquisition strategy of GNSS satellites for computational cost reduction ». In *Satellite Navigation Technologies and European Workshop on GNSS Signals and Signal Processing (NAVITEC), 2010 5th ESA Workshop on*. p. 1-8. IEEE.

Avellone, G., M. Frazzetto et E. Messina. 2007. « A new waveform family for secondary peaks rejection in code tracking discriminators for Galileo BOC(n,n) modulated signals ». In *Institute of Navigation National Technical Meeting, NTM 2007, January 22, 2007 - January 24, 2007*. (San Diego, CA, United states) Vol. 1, p. 246-251. Coll. « Proceedings of the Institute of Navigation, National Technical Meeting »: Institute of Navigation.

Avila-Rodriguez, J. A., G. W. Hein, S. Wallner, J. L. Issler, L. Ries, L. Lestarquit, A. de Latour, J. Godet, F. Bastide, T. Pratt et J. Owen. 2008. « The MBOC modulation: the final touch to the Galileo frequency and signal plan ». *Navigation. Journal of the Institute of Navigation,* vol. 55, nº Copyright 2008, The Institution of Engineering and Technology, p. 15-28.

Axelrad, P., B. Bradley, J. Donna, M. Mitchell et S. Mohiuddin. 2011. « Collective detection and direct positioning using multiple GNSS satellites ». *Navigation,* vol. 58, nº 4, p. 305-321.

Axelrad, P., B. K. Bradley, J. Tombasco, S. Mohiuddin et J. Donna. 2010. « GEO Satellite Positioning Using GPS Collective Detection ». In *Proceedings of the 23rd International Technical Meeting of The Satellite Division of the Institute of Navigation (ION GNSS 2010)*. p. 2706-2716.

Axelrad, P., J. Donna et M. Mitchell. 2009. « Enhancing GNSS acquisition by combining signals from multiple channels and satellites ». In *Proceedings of the 22nd International Technical Meeting of The Satellite Division of the Institute of Navigation (ION GNSS 2009)*. p. 2617-2628.

Baldini, G., T. Sturman, A. R. Biswas, R. Leschhorn, G. Godor et M. Street. 2008. « Security Aspects in Software Defined Radio and Cognitive Radio Networks: A Survey and A Way Ahead ».

Bardak, B., Y. Adane et I. Kale. 2011. « Hardware-Software Optimized FFT-Based Acquisition Engine for GNSS ». *International Technical Meeting of The Institute of Navigation*.

Betz, J. W. 2015. *Engineering Satellite-Based Navigation and Timing: Global Navigation Satellite Systems, Signals, and Receivers*. John Wiley & Sons.

Blunt, P. D., R. Weiler et M. S. Hodgart. 2007. « Demonstration of BOC(15, 2.5) acquisition and tracking with a prototype hardware receiver ».

Borio, D. 2008. « A statistical theory for GNSS signal acquisition ». *Doctor of Philosophy, Politecnico Di Torino*.

Borio, D. , C. O'Driscoll et G. Lachapelle. 2009a. « Coherent, Noncoherent, and Differentially Coherent Combining Techniques for Acquisition of New Composite GNSS Signals ». *Aerospace and Electronic Systems, IEEE Transactions*, p. pp. 1227 - 1240

Borio, D., et G. Lachapelle. 2009. « A non-coherent architecture for GNSS digital tracking loops ». *annals of telecommunications-annales des télécommunications,* vol. 64, nº 9-10, p. 601.

Borio, D., C. O'Driscoll et G. Lachapelle. 2009b. « Coherent, noncoherent, and differentially coherent combining techniques for acquisition of new composite GNSS signals ». *IEEE Transactions on Aerospace and Electronic Systems,* vol. 45, nº 3, p. 1227-1240.

Borio, D., et L. L. Presti. 2008. « A reconfigurable GNSS acquisition scheme for time-frequency applications ». *EURASIP Journal on Advances in Signal Processing,* vol. 2008, p. 149.

Borre, K., D. Akos, N. Bertelsen, P. Rinder et S. H. Jensen. 2007. *A Software-Defined GPS and Galileo Receiver - A Single-Frequency Approach*. University of Maryland, 189 p.

Bradley, B., P. Axelrad, J. Donna et M. Mitchell. 2010. « Performance Analysis of Collective Detection of Weak GPS Signals ». In *ION GNSS 2010*. (Portland, Oregon, USA, September 21-24, 2010), sous la dir. de ION, Proceedings of 23rd ITM of, p. pp. 3041-3053.

Bradley, B. K., P. Axelrad, J. Donna et S. Mohiuddin. 2009. « Performance analysis of collective detection of weak GPS signals ». In *Proceedings of the 23rd International Technical Meeting of The Satellite Division of the Institute of Navigation (ION GNSS 2010)*. p. 3041-3053.

Bruce, A. F. 2006. *Cognitive Radio Technology*. 649 p.

Bruno, S. 2007. « Mise en oeuvre en temps-réel d'un récepteur hybride GPS-Galileo ». Montréal, ETS, 329 p.

Canada, Natural Resources. 2015. « Station report ». < http://webapp.geod.nrcan.gc.ca/geod/data-donnees/station/report-rapport.php?id=943020&locale=en >. Consulté le Sept. 4, 2015.

Capuano, V., C. Botteron et P. A. Farine. 2013. « GNSS performances forMEO, GEO and HEO ». In *In 64th International Astronautical Congress*. (October 2013).

Carrasco-Martos, S., G. López-Risueño, D. Jiménez-Baños et E.K.A. Gill. 2010. « Snapshot software receiver for GNSS in weak signal environments: An innovative approach for galileo E5 ». In *Proceedings of the 23rd International Technical Meeting of the*

Satellite Division of the Institute of Navigation, ION GNSS 2010, Portland, Oregon, USA, 21-24 September 2010.

Celebi, H., et H. Arslan. 2007a. « Adaptive positioning systems for cognitive radios ». In *2007 2nd IEEE International Symposium on New Frontiers in Dynamic Spectrum Access Networks, 17-20 April 2007*. (Piscataway, NJ, USA), p. 78-84. Coll. « 2007 2nd IEEE International Symposium on New Frontiers in Dynamic Spectrum Access Networks »: IEEE.

Celebi, H., et H. Arslan. 2007b. « Cognitive positioning systems ». *IEEE Transactions on Wireless Communications,* vol. 6, nº 12, p. 4475-4483.

Cheong, J. W. 2011. « Towards multi-constellation collective detection for weak signals: a comparative experimental analysis ». In *Proceedings of the ION GNSS*. p. 3709-3719. Citeseer.

Cheong, J. W. 2012. « Signal processing and collective detection for Locata positioning system ». Ph. D. Dissertation, School of Surveying and Spatial Information Systems.

Cheong, J. W., A. G. Dempster et C. Rizos. 2011. « Hybrid of Collective Detection with Conventional Detection for Weak Signal Acquisition ». In *Proceedings of the International GNSS Society Symposium (IGNSS 2011)*. Citeseer.

Cheong, J. W., J. Wu et A. Dempster. 2015. « Dichotomous search of coarse time error in collective detection for GPS signal acquisition ». *GPS solutions,* vol. 19, nº 1, p. 61-72.

Cheong, J. W., J. Wu, A. G. Dempster et C. Rizos. 2011. « Efficient implementation of collective detection ». In *IGNSS symposium*. (University of New South Wales, Sydney, NSW, Australia, 15 – 17 November, 2011), sous la dir. de Society, International Global Navigation Satellite Systems.

Cheong, J. W., J. Wu, A. G. Dempster et C. Rizos. 2012. « Assisted-GPS based snap-shot GPS receiver with FFT-accelerated collective detection: Time synchronisation and search space analysis ». In *Proceeding of the 2012 International Technical Meeting of the Satellite Division of the Institute of Navigation, Nashville, Tennessee, USA*. Citeseer.

Closas, P., C. Fernández-Prades et J. A. Fernández-Rubio. 2007. « Maximum likelihood estimation of position in GNSS ». *IEEE Signal Processing Letters,* vol. 14, nº 5, p. 359-362.

Closas, P., C. Fernández-Prades et J. A. Fernández-Rubio. 2009. « Direct position estimation approach outperforms conventional two-steps positioning ». In *Signal Processing Conference, 2009 17th European*. p. 1958-1962. IEEE.

Datta, A. 2016. « How GNSS signals work within specific frequency bands ». Message envoyé à *How GNSS frequency bands for constellations work*. < https://www.geospatialworld.net/gnss-frequency-bands-for-constellations/ >.

de Salas, J., et F. van Diggelen. 2011. « Single-Shot Position: Cell-Phone Location without Ephemeris ». *GPS World,* vol. 22, nº 2, p. 28-33.

Della Rosa, F., H. Hurskainen, J. Nurmi, M. Detratti et E. P. Serna. 2010. « GRAMMAR: challenges and solutions for multi-constellation mass market user receivers ». In *Ubiquitous Positioning Indoor Navigation and Location Based Service (UPINLBS), 2010*. p. 1-6. IEEE.

DeSalas, J., et F. van Diggelen. 2010. « GNSS Position Computation without Ephemeris "Single Shot MSBased" ». In *ION GNSS 2010*. (Portland, OR, USA), sous la dir. de Navigation, Proceedings of the 23rd International Technical Meeting of The Satellite Division of the Institute of.

DiEsposti, R. 2001. « GPS PRN code signal processing and receiver design for simultaneous all-in-view coherent signal acquisition and navigation solution determination ». In *Proceedings of the 2007 National Technical Meeting of The Institute of Navigation*. p. 91-103.

DiEsposti, R. 2007. « GPS PRN Code Signal Processing and Receiver Design for Simultaneous All-in-View Coherent Signal Acquisition and Navigation Solution Determination ». *ION NTM 2007, San Diego, CA*.

Dion, A., V. Calmettes et E. Boutillon. 2007. « Reconfigurable GPS-Galileo receiver for satellite based applications ». In *National Technical Meeting of The Institute of Navigation*. p. pp. 277–287.

Dodson, A. H., W. Chen, H. C. Baker, N. T. Penna, G. W. Roberts, R. J. Jeans et J. Westbrook. 2001. « Assessment of EGNOS Tropospheric Correction Model ». *The Journal of Navigation,* vol. vol. 54, nº no. 01, p. pp. 37-55.

Dötterböck, D., et B. Eissfeller. 2009. « A GPS/Galileo software snap-shot receiver for mobile phones ». In *Proceedings of the IAIN 2009 world congress. Stockholm, Sweden*.

Dovis, F., M. Pini et P. Mulassano. 2004. « Turbo DLL: An innovative architecture for multipath mitigation in GNSS receivers ». In *17th International Technical Meeting of the Satellite Division of the Institute of Navigation, ION GNSS 2004, September 21, 2004 - September 24, 2004*. (Long Beach, CA, United states), p. 1-7. Coll. « Proceedings of the 17th International Technical Meeting of the Satellite Division of the Institute of Navigation, ION GNSS 2004 »: Institute of Navigation.

Dow, J. M., R. E. Neilan et C. Rizos. 2009. « The international GNSS service in a changing landscape of global navigation satellite systems ». *Journal of Geodesy,* vol. 83, nº 3, p. 191-198.

El-Rabbany, A. 2002. *Introduction to GPS : the global positioning system*, xv. Coll. « Artech House mobile communications series ». Boston, 176 p.

El Natour, H. A., et M. Monnerat. 2006. « A New Algorithm to Reduce AGPS Acquisition TTFF ». *ION NTM 2006, Monterey, CA*.

Electric Co., Furono. 2014. « Multi-GNSS (Multi-frequency GNSS) ». < http://www.furuno.com/en/gnss/technical/tec_multi >.

Esteves, P. 2013. « An Innovative and Efficient Frequency Estimation Method for GNSS Signals Acquisition ». In *ION GNSS*. p. 16-20.

Esteves, P. 2014a. « High-Sensitivity Adaptive GNSS Acquisition Schemes ». ISAE, University of Toulouse.

Esteves, P. 2014b. « Techniques d'acquisition à haute sensibilité des signaux GNSS ». Toulouse, Institut Supérieur de l'Aéronautique et de l'Espace (ISAE), 240 p.

Esteves, P., M. Sahmoudi et L. Ries. 2013. « An Efficient Implementation of Collective Detection Applied in a Combined GPS-Galileo Receiver ». In *Proceedings of the 6th European Workshop on GNSS and Signal Processing*. (Neubiberg, Germany, 2013), sous la dir. de 2013, SIGNALS.

Esteves, P., M. Sahmoudi et L. Ries. 2014. « Collective Detection of Multi-GNSS Signals: Vector-Acquisition Promises Sensitivity and Reliability Improvement ». *Inside GNSS*.

Fernandez-Prades, C., J. Arribas et P. Closas. 2015. « Assessment of software-defined GNSS receivers ». In *Computer Science, Computer Engineering, and Social Media (CSCESM), 2015 Second International Conference on*. p. 1-9. IEEE.

Floc'H, J. J., et M. Soellner. 2007. « Comparison between BOC CBOC and TMBOC tracking ». In *Institute of Navigation National Technical Meeting, NTM 2007, January 22, 2007 - January 24, 2007*. (San Diego, CA, United states) Vol. 2, p. 964-973. Coll. « Proceedings of the Institute of Navigation, National Technical Meeting »: Institute of Navigation.

Foucras, M. 2015. « Performance Analysis of Modernized GNSS Signal Acquisition ». INP Toulouse 275 p.

Foucras, M., O. Julien, C. Macabiau et B. Ekambi. 2012. « A novel computationally efficient Galileo E1 OS acquisition method for GNSS software receiver ». In *ION GNSS 2012,*

25th International Technical Meeting of The Satellite Division of the Institute of Navigation. p. pp xxxx.

Galileo-OS-SIS-ICD. 2016. *European GNSS (Galileo) Open Service Signal-In-Space Interface Control Document* 88 p.

Galileo OS-SIS-ICD. 2016. *European GNSS (Galileo) Open Service Signal-In-Space Interface Control Document*.

Garello, R., L. Lo Presti, G. E. Corazza et J. Samson. 2012. « Peer-to-Peer Cooperative Positioning Part I: GNSS Aided Acquisition ». *InsideGNSS*, p. 55-63.

Gerakoulis, D. and Evaggelos, G. 2001. *CDMA: Access and Switching for Terrestrial and Satellite Networks*. 284 pages p.

Gernot, C. 2009. *Development of combined GPS L1/L2C acquisition and tracking methods for weak signals environments*. University of Calgary, Department of Geomatics Engineering.

Gernot, C., K. O'Keefe et G. Lachapelle. 2011. « Assessing three new GPS combined L1/L2C acquisition methods ». *IEEE Transactions on Aerospace and Electronic Systems,* vol. 47, n° 3, p. 2239-2247.

Gernot, C., et S. Shanmugam. 2007. « A Novel L1 and L2C Combined Detection Scheme for Enhanced GPS Acquisition ». *Proceedings of ION-GNSS07, Forth Worth*.

Gold, R. 1967. « Optimal Binary Sequences for Spread Spectrum Multiplexing ». *IEEE Transactions on Information Theory,* vol. vol. 13, n° no. 4, p. pp. 619-621.

Grejner-Brzezinska, D. A., et C. K. Toth. 2013. « GPS-Challenged Environments: Can Collaborative Navigation Help? ». *Journal of Aeronautics, Astronautics and Aviation. Series A,* vol. 45, n° 4, p. 241-248.

Harper, N. 2010. *Server-side GPS and Assisted-GPS in Java*. Artech House.

He, Z., et M. Petovello. 2014. « Joint detection and estimation of weak GNSS signals with application to coarse time navigation ». In *Proceedings of the 27th International Technical Meeting of The Satellite Division of the Institute of Navigation (ION GNSS+ 2014), Tampa USA*. p. 1554-1567.

He, Z., V. Renaudin, M. G. Petovello et G. Lachapelle. 2013. « Use of high sensitivity GNSS receiver doppler measurements for indoor pedestrian dead reckoning ». *Sensors,* vol. 13, n° 4, p. 4303-4326.

Henkel, P., et J. J. Kiam. 2013. « Maximum a posteriori probability estimation of integer ambiguities and baseline ». In *ELMAR, 2013 55th International Symposium*. p. 353-356. IEEE.

Hofmann, B., H. Lichtenegger et J. Collins. 2001. *GPS theory and practice*, 4th Edition. Coll. « Springer-Verlag Wien NewYork ».

Hurd, W.J., J.I. Statman et V.A. Vilnrotter. 1987. « High dynamic GPS receiver using maximum likelihood estimationand frequency tracking ». *IEEE Transactions on Aerospace and Electronic Systems*, nº 4, p. 425-437.

Hurskainen, H., E.-S. Lohan, J. Nurmi, S. Sand, C. Mensing et M. Detratti. 2009. « Optimal dual frequency combination for Galileo mass market receiver baseband ». In *Signal Processing Systems, 2009. SiPS 2009. IEEE Workshop on*. p. 261-266. IEEE.

ICD-GPS-200. 2000. *Navstar GPS Space Segment / Navigation User Interfaces*.

Ioannides, R. T., L. E. Aguado et G. Brodin. 2006. « Coherent Integration of Future GNSS Signals ». *Proceedings of the 19th International Technical Meeting of the Satellite Division of The Institute of Navigation,* vol. ION GNSS 2006, p. pp. 1253-1268.

Jacobsen, E. , et P. Kootsookos. 2012. « Fast, Accurate Frequency Estimators ». In *Streamlining Digital Signal Processing: A Tricks of the Trade Guidebook*, sous la dir. de John Wiley & Sons, Inc., Second Edition (ed R. G. Lyons). p. pp. 107-114. Hoboken, NJ, USA.

Jacobsen, E., et P. Kootsookos. 2007. « Fast, accurate frequency estimators ». *IEEE Signal Process. Mag,* vol. 24, nº 3, p. 123-125.

Jia, Z., et M. Sahmoudi. 2016. « A type of collective detection scheme with improved pigeon-inspired optimization ». *International Journal of Intelligent Computing and Cybernetics,* vol. 9, nº 1, p. 105-123.

Jian, Z., C. Chao-hui, C. Jun-yong et S. Lei. 2009. « Cognitive radio: methods for the detection of free bands ». In *2009 International Conference on Networks Security, Wireless Communications and Trusted Computing (NSWCTC 2009), 25-26 April 2009*. (Piscataway, NJ, USA) Vol. vol.2, p. 343-5. Coll. « 2009 International Conference on Networks Security, Wireless Communications and Trusted Computing (NSWCTC 2009) »: IEEE. < http://dx.doi.org/10.1109/NSWCTC.2009.334 >.

Jiao, X., J. Wang et X. Li. 2012. « High sensitivity GPS acquisition algorithm based on code Doppler compensation ». In *Signal Processing (ICSP), 2012 IEEE 11th International Conference on*. Vol. 1, p. 241-245. IEEE.

Jiménez-Baños, D., N. Blanco-Delgado, G. López-Risueño, G. S. Granados et A. Garcia-Rodriguez. 2006. « Innovative techniques for GPS indoor positioning using a snapshot receiver ». In *Institute of Navigation-19th International Technical Meeting of the Satellite Division, ION GNSS 2006*. (Fort Worth, TX, USA, Sept. 26-29).

Joseph, A. 2010. « What is the difference between SNR and C/N0 ? ». *Inside GNSS,* vol. vol. 5, nº no. 6, p. pp. 20-25.

Julien, O., C. Macabiau, M. E. Cannon et G. Lachapelle. 2007. « ASPeCT: Unambiguous sine-BOC(n,n) acquisition/tracking technique for navigation applications ». *IEEE Transactions on Aerospace and Electronic Systems,* vol. 43, nº Compendex, p. 150-162.

Kaplan, E., et C. Hegarty. 2006. *Understanding GPS principles and applications* Coll. « Collections :Artech House mobile communications series EngineeringPro, Artech House Publishers ».

Kassas, Z. M., et T. E. Humphreys. 2014. « Observability analysis of collaborative opportunistic navigation with pseudorange measurements ». *IEEE Transactions on Intelligent Transportation Systems,* vol. 15, nº 1, p. 260-273.

Kealy, A., N. Alam, M. Efatmaneshnik, C. Toth, A. Dempster et D. Brzezinska. 2013. « Collaborative Positioning in GPS-Challenged Environments ». *Earth on the Edge: Science for a Sustainable Planet: Proceedings of the IAG General Assembly, Melbourne, Australia, June 28-July 2, 2011,* vol. 139, p. 493.

Kim, B., et S.-H. Kong. 2013. « FFT Based two Dimensional Compressed Correlator for Fast Acquisition in GNSS ». In *ION 2013 Pacific PNT Meeting*. (Honolulu, Hawaii), p. 667 - 672. Proceedings of the ION 2013 Pacific PNT Meeting.

Kong, S.-H. 2014. « Fast multi-satellite ML acquisition for A-GPS ». *IEEE Transactions on Wireless Communications,* vol. 13, nº 9, p. 4935-4946.

Kubrak, D., M. Monnerat, G. Artaud et L. Ries. 2008. « Improvement of GNSS signal acquisition using low-cost inertial sensors ». In *ION GNSS*. p. 2145-2155.

Lamontagne, G. 2009. « Conception et mise en oeuvre d'une tête de réception à échantillonnage direct RF pour les signaux de radionavigation par satellites ». Ecole de Technologie Superieure, 248 p.

Leclère, J. 2014. « Resource-efficient Parallel Acquisition Architectures for Modernized GNSS Signals ». Lausanne (Switzerland), École Polytechnique Fédérale de Lausanne (EPFL), 275 p.

Leclère, J., M. Andrianarison et R. Jr. Landry. 2017. « Efficient GNSS secondary code correlations for high sensitivity acquisition ». In *European Navigation Conference (ENC) 2017*. (Lausanne, Switzerland, May 9 - 12, 2017).

Leclère, J., C. Botteron et P.-A. Farine. 2010a. « Resource and performance comparisons for different acquisition methods that can be applied to a VHDL-based GPS receiver in standalone and assisted cases ». In *Position Location and Navigation Symposium (PLANS), 2010 IEEE/ION*. p. 745-751. IEEE.

Leclère, J., C. Botteron et P.-A. Farine. 2010b. « Resource and performance comparisons for different acquisition methods that can be applied to a VHDL-based GPS receiver in standalone and assisted cases ». In *PLANS, IEEE/ION*. (Indian Wells, CA, USA), p. pp. 745-751.

Leclère, J., et R. Jr. Landry. 2016. « Complexity reduction for high sensitivity acquisition of GNSS signals with a secondary code ».

Lee, J. K., D. A. Grejner-Brzezinska et C. Toth. 2012. « Network-based collaborative navigation in GPS-denied environment ». *Journal of Navigation,* vol. 65, nº 03, p. 445-457.

Leick, A., L. Rapoport et D. Tatarnikov. 2015. *GPS satellite surveying*. John Wiley & Sons.

Lesouple, J., F. Barbiero, M Sahmoudi, J.-Y. Tourneret et W. Vigneau. 2017. « Multipath Mitigation for GNSS Positioning in Urban Environment Using Sparse Estimation ». *IEEE Transactions on Intelligent Transportation Systems*.

Li, B., J. Zhang, P. Mumford et A. G. Dempster. 2011. « How good is Assisted GPS? ». In *Proceedings of the International GNSS Society Symposium (IGNSS 2011)*.

Li, L., J. W. Cheong, J. Wu et A. G. Dempster. 2014. « Improvement to Multi-resolution Collective Detection in GNSS Receivers ». *The Journal of Navigation,* vol. 67, p. 277-293.

Li, Q., B. Liu et H.-F. Li. 2007. « BOC modulation in Galileo ». *Computer Engineering and Applications,* vol. 43, nº Copyright 2008, The Institution of Engineering and Technology, p. 224-6.

Lin, D. M., et J. B. Y. Tsui. 1998. « Acquisition schemes for software GPS receiver ». In *Proceedings of Ion GPS.* Vol. 11, p. 317-326. INSTITUTE OF NAVIGATION.

Lin, D. M., et J. B. Y. Tsui. 2000. « Comparison of acquisition methods for software GPS receiver ». In *Proceedings of the 13th International Technical Meeting of the Satellite Division of The Institute of Navigation (ION GPS 2000)*. p. 2385-2390.

Lin, D. M., et J. B. Y. Tsui. 2002. « A weak signal tracking technique for a stand-alone software GPS receiver ». In *ION GPS 2002: 15 th International Technical Meeting of the Satellite Division of The Institute of Navigation*.

Lin, Y.-C., et S.-S. Jan. 2010. « Linear composite code acquisition method for GNSS ». In *Position Location and Navigation Symposium (PLANS), 2010 IEEE/ION*. p. 276-284. IEEE.

Linty, N., et L. L. Presti. 2016. « Doppler Frequency Estimation in GNSS Receivers Based on Double FFT ». *IEEE Transactions on Vehicular Technology,* vol. 65, nº 2, p. 509-524.

Lopez-Risueno, G., et G. Seco-Granados. 2007. « Detection and mitigation of cross-correlation interference in high-sensitivity GNSS receivers ». In *Personal, Indoor and Mobile Radio Communications, 2007. PIMRC 2007. IEEE 18th International Symposium on*. p. 1-5. IEEE.

López-Risueno, G., et G. Seco-Granados. 2004. « Measurement and processing of indoor GPS signals using a one-shot software receiver ». In *2nd ESA Workshop on Satellite Navigation User Equipment Technologies (NAVITEC 2004)*.

Luise, M., et F. Zanier. 2009. « Multicarrier signals: A natural enabler for cognitive positioning systems ». In *7th International Workshop on Multi-Carrier Systems and Solutions, MC-SS 2009, May 5, 2009 - May 6, 2009*. (Herrsching, Germany) Vol. 41 LNEE, p. 3-13. Coll. « Lecture Notes in Electrical Engineering »: Springer Verlag. < http://dx.doi.org/10.1007/978-90-481-2530-2_1 >.

Macchi-Gernot, F., M. G. Petovello et G. Lachapelle. 2010. « Combined acquisition and tracking methods for GPS L1 C/A and L1C signals ». *International Journal of Navigation and Observation,* vol. 2010.

Macchi, F. 2010. « Development and testing of an L1 combined GPS-Galileo software receiver ». *University of Calgary, Calgary Google Scholar*.

Macgougan, G. 2003. « High Sensitivity GPS Performance Analysis in Degraded Signal Environments ». *Master of Science, University of Calgary*.

Madhani, P. H., P. Axelrad, K. Krumvieda et J. Thomas. 2003. « Application of successive interference cancellation to the GPS pseudolite near-far problem ». *IEEE Transactions on Aerospace and Electronic Systems,* vol. 39, nº 2, p. 481-488.

Mattos, P.G. 2001. « Solutions to the cross-correlation and oscillator stability problems for indoor C/A code GPS ». In *Proceedings of the 16th International Technical Meeting of the Satellite Division of The Institute of Navigation (ION GPS/GNSS 2003)*. p. 654-659.

Megahed, D., C. O'Driscoll et G. Lachapelle. 2009. « Combined L1/L5 Kalman Filter-Based Tracking for Weak Signal Environments ». *European Navigation Conference 2009 – Naples, Italy, May 3-6, 2009*.

Melgard, T. E., G. Lachapelle et H. Gehue. 1994. « GPS signal availability in an urban area-receiver performance analysis ». In *Position Location and Navigation Symposium, 1994., IEEE*. (11-15 Apr 1994), p. 487-493.

Meng, X., G. W. Roberts, A. H. Dodson, E. Cosser, J. Barnes et C. Rizos. 2004. « Impact of GPS satellite and pseudolite geometry on structural deformation monitoring: analytical and empirical studies ». *Journal of Geodesy,* vol. 77, nº 12, p. 809-822.

Misra, P., B. P. Burke et M. M. Pratt. 1999. « GPS performance in navigation ». *Proceedings of the IEEE,* vol. 87, nº 1, p. 65-85.

Mitola III, J. 2006. *Cognitive radio architecture: the engineering foundations of radio XML*. John Wiley & Sons.

Molino, A., G. Girau, M. Nicola, M. Fantino et M. Pini. 2008. « Evaluation of a FFT-based acquisition in real time hardware and software GNSS receivers ». In *Spread Spectrum Techniques and Applications, 2008 IEEE 10th International Symposium on*. p. 37-41. IEEE.

Monnerat, M., R. Couty, N. Vincent, O. Huez et E. Chatre. 2004. « The Assisted GNSS, Technology and Applications ». In *Proceedings of ION GNSS 2004*. (Long Beach, CA, USA).

Narula, L., K. P. Singh et M. G. Petovello. 2014. « Accelerated collective detection technique for weak GNSS signal environment ». In *Ubiquitous Positioning Indoor Navigation and Location Based Service (UPINLBS), 2014*. p. 81-89. IEEE.

Navstar, GPS. 2000. « Space Segment/Navigation User Interfaces ». *Arinc research corporation*.

NovAtel, Inc. 2017. « Multi-Frequency, Multi-Constellation, Applications of high-precision GPS in Industries ». < https://www.novatel.com/industries/autonomous-vehicles/technology/ >.

O'Driscoll, C. 2007a. « Performance analysis of the parallel acquisition of weak GPS signals ».

O'Driscoll, C. 2007b. « Performance analysis of the parallel acquisition of weak GPS signals ». National University of Ireland.

Omar, A. B., M. Sahmoudi, P. Esteves, L. Ries, M. Andrianarison et R. Jr. Landry. 2014. « A New Method of Collective Acquisition of Multiple GNSS Satellite Signals in Challenging Environments ». In.

Pany, T. 2010. *Navigation Signal Processing for GNSS Software Receivers*. Coll. « Artech House Publishers ».

Pany, T., J. Winkel, B. Riedl, M. Restle, T. Wörz, R. Schweikert, H. Niedermeier, G. Ameres, B. Eissfeller et S. Lagrasta. 2009. « Performance of a Partially Coherent Ultra-Tightly Coupled GNSS/INS Pedestrian Navigation System Enabling Coherent Integration Times of Several Seconds to Track GNSS Signals Down to 1.5 dB-Hz ». In *Proceedings of the 22nd International Technical Meeting of The Satellite Division of the Institute of Navigation (ION GNSS 2009), Savannah, GA, USA*. Vol. 2225.

Papoulis, A. 1965. « Probability, random variables, and stochastic processes ».

Parkinson, B. W., et J. Jr. Spilker. 1996. *Global Positioning System: Theory and Applications*, vol. 1. 791 p.

Peterson, B., R. J. Hartnett, G. Ottman et L. Miller. 1995. « GPS/LORAN in an urban environment-oscillator stability considerations ». In *Proceedings of the 1995 IEEE International Frequency Control Symposium (49th Annual Symposium)*. (31 May-2 Jun 1995), p. 259-265.

Petovello, M. G., C. O'Driscoll et G. Lachapelle. 2008. « Weak Signal Carrier Tracking Using Extended Coherent Integration with an Ultra-Tight GNSS/IMU Receiver ».

Pigeon, M. 2011. « Etude et réalisation d'antennes ultra-compactes à base de métamatériaux: Application à la réalisation d'une antenne GNSS miniature ». Toulouse, Institut National Polytechnique de Toulouse - INPT, 219 p.

Polson, J. 2004. « Cognitive radio applications in software defined radio ». In *Proceedings of the SDR Forum Conference 2004*.

Pratap, M., et P. Enge. 2006. « Global positioning system : signals, measurements, and performance ». *2e édition. Lincoln, Mass.: Ganga-Jamuna Press*, p. 570.

Proakis, J. 2008. *Digital Communications*

Psiaki, M. L. 2001. « Block Acquisition of Weak GPS Signals in a Software Receiver ».

Psiaki, M. L., D. M. Akos et J. Thor. 2005. « A comparison of direct radio frequency sampling and conventional GNSS receiver architectures ». *Journal of the Institute of Navigation,* vol. vol. 52, nº no. 2, p. pp. 71-81.

Rovelli, D., P. Crosta, P. Iacone, M. Rovini, G. Gentile et L. Fanucci. 2010. « Acquisition speed-up engine for GNSS signals ». In *Satellite Navigation Technologies and European Workshop on GNSS Signals and Signal Processing (NAVITEC), 2010 5th ESA Workshop on*. p. 1-8. IEEE.

RTCM-SC104. 2001. *Recommended Standards for Differential GNSS Service (v. 2.3)*. August.

Sagiraju, P. K., D. Akopian et H. Valio. 2006. « Fine frequency estimation in weak signals for GPS receivers ». In *ION NTM Conference*.

Sagiraju, P. K., G. V. S. Raju et D. Akopian. 2008. « Fast acquisition implementation for high sensitivity global positioning systems receivers based on joint and reduced space search ». *IET Radar, Sonar & Navigation,* vol. 2, nº 5, p. 376-387.

Sahmoudi, M., P. Esteves, M. Bousquet, L. Ries, G. Artaud et M.-L. Boucheret. 2010. « A New Frequency Offset Correction Approach for Enhancing Sensitivity of GNSS Receivers ». In *Proceedings of the 24th International Technical Meeting of the Satellite Division of The Institute of Navigation (ION GNSS 2011)*. p. 1046-1055.

Sahmoudi, M., C. Yang et V. Calmettes. 2010. « The merits of the cyclostationarity of BOC signals for a cognitive GNSS receiver design ». In *2010 IEEE/ION Position, Location and Navigation Symposium - PLANS 2010, 3-6 May 2010*. (Piscataway, NJ, USA), p. 1181-8. Coll. « 2010 IEEE/ION Position, Location and Navigation Symposium - PLANS 2010 »: IEEE. < http://dx.doi.org/10.1109/PLANS.2010.5507238 >.

Scharf, L. 1991. *Statistical signal processing*, 98. Addison-Wesley Reading, MA.

Schmid, A. 2007. « Single Shot Positioning ». In *IGNSS Symposium 2007*. (Sydney, Australia, 4 – 6 December, 2007), sous la dir. de Society, International Global Navigation Satellite Systems.

Schmid, A. 2009. *Advanced Galileo and GPS receiver techniques*. Nova Science Publ.

Seco-Granados, G., J. Lopez-Salcedo, D. Jiménez-Baños et G. López-Risueño. 2012. « Challenges in indoor global navigation satellite systems: unveiling its core features in signal processing ». *IEEE Signal Processing Magazine,* vol. 29, nº 2, p. 108-131.

Shayevits, B., H. Cohen, J. Nir et E. Dochovny. 2002. « Very Efficient High Sensitivity Fully Coherent AGPS Signal Processing with Almost No Assistance Requirements ». *ION GPS 2002*.

Shiravaramaiah, N. C., et A. G. Dempster. 2011. « Cognitive GNSS Receiver Design: Concept and Challenges ». *24th International Technical Meeting of the Satellite Division of The Institute of Navigation, Portland OR*.

Soloviev, A., et J. Dickman. 2013. « Collaborative GNSS signal processing ». In *Proceedings of the 26th International Technical Meeting of the Satellite Division of the Institute of Navigation (ION GNSS+ 2013), Nashville, TN*.

Soloviev, A., J. Dickman et J. Campbell. 2013. « MUSTER A Collaborative GNSS Receiver Architecture for Weak Signal Processing ». *InsideGNSS*, p. 56-68.

Soloviev, A., F. van Graas et S. Gunawardena. 2009. « Decoding navigation data messages from weak GPS signals ». *IEEE transactions on aerospace and electronic systems,* vol. 45, nº 2.

Subirana, J. S., J. M. J. Zornoza et M. Hernandez-Pajares. 2014. « GNSS signal ». < http://www.navipedia.net/index.php/GNSS_signal >.

Sun-Jun, K., W. Jong-Hoon et L. Ja-Sung. 2006. « Design of a PC based real-time software GPS receiver ». *Transactions of the Korean Institute of Electrical Engineers, D,* vol. 55, nº 6, p. 286-94.

Ta, T. H., et S. H. Ngo. 2011. « A novel signal acquisition method for GPS dual-frequency L1 C/A and L2C receivers ». In *Advanced Technologies for Communications (ATC), 2011 International Conference on*. p. 231-234. IEEE.

Google Patents. 1984. *Navigation system and method*.

Tsui, J. B. Y. 2005. « Fundamentals of global positioning system receivers : a software approach ». *2nd. Coll. « Wiley series in microwave and optical engineering ». New Jersey: John Wiley & Sons Inc., xvi,* , p. 352 p.

Turunen, S. 2007. « Network assistance : What will new GNSS signals bring to it ? ». *Inside GNSS,* vol. vol. 2, nº no. 3, p. pp. 35-41.

van Diggelen, F. 2001. « Indoor GPS: Wireless aiding and low signal strength detection ». In *NAVTECH Seminar Course Notes, San Diego, CA*.

van Diggelen, F. 2009. « A-GPS assisted GPS, GNSS, and SBAS ». *Artech House Publishers*.

van Diggelen, F., et C. Abraham. 2001. « Indoor GPS: The No-Chip Challenge ». *GPS World,* vol. 50–58.

Van Nee, D. J. R., et A. J. R. M. Coenen. 1991. « New fast GPS code-acquisition technique using FFT ». *Electronics Letters,* vol. 27, nº 2, p. 158-160.

Waters, D. W., T. Pande et J. Balakrishnan. 2011. « Cooperative GNSS Positioning and Navigation ». In *ION GNSS 2011*. (Portland, OR, USA, Sept. 19-23), sous la dir. de

Navigation, Proceedings of the 24th International Technical Meeting of the Satellite Division of the Institute of.

Watson, R., G. Lachapelle, R. Klukas, S. Turunen, S. Pietila et I. Halivaara. 2005. « Investigating GPS signals indoors with extreme high-sensitivity detection techniques ». *Navigation. Journal of the Institute of Navigation,* vol. 52, nº Copyright 2006, The Institution of Engineering and Technology, p. 199-213.

Won, J.-H., T. Pany et G. W. Hein. 2006. « GNSS Software Defined Radio ».

Yang, C., C. Hegarty et M. Tran. 2004. « Acquisition of the GPS L5 signal using coherent combining of I5 and Q5 ». In *Proceedings of the 17th International Technical Meeting of the Satellite Division of the Institute of Navigation (ION GNSS 2004)*. p. 2184-2195.

Yang, C., M. Miller, E. Blast et T. Nguyen. 2007. « Comparative Study of Coherent, Non-Coherent, and Semi-Coherent Integration Schemes for GNSS Receivers ». In *ION GNSS*. (Cambridge, MA, USA).

Yang, R., K.V. Ling et E.K. Poh. 2013. « Optimal Parameters for the Combination of Coherent and Non-coherent Acquisition of Weak GNSS Signals ». In *ION 2013 Pacific PNT Meeting*. (Honolulu, Hawaii), sous la dir. de Meeting, Proceedings of the ION 2013 Pacific PNT, p. 1110 - 1116.

Zhang, W., et M. Ghogho. 2010. « Improved fast modified double-block zero-padding (FMDBZP) algorithm for weak GPS signal acquisition ». In *Signal Processing Conference, 2010 18th European*. p. 1617-1621. IEEE.

Ziedan, N. I. 2006. *GNSS receivers for weak signals*. 250 p.

Ziedan, N. I., et J. L Garrison. 2004. « Unaided acquisition of weak GPS signals using circular correlation or double-block zero padding ». In *Position Location and Navigation Symposium, 2004. PLANS 2004*. p. 461-470. IEEE.